Engineered Barriers for Geological Disposal of Radioactive Waste - Microbial interactions and their limits with Thermo-Hydro-Mechanical-Chemical Processes at the Waste Canister/Bentonite Interface

Student: Katie Gilmour

Supervisors: Dr Colin Davie (SoE), Professor Neil Gray (SNES)

Doctor of Philosophy

School of Engineering

June 2021

Abstract

Nuclear waste is a global problem, with many countries in the process of creating deep geological repositories to store this waste. In proposed repository designs MX80 bentonite clay has been selected as the buffer and backfill. Extensive studies have been carried out on the geomechanical properties of the clay; however, the role of microbes has not been fully investigated. Specifically, in the UK, iron-reducing bacteria are a concern as carbon steel waste canisters will contribute iron oxides and rust products to the immediate environment. Iron-reducing bacteria can reduce Fe(III) to Fe(II) and some species are adapted to high temperatures and low water availability, in keeping with conditions within the repository. Iron-interacting bacteria were found to be indigenous to MX80 bentonite and microbially-influenced iron-reduction was observed up to groundwater salinities of 0.45 M NaCl. The limits of this community at different temperatures and pressure were investigated through a series of batch experiments and subsequent enrichments, where necessary. Fe(II), Fe(Total) and pH were measured throughout the respective experiments and substrates were collected and analysed by XRD, SEM and EDX. The indigenous iron-reducing community and various iron substrates were used to investigate indirect interactions through a series of agar plate experiments. The potential bacterial production of H_2 and silica-solubilising ability was also investigated. In some experiments steel was included to represent the waste canister, results from these experiments suggest that bacteria play a role in passive protection of steel against corrosion. Significant differences in plasticity and mineralogy of MX80 were seen in all biotic experiments. Additionally, silica release coupled to metal / microbe interactions was observed. Transformation of clay minerals through iron reduction or release of silica to groundwater could significantly impact the geomechanical properties of MX80, and thus negatively affect the function of the barrier.

Acknowledgements

I acknowledge EPSRC for providing the funding for this project to take place.

There is a long list of people from the School of Engineering who I would like to acknowledge, and without which this thesis may not exist. I would firstly like to thank Stuart Patterson, Gareth Wear, and Michael Finley for turning me into something vaguely resembling an engineer, and always coming to the rescue whenever something started leaking or stopped working. I would also like to thank Melissa Ware for answering all my silly questions in the politest manner.

A huge thank you to my supervisors, Dr. Colin Davie and Prof. Neil Gray. Their enthusiasm for the project, and encouragement and guidance throughout has been of immeasurable worth. I am grateful to Dr. Anke Neumann, Harry Brooksbank, Maggie White, Jamie Gould, Ross Laws and Tracey Davey for their help with analysis. I would also like to thank the Geomicrobiology group, and its past members, especially Dr. Angie Sherry and Dr. Peter Leary, for their patience, knowledge and expertise. Additionally, I had the pleasure of being part of a wonderful PGR community within the Drummond Building – I thank you all for making 2.01 such a pleasant office to be in.

To my family, thank you for always asking how the experiments are going and listening patiently as I explain why bacteria are so exciting. An honorable mention to my cat, Cora, for needing attention so desperately she began sitting on my keyboard, forcing me to take regular breaks, and on occasion, managing to delete whole paragraphs, forcing me to rewrite them better.

Lastly, my partner Vivek for being a wonderful at-home-office-mate, and giving unending love and support, and coffee, thank you.

Contents

Abstract i

Acknowledgements ii

List of figures 1

List of tables 5

List of Abbreviations: 6

Chapter 1. Introduction 8

1.1 Nuclear Industry and Waste Overview 8

1.2 Deep geological storage of nuclear waste: 10

1.3 Role of microbes in nuclear waste repositories 12

1.4 Research Questions 14

1.5 Aims and Objectives 14

1.6 Hypotheses 15

1.7 Thesis Structure 16

Chapter 2. Literature Review 18

2.1 Radioactivity 18

2.2 Current production and future production of nuclear waste 20

2.3 Country-specific examples of nuclear waste repository concepts 21

2.3.1: Swedish nuclear waste concept (SKB): 22

2.3.2: Swiss Nuclear storage (NAGRA): 24

2.3.3: Finnish Nuclear Storage (Posiva): 25

2.3.4: French nuclear storage (Andra): 26

2.3.5 USA nuclear storage (NRC) 26

2.3.6 Canada nuclear storage (NWMO) 30

2.3.7 Russian nuclear storage concept (NO ROA) 31

2.3.8 South Korea nuclear storage concept (KORAD) 31

2.4 Host rock types 31

2.5 Disposal strategy overview for UK 33

2.5.1 Canister and storage strategy 34

2.6 MX80 Bentonite mineralogy and geomechanical properties 35

2.7 Stages of repository lifespan 40

2.8 Microbes in the repository environment 44

2.8.1 Factors limiting microbial survival in repository environments 45

2.8.2 Opportunities for microbial survival in the repository environment 48
2.8.3 General concerns about the impact of microbial activity in the repository 49
2.8.4 SRBs in the repository 51
2.8.5 Iron-interacting bacteria in the repository 55
2.8.6 Silicate solubilising bacteria in the repository 60
2.8.7 Other bacteria likely to be present in nuclear waste repositories 62
2.9 Concluding statement 63
Chapter 3. Experimental Methods 65
3.1 Introduction and safety 65
3.2 Details of MX80 bentonite 66
3.3 Preliminary experiments and groundwater choice 67
3.3.1 %moisture content of MX80 bentonite and MX80:water ratio: 67
3.3.2 Groundwater composition choice: 67
3.4 Indigenous microbial communities and their basal activity in relation to iron-reduction 68
3.4.1 Setup of anaerobic iron-reducing enrichments with MX80 bentonite: 69
3.4.2 Aerobic enrichments 71
3.4.3 High salinity enrichments 71
3.5 microbial activities of the indigenous-iron reducing community of MX80 in relation to obstacles in the repository environment 72
3.5.1 Solid media indirect microbial interactions 72
3.5.2 Solid media recolonisation on compacted MX80 73
3.5.3 Silica solubilisation 74
3.5.4 Biotic H_2 production in anaerobic conditions 40°C with MX80 bentonite and steel 76
3.6 Desiccation tolerance of the indigenous iron-reducing community of MX80 bentonite and interactions at the MX80 bentonite / steel interface 77
3.6.1 Desiccation tolerance experiment set-up 77
3.6.2 Analysis of desiccation tolerance experiments 78
3.7 Biotic clay / steel interface test cells to simulate repository pressure 79
3.7.1 Experimental set-up 79
3.7.2 Post experiment analysis 80
3.7.3 DNA sequencing and analysis 81
3.8 Experimental methods and assays 82
3.8.1 Synthesis of poorly crystalline Fe(III) oxide (PCFeO): 82
3.8.2 Fe(III) agar plates: 82

3.8.3 Fe concentration measurements (Ferrozine assay): 82
3.8.4 VFA analysis 83
3.8.5 Mineral recovery from agar plates 83
3.8.6 Significance testing: 83
3.9 Molecular techniques and 16S rRNA sequencing 83
3.10 Further analysis techniques: 84
3.10.1 XRD: 84
3.10.2 SEM and EDX 86
3.10.3 Plasticity index 86
Chapter 4. Indigenous microbial communities and their basal activity in relation to iron-reduction 87
4.1 Publication: An indigenous iron-reducing microbial community from MX80 bentonite - A study in the framework of nuclear waste disposal 87
4.1.1 Further results from anaerobic iron-reducing enrichments with MX80 bentonite 99
4.2 Enriched aerobic indigenous bacterial community of MX80 bentonite 101
4.3 Comparison of activated anaerobic iron-reducing community of MX80 bentonite and activated aerobic microbial community of MX80 bentonite 108
4.4 0.45M NaCl iron-reducing microbial enrichments with MX80 bentonite 111
4.4.1 Results 111
4.5 2.5 M NaCl iron-reducing microbial enrichments with compacted MX80 bentonite 120
4.5.1 Results 120
4.6 Comparison of anaerobic iron-reducing microbial communities at all salinities 128
4.7 Discussion 130
4.7.1 The indigenous microbial community of MX80 is putatively capable of iron reduction 131
4.7.2 Notable species identified in the indigenous iron-reducing microbial community 132
4.7.3 Fermenting bacteria are active in the indigenous microbial communities of MX80 bentonite 133
4.7.4 There are similarities and differences between communities at different salinities 134
4.7.5 There are similarities and differences between indigenous MX80 bentonite aerobic and anaerobic microbial communities 136
4.7.6 Changes to iron mineralogy occurred at all salinities 137
4.7.7 Conclusions 139
Chapter 5. Microbial activities of the indigenous - iron reducing community of MX80 in relation to conditional or ecophysiological obstacles in the repository environment 141
5.1 Introduction 141

5.2 Results 142

5.2.1 Solid media indirect interactions between indigenous iron-reducing bacteria of MX80 bentonite and iron substrates 142

5.2.2 Recolonisation experiments on solid media 152

5.2.3 H_2 production experiments by the indigenous MX80 iron-reducing community at a clay steel interface 156

5.2.4 Experiments testing the silica solubilising abilities of the indigenous microbial community of MX80 bentonite 159

5.3 Discussion 164

5.3.1 Microbes indigenous to MX80 can interact with iron substrates from a distance 164

5.3.2 Compact MX80 can be colonised by microbes 166

5.3.3 Hydrogen concentration significantly increases when microbes are present 169

5.3.4 Silica dissolution occurs when microbes are present 170

5.6.5 Changes to mineralogy could negatively impact the multi-barrier system 170

5.4 Conclusions 171

Chapter 6. Desiccation tolerance of the indigenous iron-reducing community of MX80 bentonite and interactions at the MX80 / steel interface 173

6.1 Introduction 173

6.2 Results 174

6.2.1 Mineralogical analysis of the MX80 bentonite from desiccation tolerance experiments . 174

6.2.2 Plasticity measurements of the MX80 bentonite from desiccation and temperature tolerance experiments 179

6.2.3 Visualisation of corrosion of steel coupon recovered from desiccation tolerance experiments 180

6.2.4 Community analysis of the desiccation tolerance experiments at various temperatures 181

6.3 Discussion 185

6.3.1 Survivability of indigenous bacteria of MX80 bentonite 186

6.3.2 Putative activities of the indigenous bacterial community 187

6.3.3 Potential corrosion protection afforded by microbial activity 189

6.3.4 Potential mineralogical alterations to MX80 bentonite 190

6.3.5 Conclusions 192

Chapter 7. Biotic MX80 / steel interface test cells to simulate repository pressure 193

7.1 Introduction 193

7.2 Results 193

7.2.1 Effluent measurements including pH, Fe(II), and groundwater parameters 194

7.2.2 Analysis of corrosion of the steel coupon recovered from test cell experiments 199
7.2.3 Analysis of changes to clay mineralogy and geomechanics 205
7.2.4 Iron-reducing enrichment experiments with MX80 bentonite recovered from test cells 213
7.2.5 Microbial communities of MX80 bentonite after incubation in test cell and enrichment . 218
7.3 Discussion and conclusions 225
7.3.1 Microbially influenced corrosion products may produce a protective layer on the steel surface 225
7.3.2 Putative microbial activity could alter the plasticity and mineralogy of MX80 bentonite 229
7.3.3 Iron-reducing enrichments show evidence of iron-reducing ability of indigenous microbial community after test cell incubation 230
7.3.4 Microbial communities from test cell experiments are altered during enrichment..... 231
Chapter 8. Conclusions 234
8.1 Summary of findings..... 235
8.1.1 MX80 bentonite carries a robust bacteria community capable of iron-reduction 236
8.1.2 The indigenous iron-reducing community of MX80 bentonite is capable of further activities 238
8.1.3 The indigenous iron-reducing community of MX80 bentonite can survive high temperature in desiccated environments..... 240
8.1.4 Summary of findings from microbial clay /steel interface experiments under high pressure 241
8.2 Suggestions for further study..... 243
8.2.1 Green rust analysis 243
8.2.2 Microbially influenced changes to swelling capacity 244
8.2.3 External microbial species and the role of fungi 245
8.2.4 Microbial gas production 245
Bibliography 246

List of figures

1.1 Schematic of the multi-barrier design for UK nuclear waste storage

2.1 Predictions of global nuclear power output
2.2 SKB design concept for the repository at Söderviken
2.3 Posiva nuclear storage concept based on the KBS-3V design
2.4 USA HLW repository design
2.5 Canada conceptual design of nuclear repository
2.6 Timeline of stages involved in UK site-selection for nuclear waste repository
2.7 Edge view of montmorillonite layers
2.8 Typical temperature evolution predicted for a waste package in a deep geological repository
2.9 Reaction at the canister-bentonite interface causing corrosion of carbon steel and production of hydrogen gas, occurring at phase 1 of nuclear waste storage under a hypothetical sulfate reducing system
2.10 Condensation and evaporation cycle which may occur in clay buffer during repository closure
2.11 Steps in dissimilatory sulfate reduction and energy production with H_2 as the electron donor
2.12 Proposed model of Fe(III) reduction by *Geobacter sulfurreducens*

3.1 Flowchart of experiments
3.2 Schematic of anaerobic iron-reducing enrichments experiments
3.3 Schematic of aerobic enrichments
3.4 Schematic of solid media indirect interaction experiments
3.5 Schematic of solid media recolonisation experiments
3.6 Schematic of desiccation tolerance experiments
3.7 Experimental design for test cell experiments
3.8 A simplified schematic of XRD

4.1 Compact MX80 enrichments on day 21
4.2 VFA analysis of MX80 powder experiments
4.3 XRD pattern for sample of black precipitate taken from anaerobic iron-reducing enrichments of MX80
4.4 Aerobic enrichments on day 18
4.5 pH of MX80 aerobic enrichments
4.6 VFA concentrations of aerobic experiments
4.7 Community structure of aerobic MX80 bentonite from 16S rRNA sequencing of enrichments
4.8 Phylogenic tree of aerobic bacteria population of MX80 powder constructed from 16S rRNA sequencing data and BLAST sequences

4.9 Phylogenic tree of aerobic bacteria population of compact MX80 constructed from 16S rRNA sequencing data and BLAST sequences
4.10 PCA plot of anaerobic and aerobic iron-reducing enrichments
4.11 Boxplots of bacterial families across all iron-reducing and aerobic MX80 enrichments
4.12 pH measurements of 0.45M NaCl enrichments
4.13 The concentration of Fe(II) in biotic and positive control 0.45M NaCl enrichments
4.14 VFA analysis of 0.45M NaCl iron-reducing enrichments
4.15 Community structure of 0.45M NaCl enrichments
4.16 Phylogenic tree of most dominant ASVs in the microbial community of MX80 powder from 0.45M NaCl iron-reducing enrichments
4.17 SEM images of product recovered from 0.45M NaCl iron-reducing enrichments
4.18 Bulk EDX analysis of MX80 recovered from 0.45M NaCl iron-reducing enrichments
4.19 XRD spectra of MX80 recovered from 0.45M NaCl iron-reducing enrichments
4.20 pH of 2.5M NaCl iron-reducing enrichments
4.21 Concentration of total Fe(II) from 2.5M NaCl iron-reducing enrichments
4.22 VFA analysis of 2.5M NaCl iron-reducing enrichments
4.23 Barplot of the microbial community of 2.5M NaCl iron-reducing enrichments
4.24 Phylogenic tree constructed from 16S rRNA Illumina sequencing data of 2.5M NaCl iron-reducing enrichments
4.25 SEM images of substrate recovered from 2.5M NaCl iron-reducing enrichments
4.26 XRD pattern after reitvald refinement using HighScore Plus of MX80 recovered from 2.5M NaCl iron-reducing enrichment
4.27 PCA plot of 0.45M NaCl and 2.5M NaCl iron-reducing enrichments
4.28 Boxplots of significant geneses from 16S rRNA sequencing of different salinity iron-reducing enrichments with MX80 bentonite

5.1 Agar plates after solid media experiment
5.2 pH of solid media indirect interaction experiments
5.3 Biomass measurements of solid media indirect interaction experiments
5.4 SEM images of Fe powder recovered from indirect interaction experiments
5.5 SEM images of MX80 powder recovered from indirect interaction experiments
5.6 SEM images of PCFeO recovered from indirect interaction experiments
5.7 EDX analysis of Fe powder recovered from indirect interaction experiments
5.8 XRD spectra of Fe powder recovered from indirect interaction experiments
5.9 XRD spectra of PCFeO recovered from indirect interaction experiments
5.10 XRD spectra of MX80 powder recovered from indirect interaction experiments
5.11 pH measurements of recolonisation experiments
5.12 SEM images of compact MX80 from recolonisation experiments
5.13 XRD spectra of compact MX80 from recolonisation experiments
5.14 Hydrogen production from biotic experiments with compact MX80 and steel
5.15 SEM images of steel surface from hydrogen production experiments
5.16 Silicate measurements of Sellafield-like groundwater mixed with MX80 bentonite
5.17 pH of silicate experiments
5.18 VFAs of silicate experiments

5.19 SEM images of surface of MX80 shows silicate dissolution

6.1 XRD spectra of MX80 recovered from desiccation tolerance experiments
6.2 SEM images of clay recovered from the desiccation tolerance experiments
6.3 Plasticity index for MX80 after desiccation tolerance experiments
6.4 % moisture content of MX80 bentonite after desiccation tolerance experiments
6.5 Steel discs recovered from desiccation tolerance experiments
6.6 Barplots of level 5 microbial community of MX80 after desiccation tolerance experiments
6.7 Phylogenic tree of indigenous iron-reducing microbial community of MX80 after desiccation tolerance experiments at 40°C
6.8 Phylogenic tree of indigenous iron-reducing microbial community of MX80 after desiccation tolerance experiments at 70°C
6.9 Phylogenic tree of indigenous iron-reducing microbial community of MX80 after desiccation tolerance experiments at 70°C and slowly cooled to 40°C
6.10 PCA plot of microbial communities from desiccation tolerance experiments

7.1 Steel and clay recovered from test cells
7.2 Effluent collected from test cells
7.3 pH of initial groundwater and resulting effluent collected from test cell experiments
7.4 Iron concentration in the effluent recovered from test cell experiments
7.5 Ultrameter measurements of the effluent from test cells
7.6 VFA analysis of effluent collected at the termination of test cell experiments
7.7 Steel coupons recovered from test cells
7.8 Height of rust products diffusion into the MX80 from the steel surface after test cell experiment
7.9 SEM images of steel disc recovered from test cells with microbes
7.10 SEM images of steel recovered from sterile test cell experiments
7.11 XRD analysis of corrosion products from test cell experiments
7.12 pH of the MX80 recovered from test cells at each surface
7.13 The liquid limit, plastic limit and plasticity index of MX80 bentonite recovered from test cells
7.14 SEM images of MX80 bentonite recovered from Microbe_Steel test cells
7.15 SEM images of MX80 bentonite recovered from Sterile_Steel test cells
7.16 SEM images of clay recovered from Microbe_NoSteel test cells
7.17 XRD analysis of the top of MX80 recovered from test cells including steel
7.18 XRD analysis of MX80 betonite recovered from Microbe_NoSteel test cells
7.19 pH of the iron-reducing enrichments with clay recovered from test cells
7.20 Fe(II) concentration of iron-reducing enrichments
7.21 VFA concentrations of iron reducing enrichments with MX80 bentonite recovered from test cells
7.22 PCA plots of microbial communities from Microbes_Steel
7.23 Barplots displaying the microbial communities of MX80 recovered from test cells using nested PCR

7.24 Phylogenic tree of sequences generated from 16S rRNA sequencing of the nested product of DNA extraction from Microbe_Steel_Top
7.25 Phylogenic tree of sequences generated from 16S rRNA sequencing of the nested product of DNA extraction from Microbe_Steel_Bottom
7.26 Barplots displaying the microbial communities of MX80 recovered from test cells following iron-reducing enrichments
7.27 Phylogenic tree of sequences generated from 16S rRNA sequencing of iron-reducing enrichments using MX80 recovered from Microbe_Steel_Top
7.28 Phylogenic tree of sequences generated from 16S rRNA sequencing of Microbes_Steel_Bottom after iron-reducing enrichment
7.29 Boxplots of individual species or geneses from Microbe_Steel combining top and bottom communities.

List of tables

2.1 Composition of 516 grade 70 carbon steel plate
2.2 Groundwater composition from several sites relevant to nuclear waste repositories
2.3 Mineralogical composition of MX80 Bentonite and bulk composition of FEBEX
2.4 Chemical composition of Wyoming MX80 bentonite
3.1 Sellafield-like groundwater composition
3.2 Organic substrate mixture components added to groundwater
3.3 Summary of indigenous microbial community enrichments

List of Abbreviations:

% wt.: percentage Weight
ASV: Amplicon Sequence Variant
ATP: Adeonsine TriPhosphate
aw: water activity
BLAST: Basic Local Alignment Search Tool
BLASTn: Basic Local Alignment Search Tool nucleotide
BP: Beyond Petroleum
CFU: Colony Forming Units
CNSC: Canadian Nuclear Safety Commission
cryo-TEM: three-dimensional Cryogenic Transmission Electron Microscopy
CT: Computerised Tomography
DGGE: Denaturing Gel Electrophoresis
DNA: Deoxyribonucleic Acid
EDX: Energy Dispersive X-ray analysis
EPS: Extracellular PolySaccharide
FEBEX: Full-scale Engineered Barrier EXperiment
GR: Green Rust
Gy: Grays
HLW: High Level Waste
IAEA: International Atomic Energy Agency
IC: Ion-Chromatography
ILW: Intermediate Level Waste
IRB: Iron-Reducing Bacteria
KBS: Nuclear Fuel Safety (Swedish)
Kwh: kilowatt hours
LL: Liquid Limit
LLW: Low Level Waste
MEGA: Molecular Evolutionary Genetics Analysis
MIC: Microbially Influence Corrosion
MICP: Microbially Influenced Calcite Precipitation
NAD: Nicotinamide Adenine Dinucleotide
NADH: Nicotinamide Adenine Dinucleotide with Hydrogen
NAGRA: National Cooperative for the Disposal of Radioactive Waste
NCBI: National Center for Biotechnology Information
NDA: Nuclear Decommissioning Authority
NRC: Nuclear Regulatory Commission
NU-OMICS: Northumbria University sequencing facility
NWMO: Nuclear Waste Management Organisation
OECD-NEA: Organisation for Economic Co-Operation and Development – Nuclear Energy Agency
ORP: Oxidation-Reduction Potential
OTU: Operational Taxonomic Unit
Pa: Pascals
PCA: Principal Component Analysis
PCFeO: Poorly Crystalline Iron Oxide
PCR: Polymerase Chain Reaction

PI: Plasticity index
PL: Plastic Limit
PPM: Parts Per Million
PUREX: Plutonium Uranium Redox EXtraction
QIIME: Quantitative Insights Into Microbial Ecology
RNA: Ribonucleic Acid
rRNA: ribosomal Ribonucleic Acid
RWC: Radioactive Waste Clay
RWM: Radionuclear Waste Management
SEM: Scanning Electron Microscope
SF: Spent Fuel
SKB: Svensk Kärnbränslehantering
SRB: Sulfate-Reducing Bacteria
Sv: Sierverts
TDS: Total Dissolved Solids
TEM: Transmission Electron Microscopy
THORP: THermal Oxide Reprocessing Plant
V: Volts
VFA: Volatile Fatty Acid
WIPP: Waste Isolation Pilot Plant
XRD: X-Ray Diffraction
yr: year

Chapter 1. Introduction

1.1 Nuclear Industry and Waste Overview

The nuclear energy industry is predicted to continue to provide energy for the foreseeable future, continuing into the next century. This continuation is due to the high efficiency of nuclear fission compared to fossil fuels and the lack of greenhouse gases produced at the point of generation, making it a more environmental option. Although estimates vary, the carbon footprint of nuclear power in electricity generation has been reported to be as low as 25 gCO_2/kwh on average (Warner & Heath, 2012), compared to renewable energy which is between 10-50 gCO_2/kwh (Nugent & Sovacool, 2014), and coal which is reported to generate 786 gCO_2/kwh minimum (Nie et al., 2011). In 2017, 31 countries operated a total of 403 nuclear reactors with a 1.4% increase in power generated compared to 2016 (Schneider et al., 2017). The most notable increase was in China, which had a 23% increase in nuclear energy generated and construction beginning on twenty new reactors (Schneider et al., 2017). In 2018, nuclear power accounted for 10% of the global energy output (IEA, 2019). This usage has led to 22,000 m^3 of high-level waste (HLW) from spent fuel in storage (IAEA, 2018a).

Hospitals, among other industries such as academia, are also generating an increasing volume of nuclear waste with radioisotopes being used more frequently as therapeutic and diagnostic tools. The waste generated is largely liquid and mainly contains the following isotopes: Technetium-99m (Tc-99m), Iodine-131(I-131), Iodine-125 (I-125), Iodine-123(I-123), Flourine-18(F-18), Tritium (H-3) and Carbon-14(C-14) (ICRP, 1995). Some solid waste, such as from equipment that has come into contact with liquid waste is also generated by these industries.

Therefore, the question of a disposal method is of high priority for the 31 countries which are involved in the industry and in most cases, disposal has been considered since the 1970s (Sellin & Leupin, 2013). There is currently a large proportion of nuclear waste which has been accumulating since the 1950s. Therefore, no matter the future of the industry, there will still need to be a disposal or storage solution.

The nuclear fuel industry in the United Kingdom is long established, starting in 1954 with Calder Hall, the first nuclear power station, opening in 1956. Since then, there have been several nuclear power plants built providing energy and munitions among other purposes. There are currently fifteen nuclear reactors at seven power plants still in operation in the UK, and eleven plants which have been closed and decommissioned. It is estimated that the nuclear waste industry in the UK will generate a total of 4.9 million tonnes of nuclear waste over 200 years to 2150 (NDA, 2016).

Waste is generated during almost every stage of the nuclear energy process, especially during the reprocessing of spent fuel (SF). Reprocessing allows uranium and plutonium to be recovered from spent fuel rods and reused through a process called PUREX (Plutonium Uranium Redox EXtraction) which utilises a liquid-liquid ion exchange method. Spent fuel is mainly composed of U-238, but also contains plutonium, and fission products such as caesium, strontium and other uranium isotopes. Through the PUREX process, a residual acidic, radioactive liquid is produced, which is a component of High-Level Waste (HLW). HLW and spent fuel generates 1000-2000 W of heat during the decay process (Sellin & Leupin, 2013). For safer and easier storage purposes, HLW is converted into a stable solid form through a process called vitrification (Bradbury et al., 2014). In this process the liquid waste is mixed with borosilicate glass and sealed in steel canisters. Currently a high proportion of HLW generated by the UK is stored at Sellafield above ground, a nuclear decommissioning and waste storage facility owned by the Nuclear Decommissioning Authority (NDA) in Cumbria, UK. Other waste generated by the nuclear industry is referred to as Intermediate Level Waste (ILW) (this includes cladding and filters), Low Level Waste (LLW), and spent fuel (SF). This waste can also be generated from mining, generating electricity, and decommissioning nuclear plants.

Currently, the UK LLW and short-lived ILW wastes are stored in an above ground repository at Sellafield, with a number of other countries also storing their LLW and ILW in similar facilities. Alternatively, some waste generated by reprocessing plants is released to the sea, due to its very low radioactive levels and short period of radioactive decay (IAEA, 2018). Additionally, gases produced by LLW waste are released to the atmosphere. This includes the inert gases krypton-85 and xenon-131 (Banerjee et al., 2015).

Calder Hall, at the Sellafield site was opened in 1956 as a nuclear power plant and became a reprocessing site in the 1970s and 80s. The Thermal Oxide Reprocessing Plant (THORP) was built and the PUREX method of extraction was employed in the 1990s (Leafe, 2017). It is currently the only facility in the UK able to manage all types of nuclear waste: LLW, ILW, HLW and SF. The long-term storage of this waste has been an issue since 1976. A practical long-term solution which is being adopted by several countries is the storage of nuclear waste in underground repositories. This concept has been extensively studied in Sweden at the in situ Äspö Hard Rock Laboratory and in other countries, which many, including the UK, are preparing to adopt as a solution to their own nuclear waste storage problems.

SF, in the form of irradiated fuel rods, contain pellets of uranium and plutonium compounds encased in zircaloy (Bradbury et al., 2017). The waste is currently stored in stainless steel canisters which are thought to remain a safe storage vessel for 500 years, after which point there is a risk of radionuclides entering the environment, and a new or alternative method of storage will have to be employed. Considering the half-life of selenium-79 is 65,000 years, and the half-life of plutonium-239 is 24,000 years, a longer-term solution is essential (IAEA, 1999).

LLW accounts for 90% of the volume of radioactive waste generated, despite only equalling 1% of the total radioactivity of all waste. Therefore, this waste is suitable for near-surface disposal. ILW, although more radioactive than LLW, does not require specially designed storage units to last thousands of years. It is generated from chemical sludge and requires more shielding than LLW but does not produce as much heat as HLW and has a shorter radioactive half-life. HLW and SF have long-decay periods and are heat-emitting, these types of waste therefore require the most shielding and must be stored for longer (Sellin & Leupin, 2013).

1.2 Deep geological storage of nuclear waste:

The OECD-NEA (Organisation for Economic Co-Operation and Development – Nuclear Energy Agency) includes 31 countries across Europe, Asia and America, and aims to promote international co-operation to determine solutions to nuclear waste. Most current concepts utilise a multibarrier design in mined repositories to shield the environment from the nuclear waste.

Briefly, these repositories could house low heat generating waste such as LLW and ILW; and high heat generating waste (HLW) at increasing depths. According to these current designs, HLW will be stored at 400-1000 m below ground in metal canisters surrounded by a highly plastic clay with a high swelling ability, such as bentonite (figure 1.1). These designs rely heavily on local geology and geochemistry to ensure the host rock and groundwater will allow the waste canister to remain encased for 10,000-100,000 years (Sellin & Leupin, 2013). Fractures in host rock, or pollutants and highly saline groundwaters could decrease the lifespan of the repository by allowing more access to the geosphere or increasing the corrosion of the waste canister. The ability of the clay buffer to swell and contract with changing water contents and temperatures is also important. The buffer must swell enough to seal all gaps around the canister and ensure it does not sink. The pore spaces in this clay will limit any movement of radionuclides, but this would not be possible if any cracks occur during dryer periods of enclosure (Sellin & Leupin, 2013).

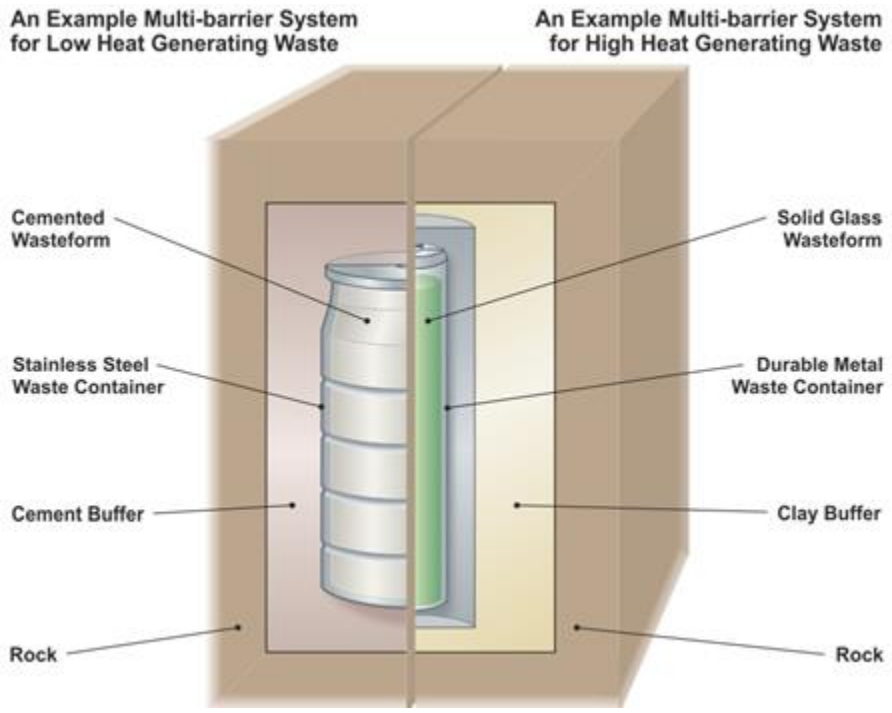

Figure 1.1: Multi-barrier design for UK nuclear waste storage (NDA, 2010)

An alternative to mined repositories is boreholes which are drilled into rock to a depth of up to 5 km. Waste canisters are then stored in the deeper sections (> 2000 m) and the shallower 3000 m is backfilled and sealed. Whilst this method has been considered by several countries, the economic cost relative to that of mined repositories makes it an unfavourable option (Freeze et al., 2019).

Currently, in the US, several boreholes are used for near surface storage of LLW at depths of under 20m (IAEA, 2009) with plans to install more boreholes of greater depths to store a wider variety of nuclear waste. Similar to mined repositories, the location of boreholes is of great importance to the safety of the storage. Sites with low levels of groundwater and limited geochemical activity are favoured.

1.3 Role of microbes in nuclear waste repositories

There are numerous concerns over the potential impact of microbial activity within nuclear waste repositories. Although some arguments have been made that microbes will not survive in the repository (West et al., 2002), there is strong counter arguments to suggest that some microbes will be present and active during repository closure (Chi Fru & Athar, 2008).

There are several sources of microbes; from the local environment (the host rock and groundwater) (Masurat et al., 2010); the engineered environment (the clay barriers, and any introduced during construction) (Lopez-Fernandez et al. 2014, RWM, 2016); and microbes introduced during manufacturing of, for example, compacted clay rings to be used as a barrier (Motamedi et al., 1996). The biggest concern is that microbes will contribute to an increased rate of corrosion of the waste canister through microbially-induced corrosion (MIC) (Leupin et al., 2017). Indeed, there is evidence that species known to be involved in MIC will be present in the groundwater at some repository sites and in the clay buffers. For example, sulfate-reducing bacteria (SRBs) are known to increase corrosion through hydrogen sulphide production, and several species have been isolated from groundwater samples at the proposed nuclear repository site in Sweden (Kotelnikova and Pedersen, 1998; Haveman & Pedersen, 2002; Masurat et al., 2010). Iron-reducing bacteria are also a concern as they may also increase the rate of corrosion of the steel canisters (Necib et al., 2017) and may reduce iron present in the clay barrier causing

mineralogical changes to the clay resulting in a change in the performance of the barrier (Wersin et al., 2008). These changes could result in transformation to non-swelling Fe(II) minerals, resulting in disadvantageous geomechanical changes to the properties of the clay (RWM, 2016; Bradbury et al., 2014). These changes could by influenced by microbes, either by directly reducing metals present within clay minerals, or indirectly through acid secretions (Kim & Gadd, 2008; Gadd, 2010). Therefore, there is a possibility that these changes could be widespread throughout the clay barrier, and as a result, decrease the swelling ability of the clay, ultimately limiting its effectiveness as a barrier.

Conversely, Videla & Herrera (2009) suggests that microbial activity could lead to a further barrier via formation of a biofilm. Moreover, it is possible that the microbial community may inhibit MIC by consuming corrosive substances such as reactive oxygen species; or some species may out compete MIC-causing bacteria (Kip & Veen, 2015).

Of further concern is the potential interactions between microbes and radionuclides; however, it is thought more likely that microbes will die on exposure to such high doses of radiation, or, as evidenced in Shukla et al. (2007), will survive and may contribute to immobilising radionuclides such as selenium and uranium (Newsome et al., 2014; Hua et al., 2006).

A final concern is microbial gas production, such as carbon dioxide which could increase the pressure in the repository (Leupin et al., 2017; Stroes-Gascoyne & West, 1997). However, microbial gas consumption of oxygen and hydrogen would be beneficial as this would decrease pressure and oxygen consumption would aid in reducing the rate of corrosion of the waste canister (West et al., 2002).

It is therefore not clear what the impact of microbial activity will be on nuclear waste storage. The outcome of microbial presence will depend on local microbial communities and geochemistry as well as the specific design materials.

1.4 Research Questions

Unlike SRBs not much is known about the potential role of iron interacting bacteria that might be associated with clay buffers or the wider repository environment. In this study we have focused on MX80 bentonite as this is likely to be the clay used in the UK concept, and so the potential for microbially mediated transformation of iron linked to the canister bentonite assemblage has been investigated. The project will aim to address the following research questions:

- Does MX80 bentonite (and by implication other bentonite clays which will be likely used in a wide range of nuclear waste repository projects around the world) have an indigenous and viable microbial community associated with it?
- In particular, how does the microbial community interact with iron?
- If present how does this community interact with the clay and canister components of the multi barrier system under the different geochemical and physical conditions relevant to the evolution of a GDF with time?
- What are geomechanical implications of this microbial activity with respect to the canister and clay components of the multi barrier concept?
- What is the likelihood that such a microbial community will be active and survive the different stages of the GDF evolution (which likely encompass changes in salinity, pressure and temperature)?

1.5 Aims and Objectives

The main aim of this project is to investigate the presence and survivability of iron-interacting bacteria and determine what effect their activity may have on the geomechanical properties of MX80 bentonite in reference to the proposed design for UK nuclear waste repositories. This overarching aim will be supported by shorter term specific objectives including;

1. To identify the indigenous microbial community of MX80 bentonite and assess whether indigenous microbes could influence iron minerals in the clay and corrosion of the carbon steel canister

2. To determine whether secreted products from indigenous microbes can interact with spatially distant iron minerals thus investigating if microbes in isolated pockets can cause widespread mineralogical changes to the clay. And, alternatively, if microbes situated further from the canister can still cause corrosion.

3. To determine whether the indigenous microbial community could affect clay properties, namely geomechanical properties which aid in its ability to function as a barrier such as plasticity.

4. To assess how the microbial community changes and survives harsh conditions relevant to the repository including high temperatures, changing salinities and pressure.

1.6 Hypotheses

a) Several species of different microbes displaying different functions and metabolisms will be identified in MX80 bentonite.

Indications in the literature support the hypothesis that at least some of these species will be thermophilic.

b) These microbes will have the potential to interact with iron in bentonite under certain conditions, but whether it will be destructive or constructive is not clear and will depend on which species are identified.

c) In the absence of microbes, geochemical reactions resulting in clay alteration and canister corrosion will be limited.

d) Microbial activity under conditions relevant to the repository environment will lead to alterations to the structural and chemical properties of the bentonite which will impact on its role in the multi barrier system.

1.7 Thesis Structure

This section explains the arrangement of this thesis and concludes Chapter 1 which set out the main aims and hypotheses of this project as well as giving a brief overview of nuclear energy and waste generation. The current UK considerations for nuclear waste disposal were also described. Chapter 2 reports on the future of nuclear energy, explores international nuclear waste repository designs including material compositions, and finally explains knowledge already gathered on microbial presence in the proposed repository environment and what speculations have been made about how this activity could affect the integrity of the repository to safely house nuclear waste.

A general methods chapter, Chapter 3, explains the experiments and general laboratory techniques used to answer the research questions outlined above. There are then 4 experimental chapters. Chapter 4 presents the indigenous microbial community of MX80 bentonite under different microbial enrichments conditions including iron-reducing, anaerobic, aerobic and highly saline. The iron-reducing ability of these communities is also presented and a comprehensive discussion on the metabolic activities of the communities is included. This chapter was used to inform the experiments presented in further chapters, and the iron-reducing community presented is used in all subsequent experiments. Chapter 5 further investigates the activities of the indigenous iron-reducing microbial community, beginning with its capacity to colonise MX80 bentonite and its ability to indirectly interact with a range of iron substrates. The H_2 produced by the microbial community over 10 months is also discussed, as is its silica solubilising abilities. The possible effects of these activities on the integrity of MX80 bentonite to act as a barrier are discussed in detail. Chapter 6 focusses on a longer-term incubation which aimed to test the survivability of the indigenous microbial community in MX80 bentonite under conditions relevant to nuclear waste repositories: namely, high temperature and low water. These experiments included steel and compacted MX80 bentonite and the changes to these materials after

incubation with microbes is assessed and discussed. The surviving microbial communities are also characterised and fully analysed. The final experimental chapter, Chapter 7, details experiments which replicated repository conditions to a greater extent than previous experiments present in this thesis. These experiments were carried out in confined test cells under high pressure with steel, compact MX80 bentonite and the indigenous iron-reducing microbial community – this is compared to an abiotic control experiment which was also carried out. The resulting corrosion products, steel surface corrosion and changes to the geomechanical properties to MX80 bentonite are described and the implications for the repository are discussed. The iron-reducing ability and metabolic activity of the microbial community after test cell incubation is measured, and a new microbial community was characterised and presented here. Finally, Chapter 8 summarises the key findings of this project and highlights areas for future work.

Chapter 2. Literature Review

This section outlines what radioactivity is, the current and future production of nuclear power – resulting in nuclear waste - and gives examples of different high-level nuclear waste disposal strategies. By considering research from different countries, particularly those with more extensive and definite repository designs, experiments relevant to the UK disposal concept can be informed.

Additionally, this section describes the materials proposed for use in the repository with a particular focus on their useful characteristics and outlines how they are suited to the repository at different phases of closure. Notably the use of MX80 bentonite and carbon-steel canisters is relevant to the UK design.

The remainder of this section will summarise published research to date which has investigated the role of microbes within a repository system, as well as describing the mechanisms of this bacterial activity more generally. This review includes which microbes have been found to be present, and what experiments have been carried out using model organisms. Through this critical review, and with reference to the repository conditions and materials selected for use in the repository, significant research gaps have been identified. The information from this literature review, further understanding of microbial activities, and previous work has been used to inform experimental design and methods (see Ch 3) to answer the research questions outlined in Chapter 1.

2.1 Radioactivity

There are three main types of ionising radiation arising from radioactive atoms; alpha, beta and gamma. Alpha radiation is the least penetrating, it occurs when an unstable atom emits an alpha particle (two protons and two neutrons – the same as a helium particle) in an effort to stabilise (Peirce et al., 1998). Beta radiation consists of high energy electrons arising from neutrons splitting into a proton and an electron in the nucleus of the atom (NRC, 2017). Gamma radiation is somewhat dissimilar to alpha and beta radiation in that it is short wavelength and high frequency electromagnetic waves which can travel long distances. Gamma is more penetrating

than alpha or beta radiation and requires lead or a thick layer of concrete (or similar) to be stopped (NRC, 2017).

Additionally, another type of ionising radiation specific to nuclear power generation is neutrons. Neutrons are even more penetrating than gamma radiation and require a thick layer of hydrogen-containing material such as concrete or water to encapsulate them. Neutrons are generated in nuclear reactors but are also widely used in the medical industry for radioactive treatments and equipment (Barschall, 1976).

There are multiple units for measuring radiation; however, the System Internationale is the most widely used and arose from the metric system. In this system, the radiation absorbed by an organism is measured in grays (Gy), and the risk of exposure to radiation is measured in sieverts (Sv) (NRC, 2017a). For context, one year of exposure to natural radiation is equal to 2.4-3 mSv (Hendry et al., 2009; Lin, 2010), and the average dose of radiation from a routine abdominal CT scan on the skin is 3.3 mGy (Mauri et al., 2011).

The biological effects of exposure and absorbance of radiation are profound. Higher doses will kill cells, while lower doses can chemically alter cells such as altering DNA. In humans, this leads to radiation sickness as well as a range of health impacts including cancer. In bacteria, radiation can cause changes to the cell, such as an increase in reactive oxygen species, a change in environmental response or cell death (Reisz et al., 2014). However, some bacteria have evolved mechanisms to combat exposure to radiation (this is further discussed in section 2.8.2) (Newsome et al., 2014).

In the conceptual design of deep geological disposal of HLW, the predicted dose of radiation released from the waste canister varies greatly in the literature. Allard & Calas (2009) predict 72 Gy per hour for the first 1000 years; however, this will not diffuse through the buffer at a fast rate and so levels of radiation at the host rock are likely to be much lower. However, Jonsson (2012) predicts a total dose of 40-200 kGy gamma-radiation. Predictions for total alpha radiation are much higher, usually around 8 MGy or higher (Sellin & Leupin, 2013; Jonsson, 2012). However, the biological and environmental risk of this radiation

escaping the confines of the repository are low, rather the possibility of radionuclides escaping the repository through breaches in the containment remains a concern. Therefore a multibarrier approach has been employed to contain HLW.

2.2 Current production and future production of nuclear waste

Although the original purpose of the early nuclear reactor plants developed in the UK was for the weapons industry, the nuclear industry now supplies a significant proportion of the energy contributed to the national grid in the UK. This increase is due to the efficiency of nuclear fission over fossil fuels, and the lower volume of greenhouse gases produced. It is primarily for this reason that the nuclear fuel industry is still growing and will continue to be an important part of the World's energy supply in the future. Although it is likely that countries within the OECD will have decreasing nuclear powder due to decommissioning of nuclear reactors, and little investment in new reactors, countries outside the OECD, in particular China are predicted to increase their nuclear power outputs over the coming decades (figure 2.1) (BP, 2019).

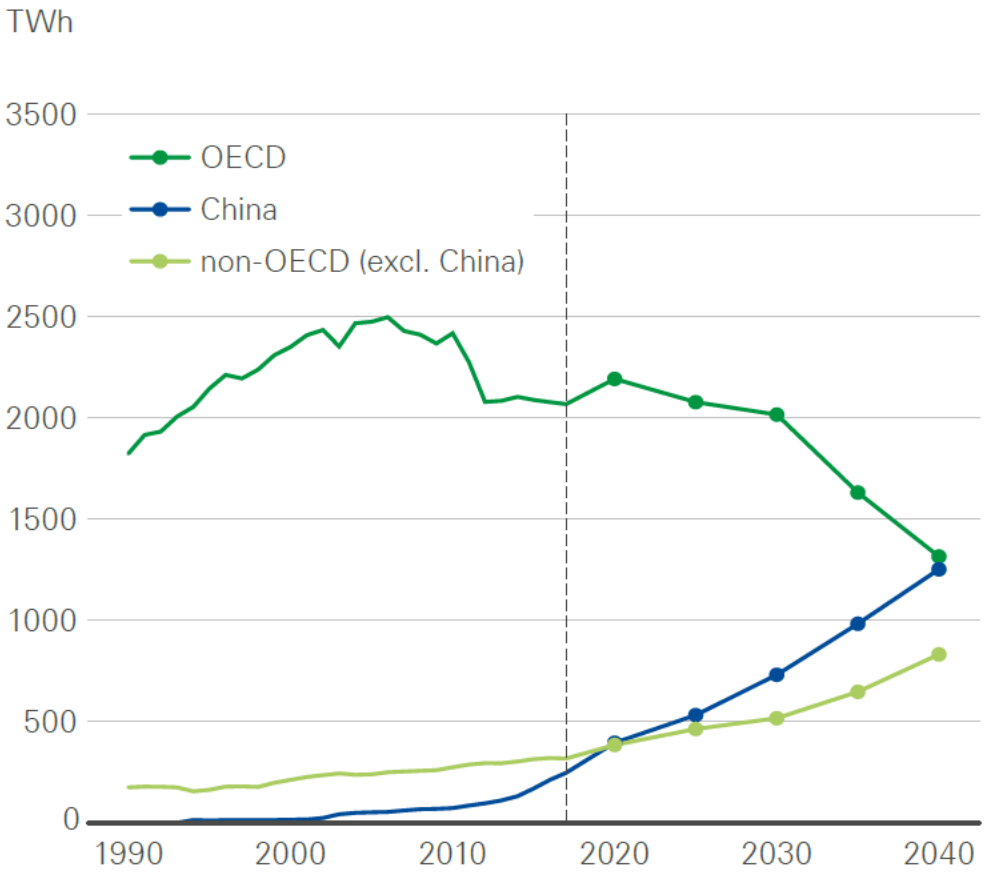

Figure 2.1: Predictions of global nuclear power output (BP, 2019)

2.3 Country-specific examples of nuclear waste repository concepts

A number of these countries, including Finland, Switzerland, Sweden, and Germany have, and are currently, developing concepts for nuclear waste disposal that have shaped the UK model, taking into consideration all geological and hydrogeological diversities relating to local settings. Although some countries, such as France, are considering a storage solution rather than disposal, in which the waste is retrievable from the repository after a period of containment. The timescale required for containment raises several additional challenges besides ensuring the longevity of the materials used. For instance, linguists and artists are currently being consulted to ensure that as language evolves, the meaning and information surrounding repositories is maintained. In France, several artists have been invited to submit designs for symbols for nuclear waste

repositories which could be understood in 10,000 years even if language changes. Further challenges are present in that the storage length is longer than that of any interval between wars – i.e., the repository is likely to experience several international conflicts and as such, the safety of these repositories is of further importance.

Most of the designs for HLW and SF currently being investigated use a multi-barrier approach and a storage depth between 400-1000 m below ground, with waste stored in metal canisters. The integrity of the multi-barrier approach should be stable for a period of 100,000 years against high pressures (4-15 MPa), provide a barrier to reduce corrosion, and withstand a shear load such as that caused by an earthquake. Additionally, the canisters must be heat and chemical resistant and have a high mechanical strength (Raiko et al., 2010). In the event of a breach of the multi-barrier system, radioactive waste in the form of SF or HLW and the radionuclides present will interact with water under reducing conditions allowing radioactive particles to enter the exterior environment and in addition radiolysis will occur.

Case studies reported on below give an outline of the various concepts and local differences between designs in different countries. These examples also highlight the different stages of planning each country is in.

2.3.1: Swedish nuclear waste concept (SKB):

The SKB began official planning in 2011 to build a repository 500 m below ground in granitic crystalline rock. The design proposed consists of three layers of barriers – a copper clad canister with an iron insert (Raiko et al., 2010); 35 cm thick MX80 bentonite of 75-90% wt. montmorillonite (SKB, 2010); and the rock face itself (figure 2.2). After vertical emplacement of the canisters encased in compacted bentonite rings, the repository will also be backfilled with bentonite and then the repository will be sealed (SKB, 2016).

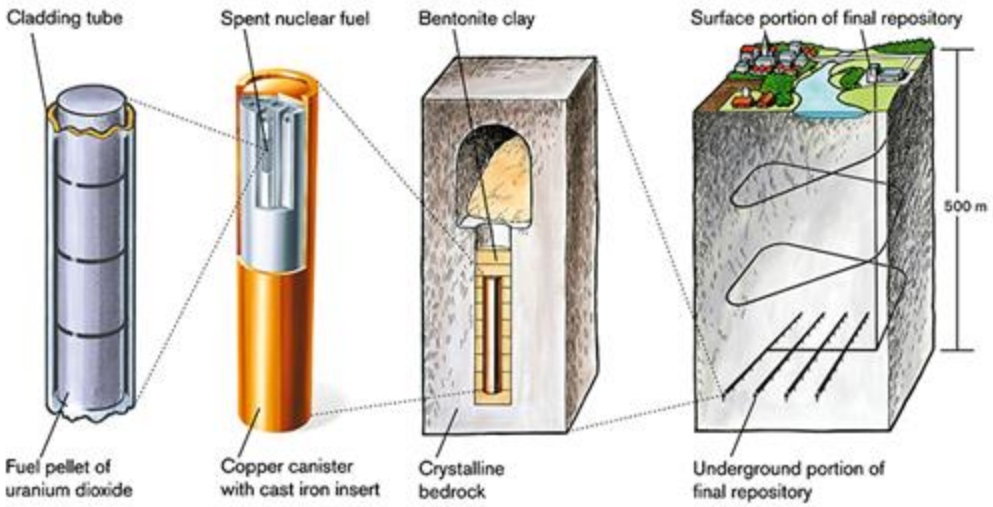

Figure 2.2: SKB design concept for the repository at Söderviken (SKB, 2015)

The 5cm thick copper canister is thought to provide a barrier to the corrosion of iron, although copper is still subject to corrosion at a slower rate. The iron insert has the purpose of protecting the copper from radioactive interaction and embrittlement. It is expected that the copper will corrode at a rate of 1 µm/yr, and so should remain stable for 50,000 years, with the total containment period being 100,000 years. These materials, along with steel can provide the strength needed for this storage and can withstand the high temperatures and pressures which they will be exposed to (Landolt et al., 2009). However, copper is susceptible to corrosion. It can corrode to form tenorite (CuO) or cuprite (Cu_2O) under oxidising conditions and chalcocite (Cu_2S) and covellite (CuS) depending on reducing or oxidising conditions and the concentration of HS^- (Amcoff & Holenyi, 1996). Corrosion of any degree will make the canister more susceptible to mechanical stress. In some cases, a patina will form on copper, providing a physical barrier to the outside environment, thus protecting the copper surface from corrosion; however, in the underground environment it is unlikely that a patina will form to give any level of significant protection.

The groundwater associated with the Söderviken site has 5.2 mM sulfate (Aunqué et al., 2006). Sulfate is considered to pose a threat to increasing the rate of corrosion of the waste canister through iron sulfide production (discussed in detail in section 2.8.4) (Valencia-Cantero et al.,

2014). The presence of sulfate and iron in Swedish groundwaters (table 2) suggests anoxic reduced conditions.

2.3.2: Swiss Nuclear storage (NAGRA):

NAGRA is a national collective of Switzerland aiming to design a suitable repository for the storage of nuclear waste. In 2002, following studies carried out at the Mont Terri Rock laboratory, a concept named "Entsorgungsnchweis" was submitted to government, proposing a repository built in Northern Switzerland. The region chosen would provide a host rock of Argillaceous Opalinus clay 110 m thick (NAGRA, 2016) and would allow storage up to 1000 m below ground (Landolt et al., 2009).

The Swiss design also uses bentonite, but stores fuel canisters made of carbon steel in horizontal tunnels. The length of each canister is 5.35 m x 1 m. The containment period with no breach in any barrier is estimated to be between 1000 and 10,000 years (Bradbury et al., 2014). Studies carried out by Patel et al. (2012) determined that 150 mm thick carbon steel canisters would be durable and strong enough to withstand the forecasted stress and corrosion that may occur during the period of storage. Table 2.1 shows the composition of the carbon steel proposed for nuclear waste canisters. This material will improve on the strength of the copper alternative and will be less susceptible to some kinds of corrosion, but, like copper, could be corroded as a result of abiotic reactions, particularly by sulfides, and anaerobic respiration of microbes.

However, the level of corrosion is linked to the elemental content of the steel (e.g., a steel with higher levels of chromium is more resistant to sulfidation). Further studies suggest that steel, when heated at intervals, is less likely to crack, which is beneficial as it will be exposed to heat emitted from the waste as it decays, and cracking would cause an unwanted breach in the canister (RWM, 2016).

Table 2.1: Composition of 516 grade 70 carbon steel plate, exact composition is dependent on grade (Bradbury, 2014)

Element	*% wt.*
Carbon	0.27-0.31
Manganese	0.79-1.3
Phosphorus	0.035
Sulfur	0.035
Silicon	0.13-0.45

The design uses steel arches to reinforce the tunnels during construction, these arches will fail due to corrosion during containment and allow a secondary creep of the host rock. This process should provide further sealing to the repositories. Compared to crystalline granitic rock, as used in the SKB concept, Argillaceous Opalinus clay is better suited to provide a barrier for radionuclides due to its hydraulic and geochemical properties. Therefore, the NAGRA concept is less dependent on compacted bentonite. The rock type proposed by NAGRA also indicates that in the event of a canister or buffer failure, the rock will still provide a suitable barrier, which explains why the canister containment period is less than that of the SKB design.

2.3.3: Finnish Nuclear Storage (Posiva):

The Finnish disposal concept is similar to the SKB, KBS-3 design. The location of the final repository will benefit from crystalline host rock located 400m underground (Idiart et al., 2013). Boreholes within the repository will allow for vertical storage (figure 2.3) of copper canisters with iron inserts (Hellä et al., 2014). Posiva is continuing to monitor borehole geochemical and geomechanical changes having selected a location in 1980s, to ensure the long-term integrity of the repository (Quiquet et al., 2016).

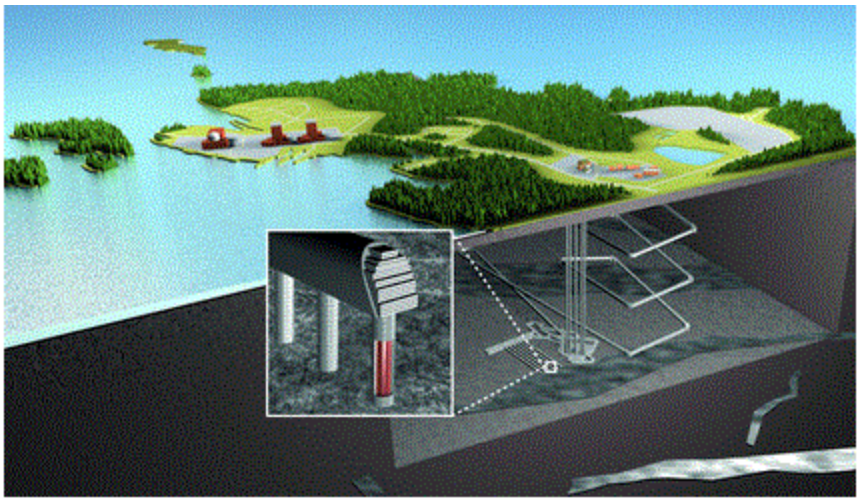

Figure 2.3: *Posiva* nuclear storage concept based on the KBS-3V design utilising metal, watertight canisters surrounded by swelling clay in vertical emplacement tunnels housed in a crystalline host rock (*Hellä*, 2016)

2.3.4: French nuclear storage (Andra):

Andra has conducted research at the French national Underground Rock Laboratory for over 20 years, as well as at the Äspö Hard Rock Laboratory. According to publications from Andra since 2005 argillaceous clay is the most likely host rock to be utilised for HLW storage in France. The current design concept uses unalloyed steel canisters to encase the waste packages which are then stored horizontally in deposition tunnels with a canister containment period of at least 10,000 years (Andra, 2005). In likeness to the NAGRA concept, this design utilises not only the bentonite to act as a barrier but relies heavily on the host rock to slow down the migration of radionuclides to the external environment.

2.3.5 USA nuclear storage (NRC)

The US currently has 4 active near-ground repositories which have been receiving LLW for over 20 years including the WIPP (Waste Isolation Pilot Plant) in New Mexico. There were plans in place for a deep geological repository to permanently house HLW in the Yucca Mountain, Nevada. Nuclear waste disposal is currently managed by the US Nuclear Regulatory Commission

(NRC, 2017). However, the project has met with challenges that suggest the site may no longer be used. There are currently no alternatives sites for the long-term storage of waste in the US, and so plans for the Yucca Mountain site are described below to demonstrate the varied approaches taken by different countries in keeping with different local geological challenges.

Measurements taken at the Äspö Hard Rock Laboratory in Sweden and boreholes in Finland, as well as in Switzerland, suggest that the groundwater at a 500m depth is of very low salinity (Posiva, 2000; SKB, 2006) (table 2.2). However, in North America the groundwater close to the Yucca site has a much higher salinity (up to 5 M) (Kang & Jackson, 2016) which could drastically increase the rate of corrosion of the steel canisters. Therefore, the disposal strategy differs slightly to the European models (figure 2.4).

Table 2.2: Groundwater composition from several sites relevant to nuclear waste repositories. All measurements shown in mol/L unless otherwise stated. (After Sheppard et al., 1995; Bath et al., 2006; Auqué et al., 2006)

	FORSMARK (SWEDEN)	**ASPO (SWEDEN)**	**GRIMSEL (SWITZERLAND)**	**UK**	**CANADA**
pH	7.2	7.7	9.6	7.1-9	7.1-7.7
Na	0.089	0.091	0.00069	0.0078	0.053
Ca	0.023	0.047	0.00014	0.00033	0.031
Mg	0.0093	0.0017	0.0000006	0.000087	0.001
K	0.0009	0.0002	0.000005	0.00013	0.00022
Fe	0.000033	0.000004	3x10-9	-	-
HCO_3^-	0.0022	0.00016	0.00045	0.0046	0.0012

Cl^-	0.153	0.181	0.00016	0.005	0.107
SO_4^{2-}	0.0052	0.0058	0.00006	0.00025	0.006
Hs^-	0	0.000005	0	-	-
O2 fugacity (bar)	<10-20	<10-20	<1	-	-
Ionic strength (M)	0.19	0.24	0.0013	-	-
TDS (g/L)	9.32	11.1	0.08	0.561	0.553
Notes	Borehole, 512 m depth	Repository depth	Intercalated Glacial waters	572m depth, sandstone	deep rock (<300m)

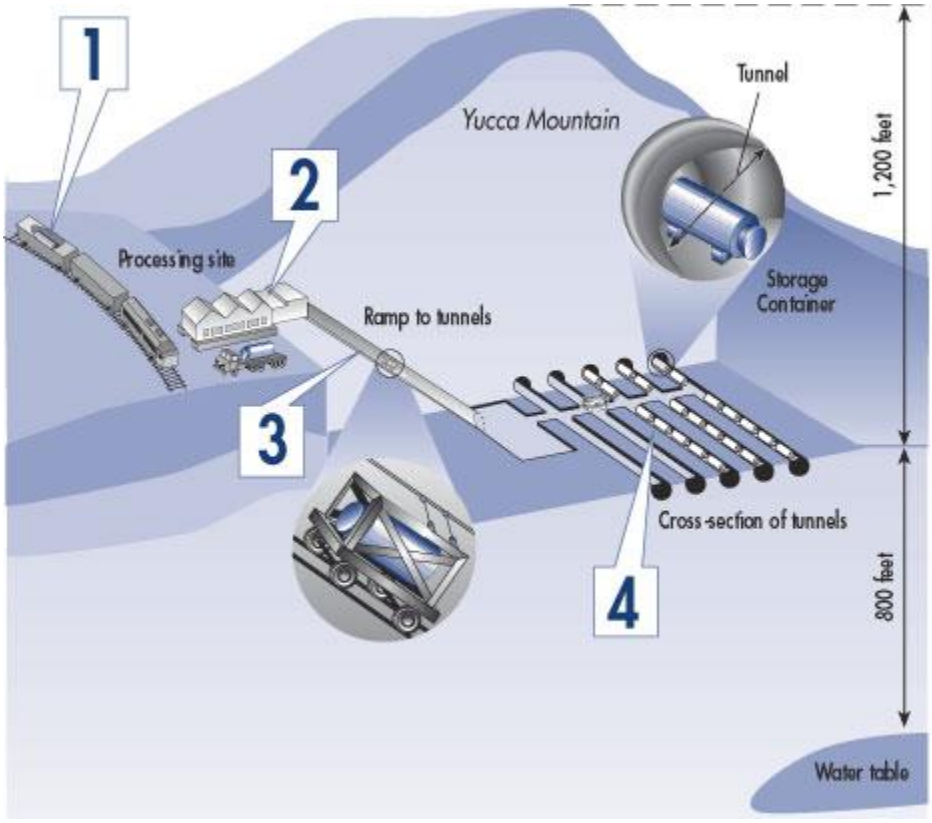

1. Canisters of waste, sealed in special casks, are shipped to the site by truck or train.
2. Shipping casks are removed, and the inner tubes with the waste are placed in steel, multi-layered storage containers.
3. An automated system sends storage containers underground to the tunnels.
4. Containers are stored along the tunnels, on their sides.

Figure 2.4: USA HLW repository design, NRC 2018

The US repository will sit 365 m (1200 ft) below the highest point of Yucca Mountain, above the water table, making the repository a largely dry environment (NRC, 2018) which acts to prevent increased corrosion from highly saline groundwaters. Several large eruptions from a caldera volcano contributed to the composition and formation of Yucca Mountain (World Nuclear Association, 2018). The resulting geology consists of alternating layers of ignimbrite (welded tuff), non-welded tuff, and semi-welded tuff. This composition is expected to be an important

component of the barrier system as it physically inhibits the movement of radionuclides (US department of Energy, 2002). A significant difference in the US design compared to those described previously is the lack of a backfill or buffer. Instead, air will be able to circulate and the double cased waste containers and host rock will be the only barrier. The entrances to the repository will be protected by titanium shields which will act as a water lock to prevent water entering the repository (US department of Energy, 2002).

2.3.6 Canada nuclear storage (NWMO)

In Canada, the Nuclear Waste Management Organisation (NWMO) and the Canadian Nuclear Safety Commission (CNSC) are responsible for finding a long-term storage solution for HLW and SF. As with other countries deep geological disposal is the favoured method with designs currently being devised (CNSC, 2006; NWMO, 2016). As with the US, groundwater in Canada has a much higher salinity (table 2.2) (Department of Environment and Climate Change, 2013) than those in Europe and so the design must reflect that (figure 2.5). The high salinity of deep groundwaters in North America is attributed to sea intrusions and is reflected in the high abundance of salt lakes (Last & Ginn, 2005; Barlow & Reichard, 2010).

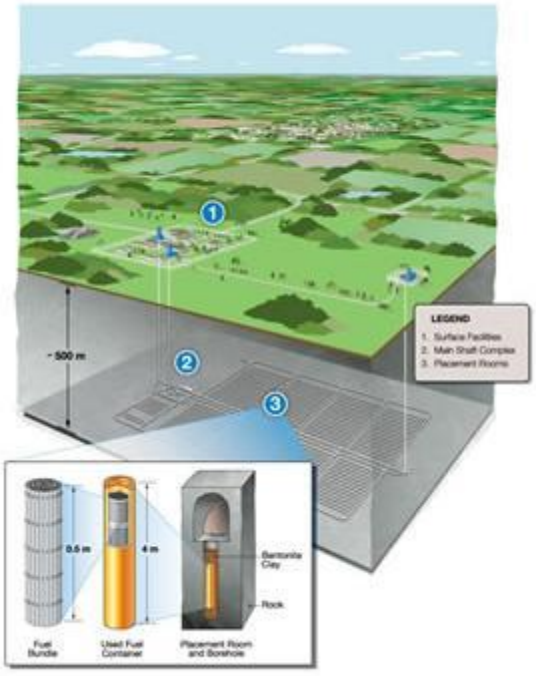

Figure 2.5: Canada conceptual design of nuclear repository, NWMO

The exact location of the repository has not been determined but it is likely to have a crystalline or sedimentary host rock. SF bundles will be encased in steel for structural strength and then clad in 3 mm thick copper to improve corrosion resistance. The buffer will be compacted bentonite and the backfill will be a mix of concrete and bentonite clay (NWMO, 2016).

2.3.7 Russian nuclear storage concept (NO ROA)

Russia has recently opened its first repository for LLW and ILW and is now focussing on finalising the design for a deep geological repository for HLW. The design is very similar to the KBS-3 design; however, steel will replace copper as the waste canister material. The host rock is also granitic, as is the SKB model but the location of the repository is in Yeniseisky, which is a site of high tectonic activity. As such multiple concerns have been raised relating to earthquakes which could increase the possibility of repository failure (Laverov et al., 2016).

The waste in Russia differs from elsewhere as it is the only country which generates HLW in the form of phosphate glass instead of borosilicate (Laverov et al., 2016). This variance leads to different rates of dissolution of the waste package. It is possible that this design may cause an increased rate of transformation of radionuclides to the aqueous phase and so further study is currently being undertaken to assess this risk (Laverov et al., 2016).

2.3.8 South Korea nuclear storage concept (KORAD)

South Korea has already begun construction on a nuclear repository for LLW and ILW and is looking towards a deep geological repository for direct disposal of HLW. Experiments are currently being carried out and a public engagement campaign is underway. However, currently all waste is in interim storage is managed under a “wait and see” policy (KORAD, 2018).

2.4 Host rock types

Evaporite deposits, or salt rocks, have a very low moisture content and are considered self-sealing – both these characteristics suggest this rock type would be favourable for waste repositories. Additionally, this rock type is the most suited to thermal conduction, which is favourable in the repository as it will allow heat to diffuse away from the canister surface. However, only a minority of countries are considering exploiting this rock type in their

designs, including USA and Germany. Salt rocks are also present in the UK. The nature of salt rocks has been shown to be less suitable for repositories due to increased risk of dissolution. There are large variations between salt deposits which greatly affect the permeability and stability, meaning that only some would be suitable for nuclear waste repositories. Furthermore, salt-groundwater interactions are not favourable in the repository environment, as it could disrupt the integrity of the host rock and / or cause migration of highly saline water to the canister surface resulting in an increased rate of corrosion. Although salt deposits are usually dry environments, many repository designs rely on groundwater to induce the swelling of the clay buffer.

Argillaceous rock encompasses a wide range of sedimentary deposits including clays, shale and mudstones. Notably, the mineralogy of argillaceous rocks can alter groundwater geochemistry, and this could interfere with repositories, either by causing interactions with bentonite or corrosion of the canister i.e., via sulfides. However, argillaceous rocks are naturally of very low permeability so the possibility of large volumes groundwater entering the repository is less likely than with other rock types. However, due to the stiffness of this rock type, it is likely that stress fractures will be present or occur during construction as a result of stress relief, or over time due to changes in expansion and contraction caused by the waste package heating and cooling. These fractures could allow contaminants such as microbes, or aggressive minerals carried in groundwater, to enter the repository and have adverse effects on the multi-barrier system (Hagdu et al., 2017).

Igneous rocks are globally widespread and favoured by several countries for nuclear waste repositories. Specifically, crystalline granitic rock which is primarily comprised of quartz, feldspars and micas (Hedin et al., 2016). The conductivity of this rock type has also been tested and deemed suitable for repositories due to the high silica content (Roxburgh, 1987) – it is important that the host rock is able to conduct heat away from the canister into the biosphere so heat does not build within the repository. This rock type is considered strong enough not to require additional supports, a property which would be advantageous for repositories, especially during construction. Conversely, a concern has also been raised over the possibility of radionuclides

migrating out of the repository through fractures in the rock face of this type; however, if the rock face were > 350 m thick (as is the case for most countries considering granitic rock) (Hedin et al., 2016) it is likely that radionuclides would decay to safe levels as they diffuse through the rock face and thus pose a reduced threat (Roxburgh, 1987). Another point which makes this rock type favourable is the knowledge accumulated through the mining industry. Throughout the World granitic rock has been explored to recover precious metals and as such there is significant knowledge collected in reference to engineering structures to build and reinforce tunnels in this rock type.

2.5 Disposal strategy overview for UK

The Swedish KBS-3 nuclear waste repository design has shaped nuclear waste storage concepts across the world including the current working model for the UK. The UK nuclear waste program is currently managed by the RWM (Radioactive Waste Management, a subsidiary of NDA).

In the UK, the host rock has not yet been chosen, and the diverse geology of the UK means that the options are not limited. One possibility is clay (argillaceous rocks) or a granitic crystalline rock. Part of this decision may depend on which local community agrees to host the waste. The UK is using a strategy reliant on effective public engagement to source a suitable location for the repository in which a council or local area will volunteer to host the nuclear waste (RWM, 2020). It works by publicising the prospect of generation of a number of jobs in the local area and the safety measures which will be put in place to ensure secure and safe storage. Several surveys will be carried out to ensure the site is suitable for nuclear storage (figure 2.6). One council, Cumbria, had indicated interest and initial non-invasive evaluations were carried out, using only above ground exploration and pre-existing surveys. During this time, more public engagement activities were carried out to ensure public support for the repository was present in the local area. However, following four years of involvement, and significant investment from the government of over £3million, the local authorities pulled out of the selection process (RWM, 2020). At the time of writing, two more sites are being considered for the repository – Hartlepool and Theddlethorpe, however, both are in the early stages of the site selection process. Therefore, as yet, no sites have been determined for the location of the repositories and so most studies

carried out for the NDA have used data from the most closely related system (KBS-V3) to demonstrate likely outcomes and scenarios. This data includes values pertaining to the rock-buffer-canister interfaces (e.g., swelling pressure, density, heat conduction); however, these will vary slightly between locations. Also important is the groundwater movements and composition at the location selected, as these could cause leakage of radionuclides; influx of ions or microbes; or interfere with bentonite structure (Bath et al., 2006). As seen in table 2.2 the pH of groundwater varies in the UK, and so it is important to fully analyse the local groundwater at appropriate depths at any proposed site.

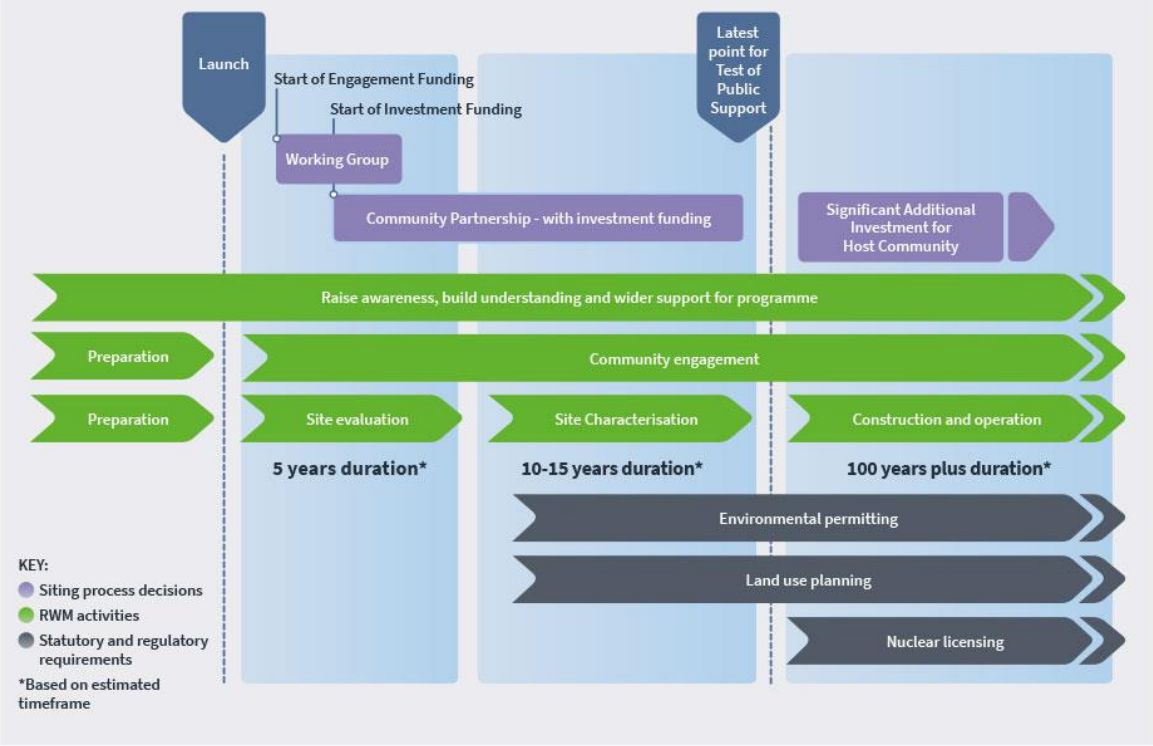

Figure 2.6: Timeline of stages involved in UK site-selection for nuclear waste repository (RWM, 2020)

2.5.1 Canister and storage strategy

In the current model adopted by the UK, vitrified waste will likely be encased in a borosilicate glass matrix within a steel canister (NDA, 2010) (figure 1.1). The container may be stainless steel, or carbon steel, and may have a copper or lead cladding (NDA, 2017). The current design uses

vertical emplacement of the canisters and does not allow for recovery of the canisters following repository closure (NDA, 2010).

2.6 MX80 Bentonite mineralogy and geomechanical properties

In almost all designs across the OECD-NEA bentonite clay plays a key role in the multi barrier containment concept. As such, this material has been extensively studied for this use (Karnland, 1998; Carlson, 2004; Gaudin et al., 2009; Milodowski et al., 2009; Wilson et al., 2010; Kiviranta & Kumpulainen, 2011; Muurinen et al., 2013; Keller et al., 2014; Savage, 2012). Although there are a variety of bentonite clays, Na-rich bentonite is widely accepted as the most suitable due to its high swelling ability and low hydraulic conductivity (Lee, 2012).

Bentonites are highly plastic montmorillonite clays. The mineral montmorillonite is a subclass of smectite and is made up of tetrahedral and octahedral sheets – T-O-T (figure 2.7). An aluminium sits centrally in the octahedral sheet, which can be replaced with magnesium primarily, or iron. Silicon is the central atom of the tetrahedral sheets and can be replaced with aluminium. The overall surface charge of the clay is always negative, but substitution of the silicon or aluminium ions can change the charge of the clay to be more or less negative. This change in charge must be balanced by cations in the interlayer space. When the clay swells, water will flow into the interlayer space and cause the distance between layers to increase (Newman and Brown, 1987), this swelling is an important property for the repository. However, loss of silicon due to substitution or clay dissolution could have a significant impact on the geomechanical properties of the clay.

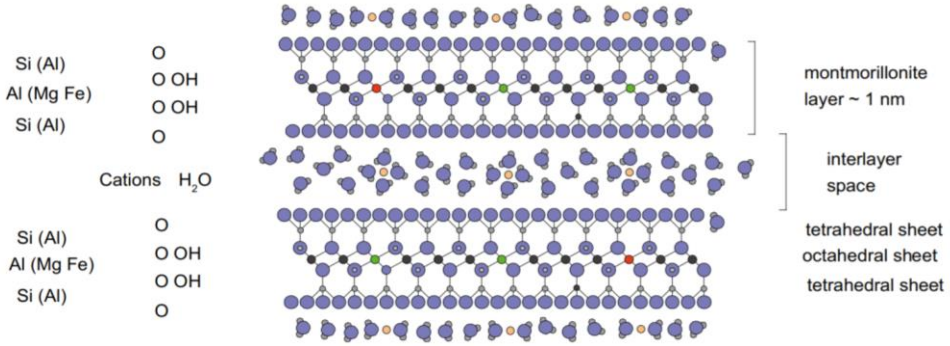

Figure 2.7: Edge view of montmorillonite layers based on description by Newman and Brown 1987 (SKB 2010)

Spain has selected FEBEX bentonite clay (table 2.3) to use as a buffer in that country's repository concept (Villar, 2015). Whereas, the UK and Sweden have selected Wyoming MX80 bentonite. A Full-scale Engineered Barrier EXperiment (FEBEX), at the Grimsel Test Site in the Swiss Alps was set up in 1997, to mimic the Spanish repository concept (Grimsel Test Site). Three steel canisters were inserted into the host rock and filled with FEBEX bentonite, the tunnel was then sealed with concrete and a total of 632 sensors were used to monitor the site. This experiment is the longest running of its kind. The canisters were heated to, and maintained at a temperature of 100°C. Two of the three canisters were recovered after 15 years and will be analysed to determine the feasibility of SF disposal according to the current design; to inform models of the geomechanical changes to the bentonite and to analyse samples to investigate their microbial populations and distributions. The third canister will be recovered in the future for further testing.

Shorter term experiments have aimed to compare FEBEX bentonite and Wyoming MX80 bentonite. It was found that MX80 bentonite has a higher swelling pressure and a slightly higher hydraulic conductivity (Villar, 2005). There are therefore pros and cons to using each clay. The high swelling pressure is advantageous because it will seal all the gaps between the canister and the host rock and it is predicted that pressures of 2 MPa and higher will eliminate all microbial activity (SKB, 2010) and therefore remove microbes as a risk to the integrity of the repository. However, the lower conductivity of FEBEX is potentially advantageous in a repository setting because it will decrease groundwater inflow from the host rock and limit the movement of any radionuclides.

Another advantage of MX80 bentonite is that it has a low concentration of soluble minerals compared to other Na-rich bentonites such as Ibeco-RWC (Karnland et al., 2010). Na-rich indicates that sodium is the dominating cation in the interlayer space. By having a low concentration of other soluble minerals, MX80 bentonite will have a higher degree of homogeneity and will be more stable in terms of density and permeability. Table 2.3 shows the mineral composition of MX80 bentonite. Due to the mineralogy of bentonite, particularly the

concentration of quartz, it is hoped that the thermal conductivity will be high enough to ensure the heat generated from the SF will dissipate. Therefore, the UK, like Sweden and many other countries globally, has selected MX80 bentonite as the buffer and backfill in its nuclear repository design.

One concern with bentonite clays, and smectite clays in general, is the risk of illitisation. This process involves alteration of the clay matrix from montmorillonite to illite through substitution of aluminium for silicon in the tetrahedral sheets, leading to silica release, and uptake of potassium in the interlayers. The result is that swelling montmorillonite clay has become non-swelling illite clay, which would be hugely disadvantageous for the repository as the clay would not be able to adjust to changes in moisture content due to temperature and groundwater changes and would be more prone to cracking.

The process of illitisation requires time, which is not limited in terms of the repository lifespan, but also requires substantial volumes of K^+. At the Äspö Hard Rock Laboratory, it was estimated that for all the bentonite in one deposition hole to undergo illitisation, all the potassium in the surrounding $9m^3$ of host rock would have to be utilised (Wilson et al., 2011). This calculation obviously does not account for potassium carried in the groundwater but does suggest that during site evaluations potassium content in host rocks and concentration in groundwater should be considered. Additionally, microbes have been implicated in illitisation, both as catalysts for the release of silica (Kim, 2012), and also by introducing potassium to the pore waters of the clay by releasing potassium from their cells as they move from saline groundwaters or seawater, to less saline waters within the clay (Aubineau et al., 2019). Therefore, groundwater salinity should also be considered when assessing potential repository sites, not only because of the risk of increased corrosion, but also because of the risk of increased K^+ release from bacteria leading to illitisation.

Table 2.3: Mineralogical composition of MX80 Bentonite and bulk composition of FEBEX (NAGRA, after Müller-*Vonmoos & Kahr*, 1983; Semenkova et al., 2018)

MINERALOGY	MX80 (%WT.)	FEBEX (%WT.)
SMECTITE	75	86.6
CALCITE	0.7	2
SIDERITE	0.7	-
QUARTZ	15.2	1.9
PYRITE	0.3	-
FELDSPAR	5.8	8.5
MICA	<1	-
KAOLINITE	<1	-
ORGANIC CARBON	0.4	-
NACL	0.007	-
$CASO_4$	0.34	-
KCL	-	0.8

Another important feature of the clay buffer is that it will not shrink away from the canister or the host rock on drying (Shariatmadari & Saeidijam, 2012). This swelling also ensures that the canisters will be supported and will not sink into the clay (Pedersen & Karlsson, 1995; Bradbury et al., 2014). The swelling and hydraulic properties of the clay are related to the montmorillonite content (SKB, 2010). For use in the repositories, it will be compacted into blocks with a dry density of 1.25 Mg/m^3 (Pusch & Kasbohm, 2002) prior to being installed.

Furthermore, bentonite in this environment is somewhat anti-microbial, which is largely due to the swelling pressure and low porosity. The pore spaces in swollen MX80 bentonite are 0.02 µm (Rättö & Itävaara, 2012) which is 100x times smaller than the average bacteria. Therefore,

bacteria will not be able to freely move around the buffer, and therefore, may not be able to access groundwater or nutrients. This limited pore size is also important to limit the movement of radionuclides to the external environment. Although larger than some ions, radionuclides may also be able to move through pore spaces at a slower rate (West et al., 2002).

However, MX80 bentonite also contains 0.19-0.4% organic carbon, which is sufficient to support microbial metabolism during the initial stages of closure, after which time it is thought that carbon availability will not be a limiting factor to microbial proliferation (Pedrial et al., 2009) due to other carbon sources such as carbon from groundwater, products of fermenting bacteria or carbon fixation from inorganic sources. In fact, some soil fungal species can survive on silica gel with no additional carbon source (Parkinson et al., 1989) and so low carbon is not a factor contributing to microbial death for many species. There is also, although not thought to be highly bioavailable, a source of iron, magnesium, potassium and phosphorus in bentonite. The elemental composition of MX80 bentonite is presented in table 2.4. Microbes pose a threat to the integrity of the canisters as they may release metabolic acids that could interact with the metal ions or minerals present in the clay, thus disrupting the reducing environment within the canister and changing the porosity.

Table 2.4: chemical composition of Wyoming MX80 bentonite, as an average across samples taken from different locations at different time points (SKB, 2010)

CHEMICAL	**% WT.**
SILICON DIOXIDE	67.4
ALUMINIUM OXIDE	21.2
IRON(III) OXIDE	4.14
MAGNESIUM OXIDE	2.61
CALCIUM OXIDE	1.46

SODIUM OXIDE	2.25
POTASSIUM OXIDE	0.55
TITANIUM DIOXIDE	0.17
PHOSPHORUS PENTOXIDE	0.05
CARBON	0.36
SULFUR	0.34

Mined repositories may need to be reinforced with additional structures such as a low-pH concrete liner. This type of liner might be used during construction but will not provide any long-term function. However, it is possible that the cement-clay interface will be the site of sharp gradients in pH and CO_2 generation, which could ultimately lead to precipitation of carbonates and hydroxides (Birkle et al., 2010), and a decrease in the porosity of bentonite. In fact, some predictions suggest that the exchange of Na^+ and K^+ between concrete and bentonite will lead to reduced swelling in the bentonite, and therefore, it is more desirable to utilise a rock type and location in which no extra support is needed during construction, which is the approached adopted by the UK.

2.7 Stages of repository lifespan

Multiple predictions have been made about the temperature of the internal environment of the repository. NAGRA (Swiss) predict temperatures of up to 150°C, but the NDA (UK) currently predict the temperature of the canister surface will not exceed 100°C (figure 2.8).

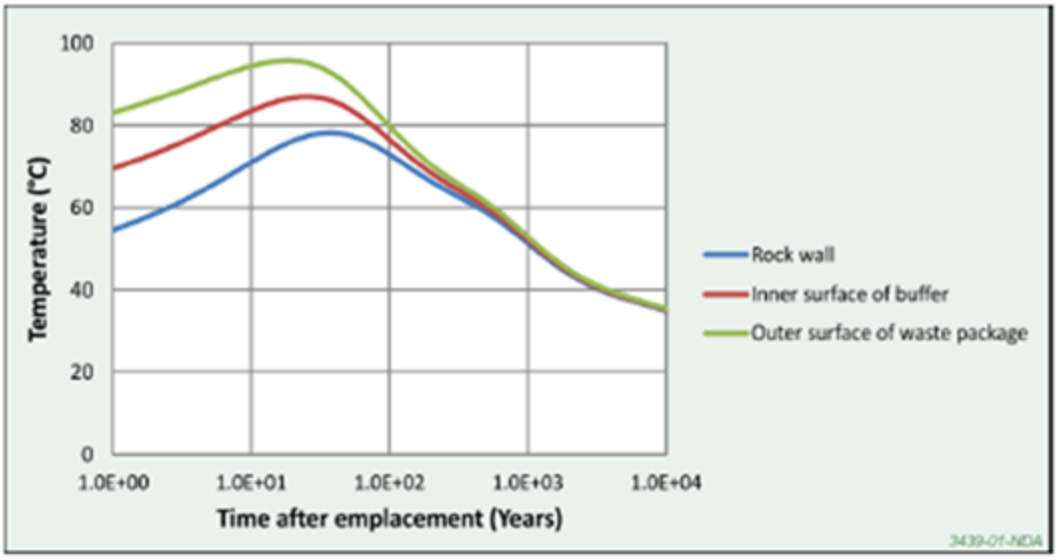

Figure 2.8: the typical temperature evolution predicted for a waste package in a deep geological repository (RWM, 2016)

During phase 1 the construction and installation of the canisters will likely increase the oxygen levels in the area, as well as the oxygen present in the bentonite, so the initial environment will be aerobic, which is not ideal as the metal canisters can begin to corrode. The level of oxygen is likely to decrease due to its reduction within the repository (Arlinger et al., 2013). These reduction reactions are linked to the corrosion of the canister and in some cases corrosion of steel mesh used to support tunnels (Landolt et al., 2009); however, there is some disagreement over whether the environment will become completely anaerobic as it is likely that oxygen will be continuously introduced by groundwater inflows. This oxygen ingress could allow bacteria to respire aerobically (Merkel & Planer-Freidrich, 2008), but nonetheless, the environment will most likely be described as micro aerobic. In the initial phase-(the first 20-30 years) the temperature is estimated to reach 50-80°C (with a maximum of 90°C (Keith-Roach & Livens, 2002)) - and thus, in addition to removal of oxygen, the water content will be reduced to less than 5% (Keith-Roach & Livens, 2002; Landolt et al., 2009). Additionally, there is some concern over whether high temperatures will accelerate abiotic reactions resulting in increased corrosion by sulfur containing compounds liberated from minerals within the bentonite (NAGRA, after Müller-Vonmoos & Kahr, 1983). Such reactions will produce iron sulfide at variable rates

throughout the full duration of the storage. The bentonite will also experience some changes; the porosity will decrease as the temperature increases and the water content drops.

The preceding paragraph describes the changes that will occur initially. Phase 2 is defined as the period of cooling, in which groundwater begins to re-saturate the bentonite. This phase is predicted to last 20-30 years (Landolt et al., 2009). However, if groundwater has a high concentration of NaCl, the non-expanding mineral sodium illite (brammallite) may be produced from the montmorillonite (Pusch & Kasbohm, 2002) through illitisation. This mineralogical change would have negative effects on the buffer because it would decrease the ability of the clay to swell and increase the risk of cracking. The associated pore size at this stage is 0.02 μm. In this phase the swelling reaches a pressure of 7-8 MPa (Rättö et al., 2012).

By phase 3, it is envisaged that all oxidation reactions will have ceased, and the environment will be truly anaerobic, signalling that the interior environment is now reducing. This phase is predicted to last for approximately 50 years. These timescales are in-keeping with other predictions which estimate a reducing state to start around 100 years after the repository is sealed (Landolt et al., 2009). During this time, the moisture content across the buffer will equilibrate and thus the swelling pressure will be uniform. The uniformity of water distribution may cause increased migration of ions, compounds or microbes across the buffer to and from the canister surface. As time proceeds, the liquid limit of the bentonite decreases in correlation with the Na/Ca ratio. The liquid limit is a component part of clay plasticity and indicates an upper moisture content limit. For the repository, a high liquid limit is favourable to ensure clay does not lose its structure during periods of high groundwater inflow. During clay swelling and increasing moisture content, the Na^+ cation in the clay has a larger radius as it is surrounded by water rather than Ca^+ (Liu, 2010). Therefore, a high Na^+ cation concentration will result in a higher liquid limit.

During phase 4, corrosion of the carbon steel canister will have started and at this stage the only oxidant available is water. Therefore, corrosion during this stage will produce hydrogen gas through reduction of water and oxidation of iron (Landolt et al., 2009). MIC is also a concern at this stage. If sulphide is present in the groundwater, large amounts of hydrogen sulfide (produced by SRBs) can be produced which contributes to the corrosion of the

canister and the production of hydrogen gas (figure 2.9) which can diffuse slowly through the buffer and increase internal pressure. The overall reaction for this type of MIC is shown below (equation 1) (Enning & Garrelfs, 2014). SRBs are discussed further in section 2.8.4.

$Fe + H_2S \rightarrow FeS + H_2$ [1]

Initially the environment will be around neutral pH, but it is thought that this will slowly increase and become more alkaline after closure due to deprotonation of water in corrosion processes (Williamson et al., 2013). The elevated pH of the environment will cause corrosion to increase, and it is likely that Fe cations will migrate through the bentonite and interact with minerals or small molecules or ions to form compounds (Leupin et al., 2017). This phase is due to last at least 1000 years and up to and even over 10,000 years.

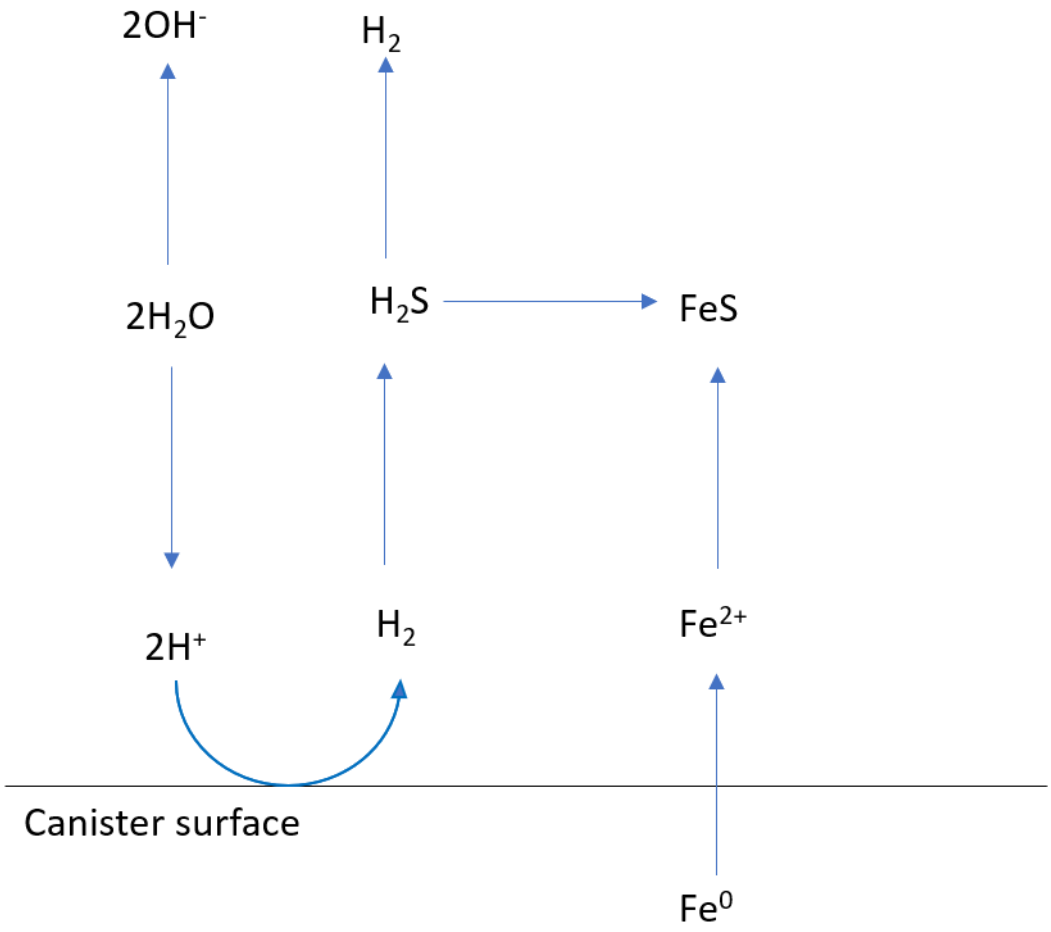

Figure 2.9: Reaction at the canister-bentonite interface causing corrosion of carbon steel and production of hydrogen gas, occurring in deep geological nuclear waste storage under a hypothetical sulphate reducing system.

Phase 4 will be the last phase, only followed by canister breeching and subsequent migration of radionuclides into the buffer and host rock. It is predicted that canisters will fail 1000 years after sealing the repository (Landolt et al., 2009). The temperatures having been cooling since phase 2 it is thought they will have reached 35-50°C.

2.8 Microbes in the repository environment

Microbes have been implicated as a potential problem for the long-term sustainability of HLW canisters. Multiple microbial species have been isolated from raw and commercially homogenised and compacted bentonite, and groundwater samples from Sweden (Arlinger et al., 2013), Spain (López-Fernández et al., 2014), Finland and the Czech Republic. Concerns have been raised over the possibility of MIC and changes to clay properties due to microbial presence in repositories, as well as impacts on gas production and consumption and interactions with radionuclides (Leupin et al., 2017). Microbial presence alone is not thought to be an important threat, but, for instance, the production of metabolites such as organic acids and sulfides is being evaluated. Organic acids and other metabolic products can interact with metals, and minerals through H^+ ions (Konhauser, 2007; Reitner & Thiel, 2011), and this could disrupt the reducing environment (Rättö & Itävaara, 2012) and thus cause negative effects to the integrity of the bentonite and possibly cause accelerated corrosion of the waste canister. However, there are some possible advantages of bacterial presence, as there are some aerobic bacteria present which will thus respire oxygen causing an acceleration to an anaerobic environment, which would be beneficial as high concentrations of oxygen would increase canister corrosion.

Whilst there is evidence of microbial presence in the clay, host rock and groundwater (Lopez-fernandez et al., 2014; Masurat et al., 2010), there are, however, several factors that will limit microbial proliferation including low water content, high pressure, low carbon availability and a lack of physical space (pore sizes). The internal environment of the repository is highly pressurised, and the compaction and swelling of bentonite greatly limits the oxygen availability.

This, combined with high temperatures, which will cause water evaporation (liquid water is essential for all forms of biological life), suggests that the environment is somewhat inhospitable to microbes (Wilson et al., 2010). However, these factors are largely transient or subject to changes by microbial activity and so the possible effects of microbes must be investigated.

2.8.1 Factors limiting microbial survival in repository environments

Studies have shown that a water activity (aw) of 0.96 is too low for microbial liFe(Motamedi et al., 1996) which is a similar water content to the repository during high temperatures. This value is of high relevance to the US concept which by design is likely to remain a very dry environment throughout the repository lifespan (US department of Energy, 2002). Further to this, the swelling and compaction greatly lower the porosity of the clay, to a size thought to be smaller than the average bacteria (Chi Fru & Athar, 2008), 0.02 μm, therefore limiting the movement of microbes through the buffer (Sellin & Leupin, 2013; Rättö & Itävaara, 2012; Kieft, 2000). However, this swelling must be somewhat limited to avoid damage to the host rock and canister (Sellin Leupin, 2013).

It has been recorded that as density or swelling of bentonite increases, bacterial activity within the bentonite decreases (Masurat et al., 2010). This study also predicted that compaction of 1.6 g/cm^3 is sufficient to inhibit bacteria within the bentonite to a point where the rate of microbial activity is below that needed to corrode through the copper or steel capsule in under 10,000 years (Masurat et al., 2010). This finding is in keeping with data which shows that prokaryotic cells can withstand turgor pressures up to 2.02 MPa but survive at lowered activity (Masurat et al, 2010). This pressure threshold is much lower than the pressures predicted to develop within the canister buffer (Rättö & Itävaara, 2012) but does suggest that pressure may not be the main limiting factor to microbial survival.

Several microbes have an optimum temperature of 30°C (+/- 10), and so the temperature alone limits how many bacteria will be able to thrive during the hottest periods of the repository lifespan when the canister surface is around 100°C and the host rock / clay interface is around 70°C (RWM, 2016); however, this is well below the temperature limit for microbial life - 121°C (Kashefi & Lovley, 2003). It is thought that during the initial phases of the repository, the

temperatures around the canister will be so high that microbes will not be able to survive in the desiccated buffer, which would penetrate tens of centimetres into the bentonite (West et al., 2002). However, during the latter stages, as the repository cools, the lowest expected temperature is 40°C which will be maintained for most of the post-closure period and may allow for some microbial life. Experiments investigating microbial activity in clays at this temperature are currently limited, with most research considering survival at higher temperatures.

Furthermore, there is a concern that the high temperatures within the canister may cause a moisture cycle (figure 2.10) which could influence the bacteria to move to the canister-bentonite interface, where they could cause most damage by corrosion (Salas et al., 2014). In this case, corrosion of a copper canister was predicted to occur at a rate of 2 mm to 25 mm over 100,000 years, depending on substrate availability (Liu et al., 2006), which may be an issue for designs using 5 cm thick copper canisters such as SKB, KBS-3 design. No similar predictions have yet been made for carbon-steel canisters, but it can be predicted that the steel would corrode at a faster rate than copper.

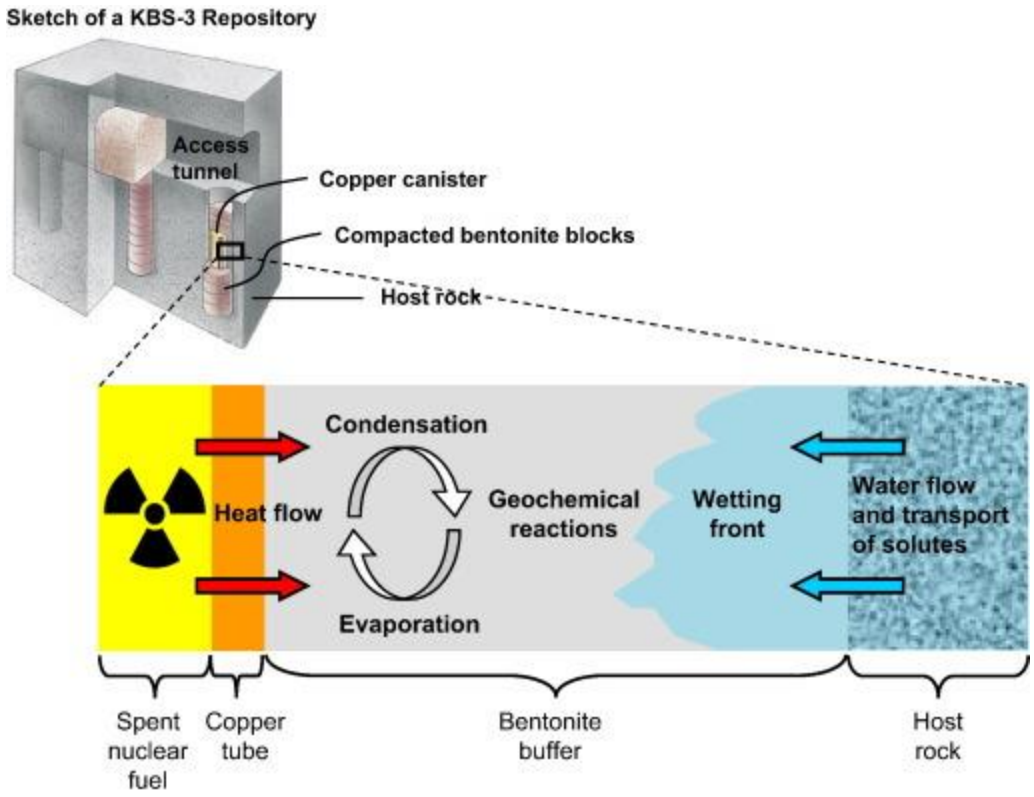

Figure 2.10: Condensation and evaporation cycle which may occur in clay buffer during repository closure (Salas et al., 2014)

A more obvious obstacle to microbial survival is the exposure to radiation. Several microbes have developed ways to adapt to exposure to ionizing radionuclides, such as increasing genome copy number; increasing rate of DNA and enzyme repair; and rearranging nucleoids (Reitner & Thiel, 2011). It is obvious that radiation will penetrate the buffer at some point during the repository lifespan. This radiation will also limit microbial life; however, some microbes have been known to recover from exposure of up to 15×10^3 Sv (Shukla et al., 2007). The ability of sediment bacteria to survive gamma radiation has been tested at continuous exposure to 30 Gy for 8 weeks, but these bacteria may be able to withstand higher doses (Brown et al., 2015). There is therefore a strong argument that radiation released from the canister will not destroy all microbial life but will become a strong selective pressure and shape the microbial community. The resulting community of radiation tolerant microbes would then be able to thrive with less competition for water, space and energy sources, however, the effect of the microbial community activity on radiation is not clear.

2.8.2 Opportunities for microbial survival in the repository environment

Despite the adverse conditions within the repository, the microbes present can increase the rate of reduction of Fe(III) (RWM, 2017) through direct or indirect mechanisms. Some thermophilic and piezophilic bacteria which exist within the bentonite could survive the high temperatures and pressures of the repository (Arlinger et al., 2013) and proliferate during the latter stages of closure. Interestingly, certain bacteria have higher survival rates in the repository environment than in the laboratory (Pedrial et al., 2009). Moreover, there are survival mechanisms which bacteria can employ to withstand inhospitable conditions until the environment becomes more favourable. For example, some bacteria (e.g., *Bacillus sp.*) can form spores which can remain dormant for hundreds of years. While these spores can recover from low water availability and temperatures above 50°C (Lindsay et al., 2006), only some species will produce spores that can survive up to 100°C as would be the situation at the canister surface.

As previously mentioned, reduced pore size is another obstacle to microbial activity, however, the pore size is not small enough to exclude the transport of any metabolite. Therefore, even if the bacteria are only able to survive in small pockets within the bentonite, there is still a method by which their secreted by-products can migrate across and through the buffer to the host rock and canister.

Other types of microbes may form biofilms or multi-species biofilms which may also aid the survival of bacteria. Biofilms are formed as a response to stress (e.g., low nutrient or water availability, high temperature, antibiotics) and can allow bacteria to share DNA, nutrients and information between one another. A biofilm also acts as a physical barrier between the bacteria and the external environment and has been very effective at withstanding external stresses such as antibiotic attacks (Bakar et al., 2018). Whilst biofilms are a survival mechanism, they are not as robust as spore formation (although they can occur at the same time) (Lindsay et al., 2006). It is also worth considering whether biofilm formation on the canister surface would create an extra barrier to corrosion and may aid in the multi-barrier design (Herrera & Videla, 2009).

Another possibility is that microbes could exist on the outer surface of the bentonite, at the bentonite/rock interface. This exploitation of the environment would be beneficial to microbes

due to greater groundwater availability and slightly lower temperatures, as well as the potential space which could exist either in fractures in the host rock (RWM, 2017a), or areas where the bentonite has not swelled efficiently to completely fill every gap. Additionally, voids within the buffer are thought to host large numbers of microbes, however, their movement is reduced by hydrogen bonding which fixes the microbes to clay gels thus inhibiting the breakdown of gel bonds (Wilson et al., 2010). Whole rock XRD revealed that pore spaces were increased or created by cell lyses and conversely, bacterial precipitates sealed other pore spaces. This is likely due to specific bacterial secretions. Additionally, microbial activity affected the overall swelling and pH of the bentonite (Pedrial et al., 2009), although the exact mechanism which caused these changes is not discussed.

2.8.3 General concerns about the impact of microbial activity in the repository

Whilst biofilm formation is a survival mechanism, there is a risk that biofilm formation prior to rising temperatures could speed up corrosion during phase 2 of repository closure in an uneven manner (West et al., 2002) because biofilms allow a microbial population to control how many metal ions or how much of a metal surface they are exposed to. Biofilms also protect the bacterial cells for years at a time by providing a physical barrier to the external environment and allowing easy nutrient exchange between individuals. Current assumptions and safeguards presume that the canister surface will corrode evenly (West et al., 2002), so the effects of uneven corrosion have not been addressed. Bacteria known to form biofilms (e.g., *Pseudomonas* and *Bacillus*) have been isolated from FEBEX bentonite samples in Spain (López-Fernández et al., 2014). Additionally, filamentous bacteria may cause micropitting on the surface of the clay, copper or steel which has the potential to cause changes in internal pressure, density and swelling. This type of microbial structure has been observed in some hydrothermal clay deposits, where a network of microtubules has been created by filamentous Fe(II)-oxidising bacteria (Konhauser, 2007). There is also a risk of illitisation by silicate solubilising bacteria.

One of the biggest concerns about microbial presence in the repository is the possibility of MIC. This risk is of most concern for the concepts that use steel canisters rather than copper as steel is likely to corrode at a faster rate (Cleary & Greene, 1967). Additionally, Cu^{2+} ions are highly toxic

to most bacteria (Dupont et al., 2011) and so MIC is of less concern in these designs. The main bacterial species known to increase corrosion are SRBs (Enning & Garrelfs, 2014). Though, steel canisters may also be attacked by iron-interacting bacteria (Valencia-Cantero & Peña-Cabriales, 2014).

Microbes will be favoured for utilising oxygen in the early stages of closure, as this will decrease the time taken for anaerobic conditions to be reached, and thus slow corrosion. Microbes may also utilise hydrogen produced during corrosion (Leupin et al., 2017; Hultquist et al., 2011; Arango & Schlegel, 1981; Williamson et al., 2013). However, a study by Stroes-Gascoyne (2002) found that gas consumption in an *in-situ* environment with bentonite did not increase with an increase in microbial presence. In fact, there was no significant differences to gas compositions between the starting composition and the composition after 6.5 years incubation with various concentrations of microbes (Stroes-Gascoyne et al., 2000). Therefore, the bacterial population may have been inactive, or the carbon sources in the bentonite may not have been bioavailable. Conversely, there are fears that microbes may produce other gases that could increase pressure within the repository, namely, H_2 and CO_2. There is also evidence to suggest that methane may be produced from the carbon dioxide and hydrogen (Stroes-Gascoyne & West, 1997). An increase in pressure in the clay barrier through gas production could be harmful as it could damage the host rock or canister (Sellin & Leupin, 2013). Although microbes will be present in the clay barrier, microbial gas production and consumption is thought to be greatest in the backfill (NDA, 2016). This is likely because the backfill will be cooler and have more space for microbial movement leading to increased microbial activity.

SRBs can promote corrosion of steel by promoting the depolarisation of its surface (Valencia-Cantero & Peña-Cabriales, 2014), through interactions with excreted compounds, namely, the by-products of metabolism. They are released to the extracellular environment and for this reason, the rate of corrosion is correlated to the rate of metabolism of the SRBs. In the case of nuclear waste canisters, these compounds have been observed to interact with copper ions to form copper sulfide, carbonates and rusts (Konhauser, 2007) and therefore could contribute to

the corrosion of the canister (Guan et al., 2016). However, the formation of FeS could also reduce corrosion by creating a protective coating (Kim & Gadd, 2008).

Additionally, iron-reducing bacteria (IRBs), which are most active at a neutral pH such as in the repository (Herrera & Videla, 2009), can increase corrosion and act on the iron rich minerals in bentonite, which could reduce the swelling pressure and compaction of the buffer (Pedrial et al., 2009). Reduction of Fe(III) present in the montmorillonite in the bentonite would result in a disadvantageous effect on the integrity of the buffer. Mass balance calculations suggested that if all the iron in the canister reacted with the bentonite, 10-30% of the montmorillonite would be converted to non-swelling Fe(II) (Wersin et al., 2008) caused by a change in lattice structure and dehydration.

A research question which is beginning to be explored is how bacteria associated with underground nuclear waste storage would interact with radionuclides in the unlikely event that a breach happened much earlier than expected. The presence of IRBs in groundwater at Sellafield suggests that the bacteria could be able to survive and can reduce uranium (U (VI) to U (IV)) (Newsome et al., 2014; Wilkins et al., 2010), although the exact mechanism is not discussed. However, this is only possible when bioavailable Fe(III) is present to encourage and select for Fe(III)-reducing bacteria. This would suggest a possible solution for microbially removing radionuclide contaminants from groundwater (Lovely, 1991) as U (IV) is insoluble and so would not be able to enter the aqueous phase, therefore, this bacterial activity would be advantageous in the repository environment as it would prevent radionuclides being able to contaminate the groundwater.

2.8.4 SRBs in the repository

SRBs have been found largely in methane and sulfide-rich areas, such as in the deep marine sediments and hot ocean currents. They belong mainly to the phylum firmicutes and proteobacteria and include spore-forming and nonsporulating species and can be facultative anaerobes, or obligate anaerobes. One commonality is that they are all able to reduce sulfate to produce hydrogen sulfide (Ehrlich & Newman, 2009).

Although bentonite clays contain some sulfur-containing minerals, the main source of sulfate is from groundwater. Therefore, MIC caused by SRBs is of most concern at sites where the local groundwater is sulfate rich, such as the Swedish site (table 2.2). Sulfur could also be released from dead biomass (RWM, 2017). SRBs can utilise this sulfate to form H_2S (Ehrlich & Newman, 2009) which is the main driver of MIC by SRBs, as it can oxidise iron in the steel producing H_2 (via reduction of H^+) and FeS (Enning, 2014). Members of this group include *Desulfotomaculum, Desulfosporosinus*, and *Thermoacetogenium*. Additionally, some SRBs can be described as piezophiles as they are able to tolerate high pressures (Rättö & Itävaara, 2012) and some (*Desulfosporosinus* sp.) have an optimum temperature of up to 65°C (Rosnes et al., 1991).

SRBs were identified by 16S rRNA gene sequencing of microbial samples from bentonite (Masurat et al., 2010; López-Fernández et al., 2014) and groundwater from the Swedish site at a variety of depths between 65-586m (Kotelnikova and Pedersen, 1998; Haveman & Pedersen, 2002; Masurat et al., 2010). Further experiments found that increased density and swelling of clay, respectively, decreased sulfide production (Masurat et al., 2010). Through community fingerprint analysis via denaturing gel electrophoresis (DGGE) differences were found between SRB communities in bentonite and communities in the groundwater (Chi Fru & Athar, 2008), therefore indicating that these environments can provide a stable habitat for a variety of SRBs. However, groundwater SRBs may not be suited to conditions within the buffer. Some species, *Sedimentibacter* and *Desulfosporosinus*, can survive in both environments (Chi Fru & Athar, 2008).

Most SRBs do not survive the extremely high temperatures and there are no reports of SRB activity above 100°C+, but several viable spores (Liu et al., 2006; Rosnes et al., 1991) have been recovered from elevated temperatures that could then produce fully functioning SRBs (Feofilova et al., 2012). The maximum temperature in which sulfur reduction has been recorded is 80°C (Hölting & Coldewey, 2019), which is within the range of the initial phase of the repository and the highest predicted temperature of the outer surface of the bentonite. Philip et al. (1991), have shown that while water availability (and the salinity of the groundwater) dictates the survival of microbial life, the limiting step of SRBs proliferation in a repository setting is the availability of

sulfate, hydrogen or organics such as acetate or lactate, which must be present for the microorganisms to anaerobically metabolise. The concentrations of sulfate in groundwater vary depending on location, but it is generally seen to be high enough to support microbial liFe(Pedersen, 2012; Kotelnikova & Pedersen, 1998). However, over the period of 100,000 years, the landscape is forecasted to be subject to several conditions that have unknown effects on the concentration of sulfate and methane concentrations.

A theory to explain the survival of SRBs at such high temperatures (such as 120°C for 15 h) which has not been fully investigated, is that the cells are desiccated. This is the process by which bacterial or microbial cells have been dried out and are able to survive in this state until they are rehydrated (Reitner & Thiel, 2011). In the canister environment, the water content is predicted to decrease to ~5% in the bentonite buffer and a study in which SRBs were able to survive 120°C began with an environment of ~10% water in bentonite (O'Sullivan et al., 2015). This theory could explain why sulfide production by SRBs is observed even after extreme heat treatment in bentonite but not in culture where the maximum temperature activity was recorded at 80°C. This could also impact findings in which low water content effectively killed SRBs, because there were no experiments in which the water content slowly decreased to a supposedly lethal concentration and then increased again. This would allow conclusions to be made about whether the cells were dead or if the bacteria are able to tolerate a desiccated state for a long period of time.

Desiccation-tolerance is possible for spore-forming SRBs such as *Desulfosporosinus*, as the spores can survive in a dormant state at high temperatures, or adverse conditions, for a prolonged period, until the environment becomes favourable for growth (Rosnes et al., 1991). This is in keeping with findings that suggest most SRBs are unlikely to survive in the bentonite. However, spore-forming SRBs were most likely to persist in pressures of 1.09 g/cm^3 with limited water and nutrient availability (Pedersen et al., 2000).

The mechanism by which SRBs reduce sulfate is complex (figure 2.11) and is coupled to ATP production. At stage 5 in figure 2.10, sulfite is reduced to S^{2-} by sulfite reductase. This last step, also the last step in the electron transport chain, is the same as for the bacterial reduction of

elemental sulfur, whereby a hydrogen ion and S^{2-} forms first sulfide, and then hydrogen sulfide on addition of a second hydrogen ion. This is then released from the cell (Cypionka, 2006; Rabus, 2013). It is well documented that SRBs can utilise hydrogen as the sole electron donor. Alternative electron donors include organic compounds such as lactate, and one study by Dinh et al. (2004) even found that some species of SRB, *Desulfovibrio*, can use metallic iron as the sole electron donor.

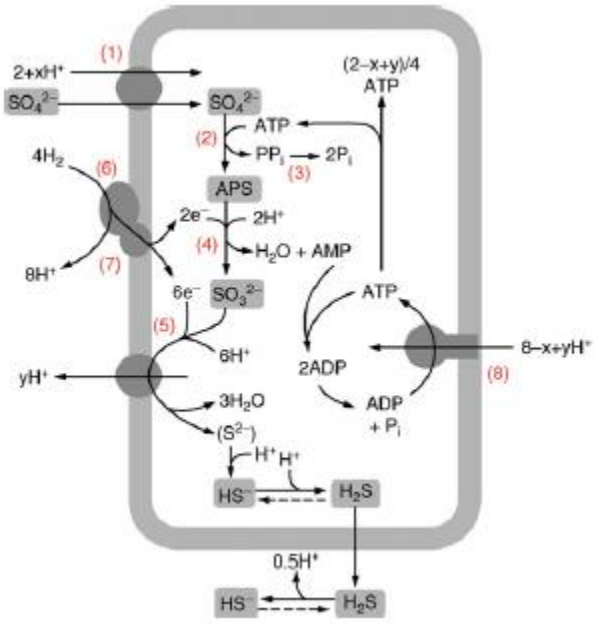

Figure 2.11: Steps in dissimilatory sulfate reduction and energy production with H_2 as the electron donor. (1) Uptake of sufate (2) ATP sulfurylase (3) pyrophosphotase (4) APS reductase (5) sulfite reductase (6) hydrogenase (7) Cytochrome C (8) ATP synthase (Cypionka, 2006)

However, the transport chains and pathways used by sulfur-reducing organisms can vary from species to species: e.g., the reductive citric acid cycle is active during sulfur reduction in *Thermoproteus neutrophilus*, whilst the hydroxypropionate pathway was active in *Acidianus* species (Rabus, 2013). Although the pathways differ, the overall equation to produce H_2S by SRBs from elemental sulfur is shown in equation 2. In *Desulfovibrio* hydrogen sulfide is produced via a different reaction (equation 3).

$4H_2 + 4\ S^0 \rightarrow 4H_2S$ [2]

$4H_2 + H_2SO_4 \rightarrow H2S + 4H_2O$ [3]

In both these examples, organic matter, such as a carbon source is utilised by the bacteria and through a series of reactions coupled to reduction to form hydrogen sulfide. Energy in the form of ATP is also produced (Welch, 1980). It has been noted that the activity and spores from SRBs are present in all samples of bentonite so far tested, and that as a result, sulfides migrate through the buffer (Keith-Roach & Livens, 2002). This would increase corrosion rates, and in the case that microbes are located on the outer edge of the buffer, this would further increase migration of sulfides through the buffer to the canister surface, and thus corrosion would increase by a predicted rate of 2 mm in 105 years (Liu, 2006).

2.8.5 Iron-interacting bacteria in the repository

Iron-interacting bacteria can also cause an increase in the rate of corrosion of steel through both iron-oxidising bacteria and IRBs. However, despite their abundance in materials and sites related to nuclear waste disposal, in comparison to SRBs, there has been little research carried out on what the outcomes of their activity in the repository could be.

IRBs, among other bacteria and archaea were also isolated from the groundwater and bentonites indigenous to Spain, and bentonite used in Finland, using 16S rRNA Illumina sequencing (López-Fernández et al., 2014; Chi Fru & Athar, 2008). They were also identified in samples from the near-field (an area geographically close - in the vicinity of the repository) and far-field (an area geographically distant such as the surrounding geosphere (1 x 25 x 25 km^3)) subsurface environment at Sellafield (Wilins et al., 2010), as well as being present in uranium-contaminated groundwater samples from Finland and Gabon (Haveman & Pedersen, 2002).

Similarly, bentonite samples collected in the Czech Republic were found to contain a few bacteria belonging to the *Gallionella* and *Nitrosomonas* families which were able to oxidise iron and sulfur as well as ammonia and manganese. *G. ferruginea* is largely considered the most active iron oxidiser, achieving theoretical rates of 1.1×10^{-11} mol Fe(III) per cell per year (Konhauser, 2007).

The bacterium has also been implicated in several clogging issues in draining systems due to its high precipitation of iron, suggesting that it is geographically widely present in groundwater.

Iron-interacting bacteria could also interact with iron, and iron-containing minerals, in the clay buffer. MX80 bentonite has ~4% wt. iron present (SKB, 2010) and interaction with this iron could lead to changes in the clays geomechanical properties leading to a less stable barrier system and possible illitisation (Bradbury et al., 2014; Sellin & Leupin, 2013). For example, iron could be transformed to non-swelling iron minerals such as hematite or magnetite which in high concentrations would increase the hydraulic conductivity of the buffer (SKB, 2010).

While oxidation of Fe(II) to ferric hydroxide ($Fe(OH)_3$) can occur in any environment where Fe(II) in solution encounters oxygen, bacteria provide the correct nucleation site for this to occur in anaerobic conditions (Konhauser, 2007). The ferric hydroxide serves as a precursor to more stable iron oxides such as goethite and hematite (Konhauser, 2007). It is the transformation of iron in the canister to these minerals which would increase corrosion and the reason why iron-interacting bacteria are a concern.

Whilst iron-oxidising bacteria can promote the oxidation of Fe(II) to Fe(III), IRBs can reduce Fe(III) to Fe(II) intracellularly and on the inner cell membrane (Ehrlich & Newman, 2009), due to a low affinity for Fe(II), the reduced product is then released from the cell. These bacteria must be specialised to recognise and attach to a surface which contains iron, and to produce proteins which are able to interact with the iron present in the extracellular environment. (Knoll et al., 2012).

Several Gram-negative IRBs have been characterised (such as *Geobacter* (figure 2.12) and *Shewanella*), and while there are some Gram-positive bacteria that are able to reduce iron, the mechanism is not fully understood. It has been observed, using cryo-TEM (three-dimensional cryogenic transmission electron microscopy), that *Geobacter* carries aggregates of Fe(III) oxides on its outer membrane. A theory has been proposed that Gram-negative IRBs collect and store Fe(III) sources on their outer membrane in preparation for a time when they do not have access to an external iron source (Luef et al., 2012). This theory would allow the iron to be stored near

the OmcS cytochrome as shown in the schematic in figure 2.11, ready for reduction. Further to this, there is evidence to suggest that *Geobacter* can not only store iron but can transfer it to other bacteria through pili (Reguera et al., 2005). This transfer is likely to be a cooperative method to sustain a microbial population, such as in a biofilm, to tackle starvation. E-pili are also employed to reach iron that is geographically distant from the bacteria. As e-pili are 3 nm in diameter (Lovely & Walker, 2019), they are not restricted by the small pore size of MX80 bentonite and so if this bacterium is found to be present, widespread iron-reduction could occur throughout the MX80 bentonite.

Due to the lack of an outer membrane, Gram positive bacteria do not have cytochrome C present in the periplasm which plays a key role in Gram-negative iron reduction as it acts as an electron reservoir for electrons destined for the outer surface (Morgado et al., 2012). This is of particular importance in the reduction of Fe(III) via acetate metabolism as acetate is metabolised in the periplasm and requires electrons to be carried across the periplasmic space (Lloyd et al., 2003). Therefore, it is possible that other types of cytochromes may play this role, however, the periplasm is an obstacle to this process (Williamson et al., 2013).

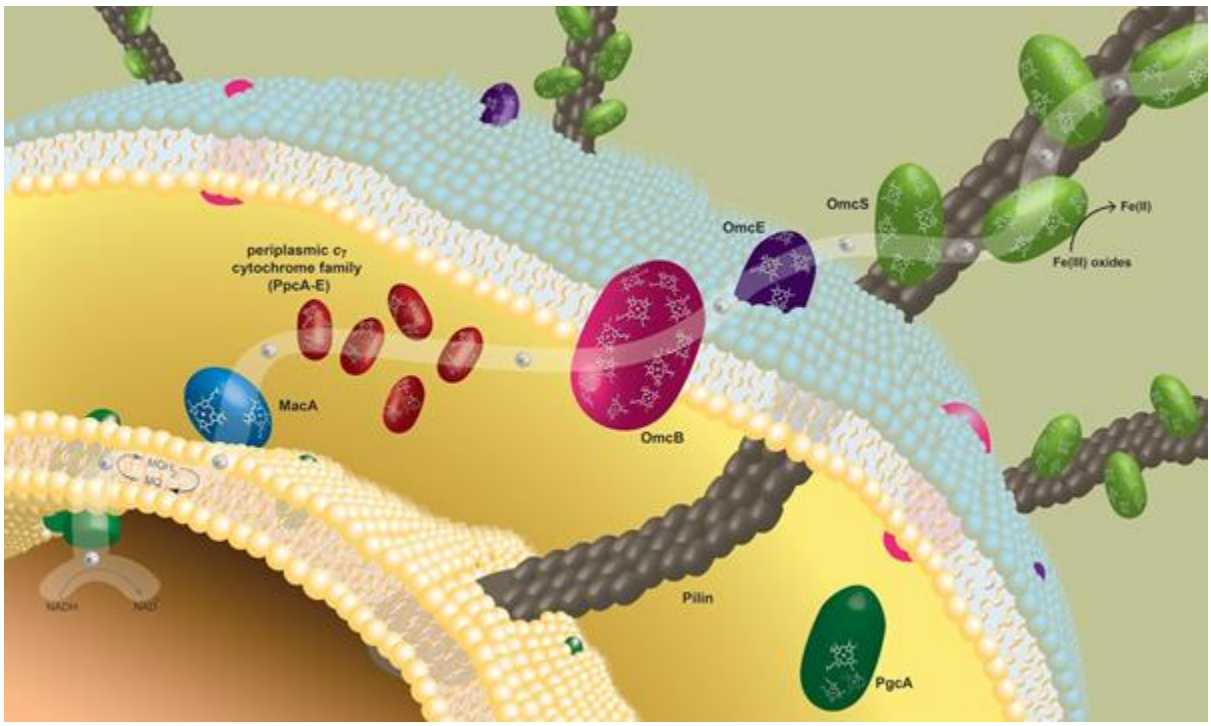

Figure 2.12: Proposed model of *Fe(*III) reduction by Geobacter sulfurreducens. The white

pathway represents the electron transfer pathway. Electrons from oxidation of NADH to NAD^+ are transferred across the periplasm by *MacA* and cytochrome C, then subsequently transferred across the outer membrane by a series of cytochromes (*OmcB*/E). In this species, *OmcS* is present on the pili and is the site of iron reduction. (Morgado et al., 2012).

Thermophilic IRBs (such as those species which would survive the high temperatures of the repository) are less able to biomineralise Fe(III) from smectite structures, than mesophilic Fe(III)-reducers (Kashefi et al., 2008). Studies showed that illite structures were formed from smectites in the presence of mesophilic bacteria (RWM, 2016), but not thermophilic IRBs. These mesophilic bacteria are anaerobic and are often found naturally to be involved in bioremediation of metal and mineral contaminants in marine environments (Kim & Gadd, 2008). It is therefore possible that these microorganisms will have adverse effects on the iron inserts, used in some designs to reinforce tunnels, or steel components within the canisters.

Certain IRBs have been extensively studied including species from the genus *Shewanella*. However, although numerous species within the *Shewanella* genera are competent iron-reducers they are not found to be indigenous to deep ground environments (Erbs & Spain, 2002) and have not been isolated from groundwater or bentonite samples. Regardless, experiments have been carried out with *Shewanella* and bentonite, using constant volume titanium test cells with Fe(III)-adapted cultures. This adaptation occurred through anaerobic incubation with Fe(III) citrate as the terminal electron acceptor, and formate as the carbon source. The results after a minimum of 3 weeks of enclosure in the test cells showed that no mineralogical changes occurred but the water content of the bentonite did change (Pedrial et al., 2009). This indicates that the microstructure of the bentonite was altered to allow more water storage in the interlayers of the clay when bacteria were present. A 3-week incubation is a relatively short incubation period when the lifespan of the repository is considered. Therefore, as significant changes were observed in a short time span, there is likely to be greater changes during the lifespan of the repository. This experiment also did not consider which other microbes may be present which could work syntrophically with *Shewanella* to potentially cause changes to the MX80. Furthermore, formate is not necessarily the carbon source likely to be available for microbial use.

S. putrefaciens is a Gram-negative bacterium which metabolises anaerobically (Kim & Gadd, 2008). *S. putrefaciens* has been used in studies to see the effects of IRBs on MX80 bentonite. It was found that the bacteria grew better on nontronite-rich clay than on smectite-rich bentonite due to the difference in Ca and Fe(III) concentrations. The study found that in both the presence and absence of *Shewanella* pyrite oxidation occurred, leading to precipitation of Fe(III) hydroxides and subsequently iron carbonates. The oxidation of pyrite can therefore be attributed to abiotic reactions. However, the bacteria had to be present for lepidocrocite formation from reactions of Fe(II) on the surface of calcite which caused changes to the pH of the internal environment (Pedrial et al., 2009) and could influence the reducing state of the canister (Kashefi et al., 2008). Furthermore, as lepidocrocite is a non-swelling iron mineral, this formation would also be detrimental to the geomechanical properties of the clay which make it an effective barrier. Whilst these experiments are useful*, S. putrefaciens* has never been identified in indigenous communities of MX80 bentonite. As with previous experiments outlined here, it would be more beneficial to understand the interaction of the entire indigenous microbial community with iron within MX80 bentonite, rather than with non-native model IRBs.

There is some disagreement over the extent IRBs contribute to corrosion of steel. While some studies show that IRBs enhance corrosion or accelerate the corrosion rates of steel, others suggest that mineral precipitates of IRBs are protective against corrosion (Herrera & Videla, 2009) depending on pH, ion distribution and oxygen concentration. Studies carried out by Schütz et al. (2015) showed that hydrogenotrophic IRBs did contribute to corrosion of carbon steel in the presence of Fe(III) and H_2, but to a limited effect that was thought to be negligible in terms of nuclear waste storage. The rate of corrosion by IRBs is inhibited by sulfide and siderite precipitation by abiotic reactions and magnetite dissolution (Dong et al., 2000) causing a protective mineral layer to form and block the bacteria from accessing the canister surface. Alternatively, it is believed that IRBs can form biofilms on the surface of steel which can support SRBs by providing a hospitable environment with direct access to the canister surface (Herrera & Videla, 2009). This would speed up corrosion of the canister due to the proximity to SRBs and the potential H_2S produced. It seems that whether biofilm formation occurs at the canister surface is dependent on whether the bacteria can colonise the area before mineral precipitates create a

protective layer. In anaerobic conditions, electrons from the carbon steel surface reduce protons, forming hydrogen and creating a protective layer over the metal (Wolzogen, 1934). IRBs among other bacteria can interact with this coating and exploit fractures in the steel caused by hydrogen embrittlement. An understanding of how this process could progress in the nuclear waste repository with microbial presence is therefore vital to accurately predict how the waste canister may corrode.

It is also noteworthy, that most IRBs are also able to reduce oxidised forms of manganese, which is present in the carbon steel canister and, to a limited extent in bentonite (Erbs & Spain, 2002). There is also evidence to support the statement that IRBs will likely use up the gas produced in the repository by their respiration (Williamson et al., 2013). This would be beneficial as it is thought that a build-up of gas in the repository could have adverse effects on the ability of the bentonite to function as a barrier due to an increase in pressure. Furthermore, less hydrogen gas would lessen the risk of hydrogen embrittlement of the steel and by extension corrosion.

2.8.6 Silicate solubilising bacteria in the repository

Chemical or mineralogical changes to bentonite will affect its geomechanical properties and change its ability to function as an effective barrier. Silica is an important component of all clays, and the silica content of clays is linked to the swelling ability and plasticity index of the clay. Loss of silica through silicate weathering in clays can lead to illitisation as previously mentioned (see section 2.6). In sediments loss of silica is coupled to release of nutrients to plants and bacteria as well as cations such as Mg^{2+} and Ca^{2+} which are involved in CO_2 sequestration. In fact, all silicate mobilisation is accompanied by release of micro and macro nutrients. Silicate-solubilising bacteria (SSB) act on silicates in clays and sediments to cause this weathering. SSB include both Gram-negative bacteria and Gram-positive bacteria, most notably, *Bacillus* sp. and *Pseudomonas* sp. (Vasanthi et al., 2016). Both these bacteria have been found to be indigenous to clays involved in nuclear waste disposal (Lopez-Fernandez et al., 2014*)*, but investigation into their silica-solubilising activity with regards to nuclear waste repositories, has not been carried out.

There are several mechanisms which are thought to be involved in silicate solubilisation by bacteria. Firstly, hydration of CO_2 during respiration results in formation of carbonic acid. This

acid when released can act on silicates. For instance, it was observed that carbonic acid can cause weathering of orthoclase ($KAlSi_3O_8$) to kaolinite ($Al_2Si_2O_5(OH)_4$) (Vasanthi et al., 2016). Similarly, feldspar can undergo chemical weathering to form muscovite (equations 3 & 4). In this example the dissolution of feldspar results in dissolved ions and dissolved silicic acid (H_4SiO_4) which form muscovite and so there is no overall yield in silicic acid, but the mineralogical change to a less plastic mineral is still detrimental to the properties of the clay buffer. Other products of chemical weathering include calcite and iron (hydr)oxides. However, it is unlikely that CO_2 will be present or generated in nuclear waste repositories, unless by microbial respiration and fermentation.

$$KAlSi_3O_8 + CaAl_2Si_2O_8 + 12H_2CO_3 + 4H_2O \rightarrow Ca^{2+} + 12HCO_3^- + K^+ + 3Al^{3+} + 5H_4SiO_4 \quad [3]$$

$$3Al^{3+} + K^+ + 3H_4SiO_4 \rightarrow KAl_3Si_3O_{10}(OH)_2 + 10H^+ \quad [4]$$

Another bacterial mechanism that causes silicate solubilisation is secretion of metabolites including amino acids, organic acids and phenolic compounds. Some of these metabolites have a high affinity for metals including aluminium and iron (Konhauser, 2007; Reitner & Thiel, 2011). By binding or reacting with metals in clays the associated silicates become soluble (Gadd, 2010). This mechanism could occur in the repository and is common among *Bacillus* sp..

Ligand, siderophore and exopolysaccharide production and secretion can also contribute to weathering in the same way as secreted metabolites – by binding metals through H^+ ions (Konhauser, 2007; Reitner & Thiel, 2011). Furthermore, SRBs have also been implicated in silicate weathering. Hydrogen sulfide production could react with iron and calcium in silicate minerals, creating iron sulfide or calcium sulfide, respectively (Ehrlich & Newman, 2009). The silicate component of the mineral would then be soluble.

Different clays and minerals have different propensities to weathering by microbes. For example, magnesium trisilicate was more vulnerable to solubilisation than quartz or muscovite (Vasanthi et al., 2018). There are also some instances in which microbes (e.g., *Actinomyces*) have become coated in silica (Suaro et al., 2018). This is most likely linked to other processes such as nitrogen fixation or iron-oxidisation and reduction (Suaro et al., 2018). It is probably used to support cell walls and increase strength of cell integrity (Vasanthi et al., 2016). Bacterial cells are also

immobilised by silica due to high adhesion. This is true for pure silica gels and silica found in clays such as bentonite (Suaro et al., 2018). It is possible that microbes promote silica dissolution or silicate solubilisation as a defence against cell immobilisation. This use of silica for structure and integrity may be an important survival mechanism for microbes in the repository to withstand high pressures and small pore sizes.

If there was a decrease in silica content of the MX80 bentonite, the effects would be detrimental to the barrier system. It would decrease the ability of the MX80 bentonite to swell and respond to changes in the environment without cracking. Despite these risks, there are not many specific studies of silicate bacteria in reference to nuclear waste disposal.

2.8.7 Other bacteria likely to be present in nuclear waste repositories

In addition to the bacteria discussed, several bacterial, archaeal and fungal species have been isolated and identified from clays and groundwater samples including nitrogen fixers, methane-oxidising bacteria, olitrophic and extremophilic bacteria, and several Gram-positive aerobic bacteria (Smart et al., 2017; Stroes-Gascoyne & West, 1997). Many of these bacteria have been disregarded, as enough is known about the species to predict that they will not survive the high temperatures, pressure or the anaerobic environment of the nuclear waste repository (West et al., 2002).

Furthermore, highly metal and uranium tolerant yeast strains from the genus *Rhodotorula* were isolated from the groundwater at the Äspö Hard Rock Laboratory. It was observed that certain yeast strains, including *Rhodotorula sp*., can precipitate U (VI). In this study, the effects of yeast under high temperatures and pressure were not tested, however, there are also a number of fungal species recorded which are able to reduce radionuclides and have a high tolerance to toxic environments. There is some concern that microbes which can tolerate and interact with radionuclides would then become active radiocolloids and transport radioactive material through groundwater movement out of the repository (West et al., 2002).

Interestingly, it was found that while bentonite is able to sustain microbial life, when groundwater containing microbes was introduced, it was found that the survival rates of the

bacteria indigenous to bentonite were much higher than that of the groundwater microbes. An explanation for this was offered: it was observed that microbes found in the clay were largely Gram positive, while soil microbes and other microbes from the groundwater were mainly Gram negative (Chi Fru & Athar, 2008). This discrepancy is perhaps due to the structure of the outer membrane on Gram negative bacteria, although no definitive explanation has been found.

2.9 Concluding statement

There are several studies surrounding the role of SRBs within the repository, however, the role and effects of IRBs has so far been largely ignored, despite studies identifying IRBs as indigenous to MX80 bentonite. Therefore, knowledge of the effects of these bacteria on corrosion, mineralogical changes to the clay or metabolic contributions are not known. This understanding is especially important for design concepts with the use of steel canisters as they will be subject to a faster rate of corrosion. The survival capabilities of these organisms are also important in understanding how they will survive in the repository, if at all. It is worth noting that due to the prolonged timescales of the repository lifespan it is not possible to run real-time experiments to accurately predict how 30 years of microbial activity will affect MX80 bentonite. Therefore, most experiments that have been carried out, excluding *in situ* long-term experiments, have used much higher concentrations of microbes than would be present in the repository. It is fair to expect that the effects seen with a higher concentration of microbes over the course of a few months, would likely be able to happen with a smaller concentration of microbes over the timespan of each phase of the repository.

Additionally, effects associated to microbial presence in the repository such as gas production and utilization, and silica solubilisation are not well understood at present. Reports of indigenous MX80 bacteria have identified a range of bacteria with diverse metabolic activities which could influence mineralogical changes to the clay. These fluctuations, amongst other changes to the internal environment, could prove important in understanding the effect microbes will have on the repository at different stages during containment. Also largely missing from the literature is a link between the microbial survival, and activity as carried out by several studies, with any measure of geotechnical changes to the clay. Indeed, many attempts to characterise the

indigenous microbial population have been unsuccessful or have not differentiated between all DNA and that of viable microbes within the clay. Aside from a limited number of isolated studies, the link between microbial activity and changes to the geomechanical properties of the clay does not appear to overlap in the literature. While some attempts have been made to indicate and model microbial life based on engineering measurements and predictions such as pressure, or some SEM, XRD techniques have been included in the analysis of some microbial studies, there is a lack of clear consequences of microbial activity on the behaviour of the clay and its ability to function as a barrier regarding its geotechnical properties.

Therefore, research gaps exist both in the understanding of which microbes can survive and become active in compact MX80 bentonite, and what geomechanical changes might occur due to the activity of these microbes. This project aims to fill these research gaps with a particular focus of iron-interactions and IRBs to complement the current UK design concept.

Chapter 3. Experimental Methods

3.1 Introduction and safety

Following an extensive literature review, the experiments designed for this project combined classical microbiology techniques and geotechnical testing to answer the research questions outlined in chapter 1 and fill the research gaps identified in section 2.9. These experiments followed a logical plan to first characterise the viable microbial community, then establish the potential activities and survival limits of this community, and finally to understand how these activities could influence the geomechanical properties of MX80 bentonite (figure 3.1). As explained previously, the UK design for a nuclear waste repository will utilise carbon steel waste canisters. As such, these experiments have a particular focus on the iron-reducing capabilities of the indigenous microbial communities. Experiments relating to characterisation of the indigenous microbial community of MX80 bentonite are described in section 3.4, 3.6 and 3.7. Those experiments which investigated the putative activities of the indigenous community are outlined in sections 3.4 – 3.7, and those with a focus on understanding potential geomechanical changes to MX80 bentonite are explained in section 3.6 and 3.7.

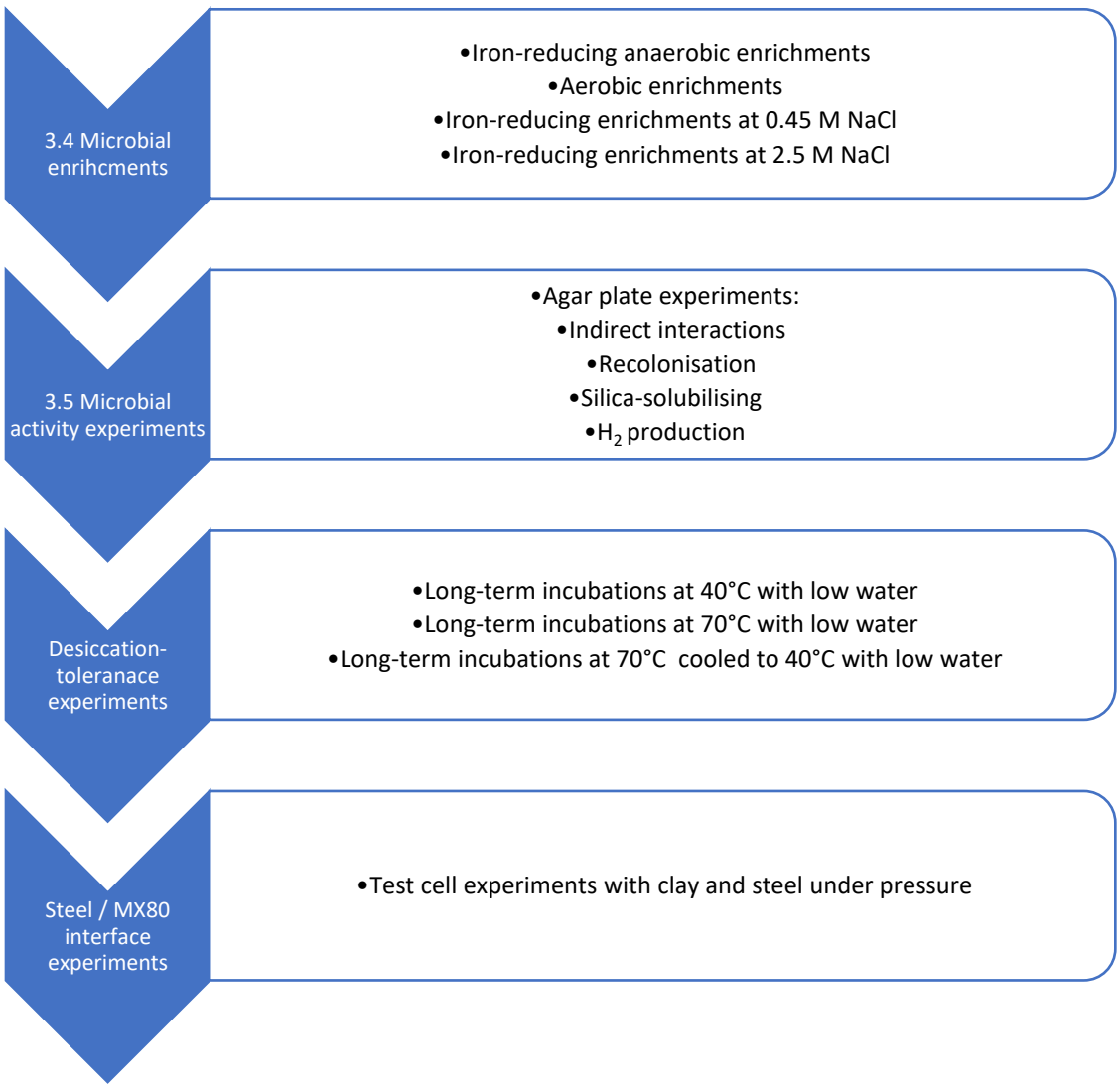

Figure 3.1: Flow chart of experiments

All microbes were handled in restricted card access labs with appropriate personal protective equipment. All biological wastes from enrichments and microcosms were autoclaved before disposal. All hazardous chemicals were handled in a fume hood, and all media stock solutions and buffers made were stored in sealed glass bottles.

3.2 Details of MX80 bentonite

Two different sources of Wyoming MX80 bentonite were used in this project: MX80 bentonite powder (known as Bentonex WB, supplied by RS minerals®) and compacted Wyoming MX80 bentonite blocks were sourced from SKB's (Svensk Kärnbränslehantering AB - Swedish nuclear waste management organisation) supplier (ClayTech AB®). Further information on these materials is presented in section 4.1.

3.3 Preliminary experiments and groundwater choice

Preliminary analyses and reagent synthesis were carried out prior to any experiments, such as determination of the moisture content of the compacted MX80 bentonite; identifying an appropriate water:MX80 ratio; selecting a groundwater composition; and synthesising poorly crystalline Fe(III) oxide according to Lovley (2013).

Anaerobic conditions refer to those created in the Coy Anaerobic Hood - 95% nitrogen:5% hydrogen – unless otherwise stated. Routine maintenance of the Coy Anaerobic Hood was carried out weekly – palladium catalysts were reactivated by heating to 125°C for 4 hours and then placing in the hood.

3.3.1 %moisture content of MX80 bentonite and MX80:water ratio:

Water content was determined according to British Standards BS1377-2:1990 (equation 5) in which clay was weighed, dried at 105°C in an oven for 24 hours and reweighed.

$$\%moisture\ content = \frac{mass\ of\ water}{mass\ of\ dry\ soil}\ x\ 100 \qquad [5]$$

Water: clay ratio tests were carried out to ensure that the swelling of the MX80 bentonite clay would still allow for routine liquid subsampling. 4g, 6g, 8g and 10g of MX80 bentonite powder were added to 100ml of deionised water. The flasks were then left overnight to allow swelling to occur. The volume of free water was then measured by slowly pouring and filtering the samples into measuring cylinders.

3.3.2 Groundwater composition choice:

A suitable Sellafield-like groundwater was identified from literature (Wilkins et al, 2007) for use in microcosm-based studies. The composition is shown in table 3.1. This groundwater was considered suitable for these experiments as it is representative of a typical UK groundwater with similar salinity to that associated with international repository sites (see table 2.2).

Table 3.1: Sellafield-like groundwater design (Wilkins, 2007)

REAGENT	CONCENTRATION (g/l)
KCL	0.0066
$MgSO_4 \cdot 7H_2O$	0.0976

$MgCl_2 \cdot 6H_2O$	0.081
$CaCO_3$	0.1672
$NaNO_3$	0.0275
NaCl	0.0094
$NaHCO_3$	0.2424

An organic substrate mixture was also used in many experiments as a source of energy and nutrients for microbial growth. The range of different carbon sources minimized the selective pressure on the microbial community. The composition of this mix is shown in table 3.2.

Table 3.2: Organic substrate mixture components added to groundwater, where the final concentration indicates the concentration in the media.

REAGENT	CONCENTRATION (g/l)
TRYPTIC SOY BROTH	3
BUTYRIC ACID	270 µl/l
PROPIONIC ACID	220 µl/l
SODIUM LACTATE	3.36×10^{-4}
SODIUM ACETATE	0.18
GLUCOSE	0.54

3.4 Indigenous microbial communities and their basal activity in relation to iron-reduction

A series of enrichment experiments were set up to characterize the indigenous iron-reducing community of MX80 bentonite at different salinities. Table 3.3 displays a summary of these experiments and the associated control experiments.

Table 3.3: Summary of indigenous microbial community enrichments

EXPERIMENT	CONTROLS	REPLICATES
Anaerobic iron-reducing MX80 microbial enrichments	1. No MX80 2. Sterile MX80 3. With *S. oneidensis*	All experiments and controls run in triplicate

Aerobic MX80 microbial enrichments	1. No MX80 2. Sterile MX80 3. No organic substrate mix	All experiments and controls run in triplicate
Anaerobic iron-reducing MX80 microbial enrichments at 0.45m NaCl	1. No MX80 2. Sterile MX80 3. With *S. oneidensis*	All experiments and controls run in triplicate
Iron-reducing MX80 microbial enrichments at 2.5m NaCl	1. No MX80 2. Sterile MX80 3. With *S. oneidensis*	All experiments and controls run in triplicate

3.4.1 Setup of anaerobic iron-reducing enrichments with MX80 bentonite:

All solutions and flasks for the preparation of iron-reducing anaerobic enrichments were left inside an anaerobic cabinet overnight (see section 3.3) prior to the setup of anaerobic microbial enrichments. Then, under these anaerobic conditions, 100 ml aliquots of synthetic groundwater (previously degassed with N_2) amended with the organic substrate mixture was added to 120 ml serum flasks. To each of these serum flasks 6 g of MX80 bentonite powder was added with poorly crystalline iron (III) oxide (PCFeO, ferrihydrite – see section 3.8.1) to reach a concentration of 20 mM Fe(III). The flasks were then sealed with butyl stoppers and 20 mm aluminium crimps and left in the anaerobic cabinet. This set-up (figure 3.2) was run in triplicate and then repeated with no MX80 bentonite powder; or sterile MX80 bentonite powder (dried in oven at 105°C for 48 hours) controls. Every 7 days 5 ml samples of each flask were taken and filtered through sterile 25 mm 0.2 µm syringe filters (Sartorius™ Minisart™). In each of the removed samples the pH, Fe(II) soluble concentration, Fe(II) total (dissolved + suspended) concentration, and Fe(total) (i.e., Fe(II) and Fe(III)) (dissolved + suspended) concentration was measured and recorded (Stookey, 1970) (see section 3.8.3) and volatile fatty acid (VFA) analysis was also carried out (see section 3.8.4). These initial enrichment experiments were then stopped on day 42 as iron reduction had taken place, this was indicated by a plateau in Fe(II) production. In addition, 1 ml

of the removed sample was centrifuged at 1500 xg for 10 mins and the pellet was frozen at -80°C for storage for DNA extraction. DNA isolation and subsequent 16S rRNA Illumina sequencing was carried out on all samples, including frozen pellets, the methods are described in section 3.9.

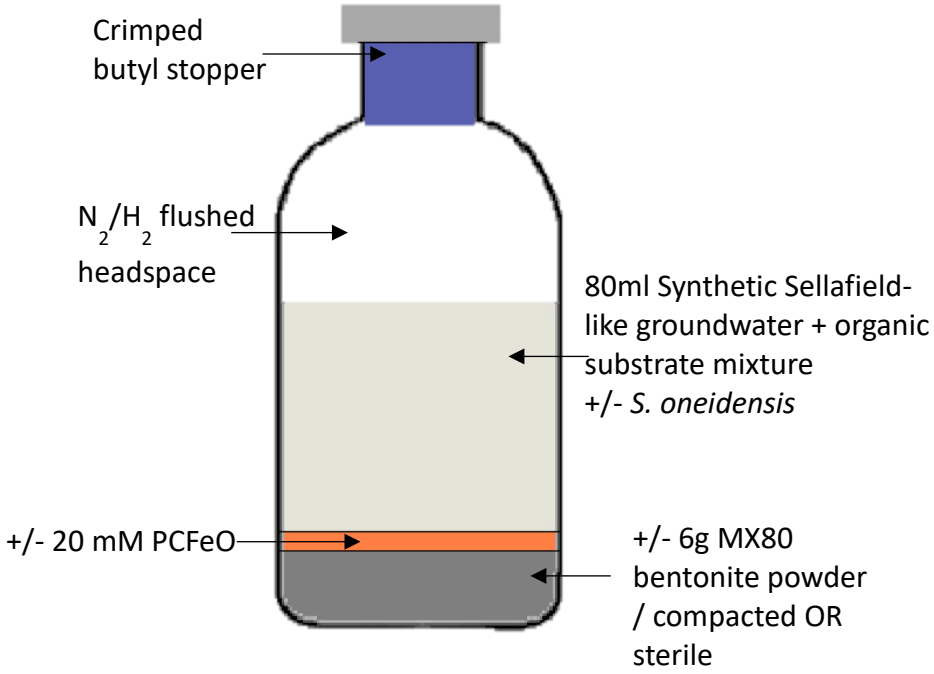

Figure 3.2: Schematic of anaerobic iron-reducing enrichments experiments. This set-up was repeated at higher salinities.

This experiment was also carried out with compacted MX80 bentonite in place of MX80 bentonite powder with the addition of a positive control in the form of *Shewanella oneidensis*. Negative controls were also used. These flasks were sampled weekly as before for 6 weeks, and eventual DNA extraction and sequencing was carried out (see section 3.9).

On day 21, 3 100 µl samples from both live and sterile experiments were spread on Fe-reducing 1.5% agar plates (see section 3.8.2) and incubated for 3 days under anaerobic conditions. The resulting colonies were then washed into 500 µl 50% glycerol stocks with 500 µl LB medium and stored at -80°C. This agar plate test also confirmed no growth in sterile flasks.

In the original iron-reducing enrichments at low salinity, it was also noticed that as the experiments progressed, a black precipitate started to form. This material was collected when

the experiments ended and was dried in an anaerobic cabinet, crushed, and analysed by X-ray diffraction (XRD) (see section 3.10.1).

3.4.2 Aerobic enrichments

Additionally, aerobic clay enrichment experiments were set up in 250 ml conical flasks and sealed with cotton wool bungs topped with tin foil. These flasks had a similar compositional set up to the anaerobic iron-reducing enrichments with experimental flasks containing 100 ml Sellafield-like groundwater with organic substrate mixture and 6 g of either MX80 bentonite powder or compacted MX80 bentonite. Controls for this experiment included flasks excluding MX80 bentonite; excluding the organic substrate mixture; and a control comprising sterile MX80 bentonite powder or sterile compacted MX80 bentonite (figure 3.3). 5 ml samples were taken every 6 days for 30 days and the pH was measured throughout the incubation period. VFA analysis was carried out with samples filtered through sterile 25 mm 0.2 µm syringe filters (Sartorius™ Minisart™). DNA isolation was carried out using a PowerSoil DNA Isolation kit and the samples were sequenced using 16S rRNA gene sequencing (see section 3.9).

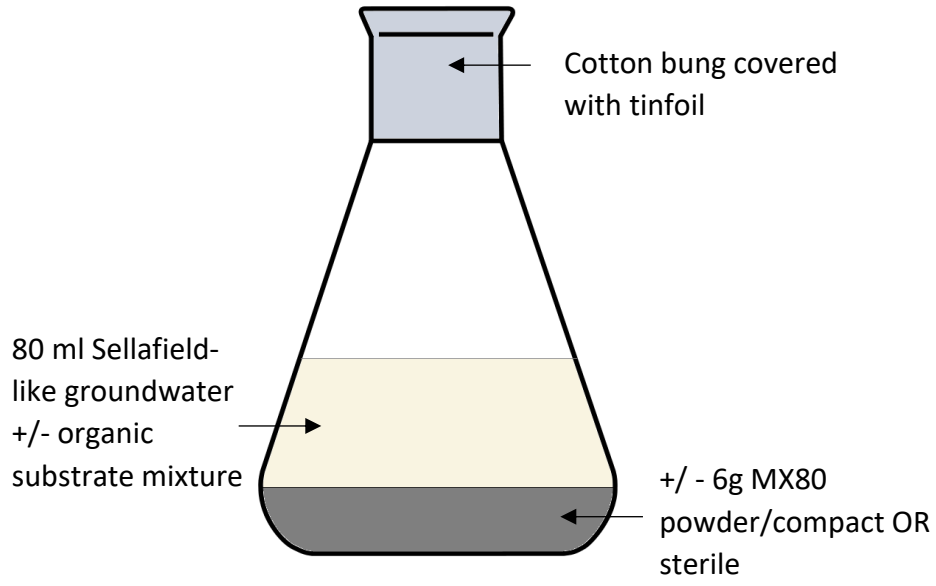

Figure 3.3: Schematic of aerobic enrichments.

3.4.3 High salinity enrichments

Anaerobic iron-reducing enrichment experiments were repeated with highly saline groundwater (2.5 M NaCl, mimicking the higher salinities of groundwaters considered likely in repository

location selections, such as those in North America) and seawater-level saline groundwater (0.45 M NaCl, which corresponds to the highest salinity predicted for UK groundwaters at possible repository sites). All other groundwater components and organic substrate mixture remained the same. Furthermore, these salinity experiments also included the same controls as previously described and were incubated under anaerobic conditions. Liquid samples were taken every 7 days for 6 weeks and analysed as previously described in section 3.4.1. These samples were also sequenced following DNA extraction which occurred on day 42, at the termination of the enrichment (see section 3.9).

3.5 microbial activities of the indigenous-iron reducing community of MX80 in relation to obstacles in the repository environment

3.5.1 Solid media indirect microbial interactions

In order to determine whether microbes need to interact directly with iron in order to reduce it, or if the microbial secretions can interact with the iron alone, a series of agar plate experiments was carried out.

3.5.1.1 Indirect interaction agar plates

2% agar plates were made-up with the synthetic Sellafield-like groundwater (Wilkins et al, 2007) with organic substrate mixture added. The agar media were then mixed with either 2% (w/v) iron powder (Sigma Aldrich), 2% (w/v) PCFeO, or 2% (w/v) MX80 bentonite powder, all of which were previously sterilised in a dry oven at 105°C for 48 hours. 6 plates with each substrate were poured and 6 more plates with no added iron powder were poured to act as controls. Plates were then dried under anaerobic conditions for 48 hours. Sterile cellulose acetate 0.2 µm membranes (Sartorius) (hence impermeable to bacterial cells) were placed on the surface of agar and 200 µl of $6x10^5$ cells/ml of iron-reducing MX80 bentonite community (see section 4.1) were added to 3 of each plate. Cells were previously grown in groundwater media with organic substrate mix from MX80 bentonite iron-reducing community glycerol stocks and counted using SYBRGold.

3 experimental and 3 un-inoculated control plates were generated for each enrichment condition (figure 3.4). Plates were incubated under anaerobic conditions at room temperature. Growth was monitored by visual inspection and changes observed over 1 month.

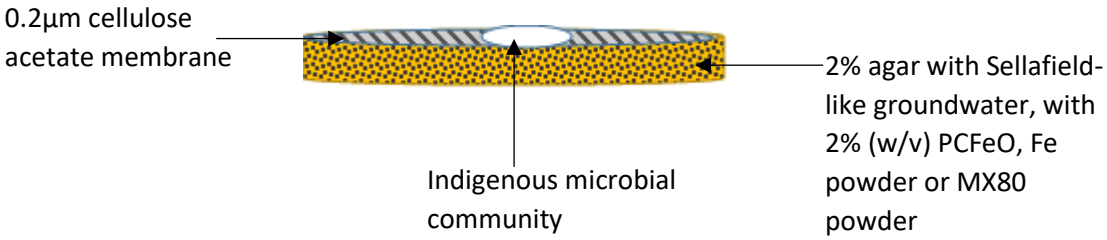

Figure 3.4: Schematic of solid media indirect interaction experiments: agar mixed with 2% (w/v) Fe(II) oxide, poorly crystalline iron oxide, or bentonite powder. Inoculated with MX80 community microbes. Abiotic controls had the same set-up but were not inoculated.

3.5.1.2 Post-experiment analysis

After 1 month of growth in an anaerobic cabinet, biomass was removed from the surface of membranes and dried in an oven at 105°C for 24 hours and weighed. Biomass was calculated as a percentage of the material removable from the membrane on the surface of the control plate with no iron substrate. The pH of membrane covered plate surface was also measured in 5 locations and the mean value calculated. Mineral recovery (see section 3.8.5) was carried out and the collected precipitates were analysed using EDX, SEM and XRD analysis using the methods described in 3.10.1-2.

3.5.2 Solid media recolonisation on compacted MX80

Recolonisation experiments were used as an indication of whether or not microbes are able to live on the MX80 bentonite, or indeed, breach the surface of the clay, which when swollen has 0.02 µm pore spaces available that would greatly limit microbial movement. The enriched microbial population used in these experiments is indigenous to the clay so should be able to recolonise it, similar to Koch's postulate which states "When a pure culture of the suspected causal agent is inoculated into a healthy susceptible host (plant), the host must reproduce the specific disease.".

3.5.2.1 Recolonisation agar plates

Six 2% (w/v) agar plates with synthetic Sellafield-like groundwater (Wilkins et al, 2007) with added organic substrate mixture were poured and left to dry in an anaerobic cabinet for 48 hours.

A 20 x 20 mm square was cut out the centre of the plates and a block of compacted MX80 bentonite (sterilised at 105°C for 48 hours) measuring 20 X 20 X 10 mm was placed in each plate. The agar was then inoculated with 200 µl of $6x10^5$ cells/ml iron-reducing MX80 bentonite community stock (see section 4.1) at a location spatially distant from the MX80 bentonite (figure 3.5). All plates were incubated for 1 month under anaerobic conditions at room temperature (21°C).

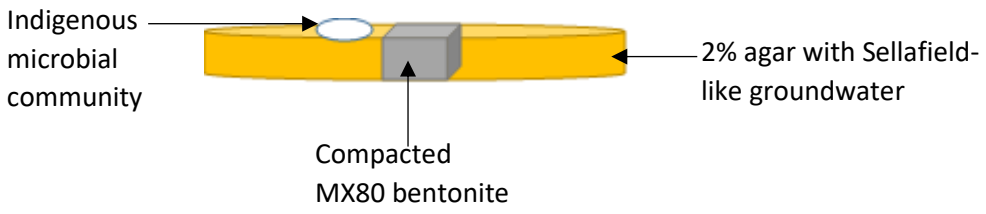

Figure 3.5: Schematics of solid media recolonisation experiments: 4cm^3 area of agar cut out and compacted bentonite inserted so flush with agar. MX80 bentonite community microbes introduced close to bentonite surface. Abiotic controls had the same set-up, but were not inoculated.

3.5.2.2 Post experiment analysis

The pH of each plate surface and the surface of the compacted MX80 bentonite block was measured in 5 different locations and the average calculated. The MX80 bentonite blocks were removed, and small amount of each block was cut off and dried for XRD, EDX and SEM analyses using the methods descried in 3.10.1 and 3.10.2. In these experiments samples for SEM analysis were not ground to allow for observation of pitting and microstructural changes to the surface of the MX80 bentonite block. The plastic limit of the remaining clay was then measured (see section 3.9.3).

3.5.3 Silica solubilisation

It was noticed in cell counts using fluorescence microscopy that bacterial cells from MX80 bentonite microbial community required extra washing prior to staining and counting to ensure SYBRGold was able to adhere to the cell surface. One possible explanation was silica released from the clay had coated the cells and was blocking the adherence of this fluorescent dye. There was also evidence of clay dissolution in some of the SEM images from enrichment studies.

Therefore, simple microcosms were set up to measure the concentration of dissolved silica over time.

3.5.3.1 Silica agar plate clearing experiments

Plate clearing experiments, like those describe in Vasanthi et al. (2018) were used as a visual measure of silica solubilising activity. In these experiments, agar mixed with silicate substrates appears cloudy and will clear if silica is removed, leaving a clear ring around bacteria colonies which are actively involved in solubilising silica.

3.5.3.1.1 Mineral clearing in agar plates

Kaolinite ($Al_2Si_2O_5(OH)_4$) or magnesium trisilicate ($Mg_2O_8Si_3$) was sterilised at 105°C for 48 hours and added to 2% (w/v) agar with Sellafield-like water (Wilkins et al, 2007) to achieve a concentration of 2% (w/v) kaolinite or magnesium trisilicate. 12 culture plates were poured and dried for 48 hours – 6 were dried under anaerobic conditions and 6 were dried under aerobic conditions. 3 plates from each environment were inoculated with 200 µl of iron-reducing MX80 bentonite microbial community at $6x10^5$ cells/ml and left to grow for 1 month under the same respective anaerobic and aerobic conditions as they were prepared under. The other plates acted as abiotic controls.

Colonies showing evidence of plate clearing after one month were transferred to new mineral plates and incubated for a further month – other experimental plates were discarded. Subsequently, mineral recovery was carried out (see section 3.8.5). Minerals from experimental and control plates were then analysed with SEM and EDX according to methods described in 3.10.1 and 3.10.2.

3.5.3.2 Silica Liquid Experiments

0.2% (w/v) MX80 bentonite powder was sterilized at 105°C for 48 hours and then added to 100 ml Sellafield-like groundwater amended with 12 mg/L acetate under anaerobic conditions. Flasks were inoculated with 100 µl of iron-reducing MX80 bentonite microbial community (see section 4.1) at $6x10^5$ cells/ml and sealed with butyl stoppers and aluminium crimps. 5 ml liquid samples were taken weekly for 10 weeks and filtered through 0.2 µm filters. The dissolved silica concentration was measured using a colorimetric method Silica Test Kit (HI-38067, Hanna

Instruments) according to manufacturer's instructions. This experiment was set up in triplicate with three control flasks containing no bacteria. A small amount of clay was dried at the end of the experiment and analysed using SEM by mounting the sample on carbon tape and coating with gold.

3.5.4 Biotic H_2 production in anaerobic conditions 40°C with MX80 bentonite and steel

It is known that hydrogen gas will build up in the repository due to steel corrosion and this will contribute to the overall pressure build. There are hydrogen-producing fermentative bacteria present in the indigenous microbial community of MX80 bentonite (see section 4.1) as well as bacteria which utilise hydrogen for energy and growth.

3.5.4.1 Microbial hydrogen production microcosms

Under anaerobic conditions 71 g of S275 steel was added to a 100 ml serum bottle divided into small coupons (12 mm diameter) with 31 g of compacted MX80 bentonite cut into cubes (10 x 10 mm) and sterilised for 48 hours at 105°C. 11 ml of sterile Sellafield-like groundwater (Wilkins et al., 2007) with 12 mg/L acetate (in the form of sodium acetate) was added to the flask as a carbon source. The flask was then inoculated with 50 µl of MX80 bentonite mixed culture community stocks ($6x10^5$ cells/ml), prepared from iron-reducing MX80 bentonite enrichments community glycerol stocks grown in groundwater media with organic substrate mix. The flasks were then sealed with butyl stoppers and aluminium crimps. This experiment was repeated in triplicate and abiotic controls were included.

Hydrogen measurements were taken on day 0 using a GC (Valco helium ionization pulsed discharged detector) using helium as the carrier gas with a flow rate of 10 ml/min. 1 ml of gas from the headspace of each sample was taken using a 1 ml gas-tight syringe (Hamilton) which was then over-pressured by compression to a 250 µl volume for injection. This over pressuring reduces the risk of contamination from the air. The temperature of the injection port was 110°C and the column was held at 60°C. A constant temp program was used so no temperature ramping was needed; H_2 has a retention time of approximately 55 seconds under these conditions. Calibration was carried out using 100 ppm H_2, and Excalibur was used to process the data.

After 10 months incubation at 20°C hydrogen measurements were taken again. Due to equipment availability and unexpectedly high hydrogen production, a different GC was used at this time point (Shimandzu, GC-2014). As previously, however, 1 ml of headspace was taken and over pressured by compression to 250 µl prior to injection. The carrier gas was nitrogen with a flow rate of 25 ml/min and temperatures of 100°C, 50°C, 100 °C for the injection loop, column, and thermal conductivity detector (TCD), respectively. Samples were run against 0.1 - 10% H_2 standards prepared as a serial dilution.

3.6 Desiccation tolerance of the indigenous iron-reducing community of MX80 bentonite and interactions at the MX80 bentonite / steel interface

In order to replicate the temperature at the clay/rock interface at different phases throughout the repository lifespan a series of batch experiments were set up. This format allowed for the microbial community at each temperature to be characterised and allowed for an understanding if any bacteria are causing changes through microbial activity at higher temperatures, or if they are inactive due to entering dormancy or not able to survive.

These experiments also allowed for observations to be made about how microbes at different temperatures affect the clay in terms of mineralogy and plasticity. Sterile controls allowed specific changes to be attributed to microbial activity.

3.6.1 Desiccation tolerance experiment set-up

Bentonite disks measuring 60 x 15 mm were heated at 40°C for 48 hours to prevent cracks developing during rapid drying and then at 105°C for 48 hours for sterilisation. S275 carbon steel disks measuring 60 x 5 mm were also sterilised in a dry oven at 105°C for 48 hours. The steel and bentonite were then put into sterile Nalgene jars (figure 3.6) along with anaerobic indicator strips (BBL ™ Gaspak ™) which change from blue to colourless in anaerobic conditions. 8 ml Sellafield-like groundwater was added (equal to 100% saturation of MX80 bentonite at 27% moisture content). After 24 hours experimental flasks were inoculated with 50 µl of iron-reducing MX80 bentonite microbial community stocks ($6x10^5$ cells/ml) (see section 4.1). Control flasks were not inoculated.

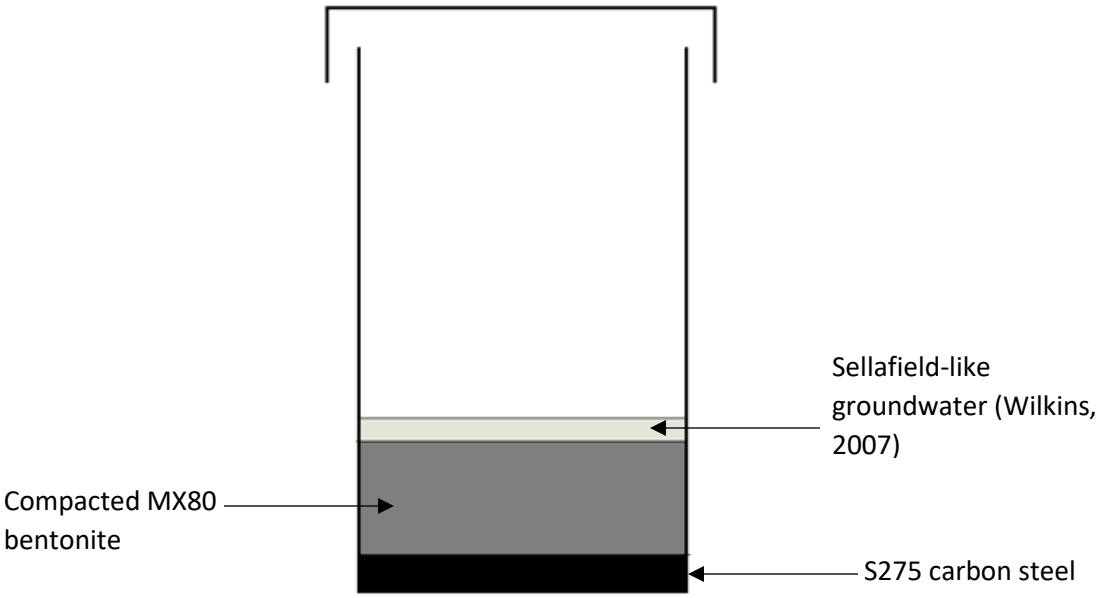

Figure 3.6: Desiccation tolerance experiments were set up with compacted MX80, S275 carbon steel coupons, Sellafield-like groundwater and indigenous microbes at 70°C, 40°C or dual temperatures (see text)

3 experimental and 3 control flasks were incubated at 70°C for 4 months and 3 experimental and 3 control flasks were incubated at 40°C for 4 months. A further 3 flasks and 3 controls were incubated at 70°C for 2 months and then cooled slowly to 40°C over 1 month and maintained at 40°C for 1 month.

3.6.2 Analysis of desiccation tolerance experiments

At the end of the experiment, scrapings from the steel surface, clay/steel interface and bentonite were dried and analysed by XRD as described in 3.10.2. MX80 bentonite was also air dried anaerobically for SEM analysis as described in 3.10.1 with observations of biological presence and changes to clay surface observed. The total area of the steel surface at the clay/steel interface was photographed. 0.5 g of clay from the steel/ bentonite interface was then used for DNA extraction. The method for extraction and analysis is described in section 3.9. Clay was also recovered to determine the plasticity index (PI) by calculating plastic and liquid limits (see section 3.10.3) and the % moisture content (see section 3.3.1).

3.7 Biotic clay / steel interface test cells to simulate repository pressure

Test cells were used to replicate pressures and temperature of the repositories during the envisaged later stage of geological storage after an initial heating to 100°C and then gradual cooling. The experimental design was adapted from Davies (2017) and allowed for observation of changes at the clay/steel interface and effluent analysis to determine if iron redox state is changing or if iron is entering the aqueous phase and being lost from the system. Mössbauer spectroscopy was due to be used to identify iron speciation; however, delays due to COVID-19 meant this was not possible.

3.7.1 Experimental set-up

All equipment, including steel and clay, was sterilized by heating, autoclaving or ethanol washing. Compact MX80 bentonite coupons, measuring 11 x 80 mm diameter, and S275 carbon steel, measuring 9 x 80 mm, were put into stainless steel test cells (figure 3.7) with a PTFE lining to prevent interactions between the steel cell and the experiment. To ensure a watertight seal, ThreeBond® (Type TB1207B) was used between the PTFE lining and the test cells. The steel coupon had a 1 mm deep 2 mm wide cross cut into the bottom side and extending up the edges to allow sufficient movement of water around the steel. Test cells were inoculated with 100 µl of iron-reducing MX80 microbial community stocks ($6x10^5$ cells/ml) isolated from iron-reducing MX80 enrichments (see section 4.1). Sellafield-like groundwater (Wilkins et al., 2007) with 12 mg/L acetate (from sodium acetate) was used for this experiment. A cell pressure of 700 kPa was applied for 48 hours to allow clay to swell using pressure controllers (GDS). Pressure was then readjusted to 1 MPa with a back pressure of 700 kPa to create a water gradient across the sample. The test cell set-up was run in triplicate and repeated for abiotic controls, and finally, repeated with inoculation but without steel – in this set up the clay measured 20 mm thickness.

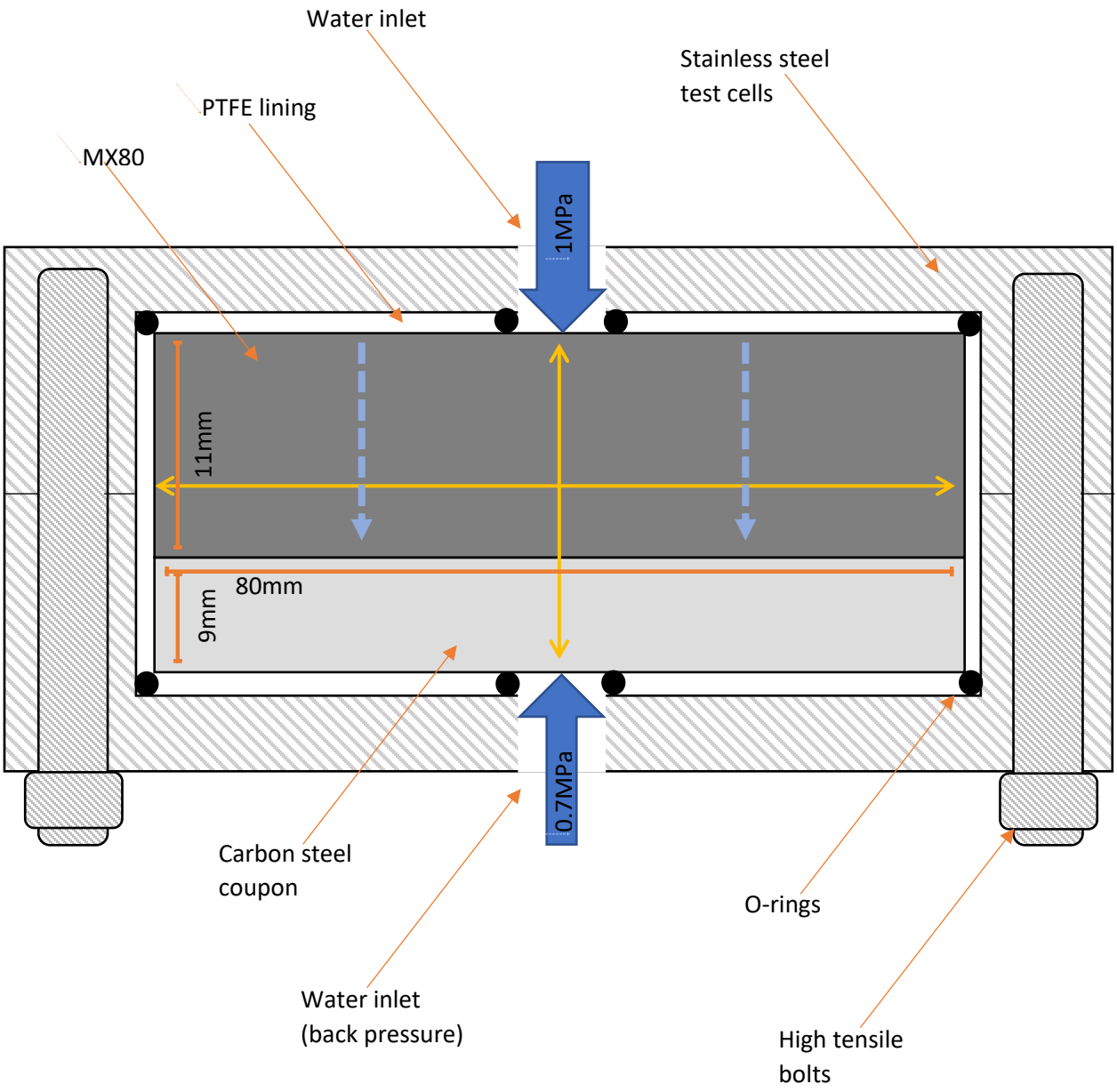

Figure 3.7: Experimental design for test cell experiments. Carbon steel and MX80 bentonite were placed inside a stainless steel test cell, an induced water gradient was created, indicated by blue dashed arrows. Yellow arrows indicate constrictive swelling area.

3.7.2 Post experiment analysis

At the end of the experiment pH, $Fe(II)_{aq}$, Fe(II) total and Fe(total) concentrations of the effluent were measured (see section 3.8.3) and VFA analysis was carried out as described in section 3.8.4. The test cells were dismantled under anaerobic conditions (100% N_2, Glovebox Systemtechnik

GS040113 (≤1 ppm O2)) and photographs taken to allow for measurements of the rust diffusion into the clay using ImageJ. Clay subsamples were air-dried anaerobically for analysis using XRD according to methods described in 3.10.2 with the exception that samples were run for 7 hours instead of 5. Whole pieces of MX80 bentonite from the top of the test cell and bottom of the test cell (closest to the steel) were also dried for SEM and EDX analysis (see section 3.10.1) along with 1 cm^3 steel samples from the center of the steel coupon and the outer edge. Additionally, small volumes of MX80 were recovered and stored between two pieces of Kapton tape to avoid contact with oxygen for subsequent Mössbauer spectroscopy. Additionally, iron-reducing enrichments using MX80 bentonite from closest to the steel/clay interface ("bottom") and furthest from the clay/steel interface ("top") were set up in triplicate and followed the same methodology as the original enrichment experiments described in section 3.4. The remaining clay recovered from the test cells was used to determine the PI (see section 3.10.3).

3.7.3 DNA sequencing and analysis

DNA extractions were carried out on samples of MX80 bentonite closest to the steel/clay interface ("bottom") and furthest from the clay/steel interface ("top") using the method described in 3.9. Due to low DNA concentrations, the extracts were amplified using a nested PCR approach whereby wide-set primers (Edwards et al., 1989) which encompass the whole 16S rRNA gene were used for the first round of PCR and then Golay barcoded primers (see section 3.9), were used for a second round of PCR amplification. Amplification was confirmed on a 1% agarose gel and samples from both the original enrichment and the nested PCR product were sequenced at NU-OMICS, Northumbria University by Illumina 16S rRNA gene sequencing, along with DNA extractions from iron-reducing enrichments with clay recovered from test cells.

Sequence library analysis was carried out using the methods described in 3.9. Significance testing was carried out using R to determine p-values for iron concentrations, pH and PI through ANOVAs (see section 3.9).

3.8 Experimental methods and assays

3.8.1 Synthesis of poorly crystalline Fe(III) oxide (PCFeO):

500 ml stock slurry of 1 M poorly crystalline Fe(III) oxide was made according to Lovley, 2013. 0.4 M $FeCl_3 \cdot 6H_2O$ was neutralised with 10 M NaOH to pH 7. The slurry was stirred constantly using a magnetic stirring rod for 30 minutes and then washed 6 times in distilled water, with centrifugation and decantation between washes.

3.8.2 Fe(III) agar plates:

Fe-reducing plates were set up by adding 1.5% (w/v) agar and 2% (w/v) PCFeO to 500 ml groundwater containing the organic substrate mixture. This medium was then autoclaved and poured into 9 cm plastic petri dishes. Half of the petri dishes were dried in an anaerobic chamber, and the other half air-dried on a bench.

3.8.3 Fe concentration measurements (Ferrozine assay):

3.8.3.1 Fe(II) soluble measurements

Measurements of Fe(II) concentrations in enrichment samples were conducted on 1 ml of 0.2 µm filtered aliquots using the ferrozine assay (Stookey, 1970) which briefly entails acidifying the sample in HCl and then adding a ferrozine buffer, a colour change from colourless to purple occurs when Fe(II) is present. The absorbance of light was then measured (562 nm) using a spectrophotometer (Jenway 6305) and Fe(II) concentrations were calculated from a standard curve. This curve was calculated using concentrations of iron (from $FeCl_3$) in a series dilution between 0.1 mM to 100 mM. Each point on the standard curve was measured 3 times and the average taken, provided there was no more than 5% difference between repetitions.

3.8.3.2 Fe(II) total measurements

Unfiltered enrichment samples (1 ml) were acidified and then centrifuged at 1000 rpm for 5 minutes. The sample was then filtered through sterile 25 mm 0.2 µm syringe filters (Sartorius™ Minisart™) and absorbance measured using a spectrophotometer at 562 nm as described by Stookey (1970) (see section 3.8.3.1).

3.8.3.3 Fe(total) measurements

Using the same Ferrozine colorimetric method detailed above (see section 3.8.3.1), 1 ml of unfiltered enrichment liquid subsample was acidified. The iron content was then fully reduced by

adding hydroxylamine hydrochloride and incubating in the dark according to the method by Stookey (1970). Samples were subsequently filtered through a 0.2 µm membrane and the light absorbance (562 nm) measured using a spectrophotometer.

3.8.4 VFA analysis

1ml of filtered sample was added to 1 ml of octane sulfonic acid (OSA) and left in a sonication bath for 30 mins in order to remove any carbonate that would co-elute with propionic. Ion-chromatography (Aquion 2) was then used to measure VFA concentrations, including acetate, butyrate and formate. A calibration curve was calculated for each VFA using 5, 10 and 100 PPM standards. The run time was 35 mins per sample. A guard column and main column were used (Ion Pac ICE-ASI). The guard column has dimensions 4 x 50mm and the main columns is 4 x 250 mm. The flow rate was 0.16 ml/min, with a Dionex suppressor (ACRS-ICE 500) and a conductivity detector. The eluent used was heptafluorobutyric acid and the regenerant was tetrabutyl ammonium hydroxide

3.8.5 Mineral recovery from agar plates

The minerals and precipitates were recovered from the underlying agar by adding deionised water to the agar followed by heating the mixture to approximately 70°C in a crystallizing dish over a Bunsen burner. The liquid was then pipetted off and discarded. Minerals were then washed and heated 3 times with deionised water before being collected and dried in microcentrifuge tubes under anaerobic conditions.

3.8.6 Significance testing:

ANOVAs were carried out on measured variables from comparisons between live and control experiments using RStudio (RStudio, 2020) to determine the significance of the difference in means according to P-values. Additionally, Stamp (Mahony & Benos, 2007; Mahony et al., 2007) was used to construct box plots and PCA plots using QIIME2 outputs.

3.9 Molecular techniques and 16S rRNA sequencing

DNA from frozen pellets derived from MX80 bentonite iron-reducing enrichments (see 3.4.1) was extracted by thawing the samples and heating to 95°C for 10 minutes. Samples were then incubated on ice for 10 minutes and centrifuged at 3000 rpm for 5 minutes. The supernatant, containing the DNA, was collected and stored in clean Eppendorf tubes at -20°C.

Further DNA extractions were carried out using 750 µl of slurry from enrichment experiments (including those conducted under anaerobic and aerobic conditions, with and without powder and compacted MX80 and the *Shewanella* inoculated control). DNA was extracted using a PowerSoil DNA Isolation Kit (MoBio) according to manufacturer's instructions. Briefly, a bead beating method is used to homogenise the soil sample; the cells are then lysed, and DNA precipitated by adding a series of chemical reagents; finally, the DNA was precipitated and purified by washing on a silica membrane. The final step was amended from the manufacturer's instructions by eluting the DNA in 50 µl of the final solution (C6) instead of 100 µl to increase the DNA concentration.

DNA extraction success was confirmed and, concentrations quantified, using QuBit. A PCR amplification was then carried out using Golay barcoded primers which target the V4 variable region of the 16S gene (515-926) (Caporaso et al. 2010). Amplification was confirmed on a 1% agarose gel stained with ethidium bromide. Samples were then sent for Illumina 16S rRNA sequencing at NU-OMICS, Northumbria University.

Illumina 16S rRNA gene sequencing outputs were received as demultiplexed .fastq files and were analysed using the QIIME2 pipeline which included amplicon sequence variant (ASV) selection using DADA2 (Casporaso et al., 2010; Callahan et al., 2016), community barplots for each taxonomic level and heatmaps were also generated from this pipeline. Further analysis was carried out through construction of phylogenic trees using BLAST (Altschul et al., 1990) to identify highly similar sequences from environmental and cultured isolate sources, and then using Muscle to align sequences. Finally, trees were constructed using the neighbour-joining method (Saitou and Nei, 1987) and bootstrap values were determined according to Felsenstein (1985).

3.10 Further analysis techniques:

3.10.1 XRD:

XRD is commonly used to analyse mineralogical composition of soils and clays among other substances. Figure 3.8, shows a simplified diagram of this method whereby x-rays diffract off crystal planes resulting in diffracted waves. By applying the Bragg's law for powder diffraction, the distance between the crystal planes can be measured and subsequent mineral identification can be conducted (Moore and Reynolds, 1997) (equation 6).

$$n\lambda = 2d_{hlk} \sin\theta \quad [6]$$

Where: *d* = d-spacing (Å)

2θ = beam deviation (º)

h,l,k = dimensional components for the lattice planes

n = an integer that represents higher order scattering (for MX80, this is assumed to equal 1)

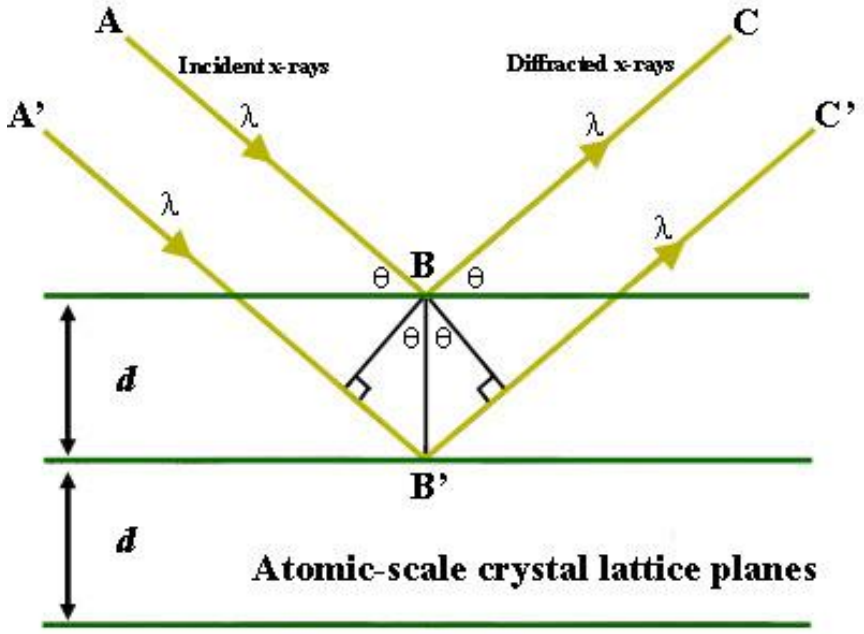

Figure 3.8: A simplified schematic of XRD. The distance between paths ABC and A'B'C' differs by an integer number of wavelengths (Henry et al., 2018)

Bulk powder scans enabled the principle mineral identification including silicates and oxides. Samples were ground with a pestle and mortar after air-drying under anaerobic conditions. Samples were then run (PANalytical X'Pert Pro Multipurpose Diffractometer) using Cu as the target metal, as standard, (λ = 0.154nm) for 5 hours.

Spectra were obtained as .raw files and analysis including mineral identification and spectrum fitting was run using HighScore Plus. As part of this analysis peaks were characterised using a mineral database (ICDD 1999 and COD 2016). Reitvald refinement was run in HighScore Plus to ensure a good fit (Chi Square ≤8).

3.10.2 SEM and EDX

Samples ground with pestle and mortar were also analysed by scanning electron microscopy (SEM) (Tescan Vega 3LMU) and electron dispersive X-ray spectroscopy (EDX) (Bruker XFlash® 6 | 30 detector). Samples were mounted on carbon tape for EDX analysis whereby X-rays and an incident beam are aimed at the sample. The resulting electron scatter allows for elemental identification and quantification. Samples were then coated with gold for SEM imaging by Electron Microscopy Research Services (Newcastle University) and analysed to observe mineralogical changes and biological forms and colonisation.

3.10.3 Plasticity index

The PI of the MX80 bentonite was calculated as the difference between the liquid limit and the plastic limit, as described in British Standards, BS:1377: 1990: Part 2, section 3.4, 3.5. Briefly, the calculation of the plastic limit entails determining the moisture content (see section 3.3.1) of the clay when it begins cracking (shears longitudinally and transversely) at a diameter of 3 mm. This diameter is achieved by hand-rolling the clay on a glass sheet. The process must use at least 10 g of sample and be repeated to ensure consistent results (consistency is defined as within 2% moisture content). The liquid limit is determined by the moisture content (see section 3.3.1) of the clay at the point which a cone of defined dimensions penetrates 20 mm into the clay over 5 seconds (in a container measuring 55 mm diameter, 40 mm depth). This is done by measuring the cone penetration at 4 moisture contents and plotting them on a graph. To ensure consistent results, the cone penetration must be repeated for each moisture content and the results must be within 0.5 mm of the first test.

Chapter 4. Indigenous microbial communities and their basal activity in relation to iron-reduction

This chapter details the results of a series of microbial enrichments of MX80 bentonite and the characterisation of the resulting microbial community. A research gap identified in the literature review was the lack of knowledge of the indigenous iron-reducing community. There had previously been few attempts to characterize the viable microbial community of MX80 bentonite. Without this information, it is not possible to infer what the potential microbially-induced mineralogical alterations could occur in the MX80 bentonite or what the possible rate of MIC of carbon steel canisters could be in the repository.

The associated methods are presented in section 3.4. Briefly, anaerobic microcosms with MX80 bentonite were set up using Sellafield-like groundwater enriched with carbon. PCFeO provided selective pressure for iron-reducers. The Fe (II), pH and volatile fatty acids were measured and the resulting microbial community was analysed. This was then repeated in aerobic conditions and with higher salinity groundwaters.

4.1 Publication: An indigenous iron-reducing microbial community from MX80 bentonite - A study in the framework of nuclear waste disposal

The following paper presents the results and discussion for the anaerobic iron-reducing enrichments and the resulting microbial community. The iron-reducing activity of these microbes is also discussed. All experimental work and analysis were carried out by the first author. DOI: https://doi.org/10.1016/j.clay.2021.106039

Applied Clay Science 205 (2021) 106039

Contents lists available at ScienceDirect

Applied Clay Science

journal homepage: www.elsevier.com/locate/clay

Research Paper

An indigenous iron-reducing microbial community from MX80 bentonite - A study in the framework of nuclear waste disposal

Katie A. Gilmour[a,*], Colin T. Davie[a], Neil Gray[b]

[a] School of Engineering, Newcastle University, Newcastle upon Tyne NE1 7RU, UK
[b] School of Natural and Environmental Sciences, Newcastle University, Newcastle upon Tyne NE1 7RU, UK

ARTICLE INFO

Keywords:
Deep geological disposal
Microbial community
MX80 bentonite
Iron
Iron-reducing bacteria
Microbial enrichment

ABSTRACT

Highly compacted MX80 bentonite has been selected as the engineered buffer and backfill material in several proposed concepts for long-term deep geological storage of nuclear waste. Iron-reducing bacteria reduce Fe (III) to Fe (II) and some are adapted to high temperatures and desiccated environments, in keeping with periods of less habitable conditions within the repository. In one potential UK repository concept, iron from carbon steel canisters may contribute to an iron-rich environment at the clay-canister interface. This could lead to changes in the mineralogy and iron-content of MX80 bentonite due to variation of the redox state and solubility, which in turn could alter the geomechanical properties of the clay. To investigate the potential role of iron-reducing bacteria in this process enrichments were carried out with both commercially available MX80 bentonite powder and compacted MX80 bentonite to identify the presence of an indigenous iron-interacting community in the clay. Throughout these enrichments Fe (II) soluble, Fe (II) total, and pH were measured, and the enrichments were subjected to 16S rRNA community analysis. Concentrations of Fe (II) total peaked at day 28 in all enrichments; however, the concentration was overall higher when accompanied by bacterial growth. Fe (II) soluble remained low throughout. 16S rRNA gene sequencing revealed the presence of several putative iron-interacting bacteria, as well as thermotolerant and spore-forming species. The indigenous community was largely comprised of firmicutes, including iron-reducers and spore-forming bacteria such as *Desulfosporosinus*. Therefore, MX80 bentonite inherently carries a viable microbial community which could potentially interact with structural iron present within MX80 bentonite or other mineral components, such as a carbon steel waste canister. Various research has shown that microbial activity is unlikely within the bulk bentonite provided high compaction is maintained. The importance of this high compaction is highlighted by the finding here of a viable, robust and functionally diverse community within the clay and activity may be possible anyway at edge sites and interfaces where, locally, swelling pressures might not fully develop.

1. Introduction

Several countries across Europe, Asia and North America are considering nuclear waste disposal by deep geological storage, including the UK (Arlinger et al., 2013; IAEA, 2018; NDA, 2010). Most designs for high level waste include a compacted clay infill to create a barrier between durable metal waste canisters and the host rock (Fig. 1).

In the UK, this method could consist of encasing vitrified nuclear waste in a carbon steel container at a depth of up to 1000 m below the surface (NDA, 2016). The clay widely proposed for use in nuclear repository multi-barrier designs is compacted Wyoming MX80 bentonite (NDA, 2016; Jönsson et al., 2009; Bradbury et al., 2014; Kiviranta et al., 2018). This clay, which will also be used as a backfill to seal the entry to repository tunnels, has been selected due to its high swelling ability; low porosity; low hydraulic conductivity; and high thermal conductivity (Sellin and Leupin, 2013; Wilson et al., 2010).

Several studies have previously been carried out to assess and predict any changes to the geomechanical properties of MX80 bentonite throughout the lifespan of the repository (Wilson et al., 2010; Leupin et al., 2017; Davies et al., 2018; Jönsson et al., 2009; Karnland, 2010). Aside from exposure to radiation and changes in moisture content, temperature, and pressure, another potential threat to the integrity and longevity of the repository is microbial activity; namely, microbially influenced corrosion (MIC) whereby microbes or secreted by-products

* Corresponding author.
E-mail address: k.gilmour2@newcastle.ac.uk (K.A. Gilmour).

https://doi.org/10.1016/j.clay.2021.106039
Received 18 July 2020; Received in revised form 19 February 2021; Accepted 22 February 2021
Available online 6 March 2021

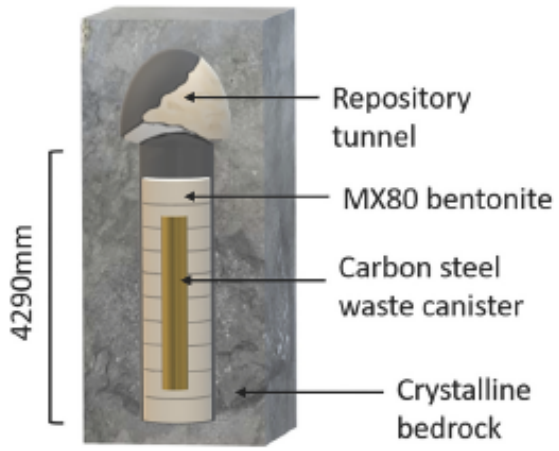

Fig. 1. Schematic of proposed method of geological disposal of nuclear waste (adapted from SKB, 2006).

(Kip and Veen, 2015) could increase the rate of corrosion of the waste canister. Certainly concerns have been raised relating to microbial micro pitting (Philp et al., 1991) of the steel and biofilms may provide a favourable environment for MIC via the creation of multiple nucleation points for iron- or sulfate-reduction (Konhauser, 2007; Konhauser, 1997). Additionally, microbial activity might cause clay dissolution or clay mineral transformation (Leupin et al., 2017) that might impact the effectiveness of MX80 bentonite as a barrier. Conversely, the formation of biofilms could be beneficial to the multi-barrier system by creating another physical barrier between the canister surface and hydrosphere (Jayaraman et al., 1997) .

The repository lifespan is predicted to be 10,000–100,000 years (Yang et al., 2019) and microbial presence and activity during this time is thought possible either from communities introduced during repository construction, or during the processing of MX80 bentonite into compacted bricks (Stroes-Gascoyne and West, 1997; Motamedi et al., 1996) or introduced from later groundwater and the host rock interactions (Pedersen, 2000; Chi and Athar, 2008). However, it is also expected that throughout the lifespan of the repository the environment will change which could have an impact on the composition of the microbial community and the properties they will possess to survive long periods of unfavourable conditions – either in an active or dormant state. For instance, it is likely to take 10s of years to fill and seal the repository (e.g. NAGRA Swiss nuclear waste management organisation, Landolt et al., 2009). Post-closure, the repository environment will likely increase in temperature, from 40 °C to 70 °C at the host rock / clay interface, and up to 100 °C at the canister surface (RWM, 2016), before decreasing again, and slowly develop to anaerobic conditions. Any bacteria present would also be subject to developing high pressure, high temperature and low water availability (Landolt et al., 2009).

This progressive change, together with the fact that the average micro (intra-aggregate) pore size of compacted saturated bentonite is $\leq$0.02 μm when compacted at a range of dry densities (dry density = $\geq$ 1.6 Mg/m^3) (Wang et al., 2013; Jalique et al., 2016) hugely limits the habitability of the barrier (Stroes-Gascoyne et al., 2011) as pore size is smaller than the average bacteria. However, areas in the backfill and at the host rock / bentonite interface, as well as fractures in the host rock, may allow for limited microbial growth and survival. These areas will not only be cooler but swelling bentonite may not have sealed all gaps and so space may be available for microbial life to proliferate (Wilson et al., 2010; Jalique et al., 2016; Stroes-Gascoyne et al., 2011).

With respect to the chemistry of the MX80 bentonite, it contains 0.11–0.4% wt. organic carbon, the upper limit of which is considered adequate to support microbial life (Sauzeat et al., 2001); however, it is considered likely that the majority of the carbon present is recalcitrant (Marshall et al., 2015) and therefore not available for microbial growth. It is also composed of several iron-containing minerals and in total contains ~4% wt. iron (Karnland, 2010) with ~20% of this iron estimated to be Fe (II) and the remainder Fe (III). Carbon steel canisters, and their subsequent rust products, would also contribute iron to the repository environment (Bradbury et al., 2014; Necib et al., 2017; Davies et al., 2018). These various sources of iron could allow growth of iron-interacting bacteria to interact with the clay barrier material. Such interactions could result in chemical changes to the mineralogy, and hence the properties of the clay barrier, including through changes to iron redox state and solubility leading to conversion of smectite to non-swelling Fe (II) rich phyllosilicate minerals (Bradbury et al., 2014). Several mineralogical changes could occur by direct or indirect bacterial interactions (Konhauser, 1997), which in the repository would allow isolated bacteria to impact a wider area of the clay barrier or canister surface. This impact could include pitting due to microbial excretion of H^+, organic acids and other metabolites (Uroz et al., 2009) which could result in an increase (Sahin et al., 2011) or decrease in the hydraulic conductivity (Glatstein and Francisca, 2014) of the clay barrier. There are also several bacteria that either oxidise elemental iron or Fe (II) to Fe (III) (Konhauser, 2007) as an electron donor or reduce Fe (III) to Fe (II) (Morgado et al., 2012). Such effects could modify the performance of the MX80 bentonite to function as an effective barrier and it is therefore important to understand if any iron-interacting bacteria are naturally present in MX80 bentonite, and if so, what their long-term survival prospects are. For instance, it is important to know how the process of homogenising and compacting the clay may facilitate or inhibit microbial growth and activity.

The ability of microbes to grow in MX80 bentonite is well documented. A number of microbial species have previously been isolated from raw and commercial bentonites, and further studies have shown that non-indigenous model organisms have been able to proliferate in MX80 bentonite under in vitro conditions (RWM, 2017; Masurat et al., 2010; López-Fernández et al., 2014; Jalique et al., 2016; Pedersen, 2000; Chi and Athar, 2008). However, indigenous iron-interacting bacteria, and their activity within the buffer, have not been extensively studied because many international designs, notably KBS-3 (Bengtsson et al., 2015) include copper canisters for high level radioactive waste containment instead of carbon steel. In such designs sulfate reduction by sulfate-reducing bacteria (SRBs) has been considered a more significant safety risk. However, both SRBs (Eydal et al., 2009) and iron-reducing bacteria (IRBs) have been isolated from groundwater at the repository sites in Sweden and Switzerland (Svemar et al., 2016). Furthermore, a study by Svensson et al. (2011) did identify the presence of IRBs in MX80 bentonite; however, only 5 species are reported in the sequencing results (all of which belong to *Clostridium* sp. or *Desulfotomaculum sp.*). The presence of IRBs is important even in the absence of a steel waste canister, as structural iron will still be present within the clay. The redox state and solubility of this iron is an important factor in the behaviour of the clay and its ability to perform as a barrier.

The purpose of this study was to identify the presence and potential iron-reducing ability of an indigenous microbial community associated with MX80 bentonite. Previously, studies to determine the indigenous microbial community of bentonite have been unsuccessful due to low DNA yields arising from sparse cell numbers or the clay interfered with DNA extraction methods (Stone et al., 2016; Poulain et al., 2008; Urios et al., 2012). Our own attempts to extract and PCR amplify DNA from the unenriched clay were also unsuccessful necessitating an enrichment approach. These experiments, therefore, did not mimic the conditions within the repository in terms of pressure, temperature or carbon availability. Enrichments were made with the specific intention of evaluating the diversity and function of the indigenous iron-reducing bacteria in a clay sourced, stored and transported without any attempts at sterilisation or acclimatisation to in situ anaerobic groundwater conditions. By using this method, the effects of the compaction process on the introduction of new species, or limitation of the existing iron-reducing community in the clay could be assessed. Unlike previous

studies, this method also allows us to characterise the activated microbial community as opposed to the dormant DNA present in the MX80 bentonite. To determine the role of the clay more generally in sustaining and carrying viable iron-reducing bacteria, enrichment microcosms were carried out with and without the provision of an exogenous iron-reducer. The nature of the enriched organisms and their responses and tolerances to different environmental conditions, such as those experienced during compaction into MX80 bentonite rings, transport and storage and the general ability of a microbe to become active in MX80 bentonite, will provide a predictive framework for consideration of real-world settings.

2. Methods

2.1. Details of MX80 bentonite

Wyoming MX80 bentonite powder (known as Bentonex WB, supplied by RS minerals®) was sourced with a bulk composition of 87% montmorillonite, ≤ 1% gypsum, ≤ 4% feldspars, ≤ 2% quartz (RS®Minerals, 2017). Compacted Wyoming MX80 bentonite blocks were sourced from SKB's (Svensk Kärnbränslehantering AB - Swedish nuclear waste management organisation) supplier (ClayTech AB®) (27% wt. water = 97% saturation, 1.56 Mg/m^3 dry density, corresponding to a swelling pressure of 4–5 MPa (Börjesson, 2010)). The mineralogical composition of this bentonite (averaged from 6 samples, (Karnland, 2010)) contained 81.4% montmorillonite, 0.9% gypsum, 3% quartz, 3.5% plagioclase, and 11.2% other. The compacted blocks were stored in sealed bags in at 20 °C for 3.5 years before this experiment. It was envisaged that the compaction process could introduce different microbial taxa (including iron-reducers) through water mixing and handling in addition to those already associated with the 'as received' bentonite. Alternatively, microbial species could be lost.

2.2. Composition of synthetic groundwater for use in microcosms

The UK has not yet selected a location for its nuclear waste repository and so for this enrichment study a Sellafield-like groundwater was used as a proxy in enrichment microcosms because it is representative of UK groundwaters, and has been used in other studies in connection with nuclear waste disposal in the UK. Synthetic Sellafield-like groundwater (Wilkins et al., 2007) composed of (g/L) KCl, 0.0066; $MgSO_4.7H_2O$, 0.0976; $MgCl_2.6H_2O$, 0.081; $CaCO_3$, 0.1672; Na_2SiO_3, 0.0829; $NaNO_3$, 0.0275; NaCl, 0.0094; $NaHCO_3$, 0.2424 was enriched with a carbon mix to give total concentrations (g/L) of tryptic soy broth, 3; butyric acid, 0.27; sodium acetate, 0.18; and sodium lactate, 0.336. The carbon sources chosen are suited to most bacterial metabolisms, allowing the added iron (see next section) to provide the selective pressure on the community.

2.3. Preparation of poorly crystalline Fe (III) oxide (PCFeO)

In order to favour and encourage proliferation of iron-reducing bacteria an exogenous iron oxide was added to enrichment microcosms. Poorly crystalline Fe (III) oxide (PCFeO) is a highly bioavailable form of ferrihydrite (Lovley, 2013) and so was considered most suitable for this study. Briefly, a 1 M solution of PCFeO was produced according to Lovley (2013) in which 0.4 M $FeCl_3{\cdot}6H_2O$ was neutralised to pH 7 with 10 M NaOH and then stirred constantly for 30 min before being repeatedly washed and resuspended in distilled water.

2.4. Preparation of Shewanella oneidensis

Shewanella oneidensis MR-1 (NCIMB 14063) is a known iron-reducer and heavy-metal tolerant species which can respire anaerobically and thus thrive in these enrichments and act as a positive control for iron-reduction. A starter culture was grown aerobically in 10 mL Luria–Bertani-50 mM (LB) medium at 20 ± 2 °C until the required cell density (given in section 2.5) was achieved; a cell count using SybrGold was used to confirm. An abiotic control was also included to ensure no contamination had occurred.

2.5. Iron-reducing enrichments

Under anaerobic conditions (using a vinyl anaerobic chamber, Coy Lab Products) - 95% nitrogen: 5% hydrogen, 4 g of unsterilized bentonite powder (as received) and PCFeO (equivalent to 20 mM dissolved Fe (III)) was added to 100 mL synthetic groundwater in 120 mL serum bottles (x 3 replicates) sealed with butyl stoppers and aluminium crimps. All enrichments were incubated at 20 ± 2 °C for 7 weeks under anaerobic conditions. As a control to attribute iron-reduction to microbial activity rather than geochemical activity (Sterile MX80 Powder), bentonite was sterilised in a dry oven at 105 °C for 48 h and used in place of the unsterilised bentonite in set of replicated (x3) microcosms. Sterility was confirmed by spreading the clay on a 1.5% LB agar plate to identify growth, plates were incubated at 20 ± 2 °C for 1 week under anaerobic conditions. No growth was observed on agar plates. Therefore, it is inferred that no microbial growth or activity occurred in the sterile controls.

An additional replicated control was included which excluded bentonite (No MX80) to ensure that any Fe (II) detected in the sterile control originated from the clay and was not due to abiotic interactions with the groundwater or carbon mix. In addition to the bentonite powder enrichments another set of microcosms were set up using 4 g of compacted bentonite (taken from a compacted block using a sterilised dry band saw) along with a set of sterile compacted bentonite controls and an additional control set in which 100 μL of a cell suspension (2×10^7 cells/mL) *S. oneidensis* was added. Sub-sampling was taken weekly for 7 weeks by shaking samples and then sampling 5 mL of representative slurry. pH was recorded and Fe (II) soluble, and Fe (II) total were measured using the Ferrozine method, (Lovely and Phillips, 1986). In order to separate Fe (II) soluble, samples were filtered (0.2 μm filters) prior to the assay.

2.6. DNA extraction and microcosm community structure analysis

The enrichment method adopted in the current study, combined with 16S rRNA gene sequence analysis, focused on a subset of the microbial community able to catabolise the added organic matter under anaerobic (specifically iron-reducing) conditions

After 7 weeks of incubation DNA extraction was performed on all the replicates of the microcosm enrichments comprising the compacted and powdered MX80 bentonite. A PowerSoil DNA isolation kit (MoBio) was used with 750 μL of MX80 bentonite/groundwater slurry according to the manufacturer's instructions, except that the final DNA elution step was performed with 50 μL instead of 100 μL elution buffer. DNA extractions were confirmed and quantified using QuBit and PCR amplification was carried out using Golay barcoded primers that target the V4-V5 region (position 515–926) of the 16S rRNA gene (Caporaso et al., 2010) which is widely used for characterisation of microbial communities. PCR amplification was confirmed on 1% agarose gel with ethidium bromide.

Following confirmation of amplification, DNA extracts from both powder and compact experiments were sent to NU-OMICS, Northumbria University for 16S rRNA Illumina sequencing. Raw sequencing data (FastQ files) obtained from the Illumina sequencing platform were then demultiplexed and analysed as part of the QIIME 2 pipeline (Caporaso et al., 2010; Callahan et al., 2016). Additionally, DADA2 was used for ASV (amplicon sequence variant) selection within QIIME2. Phylogenic analysis of representative sequences of dominant taxonomic groups were produced by using BLASTN (Zhang et al., 2000) to identify nearest neighbour and subsequently alignment and similarity values were performed using MEGA7 via the neighbour-joining method of Saitou and

Nei (1987) and bootstraps values were determined according to Felsenstein (1987).

2.7. Statistical analysis of pH and Fe (II) data

Analysis of variance (ANOVAs) were carried out between unsterilised and sterile experiments using Rstudio. The significance of the pH and concentration of Fe (II) was determined between the time-points that reflected the greatest increase of Fe (II) soluble and Fe (II) total in each experiment.

3. Results

3.1. Chemical analysis of the Fe-reducing enrichment microcosms

The pH in all unsterilised bottles decreased to acidic conditions (Fig. 2) in the first week of the incubation period. The pH drop in the unsterilized experiments, with or without the addition of *S. oneidensis*, was significantly greater ($P < 0.05$) when compared to the sterile bottles on days 7–21 (see section 4.1). However, the pH recovered to greater than pH 7 in these unsterilised experiments in the second half of the incubation period.

In all the microcosm enrichments, regardless of experiment composition and sterility, Fe (II) soluble remained low (<0.1 mM) throughout the duration of the experiment; however Fe (II) total concentrations did increase in both the powder and compacted MX80 bentonite amended experiments (Fig. 3). The increase in Fe (II) total in the compacted MX80 bentonite enrichments was similar to that observed in the positive control enrichments which included the bacterium *S. oneidensis*.

Furthermore, the concentration of Fe(II) soluble and Fe(II) total were significantly higher in the unsterilized powder enrichments when compared with the corresponding sterile control where the greatest

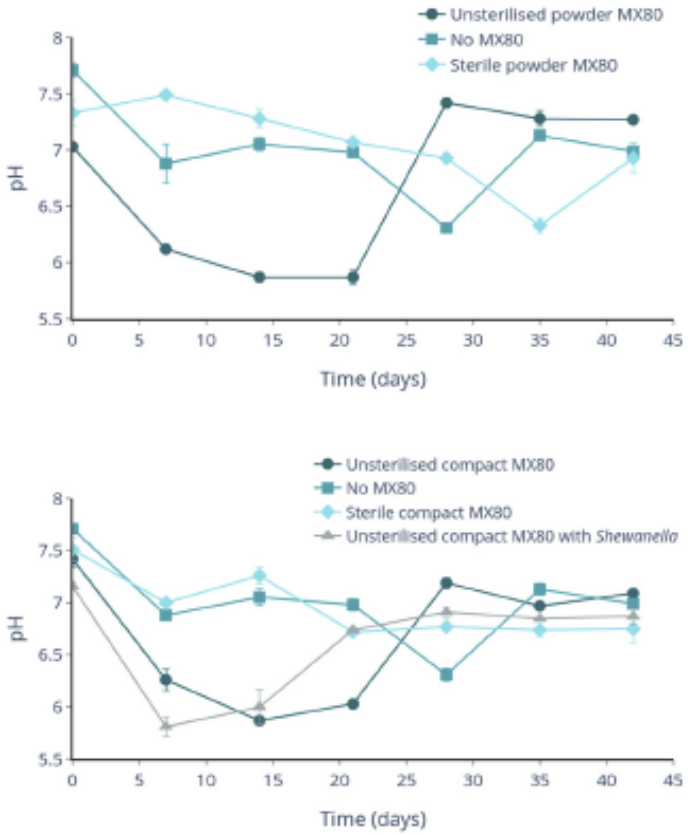

Fig. 2. pH profiles of powdered (top panel) and compact (bottom panel) MX80 bentonite amended enrichment microcosm in comparison with sterilised and bentonite free controls. Error bars represent standard error.

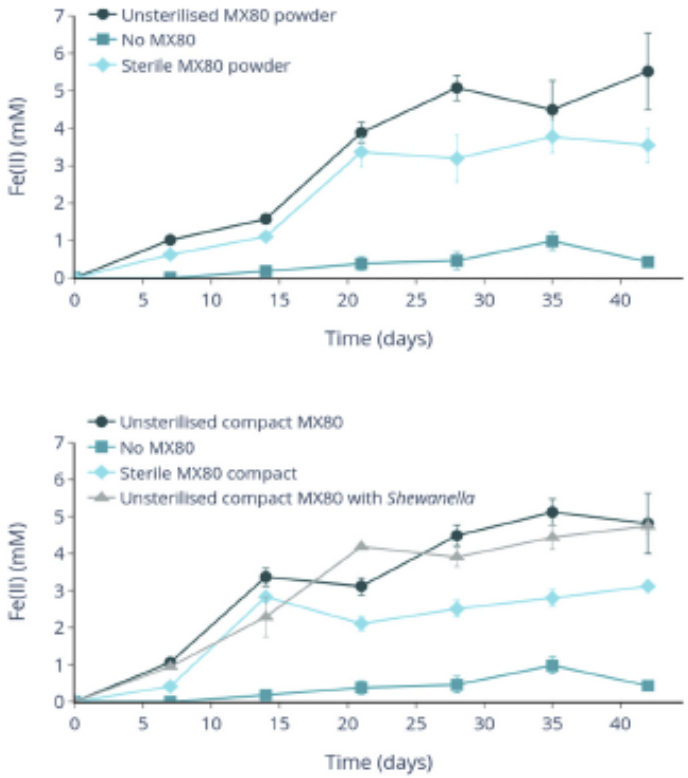

Fig. 3. Fe(II) total concentration profiles in the unsterilised powdered (top) and compacted (bottom) bentonite MX80 bentonite amended iron-reducing experiments in relation to sterilised and bentonite free controls. Error bars represent standard error.

increase in concentration was observed (*P*-values of 0.012 and 0.021, respectively). Likewise, for the compacted experiment the accumulation of Fe (II) soluble was significantly greater in the unsterilized MX80 bentonite than in the sterile control; P-value = 0.018. This was the same for the concentration of Fe(II) total (P-value = 0.014). Therefore, in both types of MX80 bentonite, bacterial presence was an important factor in Fe (II) production.

3.2. Community analysis of the enrichment microcosms amended with unsterilised powdered and compacted MX80 bentonite

Six 16S rRNA PCR amplicon libraries were prepared representing each of the individual replicate iron-reducing enrichments amended with powder or compacted MX80 bentonite. These library sequences have been deposited in the NCBI's Sequence Read Archive (SRA) available under BioProject PRJNA594313. An average total number of sequence reads per library of 65,000 (compact MX80 bentonite replicates) and 48,000 (powdered MX80 bentonite replicates) was obtained at an average length of 227 bases. From these libraries an average of 60 (compact MX80 bentonite replicates) and 110 ASVs (powder MX80 bentonite replicates) per library were identified by the QIIME 2 analysis pipeline. The diversity between samples was low in relation to other studies of bentonite community analyses (López-Fernández et al., 2014), which is likely because these communities were derived from enrichments. The activated microbial community of both the powder and compacted MX80 bentonite was largely composed of taxa assigned to the phylum firmicutes, in particular taxa related to the genera *Bacillus* and *Clostridium*, as well as a large population of *Sedimentibacter* (Figs. 4 and 5). However, there was also a small population of Proteobacterial *Pseudomonas* species which were found to be most closely related to the species *Pseudomonas stutseri* (Fig. 5). Species less than 0.5% relative abundance within the libraries include *Shewanella*, *Gracilibacter*, *Anaerocolumna*, and *Anaerosinus*. The compacted MX80 bentonite community

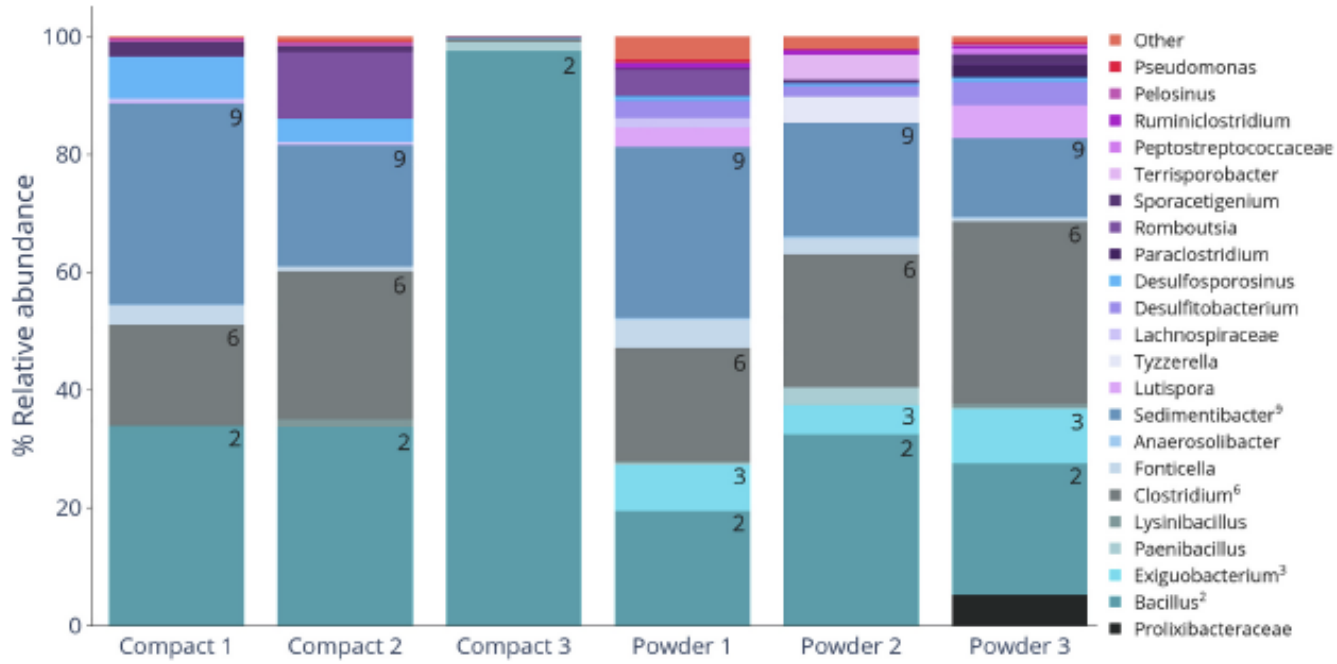

Fig. 4. Partial 16S rRNA gene-based community structure analysis of MX80 bentonite amended iron-reducing enrichments for both compacted and powder MX80 bentonite. The relative abundance (%) of the taxonomic group sequences in amplicon libraries are shown at the lowest taxanomic level to which the constituent ASVs were assignable. "Other" refers to species <0.5% relative abundance. The order the taxa appear in the figure legend corresponds to the order they appear in the stacked bars and the most abundant species have been annotated.

was less diverse than the powder community; however, neither showed high diversity when compared to other microbial communities isolated from similar clays (Engel et al., 2019). It is therefore unlikely that the commercial compaction process has led to an introduction of new species, at least not species which are able to thrive under these enrichment conditions; but rather that the compaction has limited the diversity of the cultivable microbial community. Several of the organisms identified by the 16S rRNA sequencing are putatively thermotolerant (*Desulfosporosinus*); iron-interacting (*Pelosinus* (Brown et al., 2012)); or spore-forming (*Bacillus sp.*). In some instances, species are both putatively spore-forming and iron-interacting, or in the case of *Desulfosporosinus* thermotolerant and sulfate-reducing microbes putatively capable of reducing iron (Kunapuli et al., 2010). In fact, spore-formers made up an average of 74.2% relative abundance of the microbial community of the compacted samples, compared to 56.2% relative abundance amongst the powder samples. However, there were more individual species of spore-former present in the powder samples.

4. Discussion and conclusions

There are several conclusions to be drawn from these enrichment studies related to the intrinsic and viable presence of anaerobic, hydrolytic, and fermentative bacteria and bacteria capable of iron reduction likely linked to oxidation of volatile fatty acids (VFAs). These conclusions are principally supported by the chemical data from the microcosm implying the growth and activation of anaerobic bacteria and further supported by the putative functions of such organisms identified by the community.

There may have been a motility issue with iron measurements in that the iron was not evenly distributed and may have been trapped in localised areas by swollen MX80 bentonite despite regular shaking, therefore, the results may underestimate the iron present. It is also not clear what percentage of iron reduced was structural iron in the clay as opposed to external PCFeO iron. These results suggest there is no soluble iron present at any stage which leads to the question of how much iron reduction is due to direct reduction by bacteria, or indirect by bacterial sulfate reduction or through reduction by secreted VFAs and metabolites.

4.1. Indigenous fermentative and iron reducing bacteria in the MX80 bentonite

As briefly described in the results, and indicated by both pH, and iron data – and further supported by species identification – it is likely that the majority of the energy for growth available from the organic matter added to the experimental microcosms is initially utilised by fermentative bacteria. This is likely because the initial carbon mix added to the microcosms contained various carbon sources, largely composed of amino acids and volatile fatty acids including lactate (eq. 1) which are readily fermentable to acetate and hydrogen. This variety allowed for a large range of organisms to grow without selective pressure from the carbon source or availability. These fermentation products can then be readily utilised by iron-reducing bacteria (eqs. 2 and 3). Such a sequence is evidenced by an increase in pH on day 14 after an initial decrease to acid conditions coincident with an increase in measured biotic iron-reduction, suggesting that during days 0–14, hydrolytic and acidogenic fermentation dominated as a proton generating process, resulting in VFA production and the pH drop (eq. 1). Subsequently, the dominant metabolism shifted to a consumption of acetate and hydrogen, which are the end products of mixed acid fermentation, coupled to iron-reduction (eq. 2 and 3) which are reactions that consume protons.

$$CH_3CH(OH)COOH + H_2O = CH_3COOH + CO_2 + 2H_2 \quad (1)$$

$$8Fe(OOH) + 16H^+ + CH_3COOH = 2CO_2 + 8Fe^{2+} + 14H_2O \quad (2)$$

$$2Fe(OOH) + H_2 + 4H^+ = 2Fe^{2+} + 4H_2O \quad (3)$$

In support of this theory, several species of fermentative bacteria including those that putatively utilise VFAs and amino acids, were identified in the enrichment sequence libraries. These fermenting bacteria include *Fonticella* and *Anearovorax*; both non-spore forming, thermophilic anaerobes that can metabolise amino acids (Fraj et al., 2013; Matthies et al., 2000). Interestingly, *Pelosinus* has also been classed as a fermentative bacterium that utilises Fe (III) as an electron acceptor

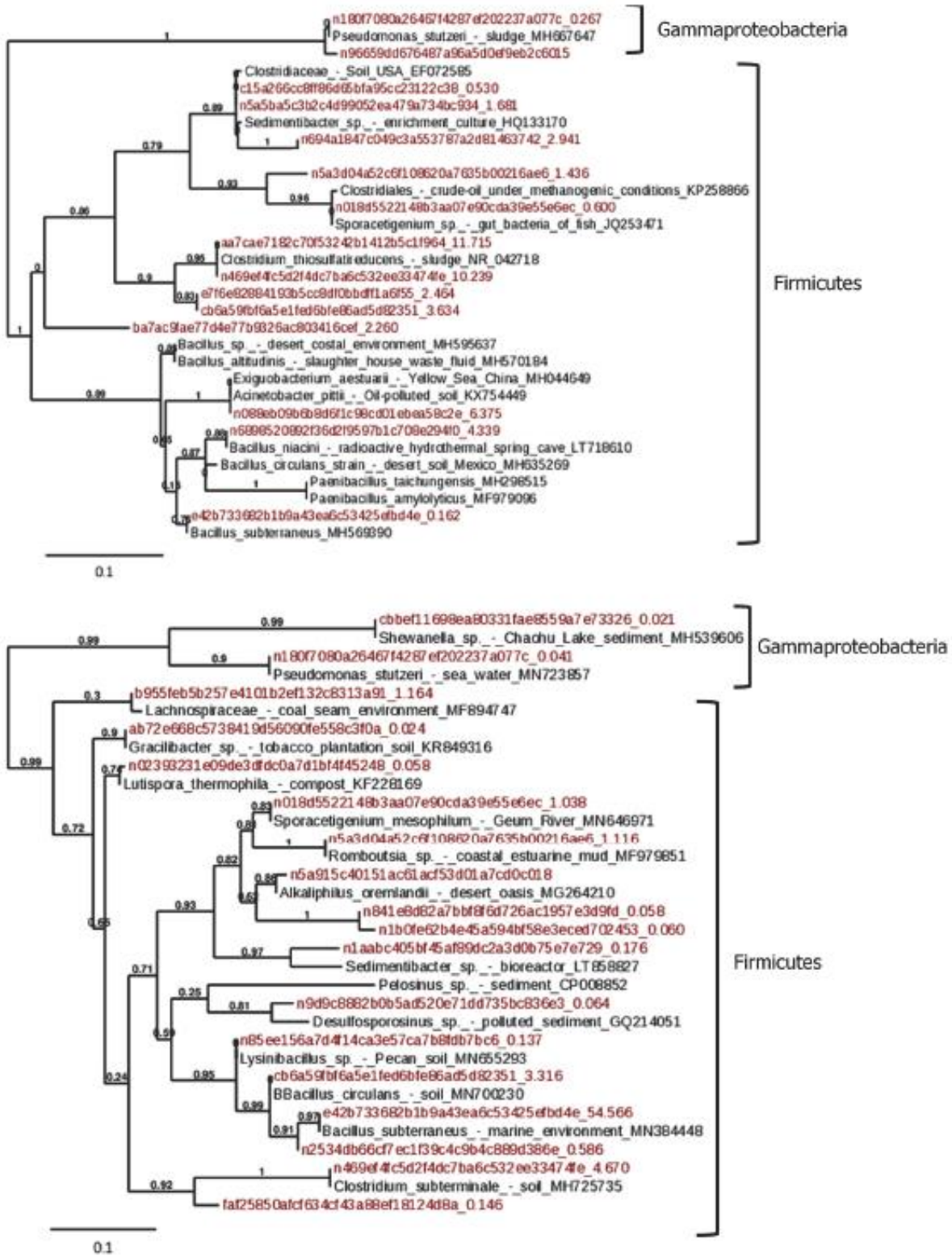

Fig. 5. Phylogenic distance trees based on comparative analysis of partial 16S rRNA sequences recovered from (Top) the iron-enrichment microcosms with MX80 bentonite powder and (bottom) from iron-enrichments with compact MX80 bentonite compared with their closest related species. Sequences were analysed to nearest neighbour using BLASTN (GenBank database), and then aligned and trees constructed using MEGA7. Scale bar denotes 10% sequence divergence.

(Shelobolina et al., 2007). Furthermore, whilst *Romboutsia* can also ferment amino acids, the genus additionally includes species that can utilise a wide variety of forms of carbon including fructose, glucose and maltose as sole carbon sources (Gerritsen et al., 2017) in addition to utilising VFAs such as acetate.

The other major VFAs produced by bacteria are butyrate and propionate. Studies carried out with sediment cores show that the bacteria present can metabolise and remove VFAs from soil (Orcutt et al., 2013; Burdige, 1993). It is likely that a similar cycle of generation of VFAs by some of the firmicutes to sustain both firmicutes and other bacteria present in MX80 bentonite is occurring in the microcosms (Fig. 6).

Also, of interest, *Sedimentibacter* is a strictly anaerobic gram-positive, spore-forming, genus. These bacteria utilise several amino acids and can perform a Stickland-like reaction by degrading glycine and lysine to

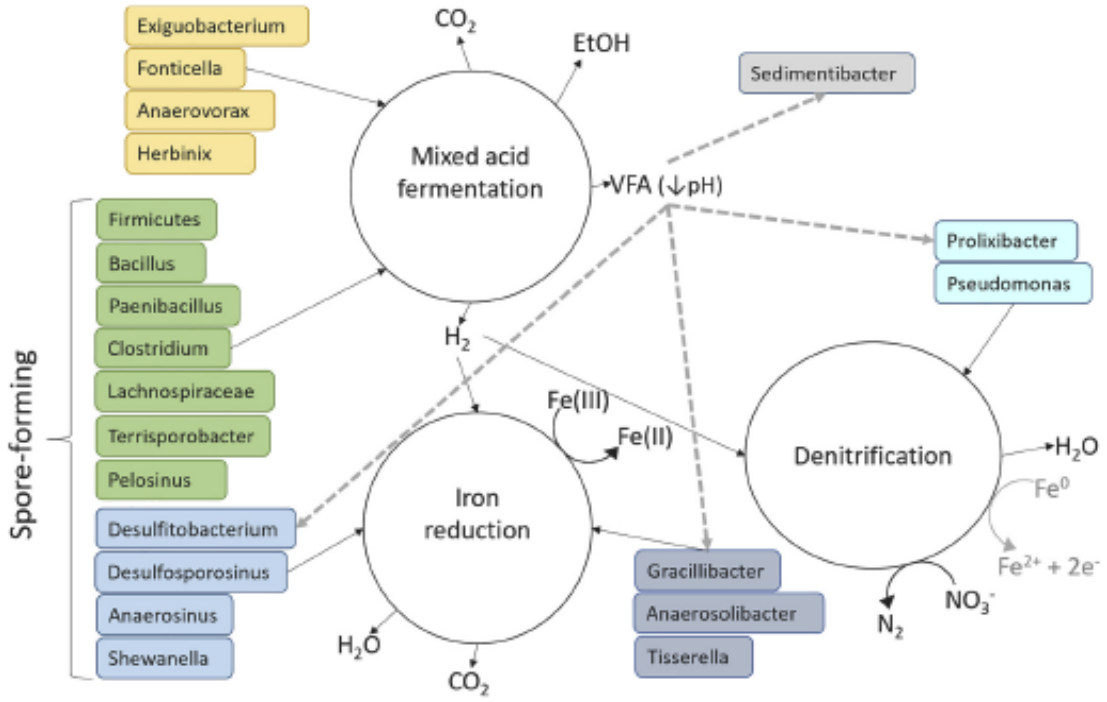

Fig. 6. Schematic of relevant microbial processes of the dominant species identified in both powder and compact MX80 bentonite enrichment. Bacteria have been grouped by function e.g. spore-forming fermentative bacteria, and denitrifying bacteria. Syntrophic relationship between VFA producers and utilisers (gray dashed line) is highlighted.

produce organic acids (Brietenstein et al., 2002; Zhang et al., 1994). In addition to amino acids, pyruvate is a common energy source for the growth of this genus. Most notably, many members of *Bacillus*, which has an average relative abundancy of 55% in the compacted enrichments and 25% in the powder enrichments, are fermenting bacteria. Interestingly, with respect to the use of MX80 bentonite in the geological disposal of radioactive waste one enriched ASV was found to be 100% similar to a *Bacillus* species identified in a radioactive spring cave (Fig. 5) which may indicate a tolerance to radiation. It is likely that the high percentage of *Bacillus* sp. in the compacted MX80 bentonite samples is responsible for the high relative abundance of spore-formers in these samples compared to powder samples. Spore-formers were expected in the compacted samples as spore formation likely allowed samples to withstand storage in the compacted MX80 bentonite, the challenges of which were not matched in the powder samples. However, as there was a larger variety of spore-forming bacteria in the powder MX80, it suggests that spore-formation alone is not sufficient to survive in compacted MX80 bentonite.

Other species identified have putative characteristics which may aid them in surviving the repository environment, including endospore formation, and facultatively anaerobic respiration (allowing the organism to survive changes in oxygen concentration). For instance, *Paenibacillus* is widespread across the enrichments with an average relative abundance of 0.88%. This genus contains anaerobic, endospore-forming bacteria. *Lutispora*, found mainly in the powder enrichments but identified in all libraries is a moderately thermophilic and anaerobic bacterial genus which has also been classed as a chemo-organotroph (Shiratori et al., 2008).

Additionally, iron-reduction within clays was observed in both unsterilised and sterile experiments. *S. oneidensis*, a model organism for iron-reduction (Ruebush et al., 2006; Arango and Schlegel, 1981) was used as a positive control but was also found to be indigenous to the MX80 bentonite; however, the compact MX80 bentonite only contained very low concentrations *of S. oneidensis*. It is therefore significant that the powder MX80 bentonite had a higher concentration of reduced iron than the positive control, and the compact MX80 bentonite had a similar concentration despite the lack of *S. oneidensis* - this indicates a high iron-reducing capability of the indigenous microbial community. However, sequences related to *Exiguobacterium aestuarii* were present in all powder enrichments (6.38% relative abundance), but were absent from compacted samples, most likely because it is non-spore forming (Kasana and Padney, 2017) and therefore was an unlikely candidate to survive in the compacted clay barrier. This species is a facultatively anaerobic bacterium that has been linked to iron-reduction through other enrichment studies, such as Sawayama (2006) which identified *Exiguobacterium* sp. in an anoxic flow-through reactor containing anaerobically digested waste treatment sludge.

There were also several iron-interacting bacteria that were indigenous to both the powdered and compacted MX80 bentonite that are able to reduce Fe (III) under favourable conditions (Fig. 6) such as *Desulfosporosinus* (Kunapuli et al., 2010). Interestingly, a study by Nixon et al. (2017) found that in addition to *Desulfosporosinus*, other bacteria presented here were also present in iron-reducing enrichments, i.e., *Pelosinus*, *Clostridium*, *Anaerosinus* and *Desulfitobacterium*. There is therefore strong evidence to implicate these bacteria, as iron-reducers, and as species involved in the iron-reduction observed in these experiments. However, whilst *Desulfosporosinus* was present in all enrichments (3.62% relative abundance in compact samples and 0.64% in powder samples), *Desulfitobacterium* was only present above 0.1% relative abundance in the powder samples. Therefore, it is not necessarily the ability to form spores which allowed survival in the compacted bentonite. In this case the bacterial survival could be due to differences in metabolism; *Desulfosporosinus* is able to: survive autotrophically with H_2; ferment lactate; and utilise butyrate as an electron donor; whereas, *Desulfitobacterium* does not use these metabolic processes (Spring and Rosenzweig, 2006). Similarly, *Anaerosinus* was also only present in the powder enrichments; however, its lack of spore formation (Strömpl et al., 1999) may account for its inability to survive in the compacted bentonite. It is also possible that these minor differences between the compacted and powder microbial communities are not due to survival but relate to the specific sample of bentonite – i.e. the microbial community is unlikely to be homogenous throughout the compacted block. Further to this, Engel

et al. (2019) found that the microbial community differed between batches of commercial MX80 bentonite, let alone local community variations within one compacted block.

The presence of these bacteria putatively capable of iron reduction is consistent with the measured reduction of the added PCFeO and potentially some of the structural iron present within the clay, to the same concentration achieved by the added *S. oneidensis*, a known iron reducer. The increase in the difference in Fe (II) total between sterile and unsterile samples coincided with the increase in pH, which is likely when fermentation no longer dominated the system and biological iron-reduction via a combination of acetate and hydrogen oxidation began; therefore, acting as further evidence of the role of VFAs in iron reduction.

Some abiotic iron reduction did also apparently occur, which was not an unexpected finding for these clay-amended enrichments. For instance, the abiotic reduction of structural iron within a clay is known to occur at edge sites because the redox-reactivity of structural Fe (III) in clay is greatly increased in the presence of Fe (II). Studies show that addition of Fe (II) can also catalyse iron reduction (Ilgen et al., 2019), but no Fe (II) was added to the MX80 bentonite microcosm enrichments presented here. However, there is some Fe (II) present in the clay (Sander et al., 2014) which could have either influenced the reduction reaction, or may itself have been represented in the iron measurements in addition to Fe (II) which has resulted from the reduction of Fe (III), therefore giving a higher concentration of Fe (II). The low concentration of soluble Fe (II) compared to Fe (II) total can be explained by Fe (II) precipitation. It is presumed that if not formed directly bound onto mineral surfaces, that any soluble Fe (II) which was dissolved then rapidly precipitated, co-precipitated (e.g. iron-rich calcite, or, although to a very limited extent, iron sulphide) or was adsorbed onto available clay and PCFeO surfaces. A proportionately small concentration of Fe (II) was also observed in the "No MX80" control flasks (< 1 mM) which may have been due to limited interactions with reagents in the groundwater and associated carbon mix.

4.2. Other putative metabolic capabilities of the indigenous MX80 bentonite community

Apart from iron-reduction, other bacterial activities could impact the ability of MX80 bentonite to perform as an effective barrier in the repository environment. This includes bacterial gas production, and interaction with other minerals within the clay.

Many iron-reducing bacteria such as those mentioned above and present in the MX80 bentonite iron reducing enrichments are also able to utilise several forms of sulfur e.g. elemental sulfur and sulfoxyanions. Two such metabolically flexible iron and sulfur reducers organisms that were identified in these enrichments are *Desulfosporosinus* (Pester et al., 2012) and *Desulfitobacterium* (Villemur et al., 2006). SulfurSulphur reduction in a repository environment has been heavily investigated, such as studies in a simulated repository environment by Bengtsson et al. (2015). Their findings show that MIC of copper canisters is largely caused by SRBs through the production of hydrogen sulfide, which can then react with copper to form copper sulfide releasing hydrogen gas to the environment – the same process is applies to iron corrosion by SRBs (Ehrlich and Newman, 2009). On balance, it seems most likely that the SRBs identified here were enriched as a result of iron reduction rather than sulfate reduction given the respective thermodynamics of IRBs compared to SRBs and the addition of Fe (III) (Stevenson et al., 2020).

Psuedomonas stutseri, a denitrifying organism, was present in both compact and powder samples, but was more relatively abundant in the MX80 bentonite powder. Although heavy-metal tolerant and facultatively anaerobic, it is a non-spore forming bacterium, which may have led to a low survival rate in the compacted bentonite (Lalucat et al., 2006). *P. stutseri* has been isolated from groundwater in Swiss boreholes at 300 m depth (Bagnoud et al., 2016; Leupin et al., 2017) and Finnish boreholes at 500 m depth (Bomberg et al., 2015) – so could be reintroduced to the repository environment through groundwaters or the host-rock. In fact, Chi and Athar (2008), identified *P. stutseri* in both MX80 bentonite and groundwater samples, identifying it as a candidate for long-term survival in the repository. This bacterium could contribute to gas production through N_2 production and possibly indirectly contribute to iron-reduction. There has been a recent study that implicated *Prolixibacter* sp. in Fe^0 oxidation as an initial step in denitrification (Iino et al., 2015); however, it is important to note that in these enrichments only one sequence was matched to *Prolixibacter* and it was not present in the compacted samples. Nonetheless, iron could be oxidised to ferrous iron, or further oxidised to ferric iron in this process (eq. 4 and 5).

$$Fe^0 + NO_3^- + 2H^+ \rightarrow Fe^{2+} + NO_2^- + H_2O \quad (4)$$

$$2Fe^{2+} + NO_3^- + 2H + \rightarrow 2Fe^{3+} + NO_2^- + H_2O \quad (5)$$

These electrons are then utilised in reduction of nitrate to nitrogen gas (Iino et al., 2015). In the unlikely event that microbes are able to proliferate, this process could impact corrosion of the carbon steel container in the proposed design for nuclear waste disposal in the UK; however, it could also permit re-oxidation of Fe (II) to Fe (III) in the MX80 bentonite.

4.3. Spore-forming bacteria may be suited to long-term repository survival

A key feature of the community analysis reported in this study is that several spore-forming bacteria were identified in both types of MX80 bentonite samples. For instance, *Sporacetigenium* is a spore-forming bacterium that was present in the majority of samples and has been recorded to grow at high temperatures (55 °C) with its spores able to withstand even higher temperatures (Chen et al., 2006). The large number of spore-forming species present in MX80 bentonite is likely due to selection pressures for persistence in the dry clay prior to enrichments.

Multiple species of biofilm and spore-forming *Bacillus sp.*, and *Desulfosporosinus* sp. were also enriched. *Bacillus* is the most dominant genus present in the enrichments many of which are known in the literature (Turnbull, 1996) to be obligate aerobes and so it might be speculated that these would remain dormant within the anaerobic clay enrichments. However, some *Bacillus* are known to be facultative anaerobes (Turnbull, 1996) and it can be concluded that the majority of *Bacillus* species present in the enrichments are thus facultative anaerobes. In addition, *Desulfosporosinus* was enriched and, as discussed above, these spore formers are prominent iron and sulfate reducers (Nixon et al., 2017) and have been isolated from high saline, high pressure environments (Pester et al., 2012), making this genus a candidate for surviving the repository conditions.

Further support for the long-term survival of spores can be found in Jalique et al. (2016), who found that the microbial community of MX80 was almost exclusively comprised of spore-forming *Bacillus* (the same dominant genus identified in the community presented above) and *Paenibacillus* species after clay was kept under confinement in fully saturated conditions for 8 years. However, these experiments did not replicate the temperature or interactions with a metal canister. Moreover, Jalique et al. (2016) did not consider iron specifically, and so here we present a more selected microbial community, which includes spore-formers specific to iron-reduction (such as *Desulfosporosinus*) that were not identified by Jalique et al. (2016).

Apart from spore-forming species, several thermotolerant species were also identified in both the powdered and compacted samples. *Thermobacterales* is able to survive up to 70 °C and the growth of *Desulfitobacterium* has been recorded at 65 °C (Rosnes et al., 1991).

The powder bacterial community was very similar to the compact MX80 bentonite community, which indicates that the compacting process does not hugely alter the microbial community. There are several similarities between this community composition and that of similar

clays, for example, Poulain et al. (2008) found that the microbial community of French argillaceous clays were largely firmicutes with some proteobacteria present. Likewise, *P. stutzeri* and *Clostridia* have been isolated from numerous bentonites including FEBEX in Spain (López-Fernández et al., 2014); however, *Bacteriodetes* were prevalent in FEBEX samples but were only present in limited numbers in powder MX80 bentonite, so local microbiology does have some impact on the overall community. Similarly, the enrichment conditions and carbon sources used may have impacted the composition of the microbial community.

Regardless of the presence of these spore forming and thermotolerant bacteria identified in this study, the enrichments did not replicate repository conditions in terms of temperature, pressure, carbon and water availability. It is likely that under true repository conditions, the bacterial community would be inhibited, and the variety of species present, and overall number of bacteria would decrease. Additionally, the compacted MX80 bentonite was not confined during these experiments; it is likely that under repository conditions the confinement of the swollen MX80 bentonite would limit microbial growth due to inhibition of movement around the bentonite (Pashang and Laursen, 2020; Jalique et al., 2016). However, there may be pockets of microbial growth in areas where swelling has not fully occurred (Wilson et al., 2010; Jalique et al., 2016; Stroes-Gascoyne et al., 2011). Therefore these results highlight the importance of highly compacted MX80 bentonite in the repository to limit the growth of a viable, functionally diverse, indigenous microbial community.

Therefore, as a preliminary finding it seems clear that with no special effort to introduce or preserve existing communities or alternatively exclude them, an indigenous microbial community, which is able to cooperatively interact with iron and iron-containing minerals, is present in the MX80 bentonite. It is also possible that a selection of bacterial species present in the bentonite remained dormant throughout this enrichment and it is therefore likely that the true microbial community of the bentonite is more diverse.

4.4. Further understanding of microbial activity in the repository environment is necessary

Further experiments should focus on long-term in situ effects of these indigenous bacteria. For instance, biogenically catalysed smectite to non-swelling phyllosilicate transformations by IRBs (such as those identified here) have been observed in bentonite clays at temperatures below 100 °C (Kim et al., 2004), this process, or illitisation, may lead to a decrease in swelling capacity and alter the sorption properties of the clay (Bradbury et al., 2014; NDA, 2016a; Liu et al., 2012). However, these microbial changes may not occur under the pressure of the repository, as Pedrial et al. (2009), found no smectite dissolution occurred in the presence of a model IRB in confined volume experiments with compacted MX80 bentonite. But the simple system considered by Pedrial et al. does not reflect the complex activities of the indigenous iron-reducing microbial community presented here.

Furthermore, several outstanding concerns also remain to be addressed; namely, bacterial gas production (H_2) and usage (CO_2) (Fig. 6); and whether iron reduction is by direct or indirect bacterial mechanisms. Overall, it is likely that microbes will be present in the repository and that there will be periods of activity and inactivity as the internal environment changes. The indigenous community of powdered MX80 bentonite is altered during the homogenising and compacting process, which impacts the functionality of the microbes. The effect of bacterial activity could alter the function of MX80 bentonite as a barrier and could lead to increases in corrosion of the waste canisters and transport across the MX80 bentonite.

4.5. Conclusions

It can be concluded that all the bacteria identified in this study are those that have been enriched through bacterial growth in the enrichment microcosms. This conclusion is justified because of our failure to be able to extract enough DNA from the indigenous microbial community of the bentonite itself prior to enrichments. Furthermore, species identified show adaptations to harsh conditions via spore-formation and thermotolerance, some of which are likely also able to reduce iron, which could alter the integrity of the barrier system within nuclear waste repositories. Differences between the indigenous, activated microbial community of the powder and compacted MX80 bentonite samples highlight the importance of spore-formation and adaptable metabolic processes in surviving in compacted clay such as that proposed for use as a barrier in the repository. VFAs have also been implicated in both the long-term survival of the microbial community in the clay barrier and in contributing to iron reduction. These findings justify the need to ensure a fully swollen and compacted clay barrier to limit microbial growth as the bentonite will carry a viable, robust and metabolically flexible community into the system.

Declaration of Competing Interest

None.

Acknowledgements

The authors would like to thank EPSRC for funding this project and NU-OMICS (Northumbria University Omics Lab, DNA sequencing research facility) for their help in sequencing.

References

Arango, M., Schlegel, H.G., 1981. The hydrogen-oxidizing bacteria. In: Starr, M.P., Stolp, H., Trüper, H.G., Balows, A., Schlegel, H.G. (Eds.), The Prokaryotes. Springer, Berlin, Heidelberg.

Arlinger, J., Bengtsson, A., Edlund, J., Eriksson, L., Johansson, J., Lydmark, S., Rabe, L., Pedersen, K., 2013. Prototype repository – Microbes in the retrieved outer section. In: Report P-13-16 Swedish Nuclear Fuel and Waste Management Co.

Bagnoud, A., Chourey, K., Hettich, R., Brujin, I., Andersson, A.F., Leupin, O.X., Schwyn, B., Bernier-Latmani, R., 2016. Reconstructing a hydrogen-driven microbial metabolic network in Opalinus Clay rock. Nat. Commun. 7.

Bengtsson, A., Edlund, J., Hallbeck, B., Heed, C., Pedersen, K., 2015. Microbial sulphide-producing activity in MX-80 bentonite at 1750 and 2000 kg m–3 wet density. Report R-15-05.

Bomberg, M, Nyyssönen, M, Pitkänen, P, Lehtinen, A, Itävaara, M, 2015. Active microbial communities inhabit sulphate-methane interphase in deep bedrock fracture fluids in Olkiluoto, Finland. Biomed Research International (979530).

Börjesson, 2010. Design, production and initial state of the buffer. SKB technical report. In: Report TR-10-15.

Bradbury, M.H., Berner, U., Curti, E., Hummel, W., Kosakowski, G., Thoenen, T., 2014. The Long-Term Geochemical Evolution of the Nearfield of the HLW Repository. In: Nagra Technical Report TR-12-01.

Brietenstein, A., Wiegel, J., Haertig, C., Weiss, N., Andreesen, J.R., Lechner, U., 2002. Reclassification of *Clostridium hydroxybenzoicum* as *Sedimentibacter hydroxybenzoicus* gen. Nov., comb. nov., and description of *Sedimentibacter saalensis* sp. nov. Int. J. Syst. Evol. Microbiol. 52 (3), 801–807.

Brown, S.D., Podar, M., Klingeman, D.M., Johnson, C.M., Yang, Z.K., Utturkar, S.M., Land, M.L., Mosher, J.L., Hurt, R.A., Phelps, T.J., Palumbo, A.V., Arkin, A.P., Hazen, T.C., Elias, D.A., 2012. Draft Genome Sequences for two Metal-reducing *Pelosinus fermentans* Strains Isolated from a Cr(VI)-Contaminated Site and for Type Strain R7. J. Bacteriol. 194 (18), 5147–5148.

Burdige, D.J., 1993. The biogeochemistry of manganese and iron reduction in marine sediments. Earth-Sci. Rev. 35, 249–284.

Callahan, B.J., McMurdie, P.J., Rosen, M.J., Han, A.W., Johnson, A.J.A., Holmes, S.P., 2016. DADA2: High resolution sample inference from Illumina amplicon data. Nat. Methods 13 (7), 581–583.

Caporaso, J.G., Kuczynski, J., Stombaugh, J., Bittinger, K., Bushman, F.D., Costello, E.K., Fierer, N., Gonzalez, Pena A., Goodrich, J.K., Gordon, J.I., Huttley, G.A., Kelley, S.T., Knights, D., Koenig, J.E., Ley, R.E., Lozupone, C.A., McDonald, D., Muegge, B.D., Pirrung, M., Reeder, J., Sevinsky, J.R., Turnbaugh, P.J., Walters, W.A., Widmann, J., Yatsunenko, T., Zaneveld, J., Knight, R., 2010. QIIME 2 allows analysis of high-throughput community sequencing data. Nat. Methods 7 (5), 335–336.

Chen, S., Song, L., Dong, X., 2006. *Sporacetigenium mesophilum* gen. nov., sp. nov., isolated from an anerobic digester treating municipal solid waste and sewage. International Journal of Systematic and Evolutionary Microbiology 56 (4).

Chi, Fru E., Athar, R., 2008. In situ bacterial colonization of compacted bentonite under deep geological high-level radioactive waste repository conditions. Appl. Microbiol. Biotechnol. 79 (3), 499–510.

Davies, C.W., Davie, C.T., Edward, C.A., White, M.L., 2018. Physicochemical and Geotechnical Alterations to MX-80 Bentonite at the Waste Canister Interface in an Engineered Barrier System. Geosciences 7 (3), 69.
Ehrlich, H.L., Newman, D.K., 2009. Geomicrobiology, fifth edition. Ch16 and 19.
Engel, K., Ford, S.E., Coyotzi, S., McKelvie, J., Diomidis, N., Slater, G., Neufeld, J.D., 2019. Stability of microbial community profiles associated with compacted bentonite from the grimsel underground research laboratory. mSphere 4 (6), 601–619.
Eydal, H.S.C., Jägevall, S., Hermansson, M., Pedersen, K., 2009. Bacteriophage lytic to *Desulfovibrio aespoeensis* isolated from deep groundwater. The ISME Journal 3, 1139–1147.
Felsenstein, J., 1987. Phylogenies and the comparative method. Am. Nat. 125 (1), 1–15.
Praj, B., HAnia, W.B., Postec, A., Hamdi, M., Ollivier, B., Fardeau, M.L., 2013. *Fonticella tunisiensis* gen. Nov., sp. nov., isolated from a hot spring. Int. J. Syst. Evol. Microbiol. 63, 1947–1950.
Gerritsen, J., Hornung, B., Renckens, B., Hijum, S.A.F.T., Martin dos Santos, V.A.P., Rijkers, G.T., Scaap, P.J., Vos, W.M., Smidt, H., 2017. Genomic and functional analysis of Romboutsia ilealis CRIBT reveals adaptation to the small intestine. PeerJ 5.
Glatstein, D.A., Francisca, F.M., 2014. Hydraulic conductivity of compacted soils controlled by microbial activity. Environ. Technol. 35 (13–16), 1886–1892.
IAEA, 2018. Contents and sample arguments of a safety case for near surface disposal of radioactive waste. In: IAEA-TECDOC-1814.
Iino, T., Ito, K., Wakai, S., Tsurumaru, H., Ohkuma, M., Harayama, S., 2015. Iron corrosion induced by nonhydrogenotrophic nitrate-reducing *Prolixibacter* sp. strain MIC1-1. Appl. Environ. Microbiol. 81 (5), 1839–1846.
Ilgen, A.G., Kukkadapu, R.K., Leung, K., Washington, R.E., 2019. "Switching on" iron in clay minerals. Environmental Science: Nano 6.
Jalique, D.R., Stroes-Gascoyne, S., Hamon, C.J., Priyanto, D.G., Kohle, C., Evenden, W.G., Wolfaardt, G.M., Grigoryan, A.A., McKelvie, J., Korber, D.R., 2016. Culturability and diversity of microorganisms recovered from an eight-year old highly-compacted, saturated MX-80 Wyoming bentonite plug. Appl. Clay Sci. 126, 245–250.
Jayaraman, A., Earthman, J.C., Wood, T.K., 1997. Corrosion inhibition by aerobic biofilms on SAE 1018 steel. Appl. Microbiol. Biotechnol. 47, 62–68.
Jönsson, B., Åkesson, T., Jönsson, B., Meehdi, S., Janiak, J., Wallenberg, R., 2009. Structure and forces in bentonite MX-80. In: SKB, TR-09-06.
Karnland, O., 2010. Chemical and mineralogical characterization of the bentonite buffer for the acceptance control procedure in a KBS-3 repository. In: *SKB, TR*-10-60.
Kasana, R.C., Padney, C.B., 2017. *Exiguobacterium*: an overview of a versatile genus with potential in industry and agriculture. Crit. Rev. Biotechnol. 38 (1), 141–156.
Kim, J., Dong, H., Seabaugh, J., Newell, S.W., Eberl, D.D., 2004. R ole of Microbes in the Smectite-to-Illite Reaction. Science 303 (5659), 830–832.
Kip, N., Veen, J., 2015. The dual role of microbes in corrosion. ISME J. 9, 542–551.
Kiviranta, L., Kumpulainen, S., Pintado, X., Karttunen, P., Schatz, T., 2018. Characterisation of bentonite and clay materials 2012-2015. In: Posiva WR-2016-05.
Konhauser, K.O., 1997. Bacterial iron biomineralisation in nature. FEMS Microbiol. Rev. 20 (3–4), 315–326.
Konhauser, K.O., 2007. Introduction to Geomicrobiology. Blackwell ch4 and 5.
Kunapuli, U., Jahn, K., Lueders, T., Geyer, R., Heipieper, H.J., Meckenstock, R.U., 2010. *Desulfitobacterium aromaticivorans* sp. nov. and *Geobacter toluenoxydans* sp. nov., iron-reducing bacteria capable of anaerobic degradation of monoaromatic hydrocarbons. International Journal of Systematic and Evolutionary Microbiology 60 (3).
Lalucat, J., Bennasar, A., Bosch, R., García-Valdés, E., Palleroni, N.J., 2006. Biology of *Pseudomonas stutzeri*. Microbiol Mol Biol Rev 70 (2), 510–547.
Landolt, D., Davenport, A., Payer, J., Shoesmith, D., 2009. A review of materials and corrosion issues regarding canisters for disposal of spent fuel and high-level waste in opalinus clay. In: Nagra technical report TR-09-02.
Leupin, O.X., Bernier-Latmani, R., Bagnoud, A., Moors, H., Leys, N., Wouters, K., Stroes-Gascoyne, S., 2017. Fifteen years of microbial investigation in Opalinus Clay at the Mont Terri rock laboratory (Switzerland). Swiss J. Geosci. 110 (1), 343–354.
Liu, D., Dong, H., Bishop, M.E., Zhang, J., Wang, H., Huang, L., Eberl, D.D., 2012. Microbial reduction of structural iron in interstratified illite-smectite minerals by a sulfate-reducing bacterium. Geobiology 10 (2), 150–162.
López-Fernández, M., Fernández-Sanfrancisco, O., Moreno-García, A., Martín-Sánchez, I., Sánchez-Castro, I., Merroun, M.L., 2014. Microbial communities in bentonite formations and their interactions with uranium. Appl. Geochem. 49, 77–86.
Lovely, D., Phillips, E.J.P., 1986. Availability of ferric iron for microbial reduction in bottom sediments of the freshwater tidal Potomac River. Applied Environmental Microbiology 52, 751–757.
Lovley, D., 2013. Dissimilatory Fe (III)- and Mn (IV)-Reducing Prokaryotes. In: Rosenberg, E., Delong, E.F., Lory, S., Stackebrandt, E., Thompson, F. (Eds.), The Prokaryotes: Prokaryotic Physiology and Biochemistry. Springer Berlin Heidelberg, Berlin, Heidelberg, pp. 287–308.
Marshall, M.H.M., McKelvie, J.R., Simpson, A.J., Simpson, M.J., 2015. Characterization of natural organic matter in bentonite clays for potential use in deep geological repositories for used nuclear fuel. Appl. Geochem. 54, 43–53.
Masurat, P., Eriksson, S., Pedersen, K., 2010. Evidence of indigenous sulfate-reducing bacteria in commercial Wyoming bentonite MX80. Appl. Clay Sci. 47, 51–57.
Matthies, C., Evers, S., Ludwig, W., Scgink, B., 2000. *Anaerovorax odorimutans* gen. Nov., sp. nov., a putrescine-fermenting, strictly anaerobic bacterium. Int. J. Syst. Evol. Microbiol. 50 (4), 1591–1594.
Morgado, L., Fernandes, A.P., Dantas, J.M., Silva, M.A., Salgueiro, C.A., 2012. On the road to improve the bioremediation and electricity-harvesting skills of Geobacter sulfurreducens: functional and structural characterization of multihaem cytochromes. Biochem. Soc. Trans. 40 (6), 1295–1301.
Motamedi, M., Karland, O., Pedersen, K., 1996. Survival of sulfate reducing bacteria at different water activities in compacted bentonite. FEMS Microbiol. Lett. 141 (1), 83–87.
NDA, 2010. Summary of Generic Designs (Geological Disposal).
NDA, 2016. Geological disposal: generic disposal facility design. In: NDA Report no. DSSC/412/01.
NDA, 2016a. Geological disposal: engineered barrier system status report. In: NDA Report no. DSSC/452/01.
Necib, S., Diomidis, M., Keech, P., Nakayama, M., 2017. Corrosion of carbon steel in clay environments relevant to radioactive waste geological disposals, Mont Terri rock laboratory (Switzerland). Swiss J. Geosci. 110 (1), 329–342.
Nixon, S.L., Telling, J.P., Wadham, J.L., Cockell, J.S., 2017. Viable cold-tolerant iron-reducing microorganisms in geographically diverse subglacial environments. Biogensciences 14, 1445–1455.
Orcutt, B.N., LaRowe, D.E., Biddle, J.F., Colwell, F.S., Glazer, B.T., Reese, B.K., et al., 2013. Microbial activity in the marine deep biosphere: progress and prospects. Frontiers Microbiology 4, 189.
Pashang, R., Laursen, A.E., 2020. Searching for bacteria in sticky situations: Methods for investigating bacterial survival at solid-air interfaces involving Wyoming MX-80 bentonite. Applied Clay Science 188.
Pedersen, K., 2000. Microbial processes in radioactive waste disposal. In: SKB Technical Report: TR-00-04.
Pedrial, J.N., Warr, L.N., Pedrial, N., Lett, M.C., Elsass, F., 2009. Interaction between smectite and bacteria: Implications for bentonite as backfill material in the disposal of nuclear waste. Chem. Geol. 264 (1–4), 281–294.
Pester, M., Brambilla, E., Alazard, D., Rattei, D., Weinmaier, T., Han, J., Lucas, S., Lapidus, A., Cheng, J.F., Goodwin, L., Pitluck, S., Peters, L., Ovchinnikova, G., Teshima, H., Detter, J.C., Han, C.S., Tapia, R., Land, M.L., Hauser, L., Kyrpides, N.C., Ivanova, N.N., Pagani, I., Huntmann, M., Wei, C.L., Davenport, K.W., Daligault, H., Chain, P.S.G., Chen, A., Mavromatis, K., Markowitz, V., Szeto, E., Mikhailova, N., Pati, A., Wagner, M., Woyke, T., Ollivier, B., Klenk, H.P., Spring, S., Loy, A., 2012. Complete Genome Sequences of *Desulfosporosinus orientis* DSM765^T, *Desulfosporosinus youngiae* DSM17734^T, *Desulfosporosinus meridiei* DSM13257^T, and *Desulfosporosinus acidiphilus* DSM22704^T. J. Bacteriol. 194 (22), 6300–6301.
Philp, J.C., Taylor, K.J., Christofi, N., 1991. Consequences of sulfate-reducing bacterial growth in a lab-simulated waste disposal regime. Experientia 47 (6), 553–559.
Poulain, S., Sergeant, C., Simonoff, M., Le Marrec, C., Altmann, S., 2008. Microbial investigations in opalinus clay, an agrillaceous formation under evaluation as a potential host rock for a radioactive waste repository. Geomicrobiol J. 25 (5), 240–249.
Rosnes, J.T., Torsvik, T., Lien, T., 1991. Spore-forming thermophilic sulfate-reducing bacteria isolated from north sea oil field waters. Appl. Environ. Microbiol. 57 (8), 2302–2307.
RS®Minerals, 2017. MX-80 Delivery Specification Sheet. Available online. http://www.rsminerals.co.uk/bentonite (Accessed 23rd October 2020).
Ruebush, S.S., Brantley, S.L., Tien, M., 2006. Reduction of soluble and insoluble iron forms by membrane fractions of *Shewanella oneidensis* grown under aerobic and anaerobic conditions. Appl. Environ. Microbiol. 72 (4), 2925–2935.
RWM, 2016. Geological Disposal: Generic Specification for waste packages containing high heat generating waste. In: *WPSGD no. WPS/240/01*.
RWM, 2017. Contractor Report to RWM FEBEX-DP: THM modelling. In: Contractor Report no. QRS-1713A-R2, V1.8.
Sahin, U., Eroğlu, S., Sahin, F., 2011. Microbial application with gypsum increases the saturated hydraulic conductivity of saline–sodic soils. Appl. Soil Ecol. 48 (2), 247–250.
Saitou, N., Nei, M., 1987. The neighbour-joining method: a new method for reconstructing phylogenetic trees. Molecular Biology Evolution 4 (4), 406–425.
Sander, M., Hoŝstetter, T., Gorski, C., Sosedova, Y., Voegelin, A., 2014. Redox properties of iron-bearing clays and MX-80 bentonite – Electrochemical and spectroscopic characterization. In: *Nagra Technical Report*, TR-13-03.
Sauzeat, E., Villiéras, T.F., François, M., Pelletier, M., Barrés, O., Yvon, J., Guillaume, D., Dubbessy, J., Pfeiffert, C., Ruck, R., Cathelineau, M., 2001. Caractérisation minéralogique, cristallochimique et texturale de l'argile MX-80 (ANDRA Technical Report).
Sawayama, S., 2006. Possibility of anoxic ferric ammonium oxidation. Journal of Bioscience and Engineering 101 (1), 70–72.
Sellin, P., Leupin, O.X., 2013. The use of clay as an engineered barrier in radioactive-waste management – a review. GeoScience World 61 (6), 477–498.
Shelobolina, E.S., Nevin, K.P., Blakeney-Hayward, J.D., Johnsen, C.V., Plaia, T.W., Krader, P., Woodard, T., Holmes, D.E., Vanpraagh, C.G., Lovley, D.R., 2007. *Geobacter pickeringii* sp. nov., *Geobacter argillaceus* sp. nov. and *Pelosinus fermentans* gen. nov., sp. nov., isolated from subsurface kaolin lenses. Journal of Systematic and Evolutionary Microbiology 57, 126–135.
Shiratori, H., Ohiwa, H., Ikeno, H., Ayame, S., Kataoka, N., Miya, A., Beppu, T., Ueda, K., 2008. *Lutispora thermophila* gen. nov., sp. nov., a thermophilic, spore-forming bacterium isolated from a thermophilic methanogenic bioreactor digesting municipal solid wastes. Int. J. Syst. Evol. Microbiol. 58 (4), 964–969.
SKB, 2006. Long-term safety for KBS-3 repositories at Forsmark and Laxemar – a first evaluation Main Report of the SR-Can project. In: SKB Technical Report TR-06-09.
Spring, S., Rosenzweig, F., 2006. The Genera *Desulfitobacterium* and *Desulfosporosinus*: Taxonomy in *The Prokaryotes* (Ch1.2.24). *Springer*.
Stevenson, M.A., Faust, J.C., Andrade, L.L., Freitas, F.S., Gray, N.D., Tait, K., Hendry, K. R., Hilton, R.G., Henley, S.F., Tessin, A., Leary, P., Papadaki, S., Ford, A., Marz, C., Abbott, G.D., 2020. Transformation of organic matter in a Barents Sea sediment profile: coupled geochemical and microbiological processes. Phil. Trans. R. Soc. A 378, 20200223.

Stone, W., Kroukamp, O., Moes, A., McKelvie, J., Korber, D.R., Wolfaardt, G.M., 2016. Measuring microbial metabolism in atypical environments: Bentonite in used nuclear fuel storage. Journal of Microbiological Methods 120, 79–90.
Stroes-Gascoyne, S., West, J.M., 1997. Microbial studies in the Canadian nuclear fuel waste management program. FEMS Microbiol. Rev. 20, 573–590.
Stroes-Gascoyne, S., Hamon, C.J., Maak, P., 2011. Limits to the use of highly compacted bentonite as a deterrent for microbially influenced corrosion in a nuclear fuel waste repository. Phys. Chem. Earth 36, 1630–1638.
Strömpl, C, Tindall, B J, Jarvis, J N, Lunsdorf, H, Moore, E R, Hippe, H, 1999. A re-evaluation of the taxonomy of the genus *Anaerovibrio*, with the reclassification of *Anaerovibrio glycerini* as *Anaerosinus glycerini* gen. nov., comb. nov., and *Anaerovibrio burkinabensis* as *Anaeroarcus burkinensis* [corrig.] gen. nov., comb. nov. Int J Syst Bacteriol 49, 1861–1872.
Svemar, C., Johanneson, L.E., Grahm, P., Svensson, D., Kristensson, O., Lönnqvist, M., Nilsson, U., 2016. Opening and retrieval of outer section of Prototype Repository at Äspö Hard Rock Laboratory. In: SKB, TR-13-22.
Svensson, D., Dueck, A., Nilsson, U., Olsson, S., Sanden, T., Lydmark, S., Jagerwall, S., Pedersen, K., Hansen, S., 2011. Status of the ongoing laboratory investigation of reference materials and test package 1. In: SKB, TR-11-06.
Turnbull, P.C.B., 1996. Bacillus. In: Baron, S. (Ed.), Medical Microbiology, 4th edition. University of Texas Medical Branch at Galveston. Ch 15.
Urios, L., Marsal, F., Pelligrini, D., Magot, M., 2012. Microbial Diversity of the 180 million-year-old Toarcian argillite from Tounemire, France. Appl. Geochem. 27 (7), 1442–1450.
Uroz, S., Calvaruso, C., Turpault, M.-P., Frey-Klett, P., 2009. Mineral weathering by bacteria: ecology, actors and mechanisms. Trends Microbiol. 17, 378–387.
Villemur, R., Lanthier, M., Beaudet, R., Lépine, F., 2006. The Desulfitobacterium genus. FEMS Microbiol. Rev. 30 (5), 706–733.
Wang, Q., Tang, A.M., Cui, Y.J., Barnichon, J.D., Delage, P., Ye, W.M., 2013. The effects of technological voids on the hydro-mechanical behaviour of compacted bentonite-sand mixture. Soils Found. 53 (2), 232–245.
Wilkins, M.J., Livens, F.R., Vaughan, D.J., Beadle, I., Lloyd, J.R., 2007. The influence of microbial redox cycling on radionuclide mobility in the subsurface at a low-level radioactive waste storage site. Geobiology 5, 293–301.
Wilson, J., Savage, D., Bond, A., Watson, S., Pusch, R., Bennett, D., 2010. Bentonite: a Review of key properties, processes and issues for consideration in the UK context. In: NDA QRS-1378ZG-1.
Yang, Q., Toijer, E., Olsson, P., 2019. Analysis of radiation damage in the KBS-3 canister materials. In: SKB TR-19-14.
Zhang, X., Mandelco, L., Wiegel, J., 1994. *Clostridium hydroxybenzoicum* sp. nov., an amino acid-utilizing, hydroxybenzoate-decarboxylating bacterium isolated from methanogenic freshwater pond sediment. Int. J. Syst. Evol. Microbiol. 44, 214–222.
Zhang, Z., Schwartz, S., Wagner, L., Miller, W., 2000. A greedy algorithm for aligning DNA sequences. J. Comput. Biol. 7 (1–2), 203–214.

4.1.1 Further results from anaerobic iron-reducing enrichments with MX80 bentonite

Further data and results not presented in the above publication are reported here. Over the course of the experiment, iron-reduction occurred in all flasks that contained microbes. Some reduction occurred in sterile controls, but at a much slower rate. Changes were identified by obvious colour changes (figure 4.1).

Figure 4.1: Compact MX80 iron-reducing enrichments on day 21, obvious colour differences were seen between each flask. The biotic flasks were black, indicating iron reduction and the precipitation of reduced iron minerals. The control flask which contained no MX80 remained orange (the colour of PCFeO), and the sterilised flasks remained orange / grey.

4.1.1.2 VFA Analysis:

MX80 powder unsterilised experiments showed an initial decrease in all three VFAs (figure 4.2). Acetic acid then increased from day 15 to 20 and remained at 850-1000 PPM until the end of the experiment. Butyric acid remained low between days 5 and 35 but increased to 600 PPM by day 42. The concentration of propionic acid was the most changeable as it decreased to 0 at day 5, increased to 440 PPM by day 20 and then decreased again from day 35 – 42 to 0 PPM. There was a slight increase in acetic acid levels in the sterile and "No MX80" controls. A similar increase occurred in all "No MX80" experiments.

An organic carbon mix had been added to these enrichments. In the compacted MX80 experiments (figure 4.2) both the unsterilised and positive control (with *S. oneidensis*) increased to 1000 PPM acetic acid by day 21, this was the highest detection of the IC instrument used. The

propionic acid concentration of the live unsterilised experiments initially decreased and then increased to 500 PPM by day 42. This trend was similar to the positive control. Likewise, the concentration of butyric acid decreased to day 5 and slowly increased to the end of the experiment. The sterile control showed some changes in acetic concentration throughout the experiment and the concentration of butyric acid slowly decreased over the course of the experiment. When compared to the sterile controls, acetic acid was significantly higher in the unsterilised live experiments with P-values of 0.028 and 0.004 for the powder and compact experiments, respectively. No other VFA measurements were found to be significant.

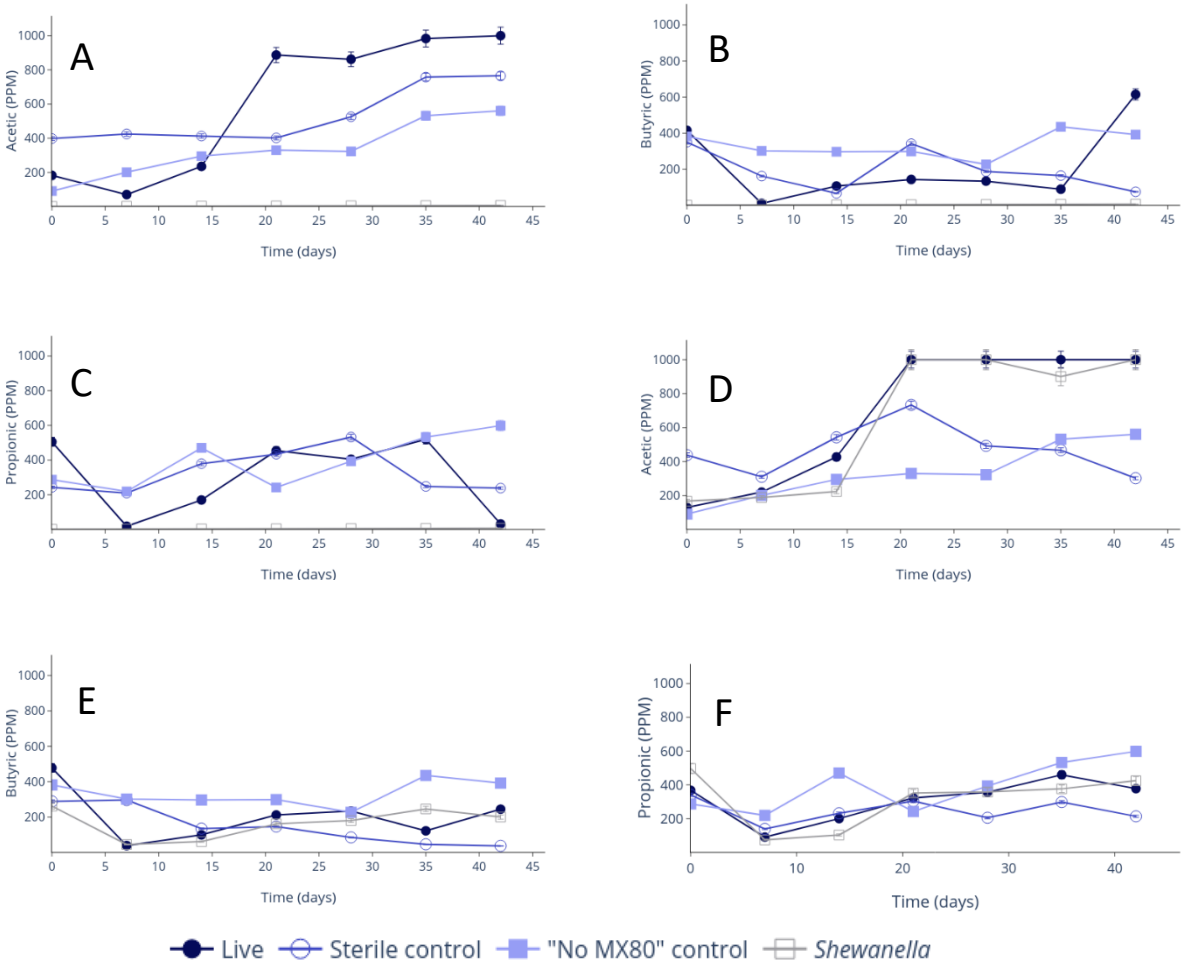

Figure 4.2: VFA analysis of anaerobic MX80 powder iron-reducing enrichments (A-C) and VFAs in compacted MX80 iron-reducing enrichment experiments (D-F). Error bars show standard error.

4.1.1.3 XRD Analysis of black precipitate from anaerobic iron-reducing enrichments:

XRD analysis was carried out on the black precipitate which was observed in enrichment flasks when microbes were present (figure 4.3). The XRD spectrum suggests this could be goethite, an iron oxide-hydroxide (FeO(OH)). Another possibility was magnetite, a mixed iron oxide, or iron sulfide; however, given the small concentration of sulfur present (< 1 mM sulfate if all gypsum present in the clay dissolves with 0.02 mM from groundwater), and the associated thermodynamics (Stevenson et al., 2020), the system is much more likely to favour iron reduction.

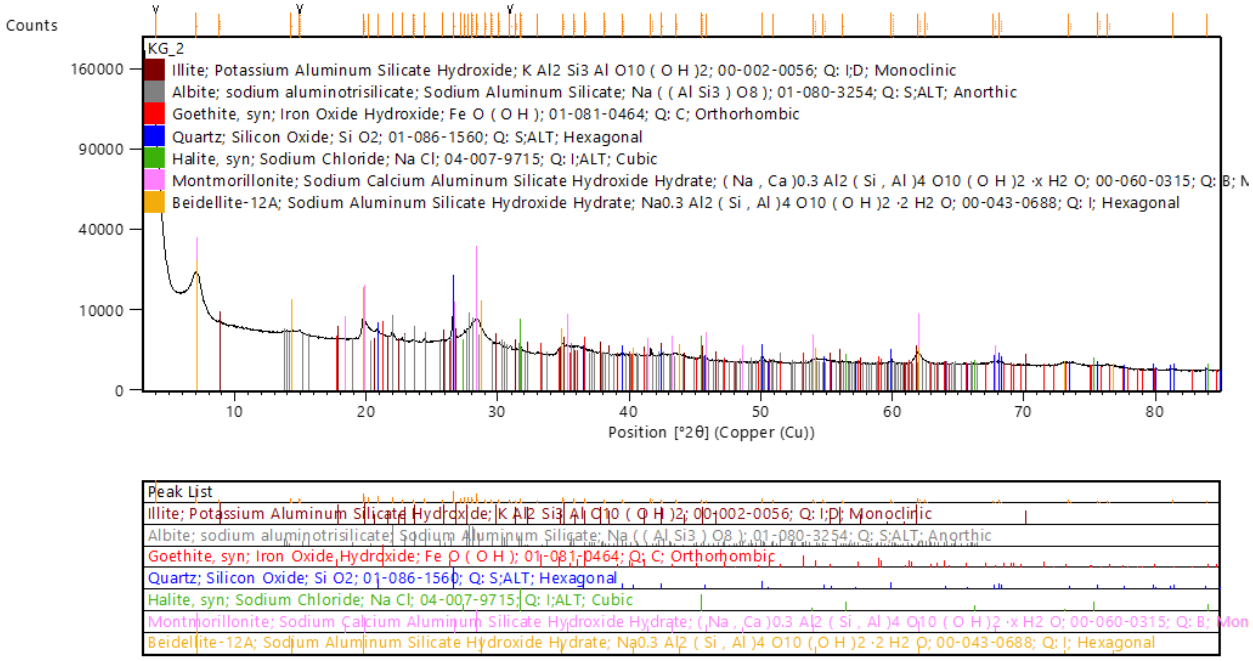

Figure 4.3: XRD pattern for sample of black precipitate taken from anaerobic iron-reducing enrichments of MX80. Pattern matches spectra for clay minerals and goethite

4.2 Enriched aerobic indigenous bacterial community of MX80 bentonite

Further bacterial enrichments of MX80 bentonite were carried out under aerobic conditions. During construction and the first 30 years post-closure, the repository environment is still aerobic or microaerobic. Furthermore, the possibility of oxygenated groundwater may introduce oxygen to the system throughout the repository lifespan. Therefore, a further understanding of the

microbial communities present is important under aerobic conditions. As previously, both powder MX80 and compacted MX80 bentonite were enriched, and the resulting bacterial DNA was extracted and sequenced. These experiments also included a control without any organic carbon added. No EDX, SEM or XRD was carried out on these samples as they were intended as a direct comparison of microbial communities to the previous anaerobic iron-reducing MX80 bentonite community.

4.2.1 Results

Colour changes from grey to black were observed in aerobic enrichments by day 18 (figure 4.4). This black mineral may be iron sulfide formation (or goethite as observed in anaerobic enrichments – see section 4.1.3). It is believed that the swelling of compact MX80 created anaerobic zones. No colour change was observed in any of the control flasks.

Figure 4.4: Aerobic enrichments of MX80 bentonite on day 18. The no carbon control shows no precipitates and is uniformly grey. The sterile controls have a small concentration of black precipitate present in small particles. The live experiments have an obvious colour change from grey to black in localised anaerobic areas. The no MX80 control (-MX80) is colourless.

4.2.1.1 pH of aerobic enrichments of MX80 bentonite

All experiments were around pH 7-8 throughout the experiment, apart from the control with no added carbon which had a higher pH. The pH of the unsterilised powder experiment ("live") when compared to the control without carbon across the second week of the experiment was significant ($P = 1.17 \times 10^{-7}$). The pH of both live unsterilised powder and compacted MX80 (figure

4.5) increased towards the end of the experiment to pH 8.59 and pH 8, respectively. The no carbon control remained alkaline until day 12. The sterile powder experiment had a circumneutral pH throughout the experiment and was found to be significantly lower when compared to the unsterilised powder experiment (P=0.0198) across days 7-14. The "No MX80" control had an acidic pH throughout the experiment.

The pH of the unsterilised compacted MX80 aerobic enrichment decreased from pH 8 to pH 6.8 before increasing back to ~ pH 8. When compared to the sterile control across the second week of the experiment, the unsterilised compacted MX80 experiment was found to be significant ($P=7.6x10^{-6}$). The pH of the unsterilised compact MX80 experiment was also significantly lower when compared to the control without carbon ($p= 6.59x10^{-4}$) across days 7-14. The no carbon control remained alkaline until day 12. The sterile experiment had a circumneutral pH throughout the experiment.

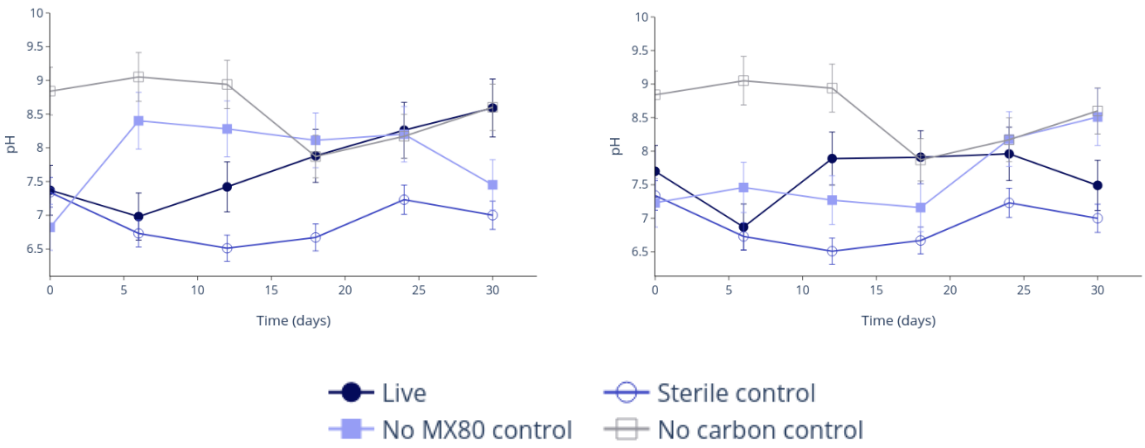

Figure 4.5: pH of aerobic enrichments of MX80 powder (left) and pH of compacted MX80 aerobic enrichments (right). Error bars show standard error.

4.2.1.2 VFA analysis of aerobic enrichments of MX80 bentonite

VFA concentrations of aerobic enrichments with MX80 powder decreased to 0 with respect to the acetic, butyric and propionic acids (figure 4.6). Acetic acid decreased to 0 from 600 PPM by day 24, this was significant compared to the sterile control (P= 0.0199). Both the sterile powder and "No MX80" controls remained constant at 50-120 PPM. The concentration of butyric acid decreased from 314 to 0 PPM by day 12. The "No MX80" control remained constant at 200-250

PPM whilst the sterile powder control decreased from 329 to 178 PPM by day 18 and then increased to 292 PPM on day 30. The concentration of propionic acid followed a similar trend to butyric acid, decreasing from 460 to near 0 PPM by day 18 in the unsterilised experiment. The concentration of propionic acid in the "No MX80" control remained constant throughout the experiment at 200-250 PPM. The sterile powder control decreased from 300 PPM on day 0 to 150 PPM on day 18 and then increased to 240 PPM by day 30. The no carbon control remained at 0 throughout the experiment in all VFAs.

Similarly, the VFAs measured in unsterilised compact MX80 aerobic enrichments all decreased (figure 4.6). Acetic acid decreased from 460 PPM to 65 PPM by day 6 and remained below 100 PPM for the rest of the experiment. As with the powder experiments, this result was significant when compared to the sterile control, p=0.05. The "No MX80" control remained constant at 75-80 PPM, whilst the sterile compacted control decreased from 364 to 81 PPM by day 12 and then increased to 689 PPM by day 24. The concentration of butyric acid decreased from 166 to below 10 PPM by day 12 in the unsterilised compacted experiment and the "No MX80" control remained constant at 200-250 PPM. The concentration of butyric acid in the sterile compacted control decreased from 254 to 18 PPM by day 12 and then increased to 134 PPM on day 30. The concentration of propionic acid decreased from 141 to 40 PPM by day 6 and remained below 100 PPM until day 30 in the unsterilised experiment. Whilst the concentration of propionic acid in the "No MX80" control remained constant throughout the experiment at 200-250 PPM and the sterile compacted control decreased from 219 PPM on day 0 to 37 PPM on day 12 and then increased to 154 PPM by day 30.

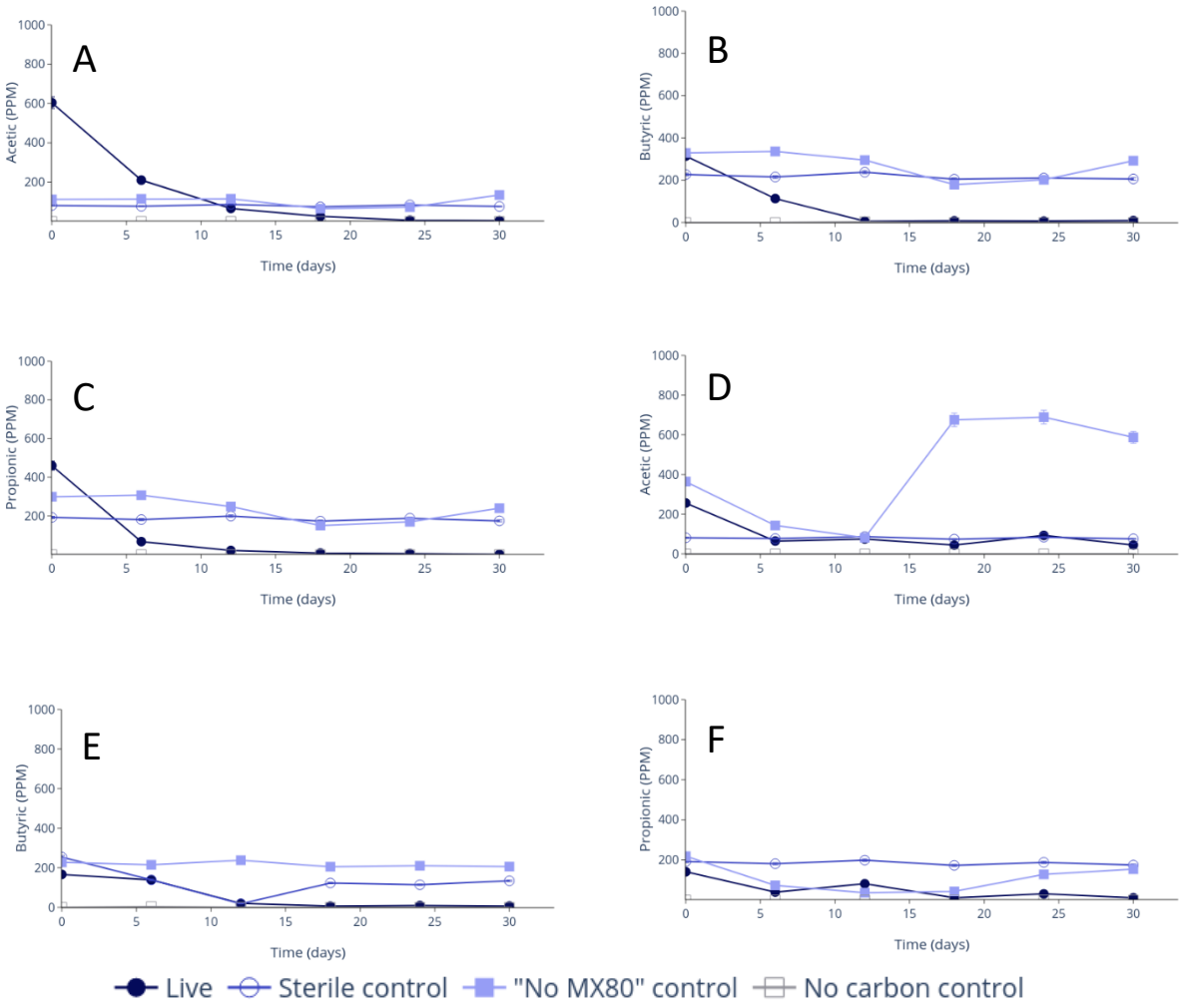

Figure 4.6: VFA concentrations of aerobic enrichments of MX80 bentonite powder (A-C) and compact MX80 bentonite (D-F). Error bars show standard error.

4.2.1.3 The activated aerobic community of MX80 bentonite:

DNA sequencing of the aerobic samples showed a low species diversity (figure 4.7) dominated by high numbers of sequences assigned to *Pseudomonas stutzeri* as well as several firmicutes including several facultatively anaerobic bacteria (figures 4.8 & 4.9). Following processing, a mean total of 107,300 sequences were identified in libraries relating to MX80 powder aerobic enrichments and a mean of 82,864 sequences were identified from libraries from compact MX80 aerobic experiments. The average sequence length was 227 bp. There were more ASVs identified in the powder MX80 (481) than the compacted MX80 (324).

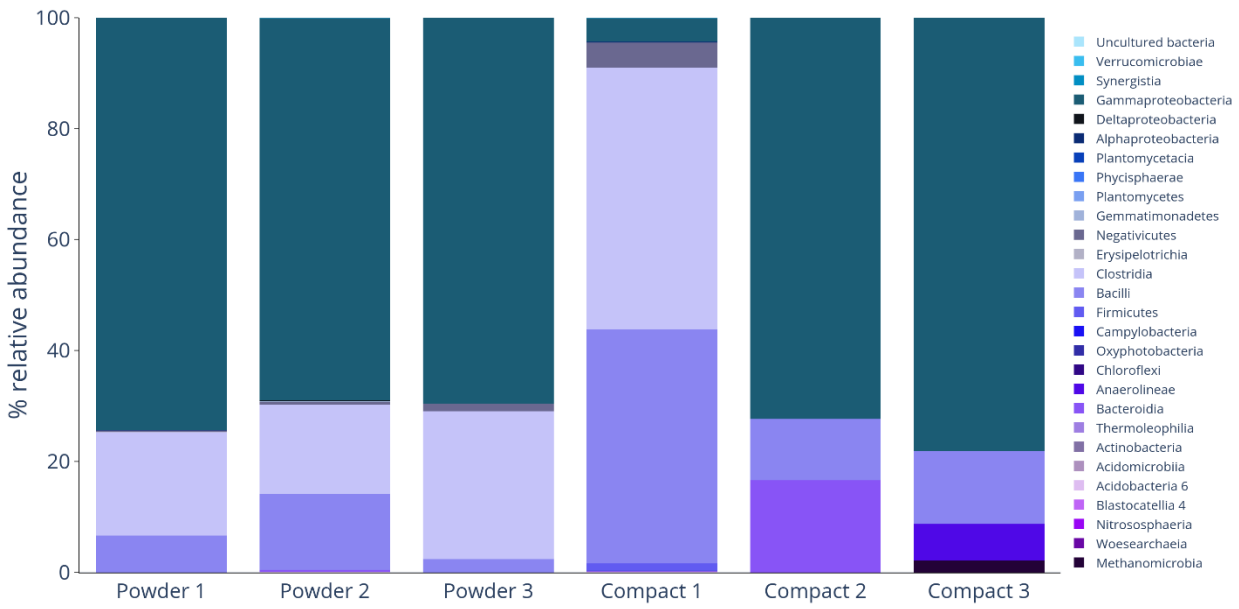

Figure 4.7: Community structure of activated aerobic bacterial community of MX80 bentonite from 16S rRNA sequencing of enrichments. The vast majority in all samples were firmicutes and proteobacteria.

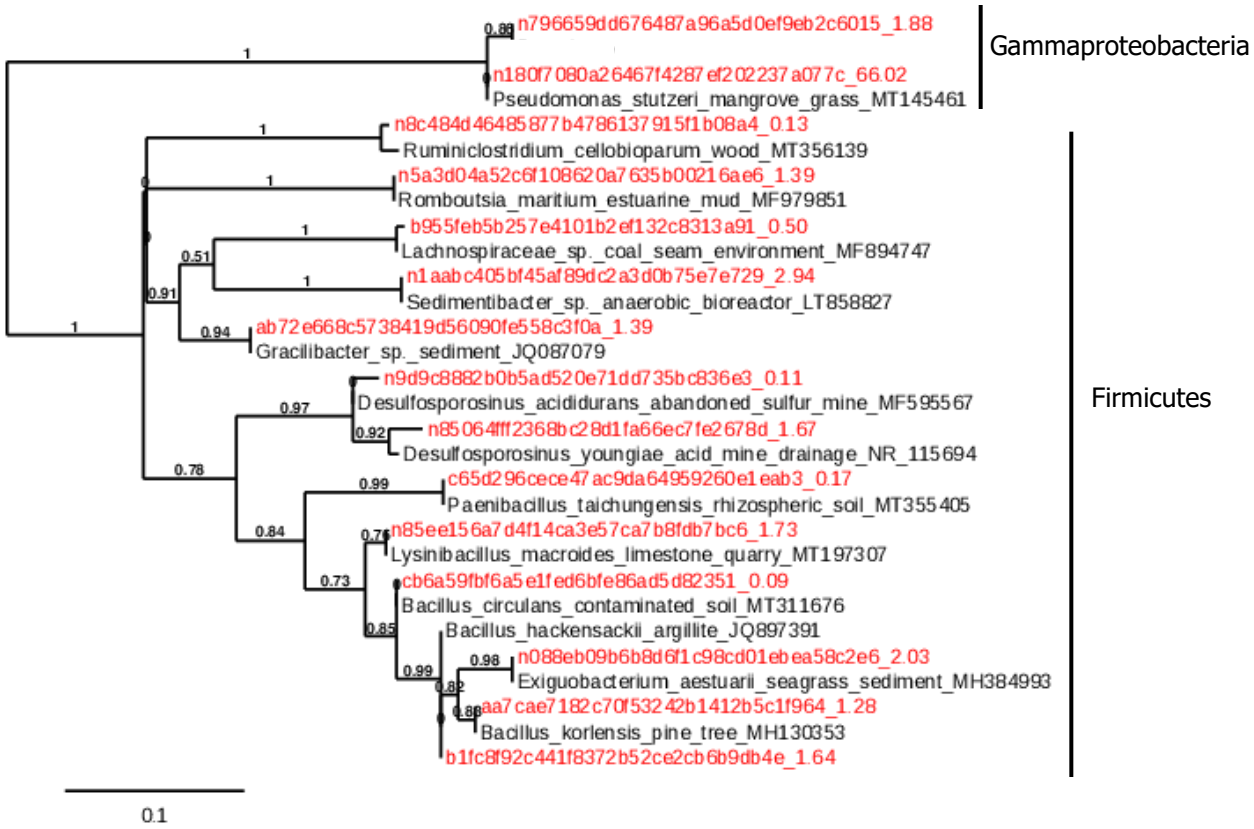

Figure 4.8: Phylogenic tree of enriched aerobic bacteria population of MX80 powder constructed from 16S rRNA sequencing data and related sequences identified by BLAST searches. % relative abundances in combined libraries (from 3 replicates) for individual ASVs is shown at the end of each leaf and bootstrap values are included on branches.

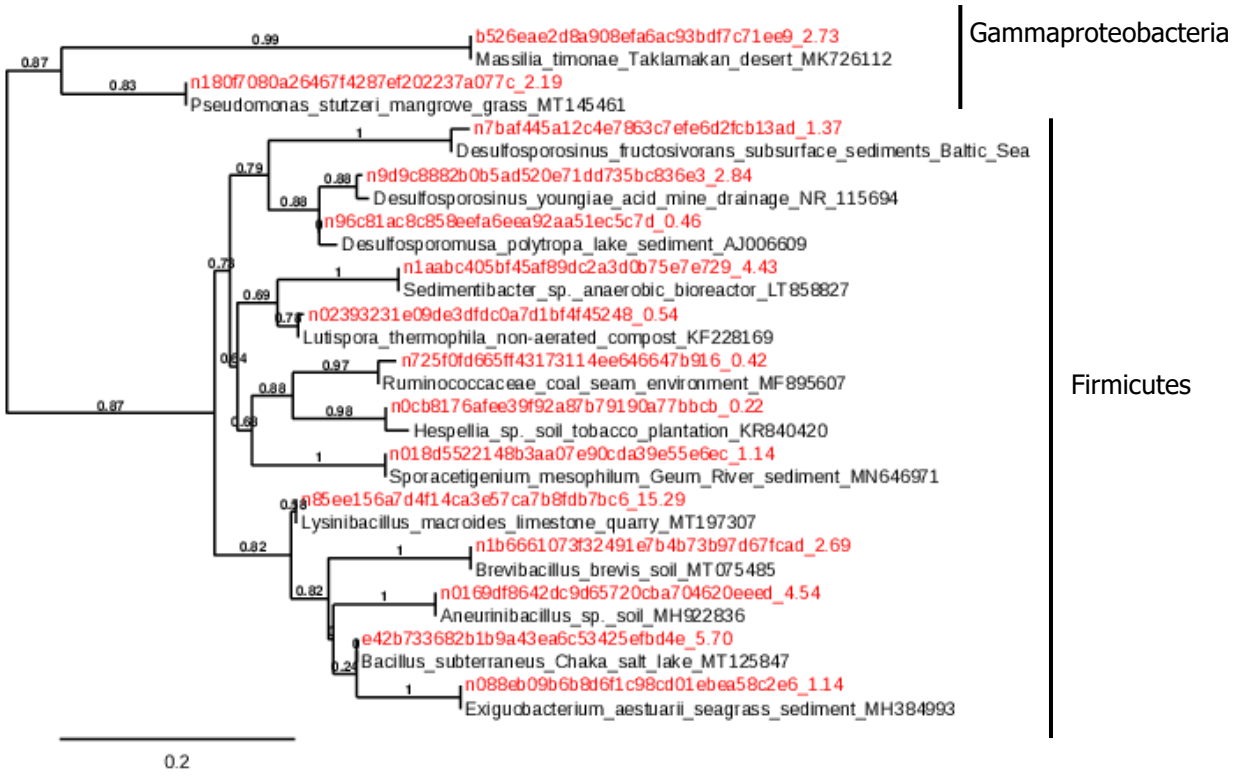

Figure 4.9: Phylogenic tree of activated aerobic bacteria population of compact MX80 constructed from 16S rRNA sequencing data and BLAST sequences. % relative abundancy is shown at the end of each leaf and bootstrap values are included on branches.

4.3 Comparison of activated anaerobic iron-reducing community of MX80 bentonite and activated aerobic microbial community of MX80 bentonite

From analyses carried out using Stamp (figure 4.10), the aerobic powder community is distinct from all other communities. The compact aerobic community is spread between an area close to the powder aerobic community and the anaerobic communities, this could be because the swelling of the compacted clay caused some areas of the flasks to become anaerobic with less ability for oxygen to diffuse – this is supported by the abundance of facultative anaerobes in the microbial community. It should be noted that samples were mixed prior to sampling for DNA extraction to ensure homogeneity across samples. The anaerobic powder community is also clustered suggesting there is a low diversity between replicates. However, the anaerobic compacted samples are somewhat distant, it could be that the powder is more homogenous as the microbes can freely move around, whereas in the compact clay the microbes cannot move around so freely after processing and compaction. Additionally, the compaction process may

have introduced new microbes and limited the survival of others. Therefore, different areas of compacted blocks may have different indigenous microbial communities.

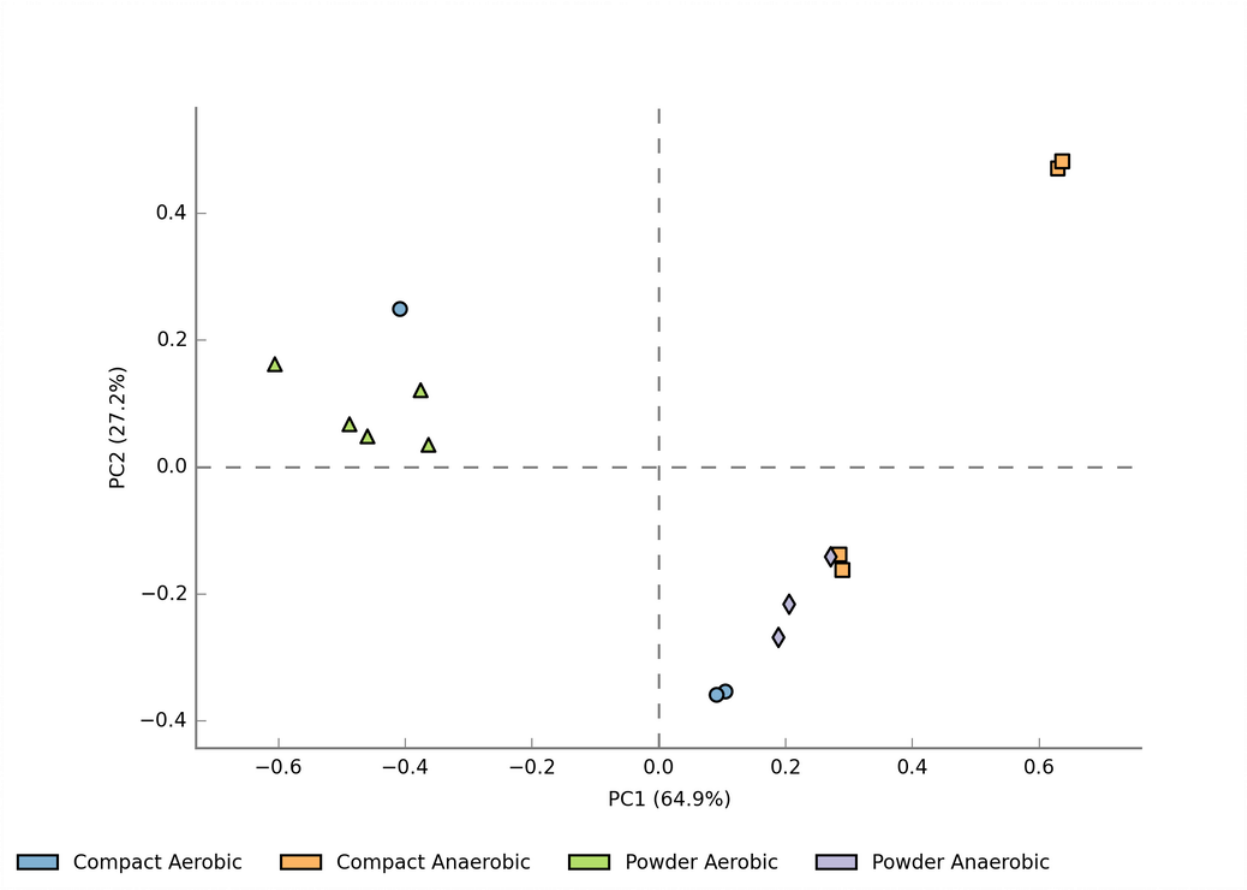

Figure 4.10: PCA plot of anaerobic and aerobic iron-reducing enrichments constructed using QIIME2 output from 16S rRNA Illumina sequencing and Stamp (see section 3.8.6)

Further to this, boxplots were created using Stamp to investigate the significance of different species present and associated abundance in each community (figure 4.11). Of particular significance was *Pseudomonaceae* which was found to be present in higher abundance in aerobic samples than in anaerobic. This refers to *P. stutzeri* which was dominant in the aerobic samples, but as it is facultatively anaerobic, it was also identified in all anaerobic samples. This species has also been identified in other bentonite samples and in groundwater from repository sites (see section 4.1). Also significant was *Clostridaceae 1* and *Bacillaceae*. Both these orders had a higher relative abundance in anaerobic samples than in aerobic, with *Clostridaceae 1* having a higher relative abundance in powder and *Bacillaceae* in compact. This figure also illustrates the

difference in range and diversity between powder and compact samples, whereby the boxes are much longer for compacted samples, further suggesting there is more variation between samples.

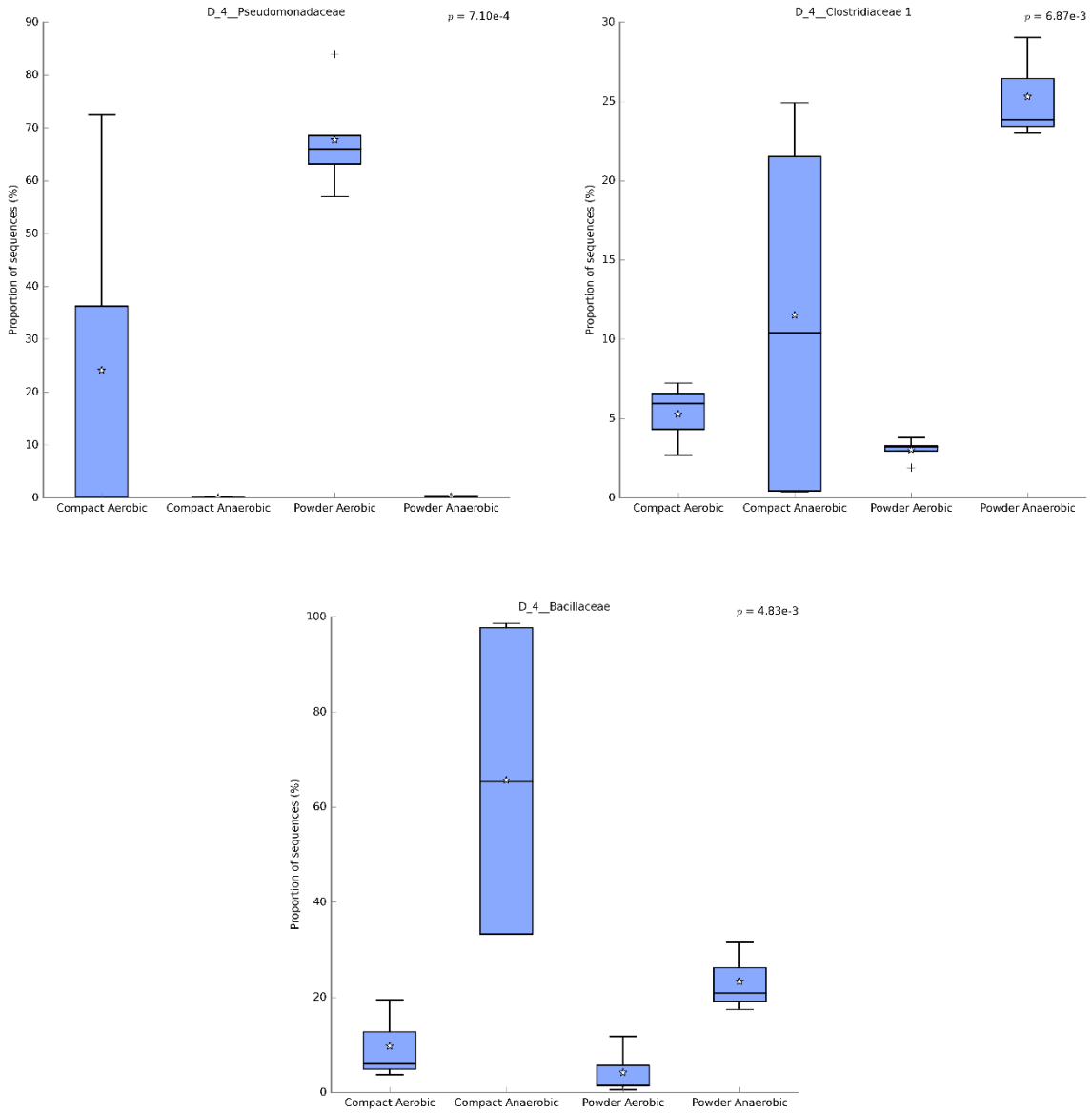

Figure 4.11: Boxplots of bacteria families identified in 16S rRNA sequencing of anaerobic and aerobic MX80 bentonite microbial enrichments were constructed using Stamp. The stars indicate the mean and the p-value is presented in the top right of each graph; Pseudomonaceae *has a p-value of 0.012,* Clostridaceae 1 *is also significant as P=0.034; and* Bacillaceae *has a p-value of 0.054 and so is not significant.*

4.4 0.45M NaCl iron-reducing microbial enrichments with MX80 bentonite

Having identified an indigenous iron-reducing community from MX80 bentonite under low saline conditions, it was necessary to consider the range of groundwater salinities that may be present at the repository site. Higher salinities would put different selective pressures on the microbial community, and likely change the composition. 0.45M NaCl was chosen as it reflects sea-level salinity which has known microbial activity and is within the range of groundwater salinities observed at international repository sites (table 2.2).

4.4.1 Results

4.4.1.1 pH of 0.45 M NaCl enrichments with MX80 bentonite

In all experiments there was an initial slight decrease in pH (figure 4.12), but the pH returned to circumneutral by the end of the experiment. There was no significant difference in pH between the different experiments.

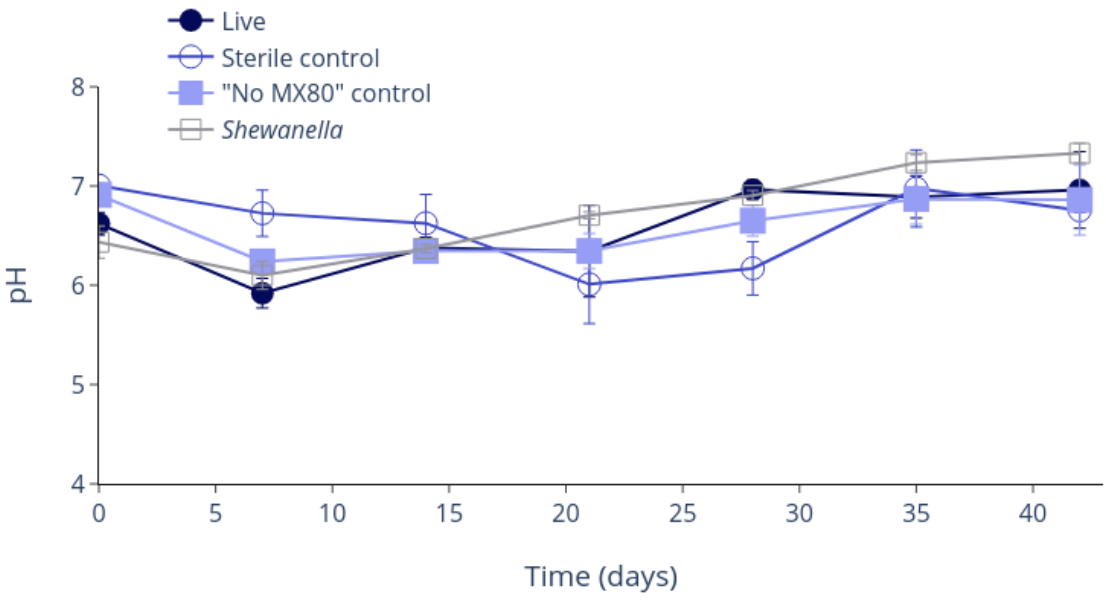

Figure 4.12: pH measurements of 0.45M NaCl enrichments with compacted MX80 bentonite were taken weekly. All flasks initially decreased to pH6-6.5 before returning to circumneutral. Error bars show standard error.

4.4.1.2 Concentration of Fe(II) throughout 0.45 M NaCl enrichments with MX80 bentonite

$Fe(II)_{aq}$ remained very low, below 0.1 mM, throughout the experiment. These concentrations are like all other enrichments presented here and are likely because Fe(II) does not stay in the aqueous form, but rather spontaneously reacts with other compounds present, possibly carbonates or sulfide (see section 4.1).

The Fe(II) concentration of 0.45 M NaCl enrichments was measured weekly (figure 4.13). The unsterilised experiments and *S. oneidensis* controls were very similar and increased from 0 mM to 4.5 mM and 4.6 mM, respectively. The "No MX80" control remained below 0.2 mM throughout the experiment, and the sterile control increased at a slow rate from 0 mM to 1.8 mM. The concentration of Fe(II) in the live unsterilised experiment was significant when compared to the sterile and "No MX80" control ($P=1.41x10^{-7}$ and $P= 8.98x10^{-12}$, respectively) between day 14 and 21, these were the time points with the biggest increase in Fe(II) concentration.

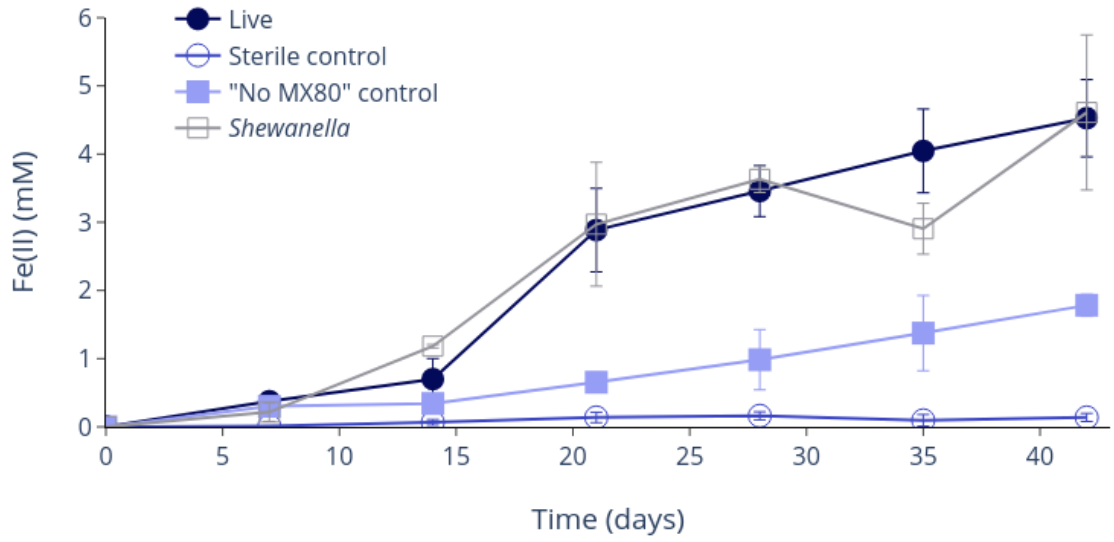

Figure 4.13: The concentration of Fe(II) in 0.45 M NaCl enrichment experiments with MX80 bentonite. Error bars show standard error.

4.4.1.3 VFA analysis of 0.45 M NaCl enrichments with MX80 bentonite

VFA analysis (figure 4.14) of 0.45 M NaCl enrichments revealed a high concentration of acetic, butyric and propionic acids in all samples. Formic acid was also present and trace amounts of isobutyric and isovaleric acids. VFAs showed no significant differences between bacterial presence and absence, apart from a couple of exceptions; the butyric acid concentration of the "No MX80" control had a p-value of 0.0069 when compared to the live unsterilised experiment between days 14-21. The sterile control was also significant; the concentration of propionic acid between days 14-21 had a p-value of 0.0267 when compared to the live unsterilised experiment. The acetic acid results are likely due to the continual production and use of secreted metabolic acids by members of the microbial community that results in no clear trend and an increase in variation between replicates. The concentration of both butyric and propionic acids decreased throughout the experiment from ~300 PPM to 0 PPM and 100 PPM, respectively. The "No MX80" control did not decrease to the same extent and reached a concentration of 137 PPM butyric acid and 122 PPM propionic acid. The concentration of formic acid in the unsterilised experiment initially increased to day 7 from 0 PPM and then decreased again to 0 PPM by day 21. The "No MX80" control remained between 50-100 PPM throughout the experiment.

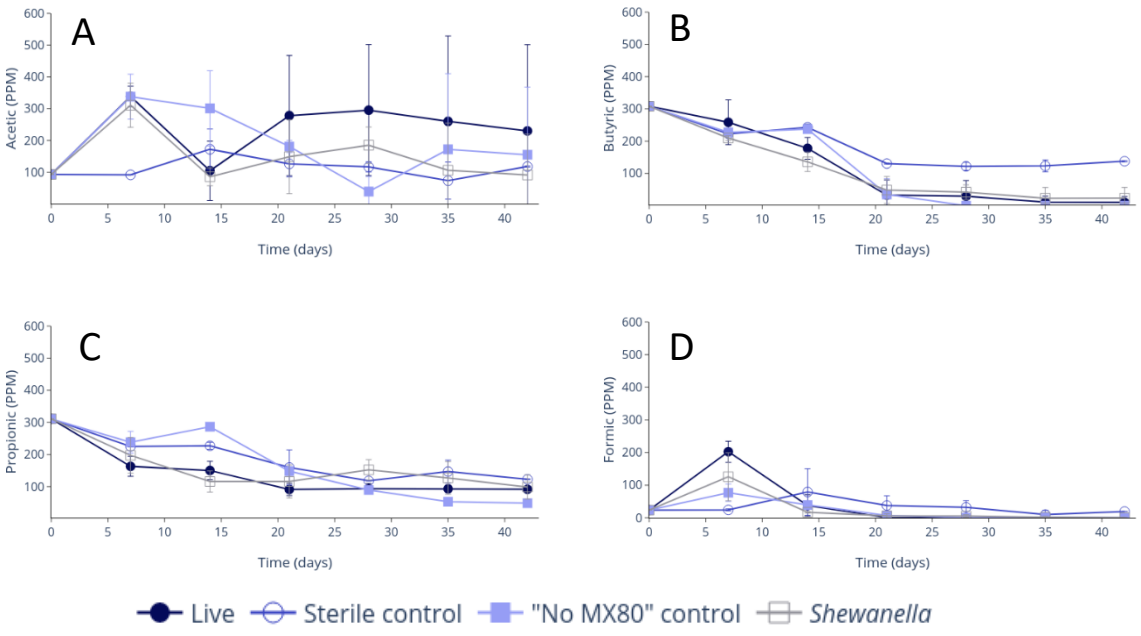

Figure 4.14: VFAs of 0.45M NaCl enrichments with MX80 bentonite. Error bars show standard error.

4.4.1.4 Indigenous activated iron-reducing community of MX80 bentonite at 0.45 M NaCl

After processing through QIIME 2, the 16S rRNA sequencing yielded an average of 96,477 sequences across the three sequencing libraries with an average length of 227 bases across 398 ASVs. The negative control returned 38 sequences which suggests there was no large-scale contamination. Across all three samples, the most prevalent bacteria belonged to the orders *Bacillales* and *Clostridales* (figure 4.15). This result is in keeping with results from previous enrichments. There were also some halotolerant species identified, such as those belonging to the order *Haloplasmatales,* which should thrive in the seawater-level salinity of these enrichments. *P. stutzeri* was also present, as with previous enrichments and other microbial community studies relevant to nuclear waste disposal (see section 4.1).

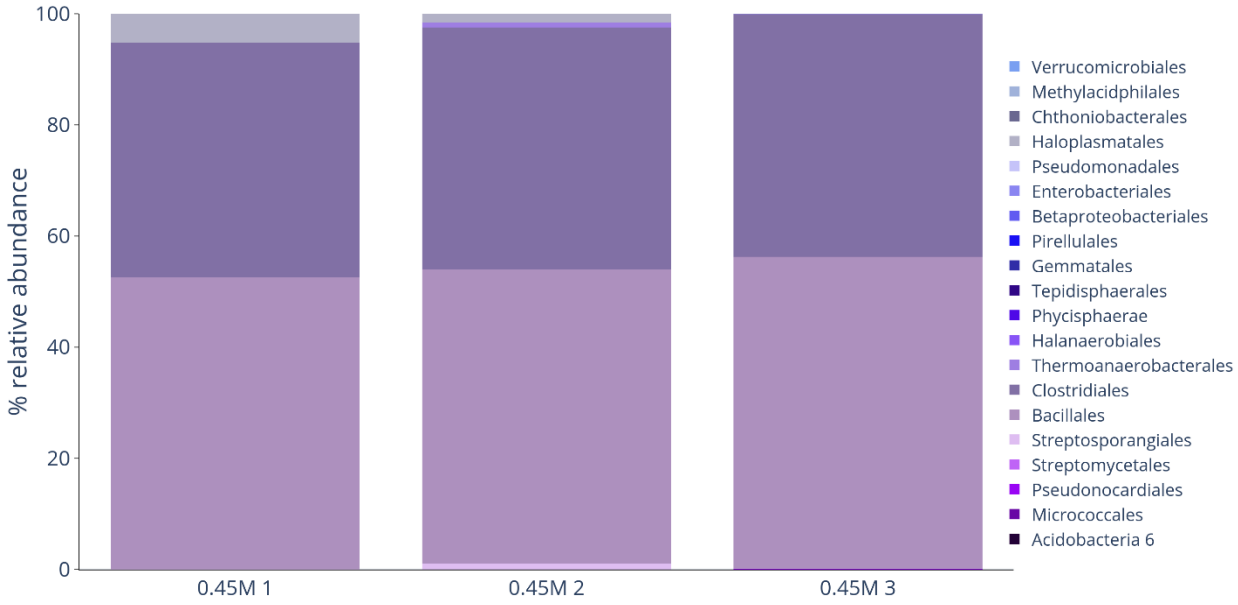

Figure 4.15: Community structure of 0.45M NaCl enrichments with MX80 bentonite using data from 16S rRNA sequencing. Data is presented at % relative abundance across a triplicated experiment. The main three orders are Bacillales, Clostridales, and Haloplasmatales.

A phylogenic tree was constructed using the most abundant ASVs and their nearest neighbour, identified using BLASTN (Zhang et al., 2000) (figure 4.16). There are also several species of putative IRB and SRB, such as *Desulfitobacterium* and *Desulfosporosinus.* Most of the community are firmicutes, which is consistent with previous enrichments (presented in section 4.1); however, in these enrichments, more halotolerant and alkali tolerant species are dominant, this includes *Alkalibaculum.*

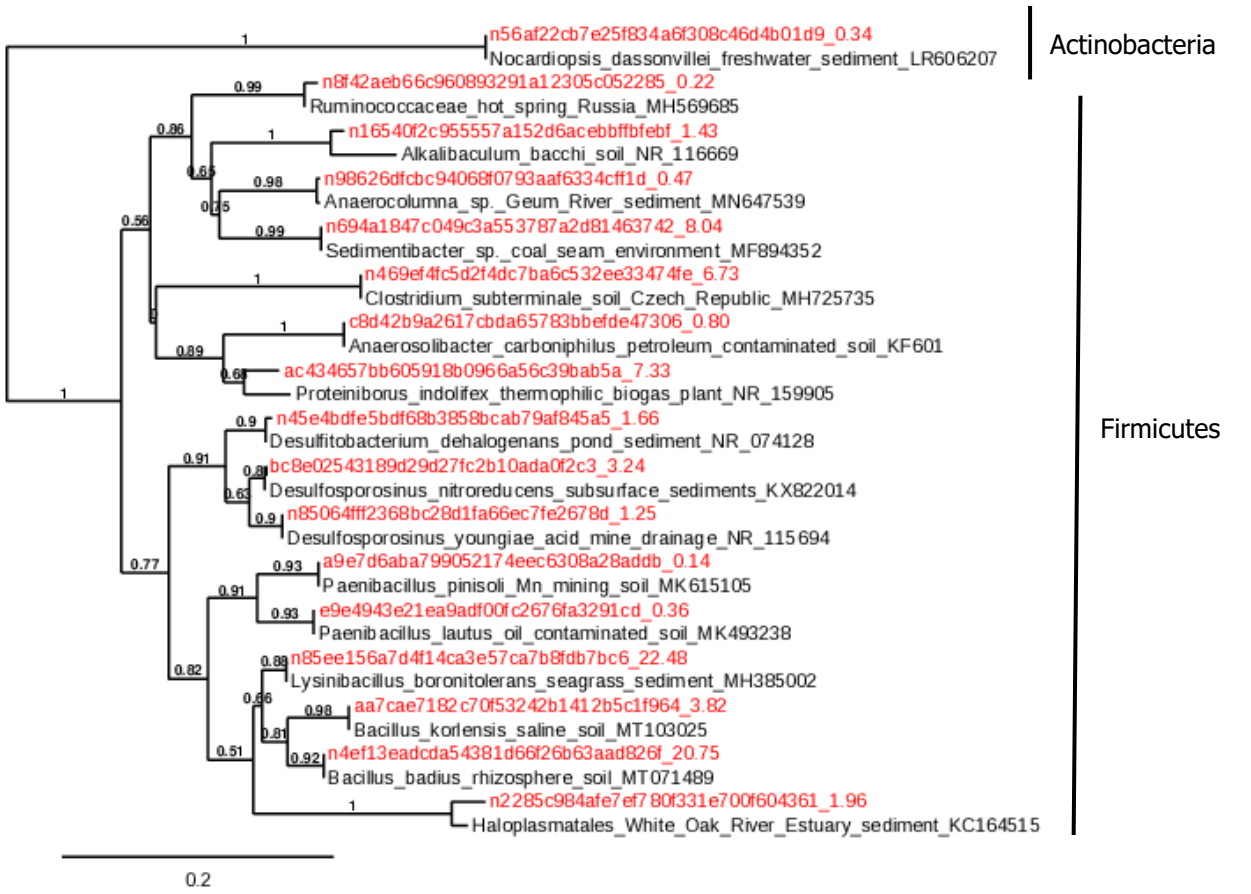

Figure 4.16: Phylogenic tree of most dominant ASVs in the microbial community of compacted MX80 constructed from 16S rRNA sequencing data and BLASTN sequences from 0.45M NaCl enrichments. % relative abundancy is shown at the end of each leaf and bootstrap values are included on branches.

4.4.1.5 SEM images of MX80 bentonite recovered from 0.45 M NaCl iron-reducing enrichments

Obvious bacterial hyphae were observed in all unsterilised experiments (figure 4.17). There was no evidence of secondary mineralization resulting in the formation of crystalline mineral textures

in the “No MX80” control, mainly PCFeO debris was observed, as added at the start of the experiments. Limited PCFeO debris was also observed in the other samples which contained PCFeO. Likewise, no specific structures were identified in the sterile control.

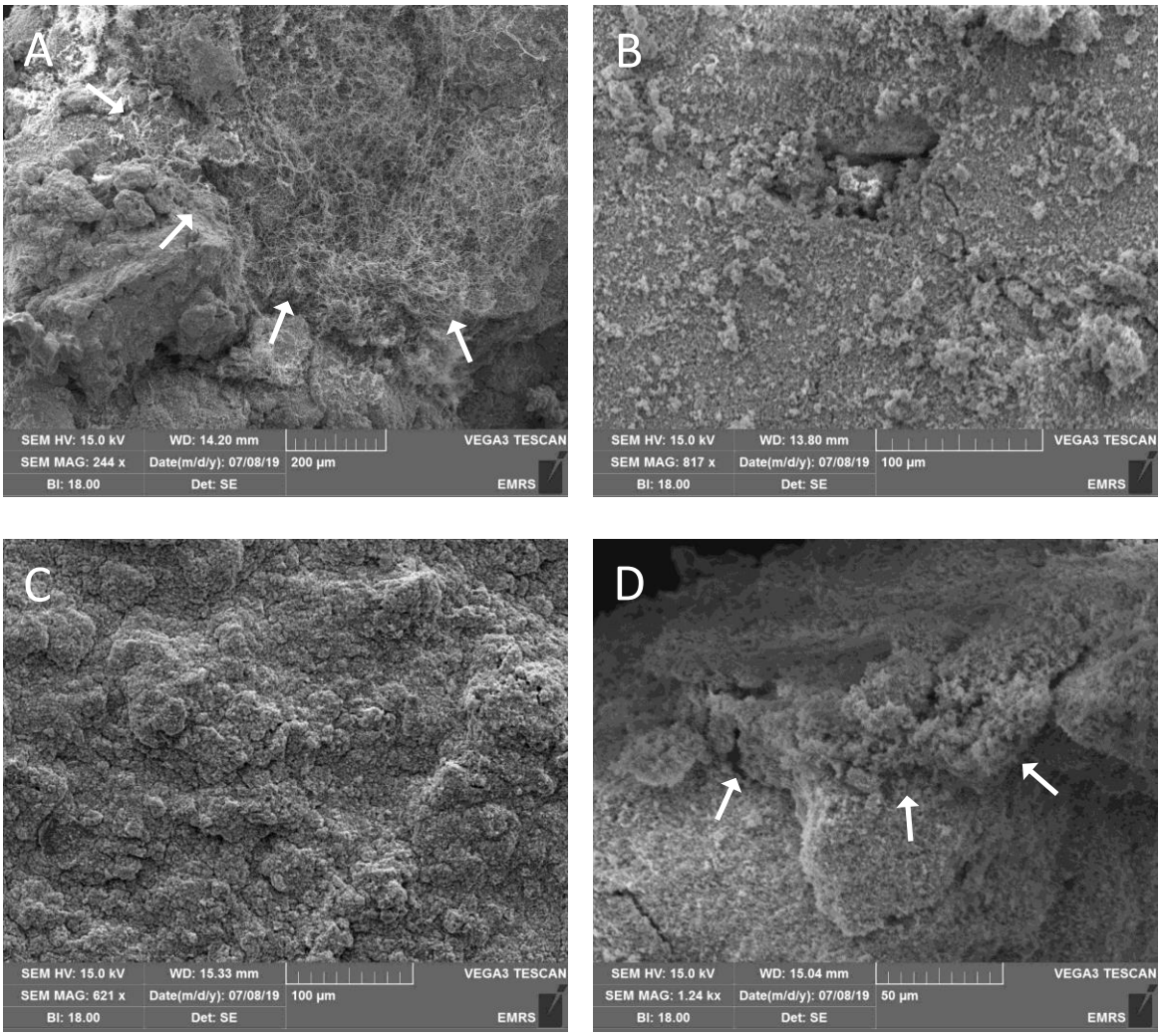

Figure 4.17: SEM images of MX80 recovered from 0.45M NaCl enrichments. There was extensive hyphae growth on the clay / iron in the experimental flask (A, arrows show the outer edge of bacterial growth). No specific structures were seen in the No MX80 control (including hyphae and secondary minerals) (B) or the sterile control (C). There was some bacterial growth on the upper surface of powder collected from the unsterilised positive, S. oneidensis*, control (D, arrows show the outer edge of bacteria growth).*

4.4.1.6 EDX analysis of MX80 bentonite recovered from 0.45 M NaCl iron-reducing enrichments

Bulk EDX analysis of samples (figure 4.18) showed that all flasks contained silicon, aluminium, sodium and oxygen apart from the "No MX80" control which only contained iron and oxygen. The samples containing microbes had a much higher percentage of carbon than the sterile control. The unsterilised experiment had relatively low iron, whereas samples from sterile flasks and flasks containing *S. oneidensis* had higher levels of iron.

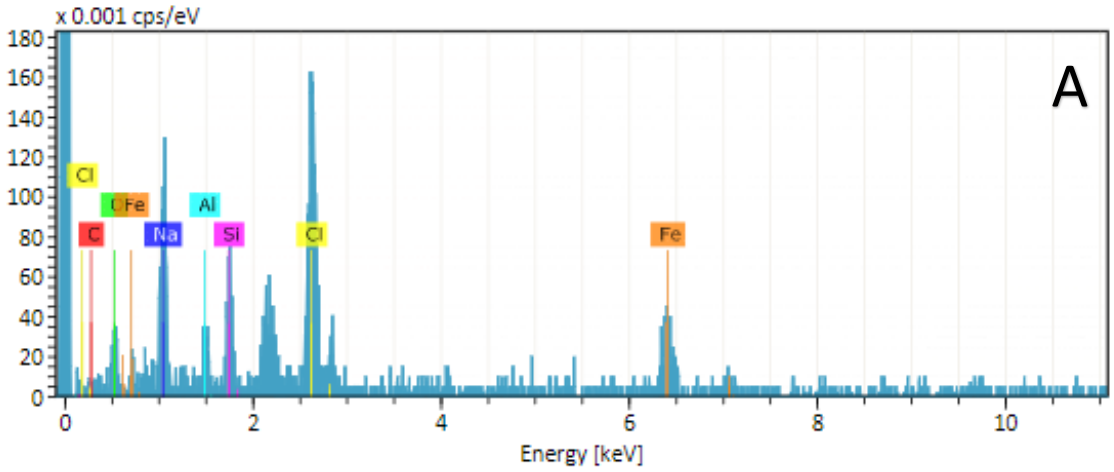
x 0.001 cps/eV
A
Cl
O
Fe
C
Na
Al
Si
Cl
Fe
Energy [keV]

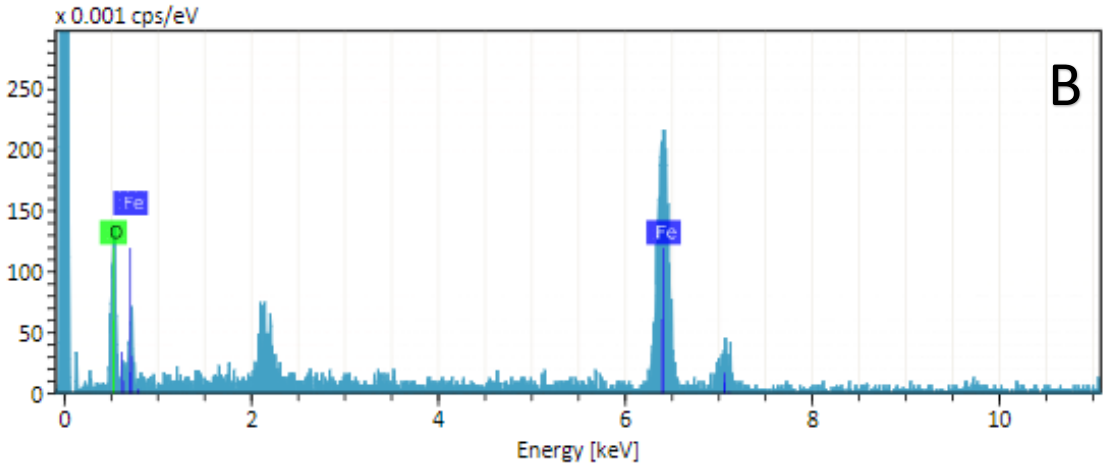
x 0.001 cps/eV
B
Fe
O
Fe
Energy [keV]

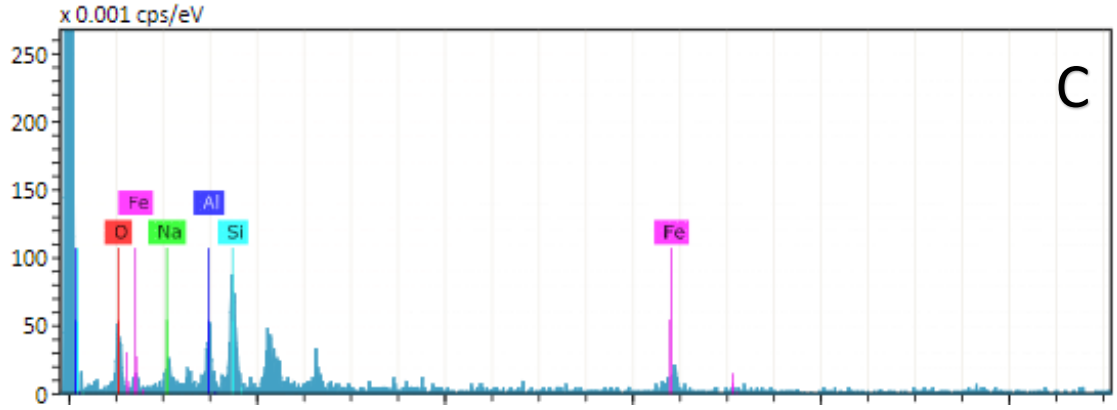
x 0.001 cps/eV
C
Fe
Al
O
Na
Si
Fe

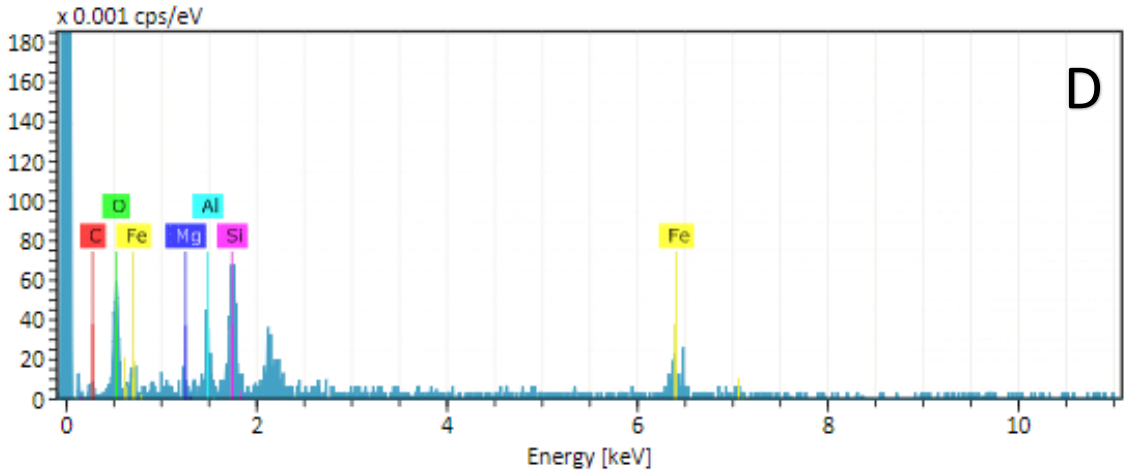
x 0.001 cps/eV
D
O
Al
C
Fe
Mg
Si
Fe
Energy [keV]

Figure 4.18: Bulk EDX analysis of MX80 recovered from 0.45M NaCl iron-reducing enrichments shows that the unsterilised experiment (A), the no MX80 control (B), the sterile control (C), and the S. oneidensis *control (D). Oxygen is shown in red (A-C) and in green (D). The unlabelled peaks represent gold from gold coating the samples.*

4.4.1.7 XRD analysis of MX80 recovered from 0.45 M NaCl iron-reducing enrichments

In order to identify any mineralogical changes to the MX80, XRD analysis was carried out (figure 4.19). The results indicate that when microbes are present magnetite (Fe_3O_4) is formed, in keeping with which flasks became black in colour and where iron-reduction was expected. Magnetite is a mixed Fe(II / III) mineral which is black in colour and a known product of biological iron reduction coupled to oxidation of organic matter (Lovley, 1991). Magnesioferrite ($(Mg(Fe^{3+})_2O_4$) is also present in this sample, which could also be a product of iron-reduction and indicates possible interaction with the magnesium in the groundwater. Both magnetite and magnesioferrite can be attributed to the black precipitate observed in the enrichment flasks; unlike previous enrichments, no goethite was observed. Halite (NaCl) is also, unsurprisingly, present in all samples, as is quartz (SiO_2) among other clay minerals. In the sterile and control flasks, no magnesioferrite or magnetite is present; however, hematite is present. This result suggests that reduction of hematite to magnetite is either much slower or not possible without the facilitation of bacteria.

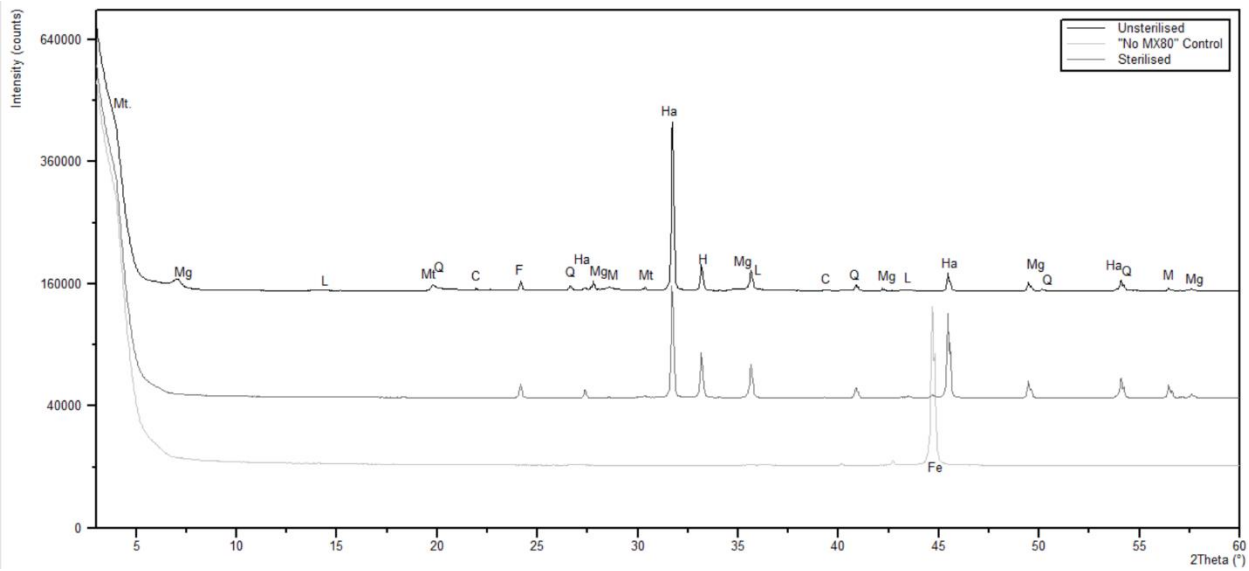

C	**F**	**Fe**	**H**	**Ha**
Calcite	Feldspar	Ferrihydrite	Hematite	Halite
L	**M**	**Mg**	**Mt**	**Q**
Lepidocrocite	Magnesioferrite	Magnetite	Montmroillonite	Quartz

Figure 4.19: XRD spectra of MX80 recovered from 0.45M NaCl iron-reducing enrichments

4.5 2.5 M NaCl iron-reducing microbial enrichments with compacted MX80 bentonite

As observed in 0.45 M NaCl enrichments, microbially-influenced iron-reduction was still possible at seawater-level salinity and the microbial community was very similar to that of the initial enrichment. However, groundwaters at potential repository sites may exceed seawater-level salinity. Therefore, further enrichments at a higher salinity were carried out to see if the microbial community could survive and iron-reduction continue under these more extreme conditions. These experiments replicated the set-up of the 0.45 M NaCl enrichments with compact MX80 bentonite.

4.5.1 Results

4.5.1.1 pH of 2.5 M NaCl iron-reducing enrichments with MX80 bentonite

No colour change was observed in these experiments. pH was measured weekly, and the averages calculated. The pH remained circumneutral across all experimental set-ups (figure 4.20) which may be because there was limited microbial activity and therefore fewer acids secreted as seen in previous enrichments. There was a slight but general increase in pH for all experiments except the “No MX80” control.

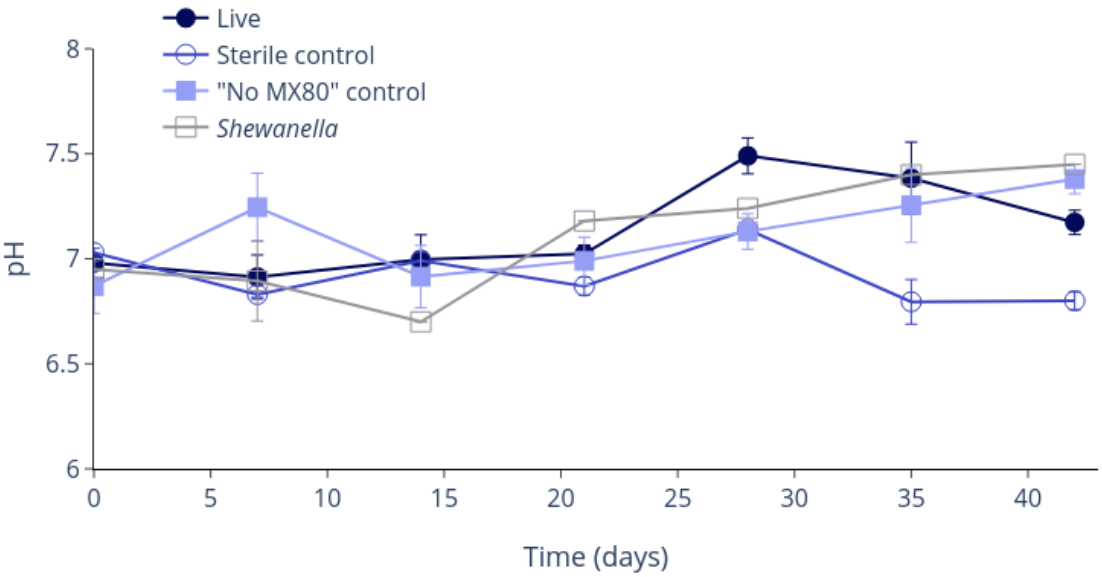

Figure 4.20: pH was measured weekly throughout high saline enrichments. pH remained between 6.7 and 7.5 throughout the experiment for all flasks. Error bars show standard error.

4.5.1.2 Concentration of Fe(II) during 2.5 M NaCl iron-reducing enrichments with MX80 bentonite

$Fe(II)_{aq}$ was not detected throughout the experiment. The concentration started at 0 mM and remained at 0 mM until day 42, reasons for this are presented in section 4.1.

The concentration of total Fe(II) was measured weekly (figure 4.21). The concentration remained at 0 mM throughout the experiment for the "No MX80" control. However, for the sterile control and *S. oneidensis* control total Fe(II) increased until day 28 before decreasing until day 42. The sterile control increased the most to 0.51 mM on day 28. The live unsterilised experiment increased from 0 mM to 0.32 mM on day 35 before decreasing to 0.26 mM on day 42. When compared to the "No MX80" control, the concentration of Fe(II) in the live unsterilised experiment between day 21 and 28 (the point at which Fe(II) concentration increased the most) was found to be significantly higher with a P-value of 0.00125.

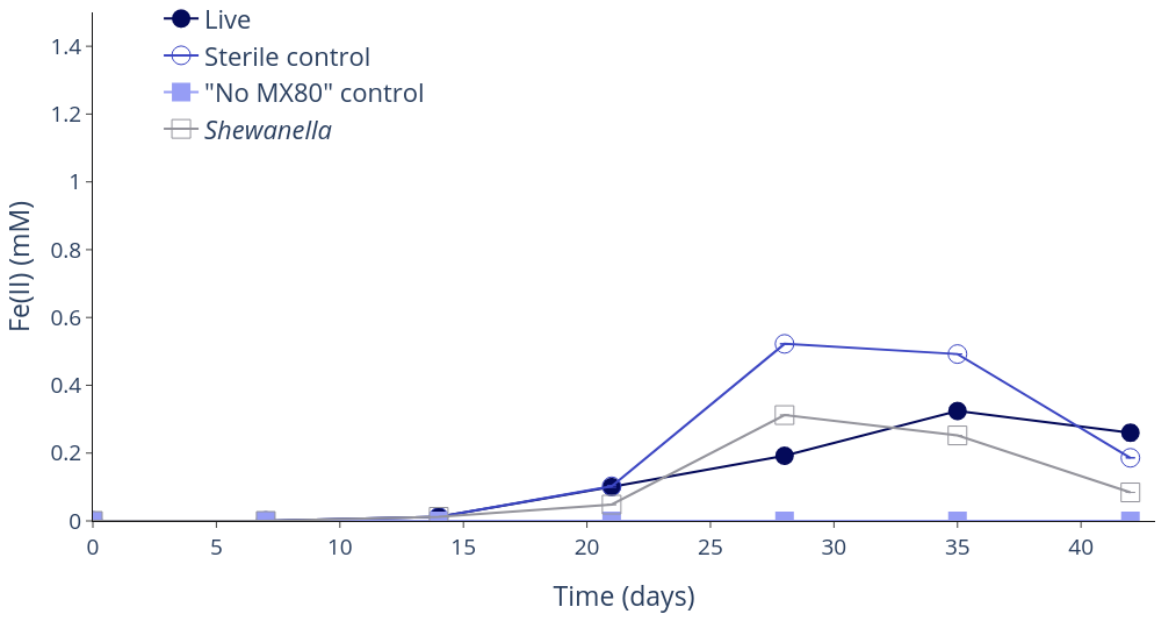

Figure 4.21: The total Fe(II) in 2.5 M NaCl enrichments increased slightly in all flasks after day 7 except the No MX80 control which remained at 0 mM throughout the experiment. However, the concentration remained below 1 mM. Error bars show standard error but are hidden by the symbols.

4.5.1.3 VFA analysis of 2.5 M NaCl iron-reducing enrichments with MX80 bentonite

IC analysis detected only 4 VFAs present: acetic, butyric, propionic and formic acids. All VFAs decreased over time with the unsterilised experiment decreasing at a slower rate than the controls (figure 4.22). Acetic, butyric and propionic acids all decreased to 0 PPM and did not increase thereafter. Formic acid did also decrease, although remained above 0 PPM in the unsterilised and sterile experiments. In the positive control with *S. oneidensis* formic acid decreased to 0 PPM and then increased to 50 PPM. The decrease towards 0PPM was slower in the "live" unsterilised experiments as the bacteria were both producing and consuming VFAs.

Formic acid was the only VFA which was found to have significantly different results between the unsterilised experiment and the control. Between day 0 and day 7 the P-value for a comparison of means of the "no MX80" control compared to the unsterilised experiment was 0.03, and between the unsterilised experiment and *S. oneidensis* control, the P-value was 4.93×10^{-4}.

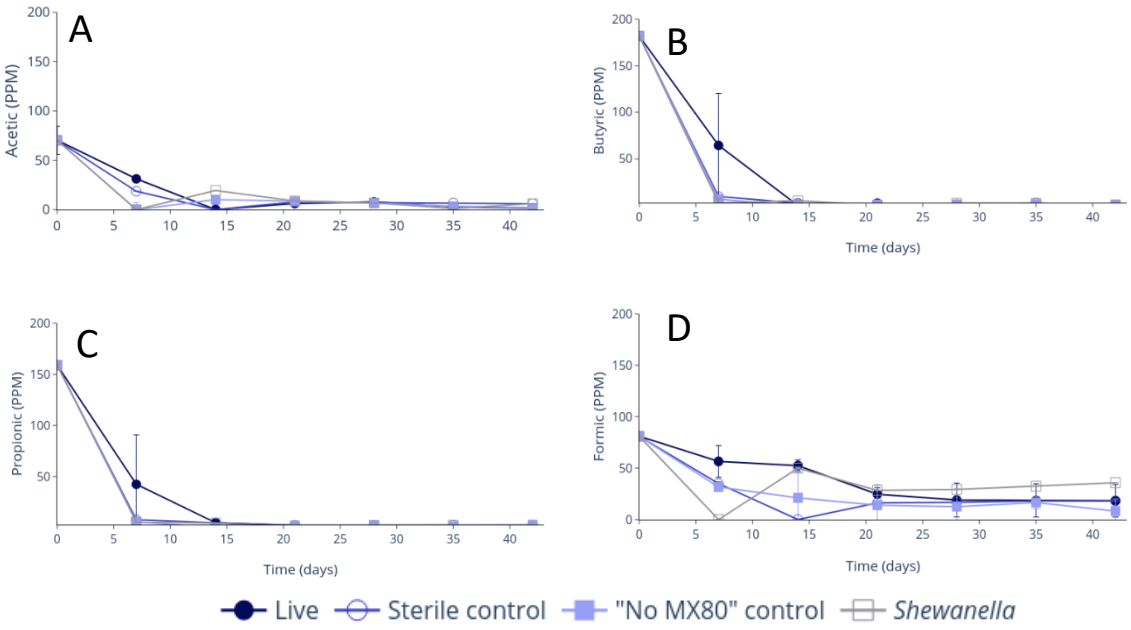

Figure 4.22: VFA analysis of the 2.5 M NaCl iron-reducing enrichments showed that all VFAs were depleted by day 7 for all controls and day 14 for the 'live' experimental flask. Formic acid was the exception, as it did not follow this trend. There was a general decrease across all experiments from 80 PPM on day 0 to below 50PPM on day 42. Error bars show standard error.

4.5.1.4 Indigenous iron-reducing bacterial community of the MX80 bentonite at 2.5 M NaCl

After QIIME2 analysis, an average of 47,558 sequences were identified across the three sequencing libraries – the unsterilised live experiments. The average sequence length was 227 and there was just 184 unique ASVs. The control sample ensured that no contamination occurred as only 23 sequences were returned.

Figure 4.23 shows the community structure as a bar plot. By far the most dominant order is *Bacillales,* accounting for over 99.3% relative abundance in all samples. Like all previous enrichments, *Clostridales* is also present and almost 100% of all samples are firmicutes. Since attempts to extract DNA without enrichment were unsuccessful, the community presented is the result of growth and enrichment under highly saline conditions. Using the data from 16S rRNA Illumina sequencing, a phylogenic tree was constructed using the most abundant ASVs and their nearest match found using BLASTN (Zhang et al., 2000) (figure 4.24).

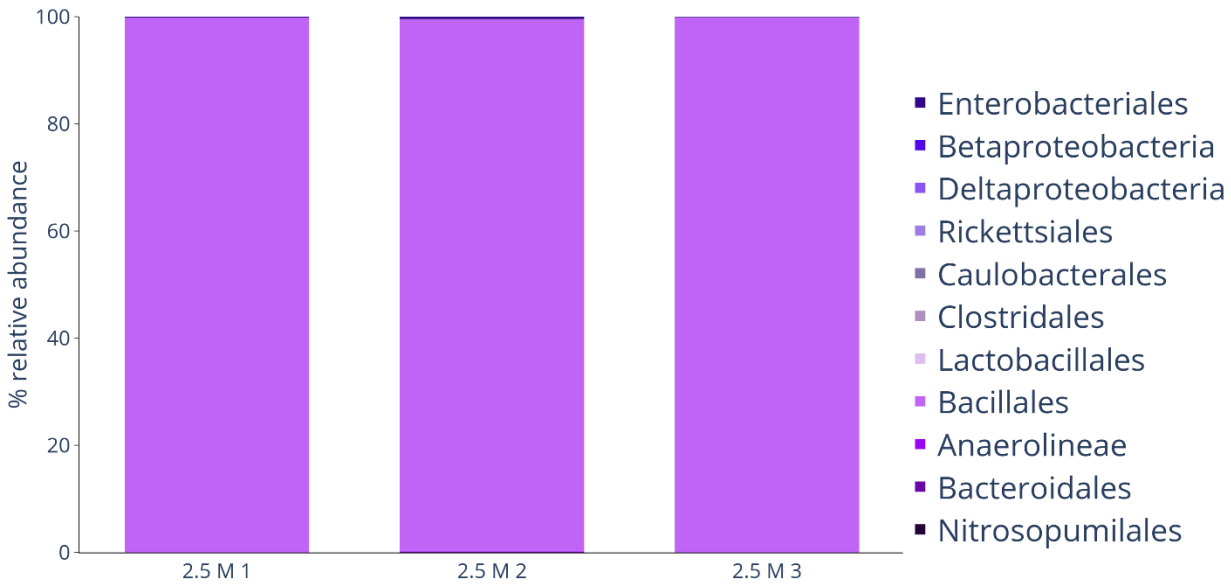

Figure 4.23: Barplot of the indiegnous microbial community of 2.5M NaCl enrichments with MX80 bentonite presented at %relative abundance of orders of bacteria across three replicates. Almost 100% of all replicates belong to the order Bacillales.

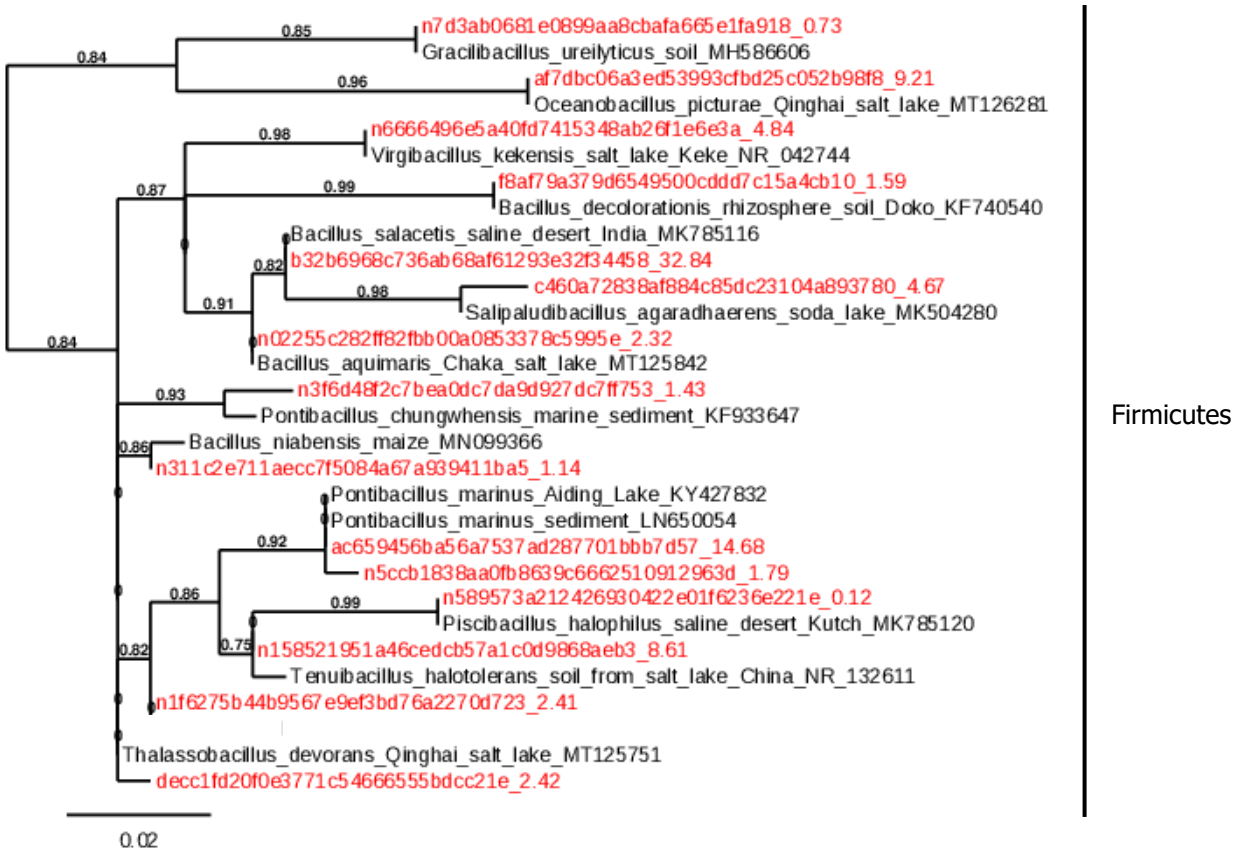

Figure 4.24: A phylogenic tree constructed from 16S rRNA sequencing data of 2.5M NaCl iron-reducing enrichments and BLASTN on NCBI database. Nearest neighbour-joining method was used and trees were constructed using MEGA7. % relative abundancy is shown at the end of each leaf and bootstrap values are included on branches.

4.5.1.5 SEM images of MX80 recovered from 2.5 M NaCl iron-reducing enrichments

SEM images of recovered substrate showed similar crystal growth in all flasks containing MX80 (figure 4.25). The observed crystal is likely halite polymorphs; however other possibilities include aragonite needle structures (possibly an iron-rich polymorph), or gypsum. The “No MX80” control contained only iron debris.

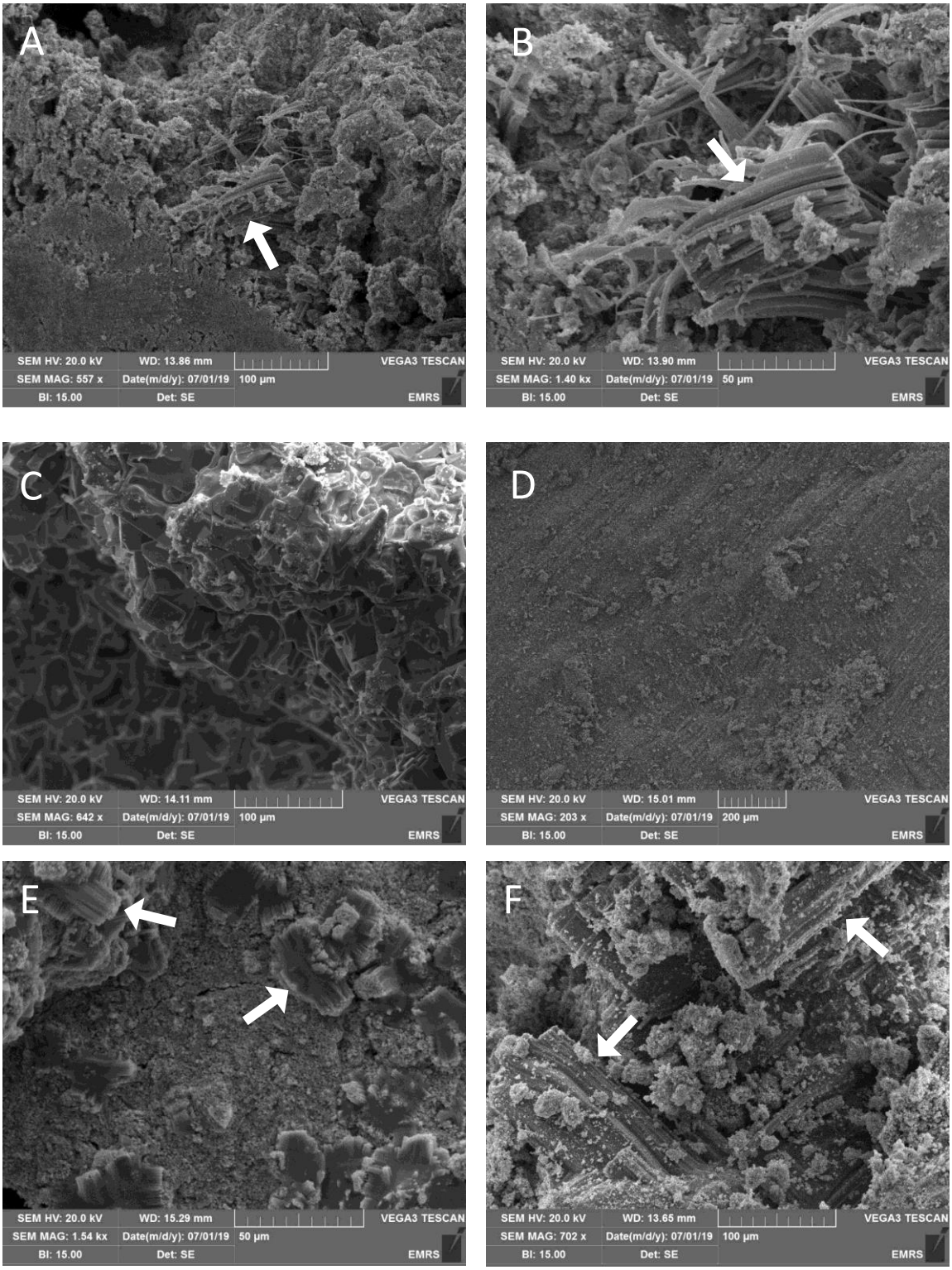

Figure 4.25: SEM images of substrate recovered from 2.5 M NaCl iron-reducing enrichments. Extensive crystal growth was observed in samples from the unsterilised experiment (A-C) including likely halite polymorphs (arrows A, B) and calcite (C), no microbes were observed. No

specific structures were observed in the No MX80 control (D). Similar crystals to that of the live experiment were seen in the sterile (E) and S. oneidensis *(F) controls.*

4.5.1.6 EDX analysis of MX80 recovered from 2.5 M NaCl iron-reducing enrichments

Due to the high levels of NaCl, spectra from bulk EDX analysis were skewed, and most elemental composition was masked. No carbon was detected in any experiment. Sodium was between 30-50% of the elemental composition of each sample.

4.5.1.7 XRD analysis of MX80 recovered from 2.5 M NaCl iron-reducing enrichments

During these enrichments there was very little iron-reduction and, unlike in previous experiments, very little black precipitate was produced. SEM images revealed the presence of salt polymorph crystals. To further investigate these crystals, and if any mineralogical changes had taken place the samples were further analysed using XRD (figure 4.26). There was little difference between the controls, the sterile and the unsterilised experiments. These similarities were expected as there were no notable changes between samples in terms of iron-reduction, VFA concentration, or SEM images. All samples contained clay minerals such as quartz and montmorillonite, and had below 2% hematite, and below 5% halite. Halite is a salt crystal, usually cubic in structure and formed from NaCl. Hematite (Fe_2O_3) is black or red in colour and could account for the small concentration of black precipitate observed. However, it may be the result of abiotic transformation of PCFeO to a more stable compound (Letini et al., 2012) which is much less readily reduced by microbes, rather than a secondary mineral product of biogenic iron-reduction.

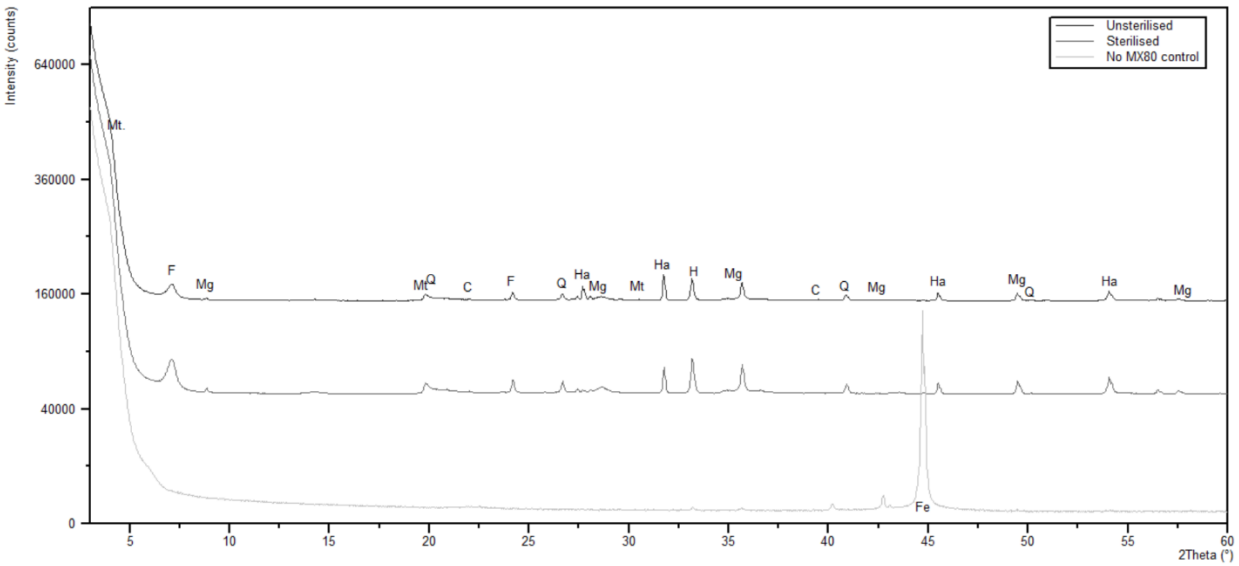

C	F	Fe	H	Ha	Mg	Mt	Q
Calcite	Feldspar	Ferrihydrite	Hematite	Halite	Magnetite	Montmorillonite	Quartz

Figure 4.26: XRD pattern after reitvald refinement using HighScore Plus of MX80 recovered from 2.5M NaCl iron-reducing enrichment

4.6 Comparison of anaerobic iron-reducing microbial communities at all salinities

In order to compare the microbial community of the original anaerobic compact iron-reducing enrichments (0.0002 M NaCl), 0.45 M NaCl enrichments and 2.5 M NaCl enrichments, a PCA plot was created using Stamp and data from QIIME2 (figure 4.27). The 0.45 M NaCl and 2.5 M NaCl are both clearly distinct from one and another, with the 0.45 M a little more spread out, indicating there are more differences between replicates. There is one outlier in the 2.5 M enrichments, but otherwise, the samples are very tightly clustered. The 0.0002M NaCl samples are split between two areas, suggesting that there are two distinct communities present, as discussed earlier, this could be due to the bacteria not being able to move around the compacted block to become homogenous.

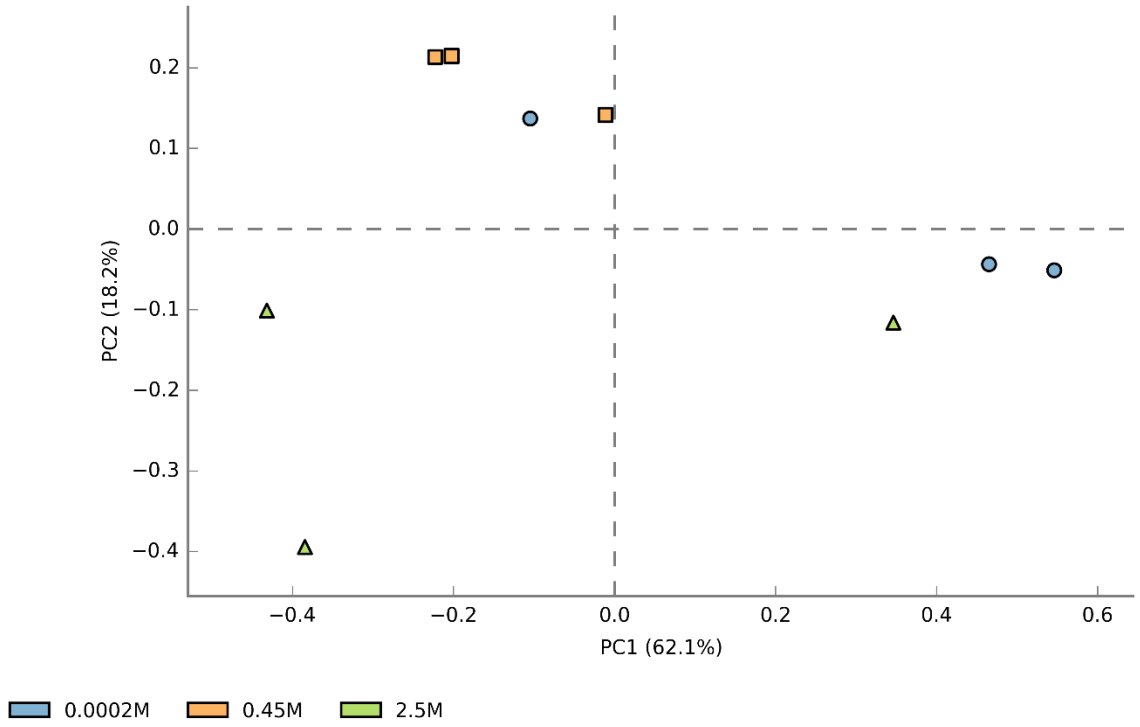

Figure 4.27: PCA plot of bacterial communities from unsterilised iron-reducing enrichments at different salinities, made using Stamp with data from QIIME2 outputs using 16S rRNA sequencing.

Further analysis was carried out by comparing individual species (figure 4.28). It was found that the abundance of some species in a particular salinity was significant, this included *Alkalibacter*, *Anaerocolumna, Desulfitobacterium* and *Lysinibacillus.* All these species were found to be significantly more abundant in 0.45 M NaCl enrichments. This result suggests that these bacteria are only mildly halotolerant and so cannot survive or thrive in the higher salinities. Their lower abundance in the 0.0002M enrichments suggests that there are other more dominant species present in the community that can outcompete in the low saline conditions.

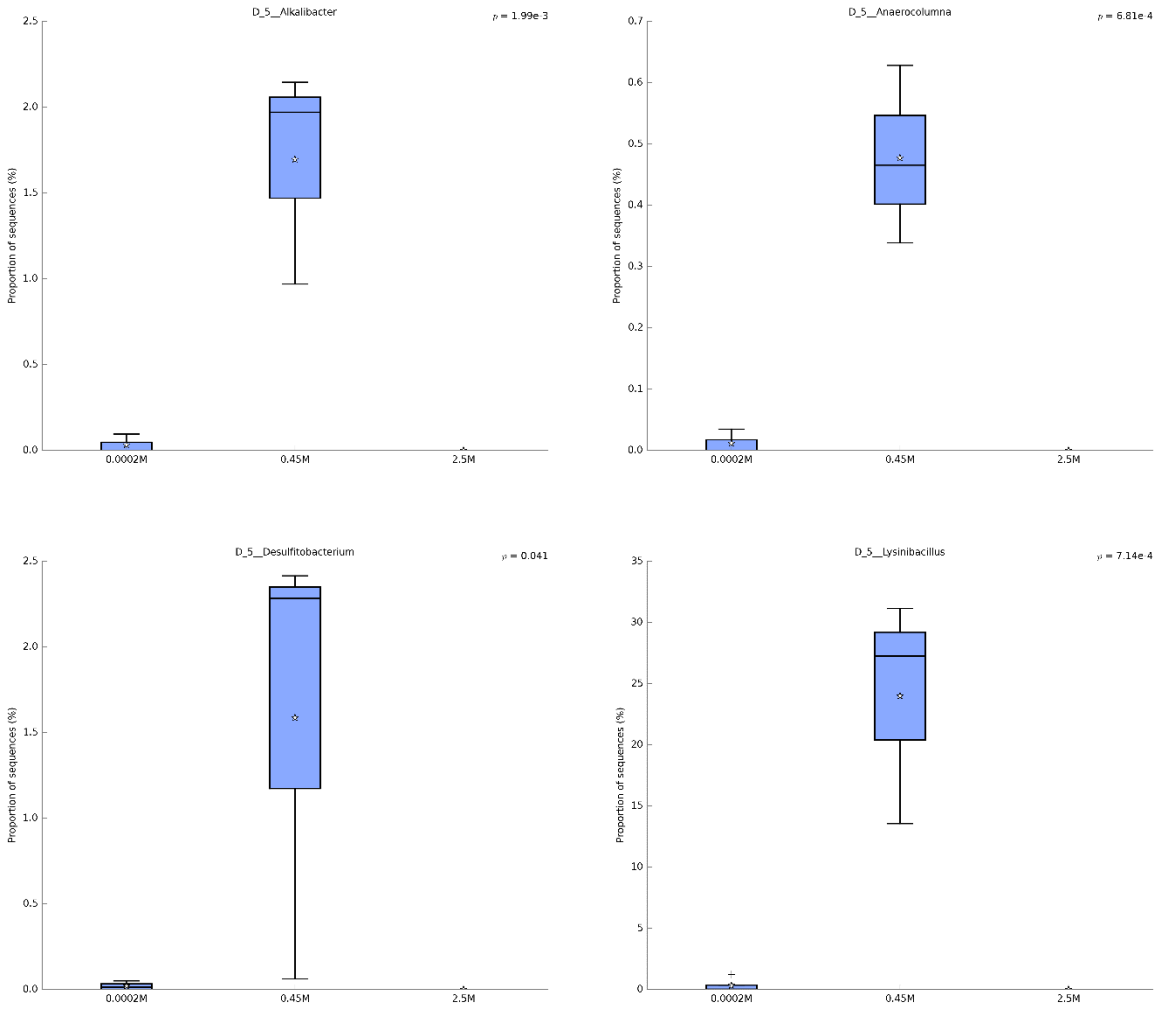

Figure 4.28: Boxplots of significant geneses from 16S rRNA sequencing of different salinity iron-reducing enrichments with MX80 bentonite were created using Stamp. Stars indicate the mean abundance and P-values are included in each graph. Alkalibacter, Anaerocolumna, Desulfitobacterium *and* Lysinibacillus *were all significantly more abundant in 0.45 M NaCl enrichments.*

4.7 Discussion

There may have been an access issue for the added iron in the iron-reducing enrichments due to the clay swelling and trapping of the added PCFeO (poorly crystalline iron oxide) at the bottom of the flask. This swelling may have also caused the formation of pockets of anaerobic environments in the aerobic enrichments. Shaking was introduced to try and homogenise the

samples; but this was not effective, perhaps increasing the water:clay ratio would have limited the trapping effect caused by swelling.

4.7.1 The indigenous microbial community of MX80 is putatively capable of iron reduction

Iron-reduction at the lower salinities (0.0002 M and 0.45 M NaCl) proceeded to the same extent and along the same trend as positive controls containing *S. oneidensis,* a known iron-reducer (Ruebush et al., 2006). Therefore, this is evidence that the indigenous community is capable of significant iron-reduction, equal to or superseding that of model organisms for iron-reduction.

PCFeO was selected as the iron substrate because it is highly bioavailable (Lovley, 1987). However, this substrate will not be present in the repository and so it cannot be concluded that iron-reduction will occur as rapidly as observed in these enrichments. The highly compacted MX80 will also decrease microbial activity due to the small pore size and confinement, limiting bacterial activity to areas at the edge of the clay buffer where swelling may not have fully occurred (Jalique et al., 2016). However, due to the long lifespan of the repository, it is likely that at least some biogenic iron reduction may occur, it may just happen more slowly. The concentration of $Fe(II)_{aq}$ remained below 0.1 mM throughout all the experiments across all salinities. This concentration likely appeared low because $Fe(II)_{aq}$ had been adsorbed onto the surface of the PCFeO to become involved in catalysing goethite or magnetite formation or it has spontaneously reacted with sulfur or carbonates (see section 4.1).

Even at the sea-water level salinity (0.45 M NaCl) similar concentrations of microbially-mediated iron reduction were observed compared to those found in the low salinity experiments. Therefore, the microbes are somewhat salt-tolerant and if the groundwater in the repository is of a similar salinity to seawater it can be concluded that this would not prohibit microbial activity in terms of iron-reduction. However, at 2.5 M NaCl, there was no increase in iron reduction in flasks containing microbes. In fact, there was less reduction in these flasks than there was in sterile experiments. While this level of salinity is not likely to occur at a UK repository site, it is interesting that the iron-reducing microbes are not halophilic and, in fact, the microbes which are active may act to inhibit abiotic iron reduction, either through Fe-oxidisation, or through inhibiting mineralogical changes which abiotically lead to reduction of Fe(III). These differences

suggest that groundwater geochemistry is an important factor in microbial community structure and associated activities and should be fully investigated as part of the repository site selection process.

4.7.2 Notable species identified in the indigenous iron-reducing microbial community

Nitrogen is present in the groundwater as sodium nitrate, this could account for the presence of the denitrifying species *P. stutzeri* in the anaerobic enrichments. In the repository the only source of nitrogen is likely to be dissolved nitrate carried in groundwater so it is unlikely that this bacterium will be active outwith aerobic conditions. In the aerobic powder enrichments, *P. stutzeri* accounted for an average of 66% relative sequence abundance and was therefore by far the most dominant species in these communities. However, it only accounted for 2.19% relative abundance in the compacted enrichments. Perhaps due to the swelling of the compacted clay which caused areas of the flasks to become anaerobic, this led to a lower abundance of certain aerobic species including *P. stutzeri*. Further discussion on this species is presented in section 4.1.

One of the principal obstacles to survival in the repository is the high temperature (40°C - 100°C). There are a few species of bacteria identified in these experiments using the MX80 clay which could survive the higher temperatures of the repository across enrichments at all salinities (figure 2.8, see section 2.7), most likely through spore-formation due to the large proportion of spore-formers identified in the community. Other methods of survival which could be employed by the species identified include biofilm formation, or through thermophilic properties, but most bacteria identified will not survive high temperatures. However, one thermophilic species which was present is *Sporacetigenium.* This bacterium was identified in the low saline (0.0002M NaCl) anaerobic samples presented in section 4.1 and a close relative been recorded to grow at high temperatures (up to 55°C (Chen et al., 2006)) with spores that can survive higher temperatures. *Sporacetogenium* has only been known to bioleach Fe from pyrite, which is only present in trace amounts in MX80, but this species could have more iron-reducing capabilities (Rawlings, 2005). *Thermobacterales* was also identified and is another thermophilic bacterium which can survive 70°C, and so will likely survive the repository environment, at least at the MX80 / host rock interface where the temperature will be lower. It is also a known IRB (Slobodkin et al., 1999).

In the 0.45 M and 2.5 M NaCl enrichments halophilic and halotolerant species are present which were not identified in the low salinity enrichments in the microbial community of the lower salinity due to different selective pressures of the enrichment. This finding provides further evidence of the diverse and varied microbial populations which are indigenous to MX80 bentonite.

Acidobacteria 6 was found to be present in the aerobic enrichments and 0.45 M NaCl anaerobic enrichments. This subdivision does not currently have any species names (Parsley et al., 2012); however, it is known to contain facultatively anaerobic organisms and, notably, has been isolated from a uranium-contaminated soil (Barns et al., 2007). This species is indigenous to both marine and terrestrial environments and has been implicated in silica mobilisation from clays via Fe-oxidising activities (Sauro et al., 2018). In terms of the repository, iron-oxidation would increase corrosion of the carbon steel canister and could liberate silica from the clay matrix if the redox state of the associated iron in the mineral was altered. These alterations could lead to a change in the geomechanical properties of the clay (see section 4.1, 5.6, 7.7). Likewise, *Actinobacter*, which was identified in the aerobic microbial community, has also been implicated in Fe-oxidising activity in relation to silica solubilisation (Sauro et al., 2018; Singh et al., 2008). Furthermore, *Actinobacteria* can grow filamentously and therefore could create channels and increase travel through the clay buffer.

4.7.3 Fermenting bacteria are active in the indigenous microbial communities of MX80 bentonite

Most bacteria indigenous to MX80 are firmicutes which includes various fermentative bacteria. These bacteria use a metabolic process called “mixed acid fermentation” under anaerobic conditions which includes secreting acids such as acetic acid, formic acid and butyric acid to the external environment (see section 4.1). This process explains the VFA results in aerobic conditions because fermentation is not taking place and so VFAs are not replenished; whereas, under anaerobic conditions VFAs are being replenished by fermenting bacteria and utilised by other members of the community. As discussed in section 4.1, the pH drop during the first 14-21 days of enrichment indicates VFA production in experiments with microbes, the pH then increases back to neutral as the VFAs are presumably utilised by other bacteria or as acetate is

used in reduction of iron. This change in pH is not seen as clearly in 0.45 M NaCl enrichments, but it does still occur. In the repository, this use of VFAs may be integral for bacterial survival because there is very low concentration of organic carbon (~0.4% wt.) present in MX80 bentonite. Although groundwater from international sites is predicted to include up to 12 mg/L acetate, this will only be available when groundwater flows in at intervals (Kotelnikova & Pedersen, 1998). The UK has not yet selected a site for the repository, and so the concentration of dissolved organic carbon could differ from groundwaters from international repository sites.

Many firmicutes produce VFAs which can interact with metals, either in compounds or pure metal states (Konhauser 2007). This interaction is one way in which iron could be reduced indirectly. In particular, *Bacillus* has been observed to liberate metals such as iron and calcium from silica (Vasanthi et al., 2017). The silica is then released from the clay into solution, which in this case would have severe, adverse effects on the integrity of MX80 as a barrier (see section 4.1, 5.6, 7.7).

The VFA results at 2.5 M NaCl enrichments show a sharp decrease to 0 PPM in all enrichments. This change could be due to the high concentration of NaCl disrupting the readings; however, the results did not change when samples were diluted. It is therefore probable that the VFAs are used up as energy for microbial growth after which point most bacteria have either died or are represented in the resulting microbial community. It is likely that the function of iron-reduction is therefore lost, but the fermentative action of the community is not.

4.7.4 There are similarities and differences between communities at different salinities

It is possible that high concentration of carbon added in these enrichments allowed dominant bacteria to thrive, thus giving them an advantage and causing the less dominant bacteria to die out. This advantage could be why *P. stutzeri* is present in such high numbers in the aerobic enrichments but may not be reflected in the actual repository due to the anaerobic conditions. Further obstacles to microbial growth in the repository which were not considered in these experiments include: low water availability; confined clay causing increased pressure and decreased pore size; and high temperature. However, in the higher salinity enrichments, it is likely that the salinity was responsible for the selective pressure.

The bacterial community of the anaerobic low salinity iron-reducing enrichment presented in 4.1 is of a similar composition to the indigenous community isolated from a Finnish Borehole at 450 m depth (Bomberg et al., 2015) and to the microbial community of argillaceous clays in France (Poulain et al., 2008) being composed largely of *Bacillus* with *Clostridia* species and *P. stutzeri* also present. This finding suggests that groundwater community, or the microbes introduced from the host rock, will be of a similar composition and so will not greatly alter the community. Of course, the UK environment may differ greatly from elsewhere, but as yet the location of the UK repository has not been confirmed and so this cannot be further investigated at this time.

As presented in section 4.1 several iron-reducing bacteria, which are also putatively capable of sulfur-reduction, were enriched in the MX80 low salinity groundwater experiments. Many of these species also appear in the 0.45 M NaCl enrichments including *Desulfitobacterium* and *Desulfosporosinus* (Bertel et al., 2011; Pester et al., 2012; Finneran et al., 2002). There are more similarities between these two communities in that both also include many of the same dominant species in much the same relative abundance, such as *Anaerosolibacter, Sedimentibacter* and *Paenibacillus*. Despite the salinity, all anaerobic enrichments in this project were composed primarily of firmicutes. This phylum includes a host of candidates which could survive the repository conditions including thermo- and halotolerant species, spore-formers and fermenting bacteria. These properties of bacterial community may be due to the bacteria having to adapt to difficult conditions in storage (dry and low carbon), leading to only the most adaptable microbes, or those that can remain dormant, surviving. In terms of iron-reduction, the concentration of Fe(II) at 0.45M NaCl is like that of the original anaerobic iron-reducing enrichment (around 4 -5 mM by the end of the experiment). However, as the salinity increased to 2.5 M NaCl, the iron-reduction was greatly reduced, and the concentration of Fe(II) did not exceed 1 mM. Therefore, the salinity tolerance of the iron-reducers in this community is somewhere between seal level and 2.5 M NaCl.

Among the halotolerant species present in the 0.45 M NaCl or 2.5 M NaCl are *Pantibacillus, Piscibacillus, Terribacillus* and *Thalassobacillus* (Saleh et al., 2017; Amoozegar et al., 2009; An et al., 2007; Sanchez-Porro et al., 2009). *Oceanobacillus* and *Salipaludibacillus* are both moderately halophilic species and alkaliphilic (Yumoto et al., 2005; Amoozegar et al., 2018). Due to the

corrosion processes likely to occur at the carbon steel canister interface, the pH of the repository could move towards a more alkaline pH from neutral over time (Schütz et al., 2015), therefore alkaliphilic bacteria may be likely to become more dominant during the later stages of the closure, such as *Alkalibaculum*¸ which was identified here. Interestingly, every member of the 2.5 M NaCl microbial community is a spore or endospore-forming species. Although all these bacteria must have been active to be enriched and isolated during DNA extraction, all these species are capable of forming spores and remaining dormant until conditions are more favourable.

4.7.5 There are similarities and differences between indigenous MX80 bentonite aerobic and anaerobic microbial communities

There were several similarities between the powder and compacted samples in both the aerobic and anaerobic enrichments. It is possible that the dry storage of these clays has limited the microbial community to those which are best suited to survival more generally on the clay and so differences are less noticeable. It was thought that the human interaction and the process of mixing MX80 with water during the commercial compaction process would introduce a large concentration of non-native bacteria; however, these results suggest that the compaction process does not alter the composition of the viable microbial community in any significant way.

When comparing the anaerobic and aerobic enrichments there is a higher relative abundance of *Clostridia* and *Bacillus* in the anaerobic compared to aerobic experiments. This difference may be because facultative anaerobes are thriving, especially fermenting ones which would otherwise be outcompeted by aerobic bacteria. It is important to remember that these communities are derived from enrichments, without which no DNA could be isolated, and so different bacteria could dominate under different conditions but still be present in dormant forms. In order to reveal this, several different experiments were run to impose different selection conditions on the indigenous community. Therefore, as the repository shifts from aerobic to anaerobic conditions over the first phase post-closure (Landolt, 2009) the aerobic microbial community presented here could begin to shift towards the anaerobic community. Throughout the lifespan of the repository groundwater could bring in oxygen, in which case facultative anaerobes could have a survival advantage over strict anaerobes. Many of the results from BLASTN revealed sequences which matched to samples from saline or hypersaline environments, such as salt

planes or highly saline lakes and their sediments. It is therefore important to note that even in repositories with highly saline groundwaters, there could still be a viable, if relatively small, microbial community if MX80 bentonite clay is used.

4.7.6 Changes to iron mineralogy occurred at all salinities

From the XRD data presented, there has been some alteration to PCFeO or to the Fe(III)-minerals within the MX80 bentonite when microbes are present. A black precipitate was observed in all enrichments, both aerobic and anaerobic, up to 0.45M NaCl. This mineral was thought to be some form of iron oxide. Hematite, goethite and magnetite are all iron oxide minerals which could develop as secondary minerals when Fe(II) forms from PCFeO (Shimizu et al., 2013). However, hematite may also form abiotically from PCFeO as a more stable compound (Lentini et al., 2012). The black precipitate which was isolated from the 0.0002 M NaCl enrichments presented in the paper was found to be goethite according to XRD, although magnetite was observed to form in other microcosm experiments.

Goethite readily forms from ferrihydrite if Fe(II) is present to act as a catalyst at neutral pH, without this the process is naturally much slower and requires significantly more energy because ferrihydrite is not soluble at neutral pH (Yee et al., 2006). Therefore, ferrihydrite solubility is often the rate limiting step in goethite formation. Ferrihydrite is a poorly crystalline iron oxide such as the one used in this experiment and could transform to goethite under the correct conditions through dissolution and reprecipitation. Therefore, the bacteria are necessary for this transformation as they allow for the production of Fe(II) which in turn allows for the transformation of PCFeO to goethite. Indeed, no black precipitate was observed in any of the abiotic flasks. It is possible that other elements have been incorporated into the goethite crystal such as silica, this would alter the structure of the crystal resulting in a polymorph.

In the 0.45 M NaCl enrichments XRD data identified magnetite (Fe_3O_4) and magnesioferrite ($Mg(Fe^{3+})_2O_4$) formation. Magnesioferrite is a spinel form and part of the magnetite series. Magnetite is a black ferrimagnetic mineral which is widespread in nature. The formation of magnetite differs from hematite in that it requires a higher ratio of Fe(II) / Fe(III). It is a product of iron mineral weathering and can transform to hematite through oxidation of structural Fe(II)

to Fe(III). Studies have shown that magnetite formation from ferrihydrite can occur at up to 3 M salinity but is much reduced as salinity increases (Park et al., 2010), as such no magnetite was observed in the higher salinity experiments presented here. The Fe(II) must be absorped onto the ferrihydrite and a solid-state transformation occurs to produce magnetite (Lovley et al., 1987). This transformation may explain why magnetite formation was not observed at 2.5 M NaCl where very little Fe(II) was present. Like goethite, magnetite can form abiotically from ferrihydrite (or goethite) in the presence of Fe(II) (Schwertmann & Murad, 1983; Lovley et al., 1987); however, this process is often very slow in natural environments. Therefore, the bacteria present in these enrichments not only drive the production of Fe(II) but also aid in the formation of magnetite by being either directly or indirectly involved in the restructuring process (Han et al., 2018; Bazylinski et al., 2006). Indeed, Lovley (1991) observed magnetite formation coupled to oxidation of organic matter during dissimilatory iron-reduction. The formation of magnetite by *S. oneidensis* has also been investigated. Han et al. (2018) found that during Fe(III) reduction by *S. oneidensis* it took longer for magnetite to form as a secondary mineral than hematite or goethite. Magnetite is more reduced than goethite and that in this pathway ferrihydrite could form goethite which could in turn, eventually transform to magnetite.

It is not clear why magnetite formed in this enrichment, but not in the original 0.0002 M NaCl enrichment. It is possible that the clay minerals, silicates, or the organics present blocked the transformation of the goethite by blocking sites for reconstruction on the iron oxide surface (Taylor, 1995). In the 0.45 M NaCl experiments this may not have been an obstacle due to the high salt concentration disrupting the clay matrix (Stewart et al., 1998). Another possible explanation is the difference in microbial community. However, the communities share far more similarities than differences and no specific species which could aid in iron mineral transformation was identified from the 0.45 M NaCl community, other than those previously identified in the 0.0002 M NaCl community.

Hematite formation was observed in the 2.5 M NaCl enrichments. However, this may have been due to abiotic transformation during the drying of ferrihydrite aggregates as opposed to microbial effects. This process would also explain why hematite was identified in all the 2.5 M NaCl enrichments, regardless of whether microbes were present. Furthermore, it has been

shown that in the absence of Fe(II), ferrihydrite will preferentially transform to hematite at a slow rate (Yee et al., 2006) in place of goethite, taking up to 112 days for half conversion at room temperature and neutral pH (Schwertmann & Murad, 1983). This long conversion time could be why only a small percent of black precipitate was observed in these enrichments; however, the conversion has been observed to occur faster at high ionic strengths (Cornell & Schwertmann, 2003).

Halite is a cubic NaCl crystal which is commonly known as salt. Halite was identified in all 0.45M NaCl and 2.5M NaCl enrichments. Halite formed on drying simply due to the high concentration of NaCl that was included in these enrichments. The high salinity also caused changes to the clay as seen in the SEM images. Other studies have indicated that high salinity can decrease the swelling ability and plasticity of montmorillonite clays by disrupting the clay layers through dissolution of silica (Zhang & Wang 2019; Davies et al., 2017). Polymorphs of halite may have formed due to elements from the clay layers being absorbed into their crystal structure.

There are only a few members of the 0.45 M NaCl community which are halotolerant, but, like the 2.5 M NaCl community, the effects due to the high salinity are masking any microbial alterations to the clay mineralogy or appearance under SEM, or the active bacteria do not interact with clay. Therefore, while groundwaters with this high a salinity is effective at limiting undesirable microbial effects, the potential for increased corrosion, and halite and hematite formation suggests these groundwaters are less suitable for repository environments than lower salinity groundwaters.

4.7.7 Conclusions

There was plentiful carbon in this system to encourage microbial growth; the repository will likely be much less favourable in this respect and so all microbial activity will be greatly reduced, including MIC, VFA production and microbially-mediated iron or sulfate reduction. Furthermore, the microbes in this experiment were not subject to the challenges which will be present in the repository such as pore space and pressure due to clay swelling (Vorhies & Gains, 2009). These constrictions may inhibit all movement and growth of bacteria within the clay, resulting in much more localised effects or effects on iron-mineralogy due to bacterial secretions rather than

through direct contact with microbes (Konhauser, 2007). Microbes could exploit pockets at the host rock / clay interface where the temperature is cooler, there is more space due to gaps where swelling of the clay has not fully occurred (NDA, 2016a; Jalique et al., 2016; Wilson et al., 2010). This interface will also allow more access to groundwater which may carry some organic carbon, therefore avoiding some of the obstacles posed in the buffer.

However, there is a robust, functionally and metabolically diverse viable indigenous microbial community in MX80, capable of iron-reduction up to at least salinities equal to that of seawater, which will be present in the repository. There are also spore-forming and thermotolerant species present as well as filamentous bacteria. Spore-forming bacteria may survive the repository by entering dormancy until conditions become more favourable during latter stages of closure. MX80 bentonite will also carry some halotolerant species into the repository which can survive upwards of 2.5 M NaCl; however, it can be concluded that the bigger risk to the clay properties at higher salinities in terms of iron reduction is not the microbes, but the salinity itself.

Chapter 5. Microbial activities of the indigenous - iron reducing community of MX80 in relation to conditional or ecophysiological obstacles in the repository environment

5.1 Introduction

The series of experiments described in this chapter aimed to determine whether microbes could overcome certain physical and chemical obstacles which they are likely to face during the evolution of a repository. These experiments also aimed to further understand the activity of the indigenous iron-reducing microbial community (as presented in section 4.1) in relation to the multi barrier system.

Firstly, it was hypothesised that the physical obstacle of pore size will limit microbial travel through the MX80. It was therefore necessary to understand whether microbes had to be in direct contact with iron or iron-containing minerals in order to interact with them, or if this interaction could be achieved remotely. For example, the mechanism by which *Geobacter sulfurreducens* is known to reduce iron through an enzymatic system which requires direct contact of the iron with OmcC located on the pili (Morgado et al., 2012). However, there are also mechanisms by which secretory products can reduce iron, eliminating the need for direct contact (Gadd, 2010). One such secretory mechanism is flavins which can be secreted by *Shewanella oneidensis* to act on metal surfaces such as Fe (III) (Marsili et al., 2008). These experiments have also investigated which type of iron substrates the indigenous microbial community could act on.

Secondly, recolonisation experiments aimed to determine whether microbes were able to recolonise the clay or if they had to be introduced prior to compaction. For example, if all microbes died during the initial stages post-closure, when the temperature is highest (Keith-Roach & Livens, 2002), could microbes recolonise the clay at later stages.

In terms of microbial activities, a process which could impact the barrier might include microbially-influenced changes to clay mineralogy through silica loss. As previously known, microbes can interact with structural iron in clay (Kostka et al., 2002), which is likely to cause some changes to the clay mineralogy. However, another important factor which may lead to detrimental mineralogical changes for the barrier is the silica content of the clay. A high silica

content is important for the high swelling capacity of MX80 bentonite a key component of the repository design. From the previously described community analysis there are some indications that there are silica solubilising bacteria present in the indigenous community (such as *Bacillus* (Vasanthi et al., 2018; Vasanthi et al., 2016) and *Actinobacteria* (Singh et al., 2008) (see section 4.7.2)), and further evidence of interaction with silica was observed during cell count studies whereby it was found that dye could not adhere to cells taken directly from clay incubations. Therefore, cells were first grown in synthetic groundwater media with organic substrate mixture.

The final microbial activity investigated in this series of experiments was microbial gas production. Due to the high abundance of fermenting bacteria, there is very likely to be CO_2 and H_2 production, as well as gas utilisation. An increase in gas is predicted to produce a detrimental increase in pressure in the repository which could eventually result in fracturing (Stroes-Gascoyne & West, 1997; Zhang et al., 2020) More specifically H_2 in the clay could lead to a desaturation of the MX80 bentonite which would alter the properties of the barrier (Bardelli et al., 2014).

5.2 Results

5.2.1 Solid media indirect interactions between indigenous iron-reducing bacteria of MX80 bentonite and iron substrates

Anaerobic agar plate experiments inoculated with the indigenous iron-reducing microbial community (as presented in section 4.1) were used to assess the potential for indirect interactions between microbes and iron minerals through use of a 0.2 µm membrane, abiotic controls were included (figure 5.1). During these experiments, an orange precipitate was observed in all biotic Fe powder plates which appeared after 14 days of incubation and remained to the end of the experiment; however, due to its solubility it was lost during mineral recovery. No other significant visual changes were observed. The methods for these experiments are presented in section 3.5.1.

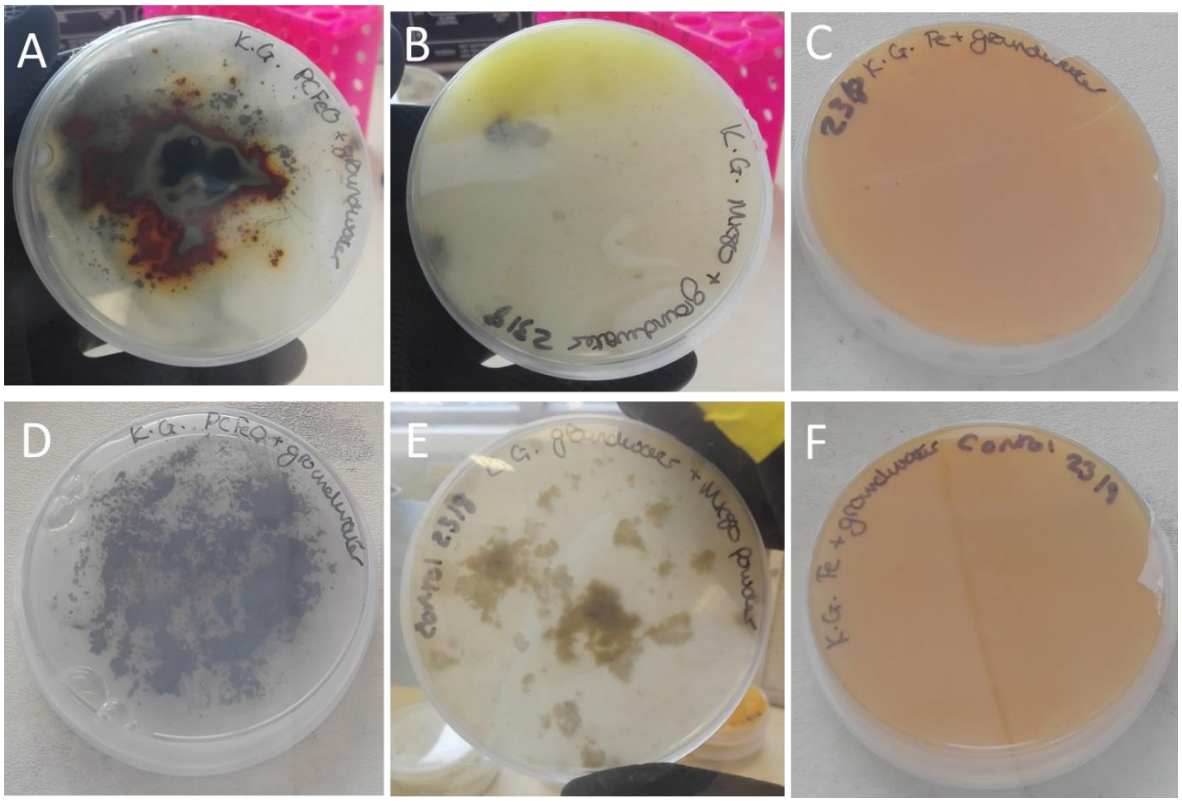

Figure 5.1: Agar plates after solid media experiment containing Fe powder (A), MX80 bentonite (B) and PCFeO (C). The corresponding abiotic controls are shown D-F.

5.2.1.1 pH changes in solid media indirect interaction experiments

Measured pH values were unexpectedly high across all experimental agar plates (figure 5.2). All inoculated plates had a higher pH than the corresponding control plates, apart from the inoculated plate containing PCFeO which had a mean pH of 7.73 ± 0.37 compared to the abiotic control plate which had a pH of 7.93 ± 0.02; however, this pH did vary between replicates. The inoculated Fe powder plates had the highest pH at 8.56 ± 0.09 and the corresponding abiotic control plates had the lowest pH at 7.66 ± 0.01, this difference was significant with a p-value of 7.23×10^{-8}. Likewise, the pH of the inoculated MX80 powder plates were significantly higher ($p = 0.0463$) when compared to the abiotic control MX80 powder plate.

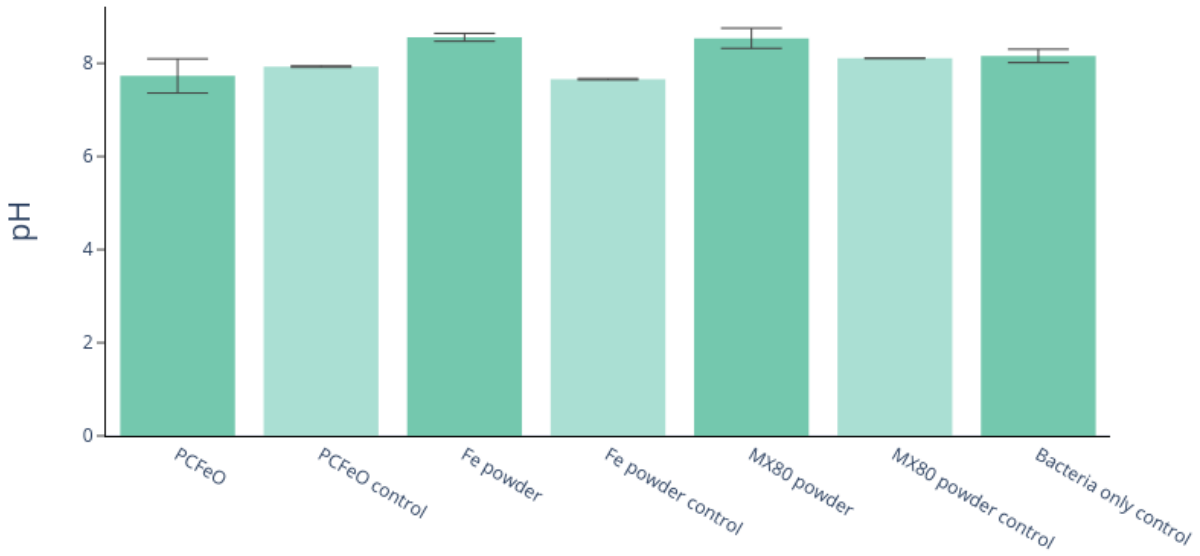

Figure 5.2: The pH (mean values) of solid media indirect interaction experiments measured at 5 points per plate across 3 replicates at the end of the experiment. Error bars show standard deviations. All experimental plates had a higher pH than their corresponding controls apart from the PCFeO amended plates

5.2.1.2 Biomass measurements of solid media indirect interaction experiments

Biomass measurements showed that all inoculated plates had growth, albeit at levels below that recorded for the bacteria only control (figure 5.3). Inoculated Fe powder showed the lowest biomass growth at 79% of that observed in the control whilst the inoculated MX80 powder plates had the highest biomass at 94% of that measured in the controls. Based on these differences there was therefore no significant effect on biological growth putatively caused by iron toxicity, apart from in the inoculated iron powder experiments which when compared to the control was

found to be significantly lower (p=0.043).

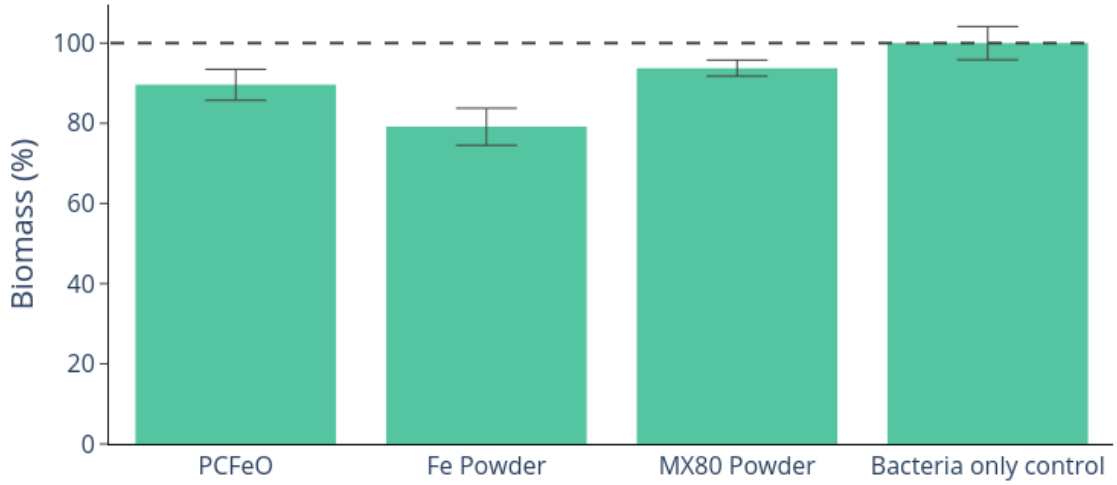

Figure 5.3: Biomass measurements of the solid media indirect interaction experiments measured and presented as a percentage of the bacteria only control. Error bars show standard error

5.2.1.3 SEM images of minerals recovered from solid media indirect interaction experiments

SEM images of Fe powder experiments (figure 5.4) showed visible differences between the inoculated and abiotic control plates. The inoculated plates had very few spherical crystals and largely consisted of irregular shaped particles with limited mineralisation on the surface, whilst the control was solely spherical crystals measuring up to 5 µm in diameter, as seen in the original iron powder. SEM images of MX80 powder (figure 5.5) showed some dipyramidal octahedral crystals (identified as magnetite or a magnesioferrite polymorph (see section 5.6)) whilst the control had no regular crystal structures. inoculated and control PCFeO plates were also analysed by SEM images (figure 5.6). There were obvious differences between the control, which had numerous small cubic crystals and the inoculated plate which had no cubic crystals but did consist largely of spherical crystals that were up to 20 µm in diameter. The starting material showed no significant crystal structures, and so some abiotic interactions with the $CaCO_3$ in the groundwater has likely occurred. There does appear to be

microbial contamination in the inoculated samples from PCFeO amended experiments; however, given that microbes are unlikely to have survived the boiling washing process to recover minerals, it can be assumed that this contamination occurred after the experiment was completed. During the experiment, a orange colour was observed in Fe powder inoculated experiments but not in the abiotic control. This colour leaked into the agar and was soluble and so was not recovered for subsequent analysis.

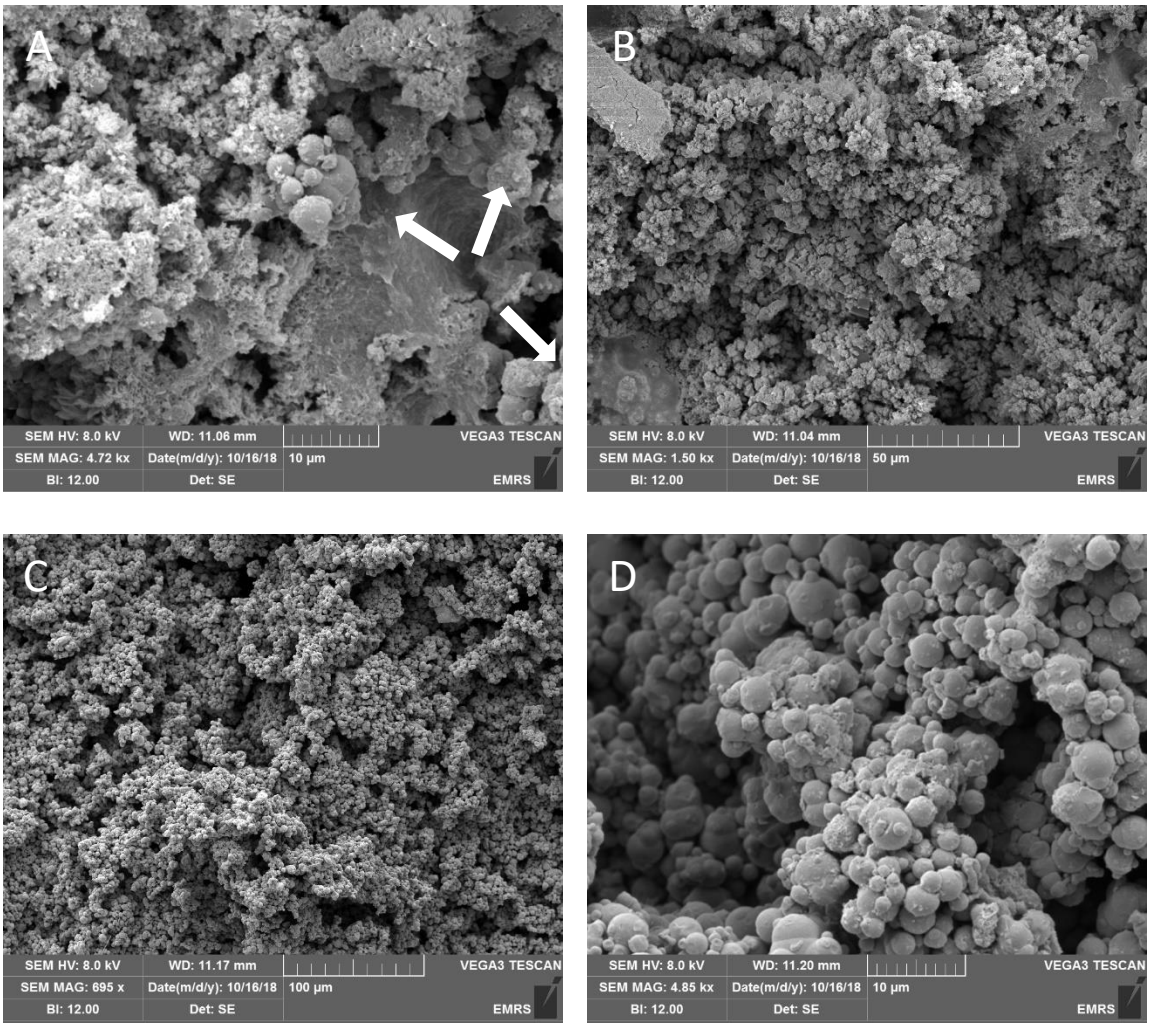

Figure 5.4: SEM images of Fe powder recovered from solid media indirect interactions experiments revealed visible differences between experimental and abiotic controls. Powders from inoculated plates (A + B) show some crystallisation and a few spherical crystals (arrows A). Abiotic controls (C + D) were uniformly spherical.

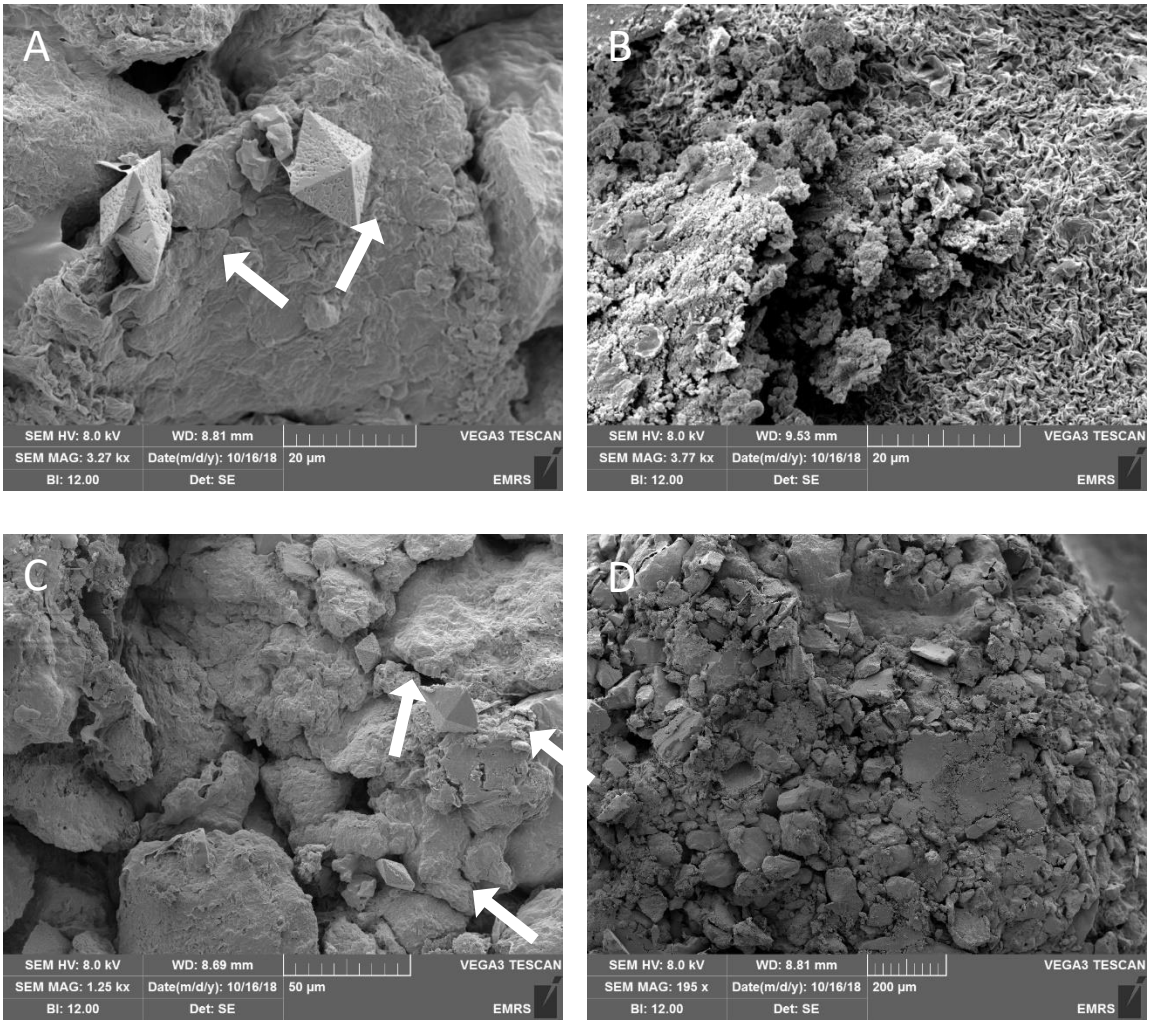

Figure 5.5: SEM images MX80 powder recovered from solid media indirect interactions experiments. Mineralisation (B) and octahedral crystals (A +C, arrows) appeared in the inoculated samples. The control had no obvious mineralisation or crystals (D).

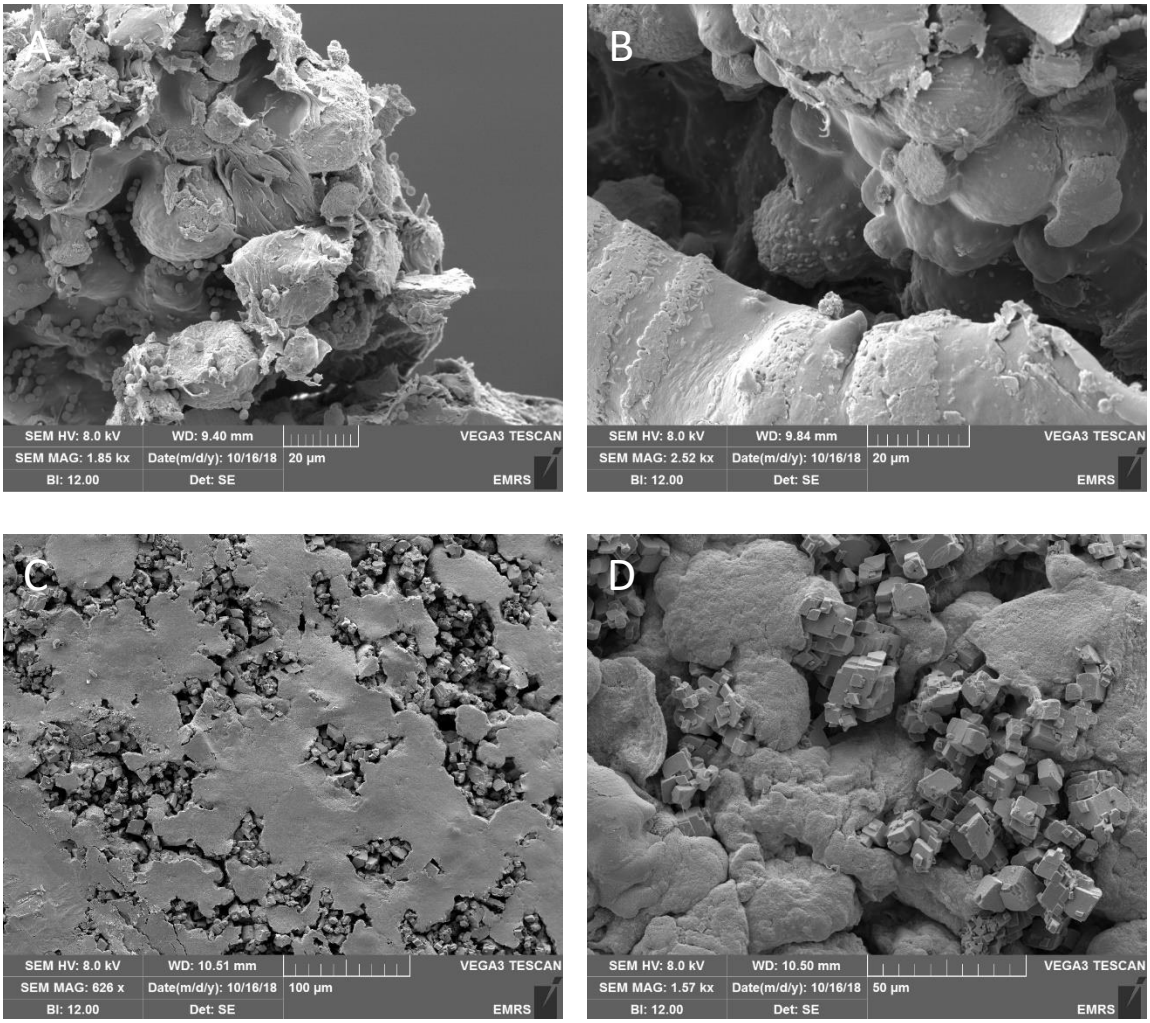

Figure 5.6: SEM images of PCFeO recovered from solid media indirect interactions experiments. There were visible differences between the inoculated (A + B) and the control (C + D) samples. The inoculated samples had large spherical shapes whilst the control had several cuboidal crystals (calcite). Microbial contamination can be seen in the live experiments.

5.2.1.4 EDX analysis of mineral textures recovered from the solid media indirect interactions experiments

Bulk EDX analysis of inoculated Fe powder experiments showed that the minerals recovered contained iron, carbon and oxygen (figure 5.7). The abiotic control was found to be 100% iron, suggesting that some biogenic mineralisation had taken place in the inoculated samples, either to form carbonates or oxides. Bulk EDX analysis of inoculated MX80 powder showed it contained carbon, sodium, aluminium, silicon, potassium, calcium and iron. The abiotic equivalent had half

the amount of carbon but was otherwise very similar (data not shown). Inoculated PCFeO powder EDX analysis showed that the sample contained carbon, sodium, calcium, iron and magnesium whilst the abiotic control contained only calcium, carbon and iron (data not shown).

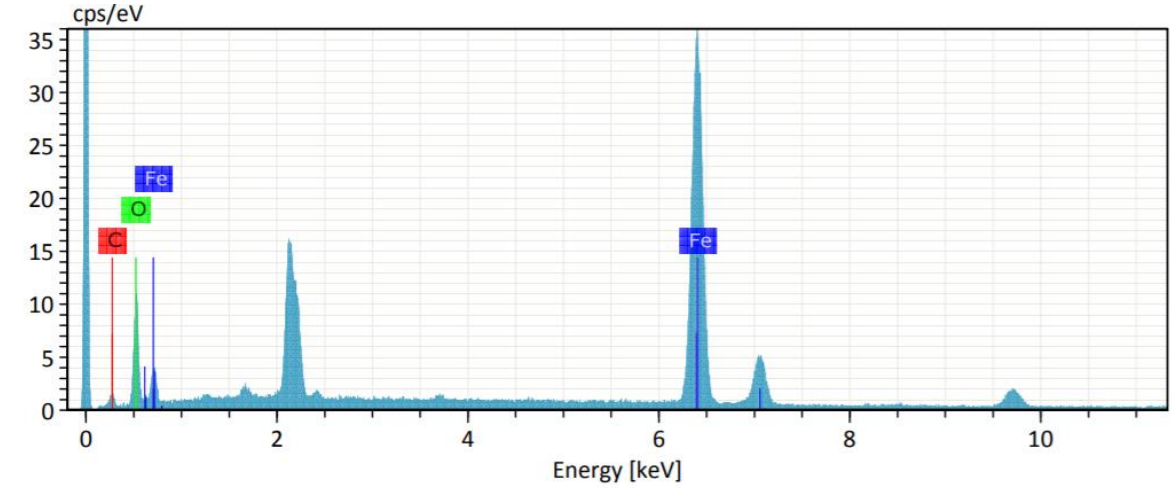

Name	Date	Time	HV [kV]	Real time [s]	Dead time [%]	Pulses [kcps]
Fe powder 1300	10/16/2018	10:02:51 AM	20.0	14.273	11	19.713

Spectrum	C	O	Fe
Fe powder 1300	11.18	26.27	62.55

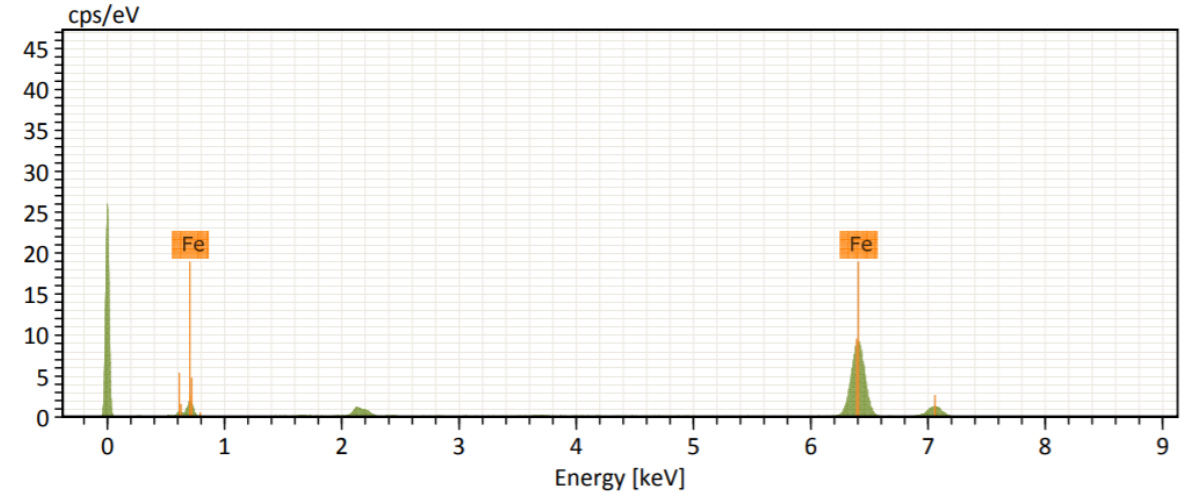

Name	Date	Time	HV [kV]	Real time [s]	Dead time [%]	Pulses [kcps]
Fe powder control 1302	10/16/2018	10:10:10 AM	20.0	81.466	2	3.120

Spectrum	Fe
Fe powder control 1302	100.00

Figure 5.7: EDX analysis of Fe powder recovered from inoculated plates (Top). EDX analysis from abiotic control plates contained 100% iron (Bottom).

5.2.1.5 XRD analysis of minerals recovered from solid media indirect interaction experiments

XRD spectra of recovered minerals from Fe powder experiments showed that in the presence of bacteria some of the Fe powder had been transformed to goethite (FeO(OH)), magnetite (Fe_3O_4) and magnesioferrite ($Mg(Fe^{3+})_2O_4$) (figure 5.8). The control remained mostly elemental iron. The XRD spectra for inoculated PCFeO contained goethite, as well as calcite and vaterite ($CaCO_3$), whereas the control contained ferrihydrite and calcite, but no vaterite (figure 5.9). Both MX80 samples, live and sterile, contained mainly montmorillonite as well as quartz, magnetite and calcite (figure 5.10 however, the live experiment also contained a mordenite-like silicate mineral. The sterile control also contained cristobalite and hematite.

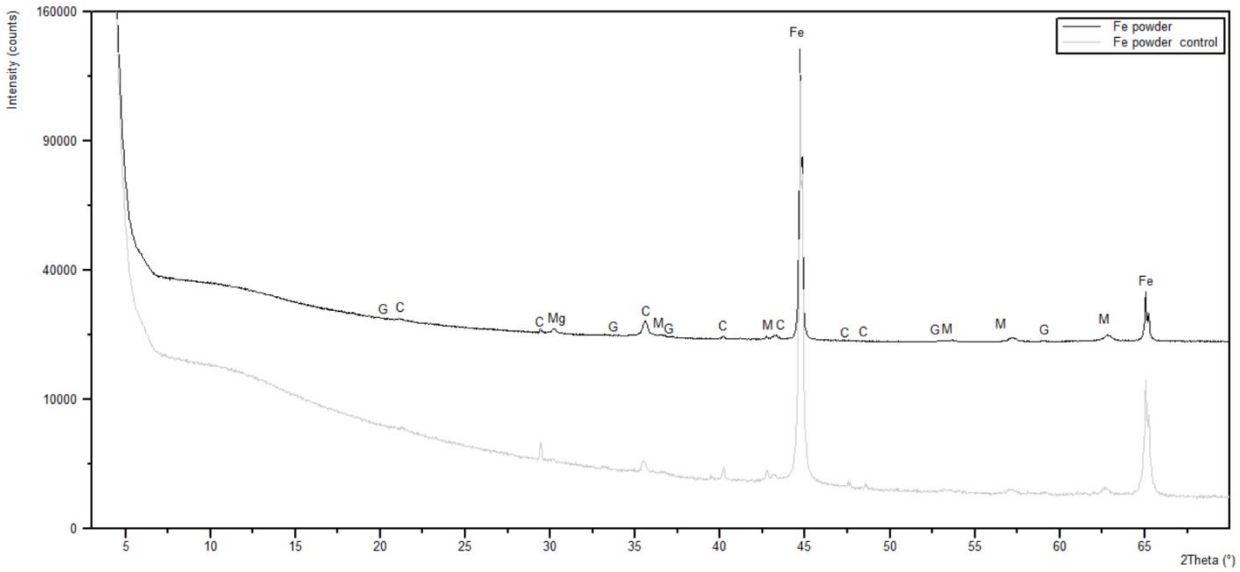

C	**Fe**	**G**	**M**	**Mg**
Calcite	Elemental iron	Goethite	Magnesioferrite	Magnetite

Figure 5.8: XRD of Fe powder recovered from solid media indirect interactions experiments. The powder from the inoculated plate and the Fe powder abiotic control is shown.

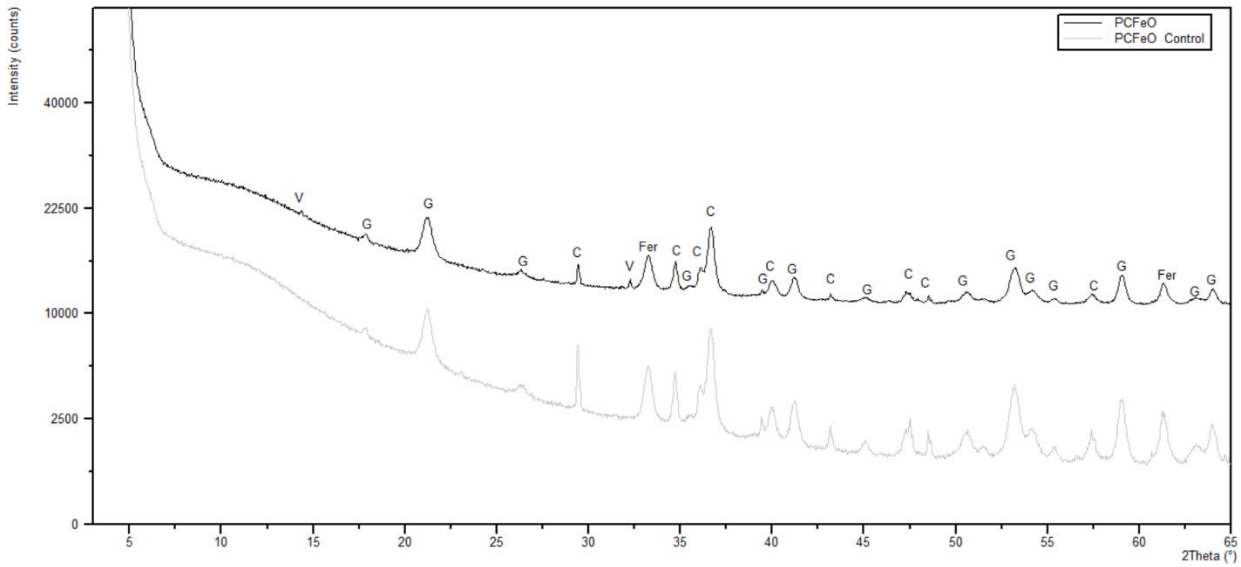

C	Fer	G	V
Calcite	Ferrihydrite (PCFeO)	Goethite	Vaterite

Figure 5.9: PCFeO analysed by XRD after after recovery from indirect interaction solid media experiments. The XRD spectra from inoculated plates and the PCFeO abiotic control is shown.

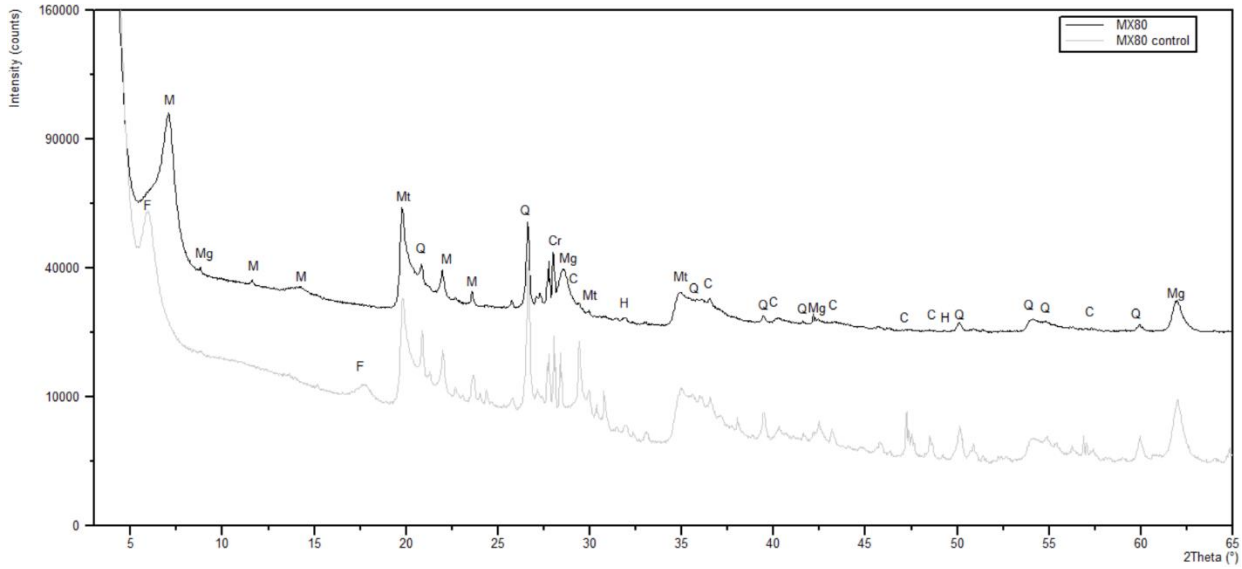

C	Cr	F	H
Calcite	Cristobalite	Feldspar	Hematite
M	**Mg**	**Mt**	**Q**
Mordenite-like	Magnetite	Montmorillonite	Quartz

Figure 5.10: XRD of MX80 recovered from indirect interactions experiment. The inocculated experiment and the sterile control is shown.

5.2.2 Recolonisation experiments on solid media

In order to determine if the iron-reducing microbial community indigenous to MX80 could recolonise the clay after a period of harsh conditions (e.g. after high temperatures and low water conditions as expected by year 50 post-colsure (Landolt et al., 2009), plate experiments were set up. The method used is presented in section 3.5.2.

5.2.2.1 pH of agar and clay surface at the termination of etching experiments

In keeping with the above results, the pH of the inoculated plates was higher than those of the corresponding abiotic control plates (figure 5.11), this was true for both the agar and the surface of the compacted MX80. The MX80 from the inoculated plate had a pH of 8 compared to the control which was recorded at pH 7.4. Whilst the pH of the MX80 surface was not significant, the pH of the agar was significantly higher when compared to the control (p-value of 0.004).

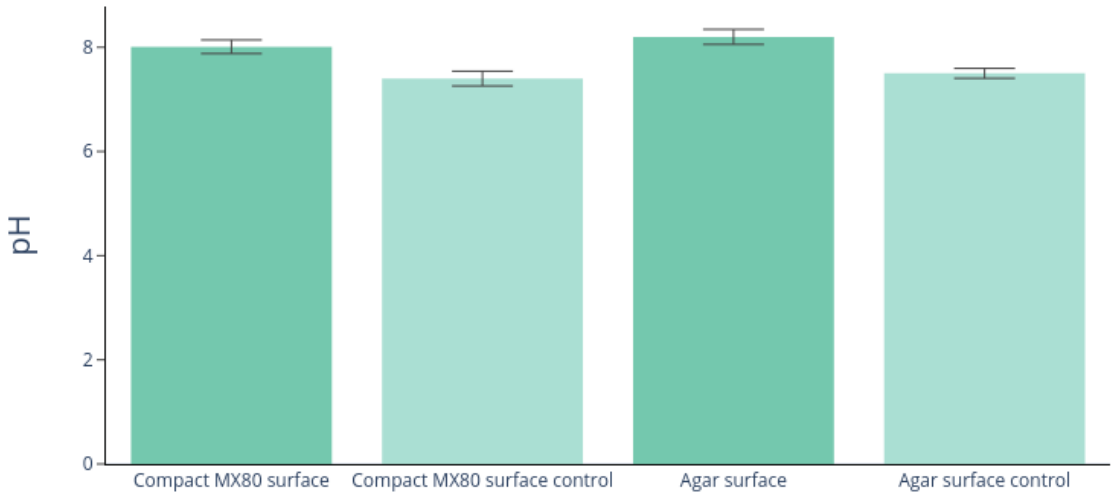

Figure 5.11: mean of pH measurements of recolonisation experiments taken at 5 points on the agar and clay surface of all 3 replicates at the end of the experiment. Error bars show standard

deviation.

5.2.2.2 Plasticity index of MX80 recovered from etching experiments

The plasticity index (PI) of the inoculated samples was 243, with the abiotic control having a higher PI of 303. The plastic limit was reached at 50% moisture content and the liquid limit was reached at 293% moisture content. The control had a plastic limit of 45% and a liquid limit of 348%.

5.2.2.3 SEM images of MX80 recovered from etching experiments

SEM images (figure 5.12) of MX80 from inoculated etching experiments revealed that extensive surface colonisation had occurred, as well as string-of-bead bacterial growth and actinohyphae. Further images of a cross section of the compacted MX80 showed hyphal growth inside the MX80. There were no bacteria observed in SEM images of the abiotic control which confirms that sterilisation was successful and that the bacteria observed in the inoculated experiments was new growth.

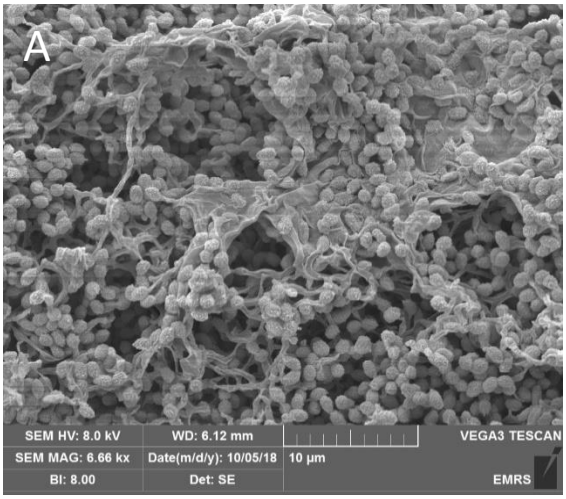
A
SEM HV: 8.0 kV
WD: 6.12 mm
VEGA3 TESCAN
SEM MAG: 6.66 kx
Date(m/d/y): 10/05/18
10 µm
BI: 8.00
Det: SE
EMRS

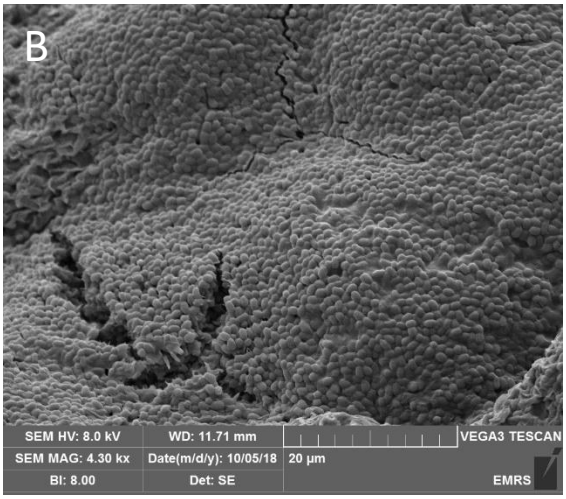
B
SEM HV: 8.0 kV
WD: 11.71 mm
VEGA3 TESCAN
SEM MAG: 4.30 kx
Date(m/d/y): 10/05/18
20 µm
BI: 8.00
Det: SE
EMRS

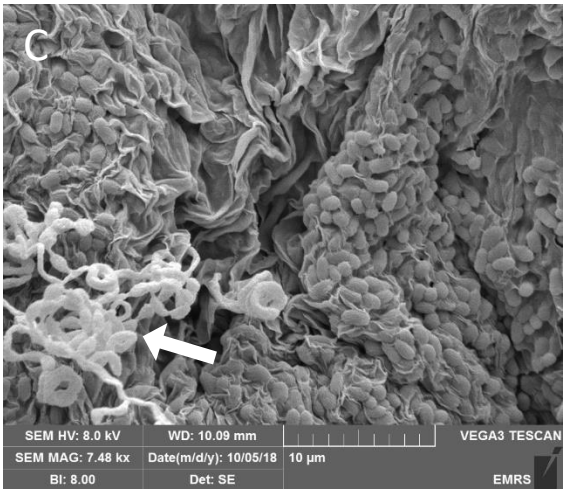
C
SEM HV: 8.0 kV
WD: 10.09 mm
VEGA3 TESCAN
SEM MAG: 7.48 kx
Date(m/d/y): 10/05/18
10 µm
BI: 8.00
Det: SE
EMRS

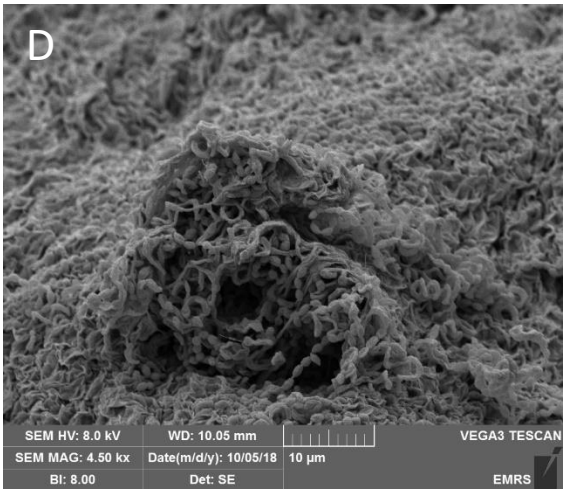
D
SEM HV: 8.0 kV
WD: 10.05 mm
VEGA3 TESCAN
SEM MAG: 4.50 kx
Date(m/d/y): 10/05/18
10 µm
BI: 8.00
Det: SE
EMRS

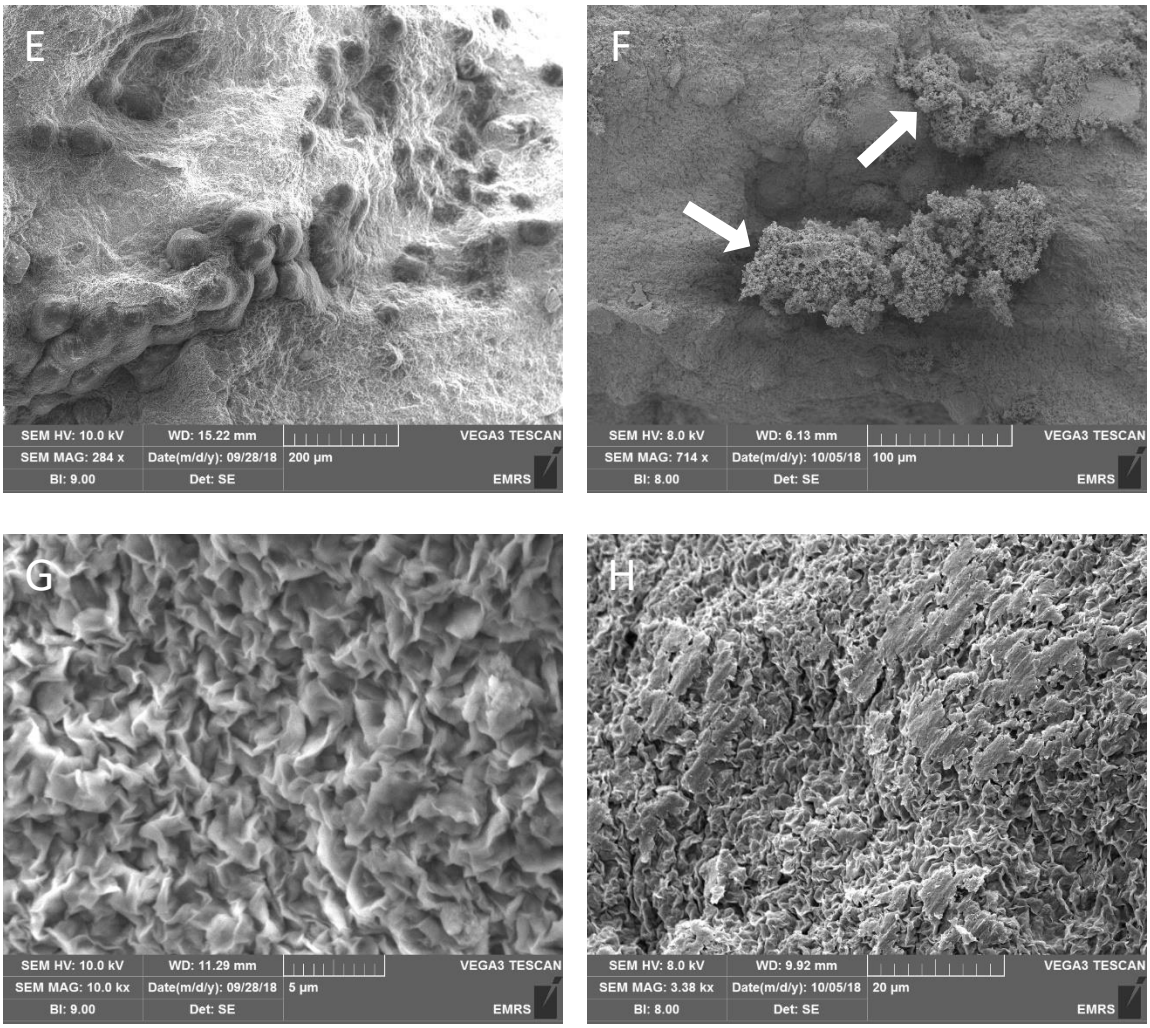

Figure 5.12: Compact MX80 was analysed by SEM. Significant colonisation occurred on the inoculated sample (A-D) including biofilm formation (A) and string of pearl growth (C, arrow) and several egg-shaped clay growths were observed (E). SEM images were also taken of a cross-section of the compacted block (F, arrows). The abiotic control sample had no evidence of colonisation, or growth (G + H)

5.2.2.4 EDX analysis of MX80 recovered from etching experiments

The inoculated compact MX80 EDX spectra indicated the sample was composed of carbon and silicon with trace amounts of nitrogen, sodium, magnesium, aluminium, calcium and iron. The abiotic control had only carbon, silicon and aluminium as well as sodium, magnesium, calcium and iron (Data not shown).

5.2.2.5 XRD analysis of MX80 recovered from etching experiments

XRD spectra of the inoculated compact MX80 recovered from etching experiments showed that the samples contained montmorillonite, quartz, magnetite, cristobalite and calcite (figure 5.13). The abiotic control contained similar volumes of montmorillonite and quartz but had much less magnetite. Calcite and cristobalite were also present in the sterile control.

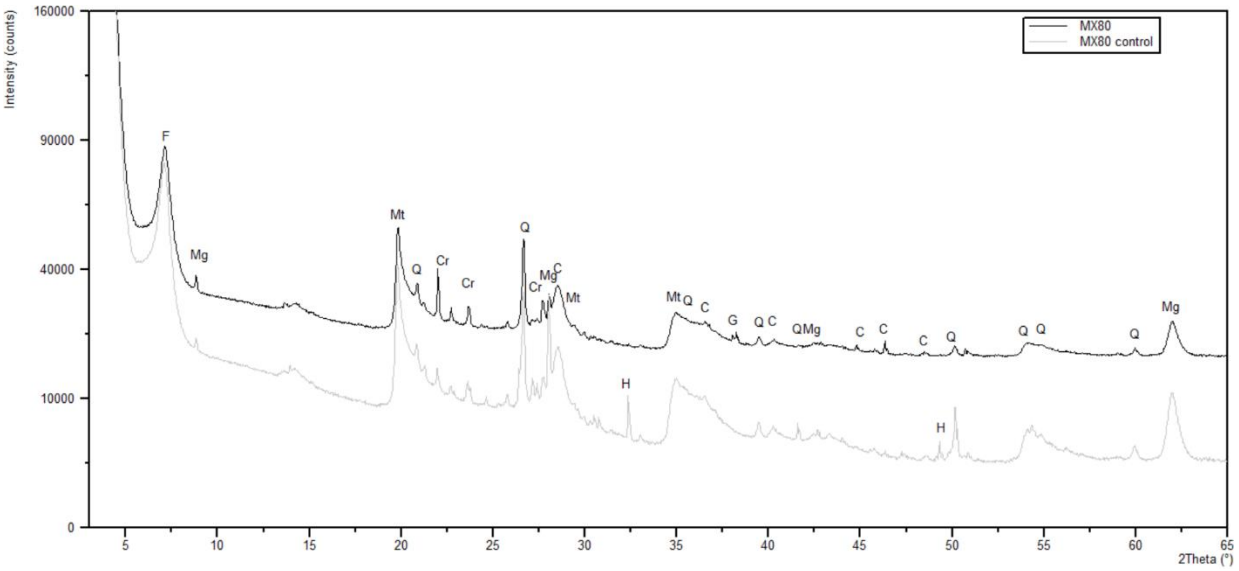

C	**Cr**	**F**	**G**
Calcite	Cristobalite	Feldspar	Goethite
H	**Mg**	**Mt**	**Q**
Hematite	Magnetite	Montmorillonite	Quartz

Figure 5.13: Compact MX80 from recolonization experiments was analysed by XRD, as was the abiotic control

5.2.3 H_2 production experiments by the indigenous MX80 iron-reducing community at a clay steel interface

Within the repository, there is likely to be production of H_2 as a result of the anaerobic corrosion of the carbon steel waste canister (Landolt et al., 2009). Therefore, steel was included in these experiments. After 10 months incubation, there was an increase in hydrogen in both biotic and abiotic flasks (figure 5.14). In the inoculated, biotic samples, with microbes present, the mean H_2 increased from 106 PPM ± 10 to 15497 PPM ± 3100; whereas the abiotic controls increased from

121 PPM ± 10 to 8104 PPM ± 1200. There was found to be a significant difference in hydrogen production between the biotic and abiotic samples (P-value of 0.0432).

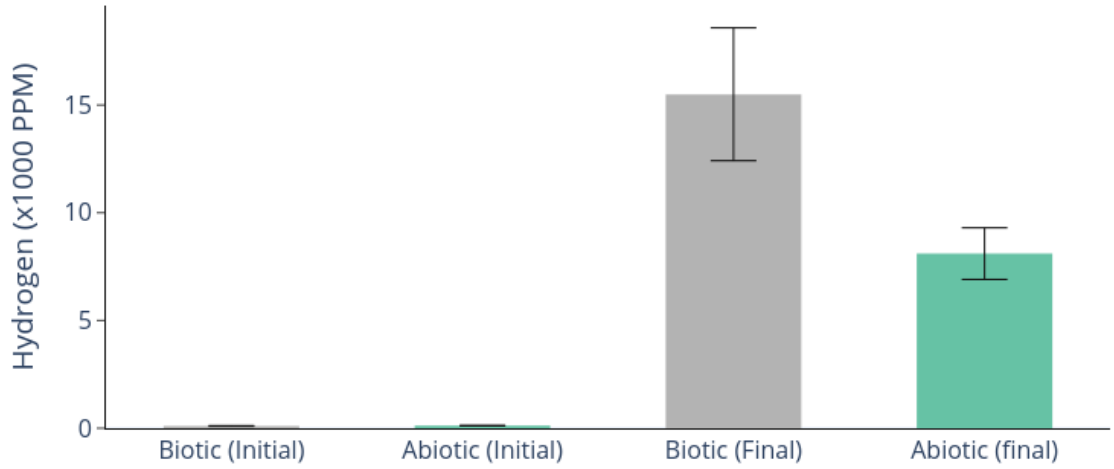

Figure 5.14: Hydrogen production after 10 months incubation increased in both the biotic and abiotic samples. Initial measurements were taken on day 0 and final measurements were taken after 10 months. Error bars show standard error.

5.2.3.1 SEM images of steel coupons recovered from H_2 production experiments

SEM images were taken of the steel coupons recovered from the flasks (figure 5.15). In the biotic samples, evidence of blistering or bubbling of the steel surface was observed (tentatively thought to be due the formation of toroidal magnetite (Alcántara et al., 2016)), this alteration is not uncommon for carbon steel corrosion. There was also some crystallisation, most likely FeOOH, lepidocrocite (γ-FeO(OH)). The surface of the steel (figure 5.15C) seemed to be covered in amorphous debris. In the abiotic samples, more blistering was evident as well as cracking of the steel surface, possibly due to hydrogen embrittlement. However, there may have been similar cracks present under the debris from the inoculated samples. It is possible that if greater magnification had been possible, corrosion products would have been observed around the

blisters; however, at the magnification achieved they appeared smooth. It is apparent (albeit qualitatively) that much more damage and corrosion of the carbon steel surface occurred when microbes were absent, indicating that microbes may aid in protection of the steel surface from corrosion, or prevention of corrosion.

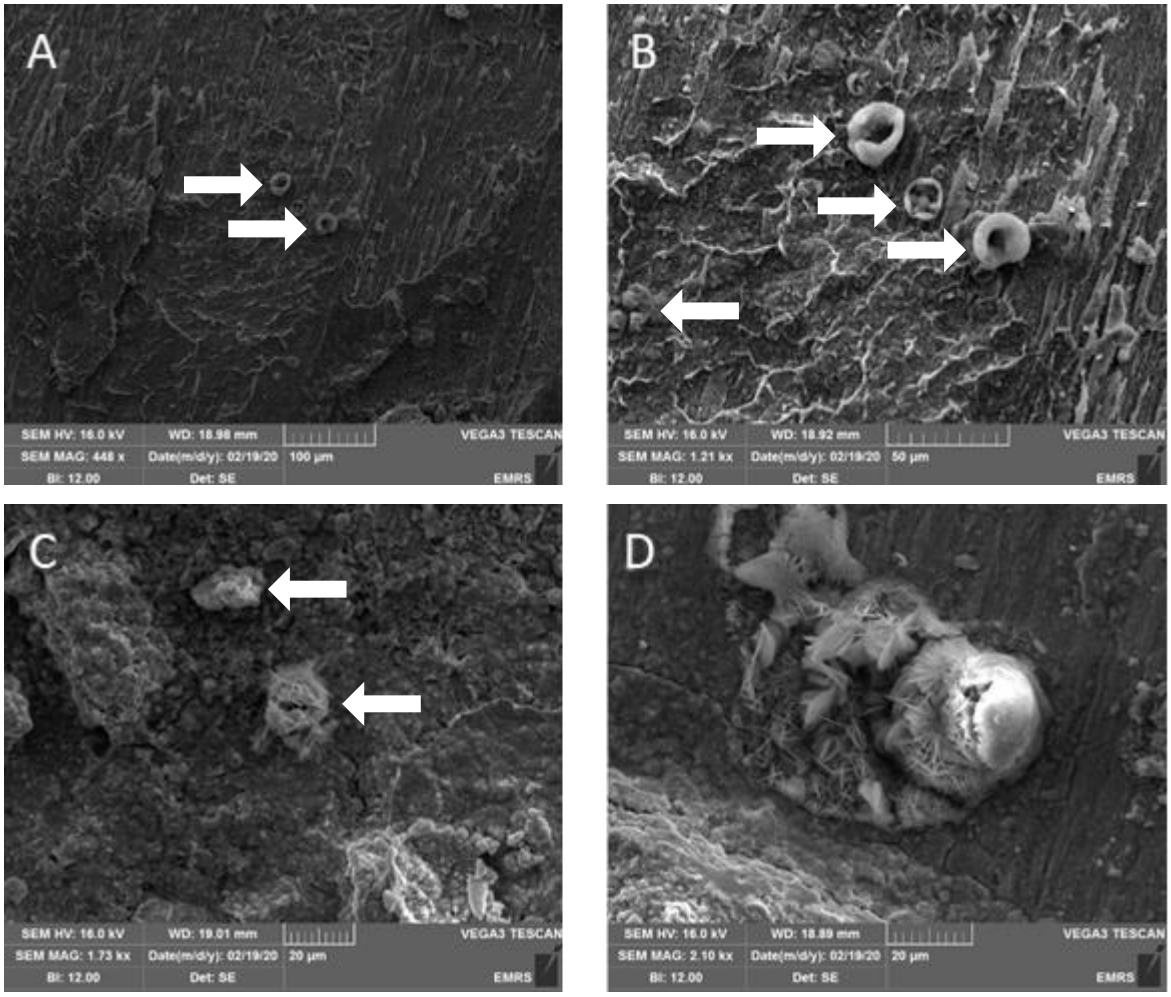

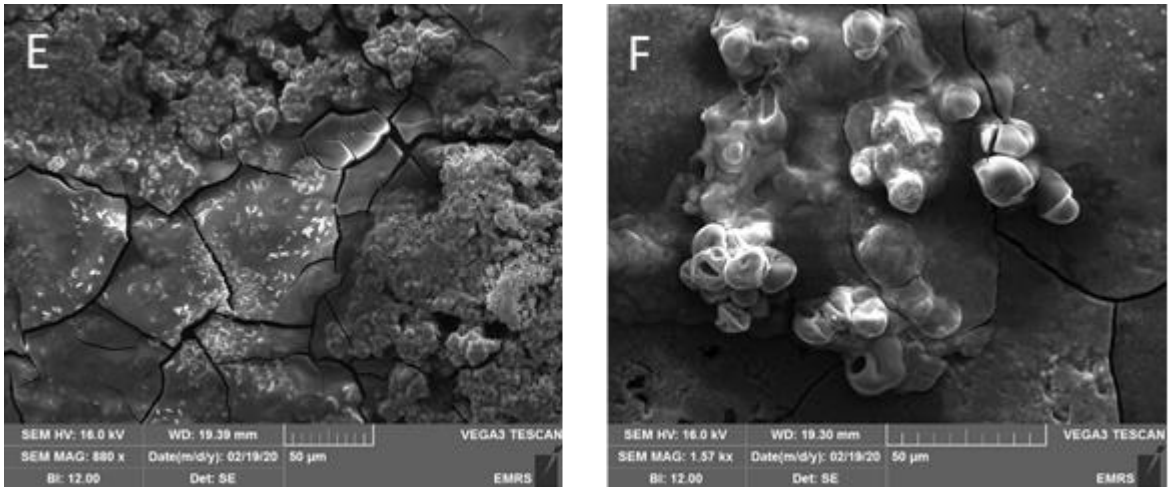

Figure 5.15: SEM images of steel surface from hydrogen production experiments. The biotic experiment (A-D) displayed crystallisation and corrosion (A, B, arrows) and lepidocrocite (C (arrows), D). The abiotic controls had more extensive corrosion including embrittlement (E) and toroidal magnetite (F).

5.2.4 Experiments testing the silica solubilising abilities of the indigenous microbial community of MX80 bentonite

Silicate dissolution experiments were informed by previous experiments as dissolution of clay minerals was identified in SEM images, and there were issues with cell counting using SYBRGold. Therefore, it was hypothesised that the cells may be coated in silica (Suaro et al., 2018) which would prevent the dye from reaching the DNA and would also indicate that silica is being removed from the clay.

Although a simple colorimetric assay, it was important to determine if silica was being lost from the clay matrix because this would result in a detrimental effect on the geomechanical properties of the MX80 which make it an effective barrier. Most notably, loss of silica could lead to illitisation (Wilson et al., 2011) which would result in a decrease in overall swelling ability and plasticity – the effects of illitisation are further described in section 2.6.

5.2.4.1 Silica solubilising abilities of indigenous iron-reducing MX80 microbial community on solid media

5.2.4.1.1 Kaolinite

After 3 days of growth all plates had more than 300 CFUs. No plate clearing was observed in aerobic plates. However, limited plate clearing was observed in anaerobic plates. Colonies which showed obvious clearing were transferred to new plates and typically showed 3 mm diameter plate clearing after growth.

5.2.4.1.2 Silicon carbide

After 3 days of growth all plates had more than 300 CFUs. No plate clearing was observed in aerobic plates. Very limited plate clearing was observed in anaerobic plates.

5.2.4.2 Silica solubilising abilities of indigenous MX80 microbial community in liquid media

5.2.4.2.1 Concentration of dissolved silica in silica solubilizing liquid media experiments

Silica content in filtered liquid samples (figure 5.16) remained below 4 mg/L until week 4. The silica content in the inoculated experiment then increased to 8 mg/L. The abiotic control fluctuated between 5 mg/L and below 4 mg/L. These results were found to be significant (P = 0.0433) when the inoculated experiments were compared to the abiotic controls across day 21 to day 28.

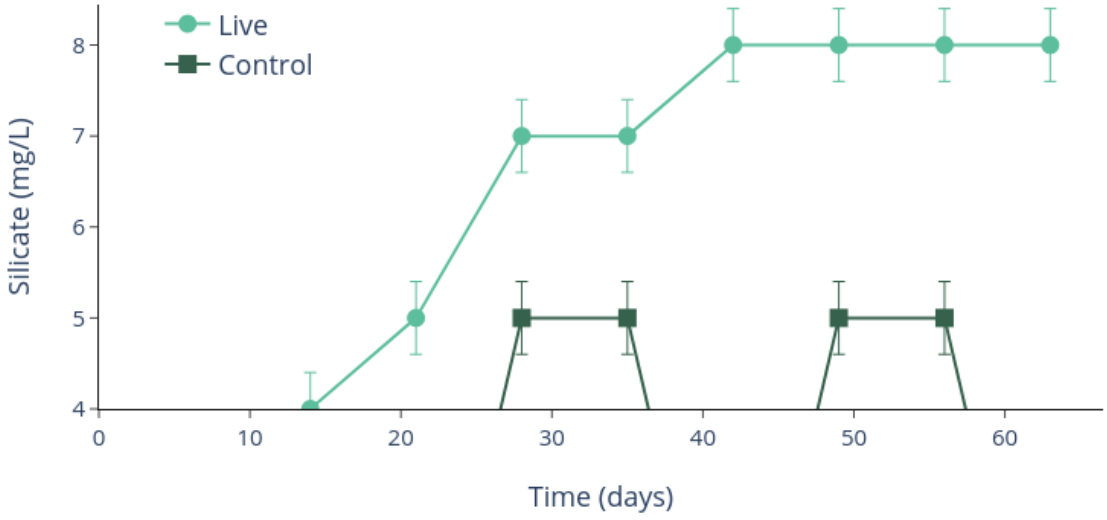

Figure 5.16: Dissolved silicate measurements of Sellafield-like groundwater mixed with MX80 bentonite taken weekly. Error bars represent the accuracy of the assay.

5.2.4.2.2 pH of silica solubilizing liquid media experiments

The pH decreased to 5.5 from circumneutral in all flasks including abiotic controls (figure 5.17), although the abiotic controls did have a higher initial pH and so decreased at a faster rate. There was limited recovery towards a neutral pH towards the end of the experiment. There was no significant difference in pH between the biotic samples and abiotic controls.

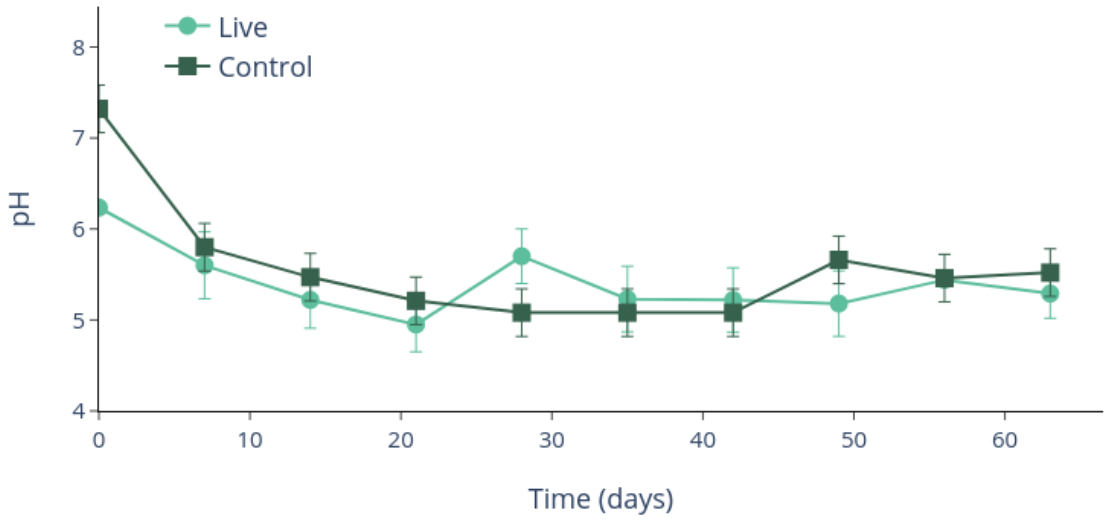

Figure 5.17: pH of silicate liquid media experiments. Error bars show standard error

5.2.4.2.3 VFA analysis of silica solubilsing liquid media experiments

All VFAs in biotic experiments increased over the duration of the experiment apart from for formate which remained constant at 140 PPM. All VFAs in the abiotic controls decreased over time or did not change from starting concentrations, apart from acetate which increased albeit still at lower concentrations than in the inoculated flasks (figure 5.18). Similarly, there was a small increase in propionate which was significant when compared to the abiotic control between day 21 and day 28 ($P = 0.0245$). Butyrate concentrations increased from days 0 to 7 in live experiments from 0 to 446 ppm and remained at a high concentration to the termination of the experiment. The difference between the biotic and abiotic control for the concentrations of butyrate on day 21-28 was significant with (p-value of 0.0436). The concentration of isobutyrate

remained low throughout the experiment, but the live experiment did have a consistently higher concentration of this VFA compared to that observed in the abiotic control. When the concentration of isobutyrate between day 21 and 28 was compared to the control, the result was significantly higher (P = 0.0391). Formate concentrations remained at 140 PPM in the live samples for the entirety of the experiment but decreased to ~0 PPM in the abiotic control by day 7. Isovalerate increased from 0 ppm to 171 ppm over the duration of the experiment, with concentrations found to be significantly higher compared to the abiotic control over day 21 to day 28 (P = 0.0496).

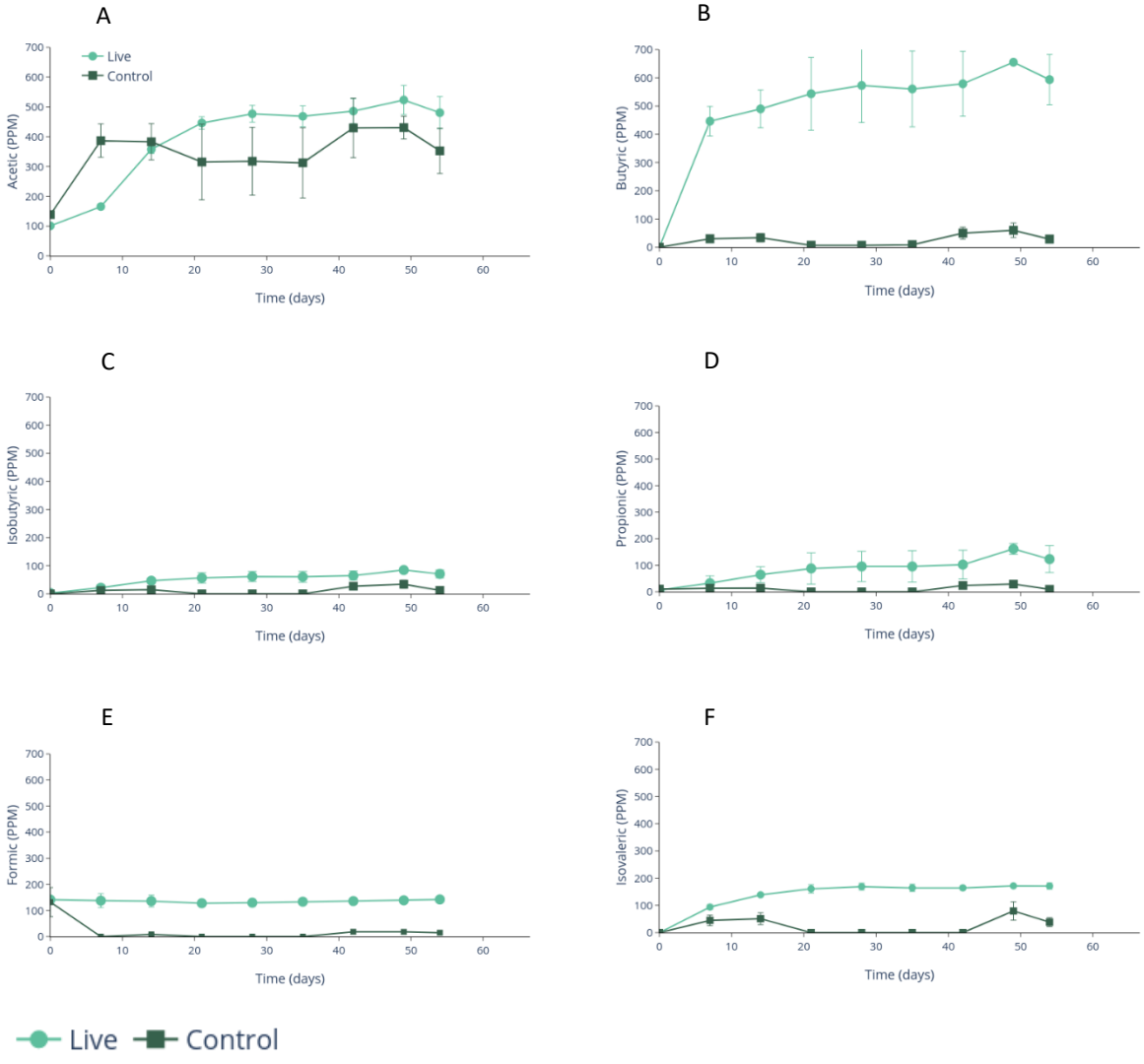

Figure 5.18: VFAs measurements over time in silicate dissolution experiments. Acetate acid (A). Butyrate (B). Isobutyrate (C). Propionate (D) Formate (E). Isovalerate (F).

5.2.4.2.4 SEM images of MX80 recovered from silica solubilizing liquid media experiments

SEM images of inoculated MX80 silicate experiments (figure 5.19) showed that the surface was studded with holes, as if burst open, this is likely to be silicate dissolution. Further crystal structures were observed around the edges of the areas of dissolution; however, the rest of the clay surface was smooth. These 'open' structures may be areas in which bacterial colonies were in direct contact with the clay resulting in silicate release and dissolution. Crystal growth around the edges of these sites were thought to be calcite precipitation and aragonite needles. The abiotic control did not show any mineral structures or evidence of silica dissolution.

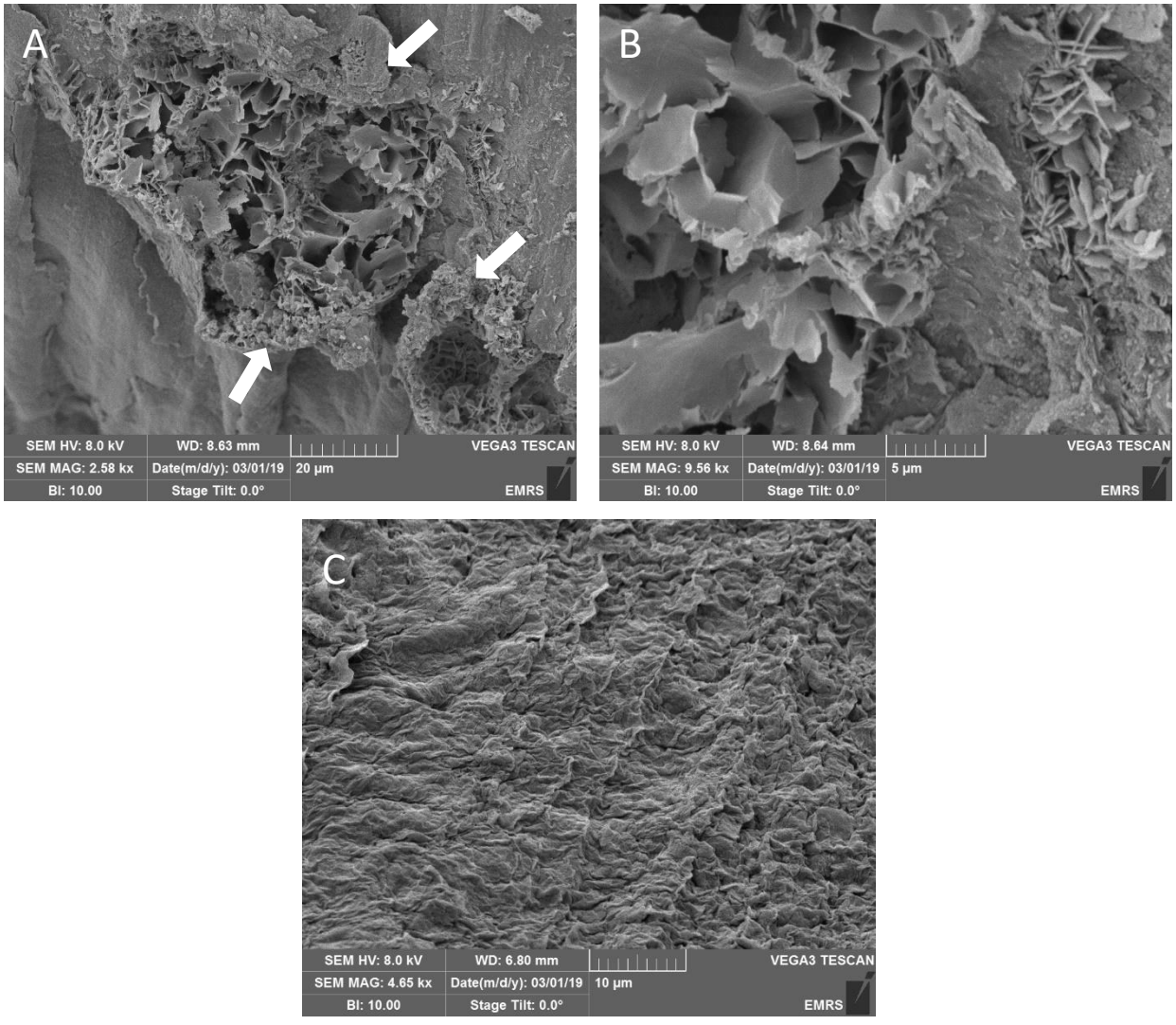

Figure 5.19: SEM images of surface of MX80 shows silicate dissolution, and possible reordering

of clay layers (A). "Fluffy" crystal formations can be observed around the edges (A (arrows), B). No such dissolution was observed on the abiotic control (C).

5.3 Discussion

5.3.1 Microbes indigenous to MX80 can interact with iron substrates from a distance

Indirect interactions on solid media resulted in significant changes to all the iron substrates and so it can be concluded that metabolites and secretory products from microbes indigenous to MX80 can interact with iron from a distance. The dissolution of the iron powder from spherical crystals suggests that there are iron-oxidisers present, in addition to the iron-reduction described in previous chapters. Changes were also observed in the MX80 powder plates in which various mineralisation recrystallisation processes were evident in the SEM images – and further supported in the XRD results. It is likely that the octahedral crystals observed are magnetite, or a polymorph of magnesioferrite (Malik et al., 2016). Due to the small incidence, they may not have been identified in XRD; however, the crystals are similar in size and appearance to magnetite from Malik et al. (2016). Malik et al. describes different magnetite nanoparticles and attributes the octahedral structures to a biogenic origin, which would be in keeping with the crystals observed on the MX80 powder.

Furthermore, the XRD results of the MX80 powder identified a "morden-like" crystal. Mordenite ($(Na_2,K_2,Ca)\ Al_2Si_{10}O_{24}\cdot 7H_2O$) which is an expanding silicate crystal that is a well-documented synthetic mineral but also appears widely in nature (Simoncic & Armbruster, 2004). It is a member of the zeolite category of minerals and grows in needle-like structures, which could be the "fluffy" crystalisation that appears in the SEM images around the edge of the clay dissolution; however, Fe(II) carbonates have also described as "fluffy" in appearance (Etique et al., 2014). The presence of this mineral indicates an obvious restructuring or dissolution of the clay layers within the MX80 and a disruption of the clay matrix which is not seen in the abiotic control. The abiotic control also contained some iron minerals, namely magnetite (mixed Fe(II / III)) and hematite (Fe(III)), both of which have been discussed previously in section 4.7.5. This oxidation is likely to have occurred during the drying process which can inadvertently cause oxidation of iron-minerals. It is, however, important to remember that up to 20% of the iron in MX80 is reduced (Fe(II)) and so there should be some minerals containing reduced iron present in the MX80 prior

to any experiments, and this iron may act to abiotically catalyse reduction of Fe(III) (Yee et al., 2006) (see section 4.1).

There were also changes to PCFeO in both the biotic and abiotic controls in the indirect interaction solid media experiments. Whilst the abiotic controls showed significant calcite precipitation from the calcium carbonate present in the groundwater. As evidenced in SEM images and XRD results, the biotic plates contained large spherical structures which could be an iron-rich carbonate as described by Jiang and Tosca (2019) and which were identified as vaterite – an unstable calcite polymorph. Indeed, Li et al. (2019), found that microbial secretions play a key role in vaterite formation over other calcite polymorphs. According to XRD, reduction to magnetite had occurred. Like the last chapter (see section 4.7.5), it seems that without microbes only transformation of PCFeO to goethite is possible but slow. With microbial presence, transformation of PCFeO can proceed faster to produce iron minerals and secondary minerals such as goethite (Shimizu et al., 2013). The production of goethite may have been promoted in these experiments by the alkaline pH observed in all agar plates (Das et al., 2011). There may have been reduction to soluble Fe(II) which was then lost during mineral recovery and therefore not observed in SEM images.

Therefore, it can be speculated that microbes located at the MX80/host rock interface could interact with the canister surface and iron-interacting minerals throughout the buffer, despite being geographically distant. This scenario has not yet been considered a factor as the small pore size was thought to limit bacterial travel through the repository, thus limiting activity to areas where swelling has not fully filled all gaps (Jalique et al., 2016; Wilson et al., 2010).

The high pH recorded in solid media experiments was unexpected, it is possible that VFAs are being utilised at the same rate as they are being produced and so did not contribute to the overall pH. Another possibility is that hydrogen is being used in respiration (Arango & Schlegel, 1981; Liu et al., 2020), or in iron-reduction. Similarly, acetate could also be utilised in iron-reduction (Reitner & Thiel, 2011) and so this would therefore negate the effect of H^+ and $CHCOO^-$ on pH (see section 4.1).

It is possible that some compounds or minerals may have been lost during mineral recovery. For example, the appearance of the Fe powder plates was orange in some areas which may have been the result of iron oxidation to produce a soluble iron containing compound, which may have been lost due to solubility during the boil washes with water or due to presence of secretory acids.

As the iron powder is already fully reduced, all changes observed in Fe powder plates must have been due to iron-oxidisation (equation 7). A possible explanation for this is that microbes could have aided in Fe-oxidation through indirect interactions with some secreted acids and hydrogen scavenging (Lyles et al., 2014) which would favour iron oxidation based on Le Chatalier's principle. Biotic iron-oxidisation has largely been linked to *Proteobacteria*, particularly nitrate-reducers such as *P. stutzeri* (Hedrich et al., 2011); however, within this community as specified previously (see section 4.7.2), some species of *Acidobacteria, Actinobacteria, Thiobacillus* and *Burkholderiales* are present and all have iron-oxidising activity (Sauro et al., 2018). It would be expected that once the carbon sources supplied had been exhausted, and the microbes enter dormancy or die, the Fe(II) concentration would stop increasing and plateau. Abiotically, iron oxidation can occur through interactions with oxygen and water at neutral pH, this is discussed further in chapter 7.

$$3Fe_{(s)} + 4H_2O \leftrightarrow Fe_3O_4 + 8H^+ + 8e^- \quad [7]$$

In terms of the repository, the presence of microbes able to oxidise iron would not be considered favourable, most notably because this could increase corrosion of the carbon steel waste canister. As oxidation of iron was observed indirectly in these experiments, it suggests that microbes geographically distant to the canister may still have an effect. Therefore, the high temperatures of the canister surface (up to 100°C) (Keith-Roach & Livens, 2002) and small pore size, which is thought to eliminate microbial activity, may not limit all MIC as previously predicted (Jalique et al., 2016).

5.3.2 Compact MX80 can be colonised by microbes

A cross-section of the compacted MX80 from the etching experiments revealed bacterial growth in the form of filamentous bacteria. It can therefore be surmised that microbes can colonise the

MX80 bentonite. *Actinohyphae* may be especially prone to causing micro-pitting as they have a smaller diameter, up to 2 µm (Dhanasekaran & Jiang, 2016) than other hyphae. These smaller hyphae can therefore travel through smaller pore spaces, and additionally can give rise to spore-forming mycelium which has the same diameter (Dhanasekaran & Jiang, 2016). This mechanism again indicates that the pore size may not be as significant an obstacle to microbial activity as previously thought. It is also important to note that the clay was not fully confined in these experiments, so may have been able to expand allowing pore sizes to increase.

When compared to the literature (Wilson et al., 2010), the plastic limit (PL) of the clay is relatively high in the control at 45% as opposed to 33-39%. Therefore, the agar itself may have had some influence of the geomechanical properties of the clay. The PL of the clay with microbes was even higher – 50% - suggesting that the microbial activity also influenced the geomechanical properties of MX80 or caused structural alterations to the clay matrix – possibly through silicate solubilising bacteria. The higher PL in conjunction with a lower liquid limit (LL) results in a significantly lower PI than the abiotic control. The PI of the clay is a good indication of the swelling ability of the clay and specifies how dry the clay will become before it cracks (Haigh et al., 2013). Given that there are periods of time post-closure when the clay will be very dry, and repeated episodes of groundwater flowing in (Landolt et al., 2009), it is important that the MX80 can respond to these conditions without cracking and causing a breach in the barrier. Therefore, a low PL, in combination with a high LL is desirable. These results are of importance when considering the repository as it indicates that the clay may be less likely to swell and contract and behave as an effective barrier throughout changing temperatures and moisture contents.

As in the indirect interaction solid media experiments, the pH of the etching experiments was higher than expected. An alkaline pH of 8 when microbes were present suggests that any VFAs or hydrogen produced by the microbes are being utilised either in reduction of iron (Luidold & Antrekowitsch, 2007; Konhauser, 1997) or as energy by other members of the community instead of contributing to the overall pH of the environment (Kim & Gadd, 2008).

The XRD results for the etching experiments highlight the differences in the mineralogy between the sterile samples and those exposed to bacteria. While the composition was similar between

these samples from different conditions in terms of montmorillonite, quartz, and cristobalite, there were differences in terms of iron-oxides produced and calcite precipitated.

Iron transformation to magnetite can be blocked by clay minerals and silicates, therefore it is likely that the microbes are liberating the iron from the associated clay minerals, thus allowing magnetite transformations to take place. Calcite precipitation can be promoted by microbial activity, and indeed a lot of naturally occurring calcite deposits are of biogenic origin (Gadd, 2010). Bacterial products such as urease (Hammes et al., 2003), and bacterial processes such as denitirification and sulfate reduction can all contribute to the formation of calcite, each producing different morphologies (Chekroun et al., 2004; Bosak & Newman, 2005). Moreover, microbially induced calcite precipitation is most likely to occur at alkaline pH. Lüttge and Conrad (2004) even implicated *S. oneidensis* in inhibition of calcite dissolution. Therefore, the evidence would suggest that we should observe more calcite in these experiments. Carbonate precipitation is known to be a microbially driven process, largely through bacteria secretions and sulfate and iron-reduction (Ronholm et al., 2014). Biogenic precipitation of calcium carbonate is thought to be a passive or inadvertent process, rather than as an active provision of a biological advantage. Several explanations have been offered, such as negatively charged proteins or membrane porins attracting Ca^{2+} (Beveridge & Murray, 1976); cell processes such as sulfate reduction cause an increase in pH in the immediate environment promoting precipitation (Gallagher et al., 2012); or metabolites and secreted siderophores interacting with Ca^{2+} in place of other metals (Braissant et al., 2004). However, this process would require supersaturation of calcite. Modelling of the groundwater using SPECE8 suggests that this was not the case, but addition of calcite from the clay could have influenced this.

However, there is also evidence to suggest that some microbes and microbial processes promote the dissolution of carbonate (equation 8) through organic acid production, and production of carbon dioxide. Moreover, certain species of bacteria including *Acidobacteria* and *Actinobacteria* have been historically involved in breaking down calcareous rocks (Campbell & Cole, 1984; Sauro et al. 2018). Therefore, it is likely that within this microbial community both processes of calcite precipitation and dissolution are occurring.

$CO_2 + H_2O + CaCO_3 \rightarrow Ca^{2+} + 2HCO^-_3$ [8]

5.3.3 Hydrogen concentration significantly increases when microbes are present

Results from hydrogen production experiments clearly show that microbial presence leads to an increase in H_2. This result contrasts with previous predictions which stated that microbial presence would utilise available gas sources (Stroes-Gascoyne et al., 2000; West et al., 2002). The increase in gas production is detrimental to the integrity of the multibarrier system as it would contribute to an increase in gas pressure which may cause cracking of the MX80 barrier (Landolt et al., 2009). H_2 in particular could also lead to an increase in corrosion through hydrogen embrittlement (Raman et al., 2005; Okonkwo et al., (2017)). The process of hydrogen embrittlement involves H^+ ions adhering to electrons on the metal surface which leads to blistering and hydrogen absorption. Once the hydrogen has diffused into the metal it forms a brittle compound (such as hydride), this, coupled to an increase in hydrogen concentration on the surface, results in an increase in pressure and eventual cracking at the metal surface (Wang et al., 2016).

Hydrogen embrittlement by microbial activity has been linked to iron-oxidising bacteria (Ashassi-Sorkhad et al., (2012)) which are present in the indigenous iron-reducing MX80 bacterial community (see section 4.1). However, here hydrogen embrittlement was only observed in abiotic experiments. It is possible that hydrogen entry to the metal has been blocked by aragonite, lepidocrocite or calcite deposits on the surface (Liu 2020) caused by microbial activity. Buildup of these mineral layers has been known to protect steel from corrosion (see chapters 6 & 7), therefore, it is unlikely that cracking of the surface has occurred under these layers. Calcite was identified in XRD spectra only when microbes were present, therefore this may have contributed to reduced corrosion.

Interestingly, these results do suggest that the microbial community, under these conditions, is much more dominated by active fermenting bacteria than hydrogen consumers – this may change in aerobic environments. There is therefore also likely to be a lot of acetate produced by these species, which could increase iron-reduction within the MX80, as could the excess of H_2 (see section 4.1). No CO_2 increase was observed during these experiments; however, there is

almost certainly CO_2 produced as part of fermentation. Therefore, further experiments should investigate what happens to this CO_2.

5.3.4 Silica dissolution occurs when microbes are present

Silica dissolution occurs both when microbes are present and, to a limited extent, when they are absent. Bacteria may be coating themselves in silica (Suaro et al., 2018), or, more likely, metabolites interacting with iron may cause associated silica to enter the aqueous phase. A decrease or loss of silica from the clay matrix could be extensively damaging to the MX80 barrier in the repository setting. Loss of silica would make the clay more prone to weathering and lead to possible illitisation (Pusch & Kasbohm, 2002), as well as a decrease in swelling ability and a decrease in clay plasticity (see section 7.7.2), all of which are important characteristics for the clay barrier to remain effective whilst adapting to changing temperature and moisture contents. The overall effect of these potential changes could be that the MX80 is less able to respond to changes in moisture content and becomes less effective as a barrier.

5.6.5 Changes to mineralogy could negatively impact the multi-barrier system

The transformation of structural iron within MX80 to other minerals such as magnetite as seen in the Fe powder plates, and all MX80 samples, could have adverse effects on the multi-barrier system. This transformation could happen relatively quickly in terms of the repository lifespan as the immediate post-closure period will have moderately favourable conditions for microbial growth and these will last for 30 years (Landolt et al., 2009). As this activity observed in the experiments occurred in only 1 month, with added carbon, it is likely that significant microbial activity could occur in the post-closure period despite the absence of excess carbon given the long lifespan of the repository. MX80 contains 0.4 % wt. organic carbon which is considered adequate to support microbial growth (Pedrial et al., 2009; Parkinson et al., 1989), although other predictions suggest it is not bioavailable (Marshall et al, 2015). Nonetheless, there is likely to be some fermentable matter in the groundwater, as found at international repository sites (Kotelnikova & Pedersen, 1998) to support microbial growth.

5.4 Conclusions

It is necessary to note that these experiments did not replicate the repository conditions in terms of temperature, pressure, and carbon, water and nutrient availability, all of which would limit or promote microbial growth dependent on their variation. A higher concentration of bacteria was also used in these experiments than would be present in the repository. It is likely that microbial growth will be limited to the edges of the clay barrier with very limited growth within the barrier provided it is compacted correctly and swells as predicted (Jalique et al., 2016). Therefore, the effects observed may not be a true representation of 'real world' microbial interactions; however, given the long timescales of the repository, it is possible that microbial activity will eventually result in large-scale alterations. The biomass measurements indicate that the presence of the clay or iron did not significantly inhibit bacterial growth, suggesting that there is a low toxicity to this bacterial community.

Etching experiments demonstrated that, microbes were able to colonise MX80 bentonite. Therefore, over time microbes from the groundwater or host rock that are introduced to the repository environment could colonise MX80 bentonite, especially as it corrodes (Nakano & Kawamura, 2010), or if there is any decrease in swelling leading to an increase in pore size. While studies have shown that groundwater communities are not necessarily suited to surviving in MX80 due to being largely Gram-negative, there are some exceptions to this rule, for example, *Desulfosporosinus* and *Sedimentibacter* (Chi Fru & Athar, 2008).

From the results presented in this chapter, it is clear that microbial presence and activity in MX80 results in an increase in H_2 production. High concentrations of H_2 could lead to an increase in gas pressure and possible subsequent hydrogen embrittlement of the canister. However, interestingly microbial presence actually seemed to protect the canister surface – possibly through armoring of the metal surface through lepidocrocite precipitation (Alcántara et al., 2017; Hofstetter et al., 2003).

It is also clear that microbial activity in MX80 could lead to a loss of silica from the clay matrix, which would decrease swelling and plasticity thus making the clay a less effective barrier. Loss of silica could also lead to illitisation which could result in a decrease in swelling capacity. This

process may also increase MX80 corrosion at the edge sites to a rate greater than currently expected (Nakano & Kawamura, 2010). It is not clear if this silica dissolution requires direct interactions with the microbes; however, it seems likely that metabolites may be able to act on metals in silicate-containing minerals to liberate the silica, such as Fe(III) reduction by acetate.

The results of these interactions are likely to cause a detrimental effect on the ability of the clay to act as an effective barrier, as suggested by the PI results and silica loss. However, in order to more accurately predict the changes to MX80, swelling ability after incubation with microbes should be assessed. Further experiments should also be carried out which more closely mimic the repository environment.

Chapter 6. Desiccation tolerance of the indigenous iron-reducing community of MX80 bentonite and interactions at the MX80 / steel interface

6.1 Introduction

These experiments were carried out to further understand the activity and survival of the indigenous iron-reducing community of MX80 bentonite in reference to nuclear waste repositories. The indigenous iron-reducing microbial community of MX80 bentonite was previously characterised at ambient temperatures with excess carbon (see section 4.1). During the repository closure, after 30 years of relatively favourable conditions, the temperature will increase causing water availability to decrease. This environment will last until around 100 years post-closure, after which time the temperature will decrease to 40-50°C across the clay barrier for the rest of the repository lifespan (Landolt et al., 2004). It was therefore important to test the temperature limits of this community under low water / low carbon conditions as this will be a large factor in determining microbial survival in the repository.

Furthermore, it is important to understand how the activity of this community (in addition to iron-reduction), will affect the multi-barrier system within the repository under these unfavourable conditions. For example, gas production and consumption could increase pressure causing detrimental effects (Landolt et al., 2009; Bardelli et al., 2014), or decrease oxygen levels aiding in reaching anaerobic conditions and thus inhibiting corrosion (Landolt et al., 2009). Another important factor to consider is the mineralogical and structural changes that could occur in MX80 bentonite. Although there are many possible biogenic changes that could occur, evidence from previous experiments suggested that species indigenous to the MX80 included IRBs, fermenting bacteria and possibly silica-solubilising bacteria (see ch4 and ch5).

Batch experiments were carried out using carbon steel (to represent the canister material for the UK-concept (NDA, 2016)) and compacted MX80 bentonite (from SKB's commercial supplier (ClayTech^{AB})). These experiments aimed to investigate the effect of temperature at different points within the repository lifespan. In the repository, the outer layer of the buffer is predicted to reach a maximum temperature of 70°C (RWM, 2016) within the first 100 years post-closure and then cool to 30-50°C for the remainder of the lifespan of the repository. It is therefore important to know if this initial spike in temperature would eliminate all microbes, or if some

could survive to later become active. It was expected that bacterial activity would be lower at higher temperatures and only some species would survive. To test this, following exposure to 70°C some experiments were cooled to 40°C. In these cases, any bacteria that were dormant during the higher temperatures may have been able to proliferate again as the experiment proceeded. All experiments were initially anaerobic, however, as the clay dried, oxygen may have entered the system.

The method for this chapter is presented in section 3.6. Briefly, jars containing sterile bentonite discs on top of steel coupons with a low volume of Sellafield-like groundwater were inoculated with the indigenous microbial community as characterised in section 4.1. The experiments were then incubated at 40 - 70°C with allowance for evaporation. At the termination of the experiment, the moisture content, plasticity and mineralogy of the clay was analysed. Additionally, observations of corrosion were made and the microbial community was analysed.

6.2 Results

6.2.1 Mineralogical analysis of the MX80 bentonite from desiccation tolerance experiments

Differences between the mineralogy of the MX80 bentonite were observed, both between microbial and abiotic control samples, and samples at different temperatures (figure 6.1). Notably, magnetite (Fe_3O_4) was identified in biotic samples from all incubation temperature regimens, but only in abiotic samples at 70°C. Other differences include the presence of a sodium iron oxide ($NaFeO_2$) at 40°C and 70°C incubations when microbes are present but not in abiotic controls. However, both the biotic and abiotic samples from the 70°C incubation contained goethite ($Fe^{3+}O(OH)$). All samples contained clay minerals known to exist in MX80 bentonite (Karnland, 2010) (quartz, montmorillonite, feldspar), however, the abiotic samples from the dual temperature control were also found to contain another member of the feldspar mineral series, not present in any other samples: anorthite ($CaAl_2Si_2O_8$). Although bulk XRD analysis is adequate to identify the iron oxide minerals present, there are limitations to the identification of clay minerals due to the interlamellar spacing. Therefore, limited conclusions can be drawn from the presence or absence of specific clay minerals such as anorthite.

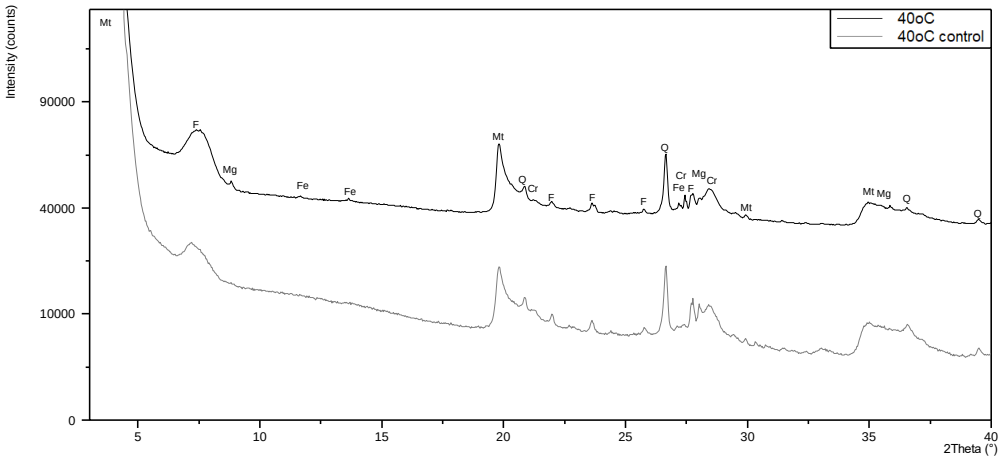

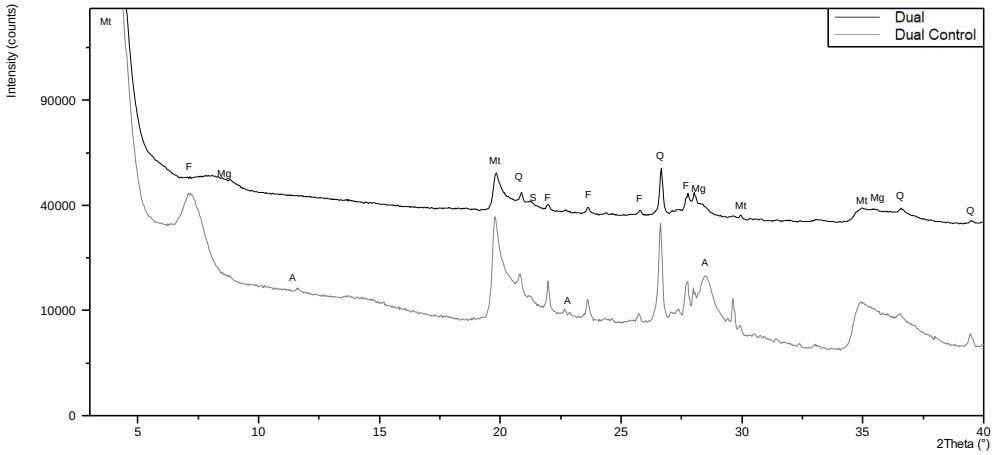

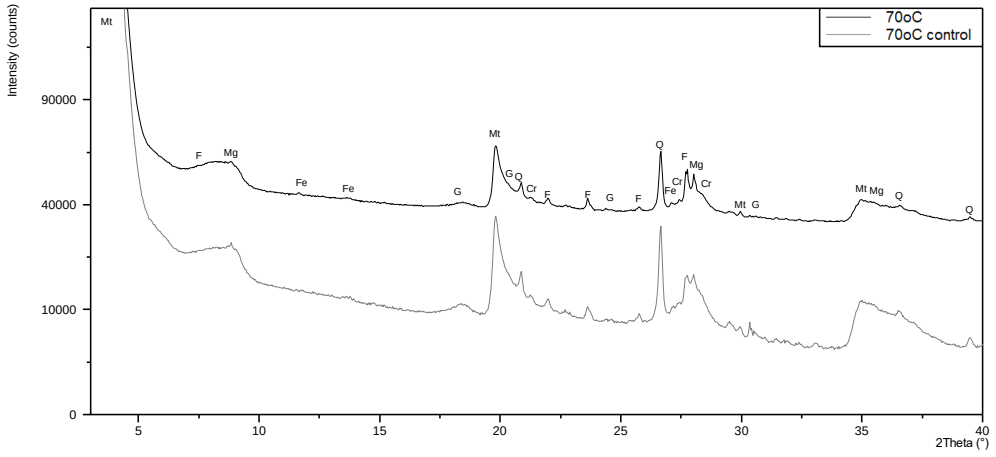

A	Cr	F	Fe	G	Mg	Mt	Q	S
Anorthite	Cristobalite	Feldspar	Sodium iron oxide	Goethite	Magnetite	Montmorillonite	Quartz	Sanidine

Figure 6.1: XRD spectra of MX80 bentonite recovered from desiccation tolerance experiments were analysed using HighScore Plus. Images show raw spectra with key mineral peaks labelled. Dual refers to experiments at 70°C, cooled to 40°C. Control refers to sterilised experiments.

Some changes to the bentonite surface were also observed in SEM images of MX80 bentonite from the steel / clay interface (figure 6.2). Extensive mineral precipitation was observed on the surface of MX80 bentonite from experiments at 40°C, which has been identified as cristobalite (images are comparable to those generated by Horwell et al. (2013)), and octahedral magnetite, although, other minerals may also be co-precipitated. Similar minerals were observed on the surface of MX80 bentonite from the dual temperature experiments, but this was more localised. The samples analysed from MX80 bentonite from desiccation tolerance experiments at 70°C indicated iron oxide formation on samples from the centre of the MX80 bentonite disk closest to the steel coupon, which could be the sodium iron-oxide identified in the XRD. Similar iron-oxides have been identified by Leban & Kosec (2017) who found that goethite was replaced by magnetite or lepidocrocite formed on mild steel.

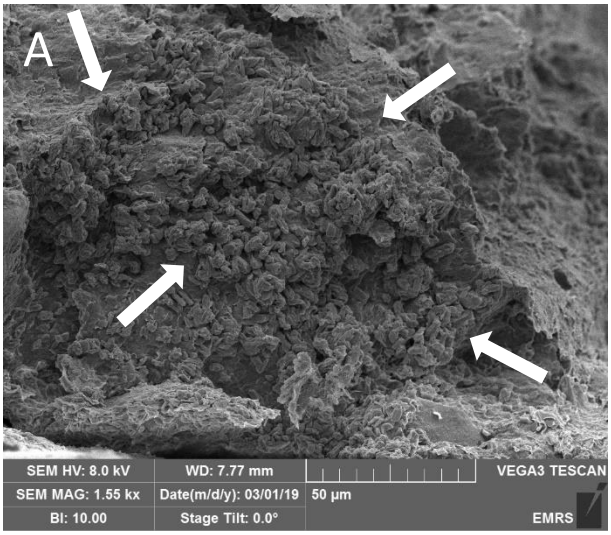
A
SEM HV: 8.0 kV
WD: 7.77 mm
VEGA3 TESCAN
SEM MAG: 1.55 kx
Date(m/d/y): 03/01/19
50 µm
BI: 10.00
Stage Tilt: 0.0°
EMRS

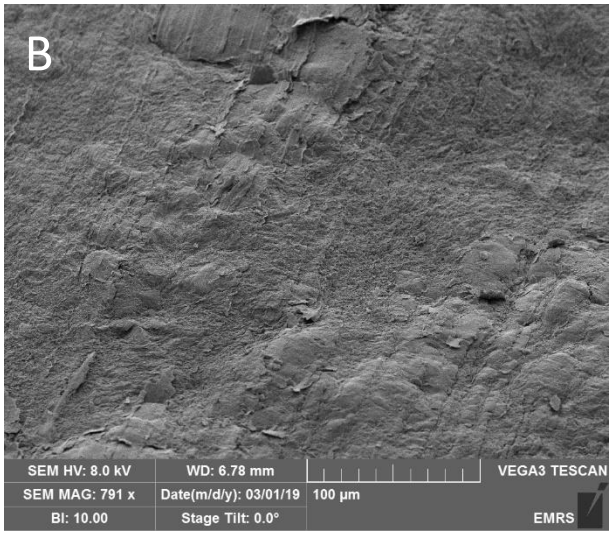
B
SEM HV: 8.0 kV
WD: 6.78 mm
VEGA3 TESCAN
SEM MAG: 791 x
Date(m/d/y): 03/01/19
100 µm
BI: 10.00
Stage Tilt: 0.0°
EMRS

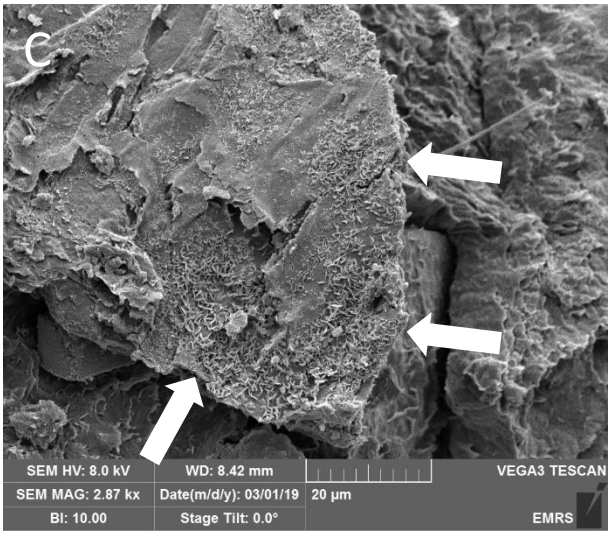
C
SEM HV: 8.0 kV
WD: 8.42 mm
VEGA3 TESCAN
SEM MAG: 2.87 kx
Date(m/d/y): 03/01/19
20 µm
BI: 10.00
Stage Tilt: 0.0°
EMRS

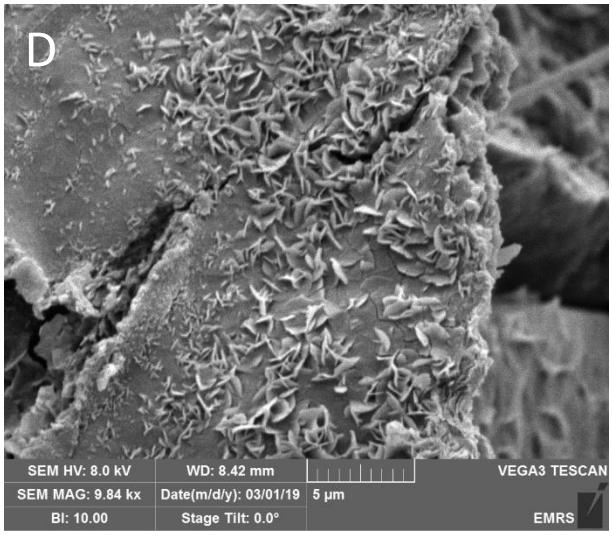
D
SEM HV: 8.0 kV
WD: 8.42 mm
VEGA3 TESCAN
SEM MAG: 9.84 kx
Date(m/d/y): 03/01/19
5 µm
BI: 10.00
Stage Tilt: 0.0°
EMRS

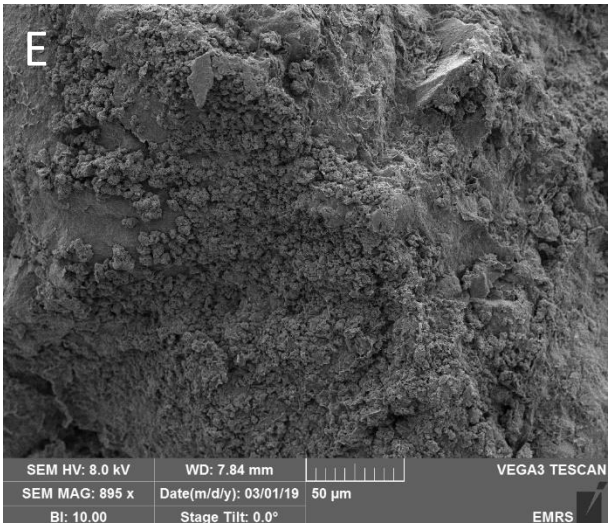
E
SEM HV: 8.0 kV
WD: 7.84 mm
VEGA3 TESCAN
SEM MAG: 895 x
Date(m/d/y): 03/01/19
50 µm
BI: 10.00
Stage Tilt: 0.0°
EMRS

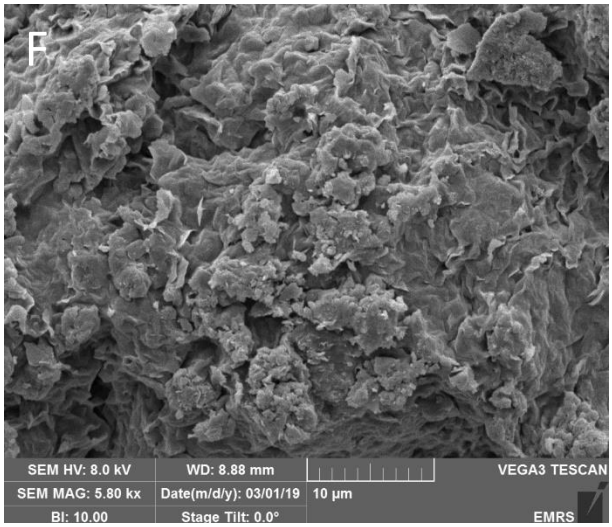
F
SEM HV: 8.0 kV
WD: 8.88 mm
VEGA3 TESCAN
SEM MAG: 5.80 kx
Date(m/d/y): 03/01/19
10 µm
BI: 10.00
Stage Tilt: 0.0°
EMRS

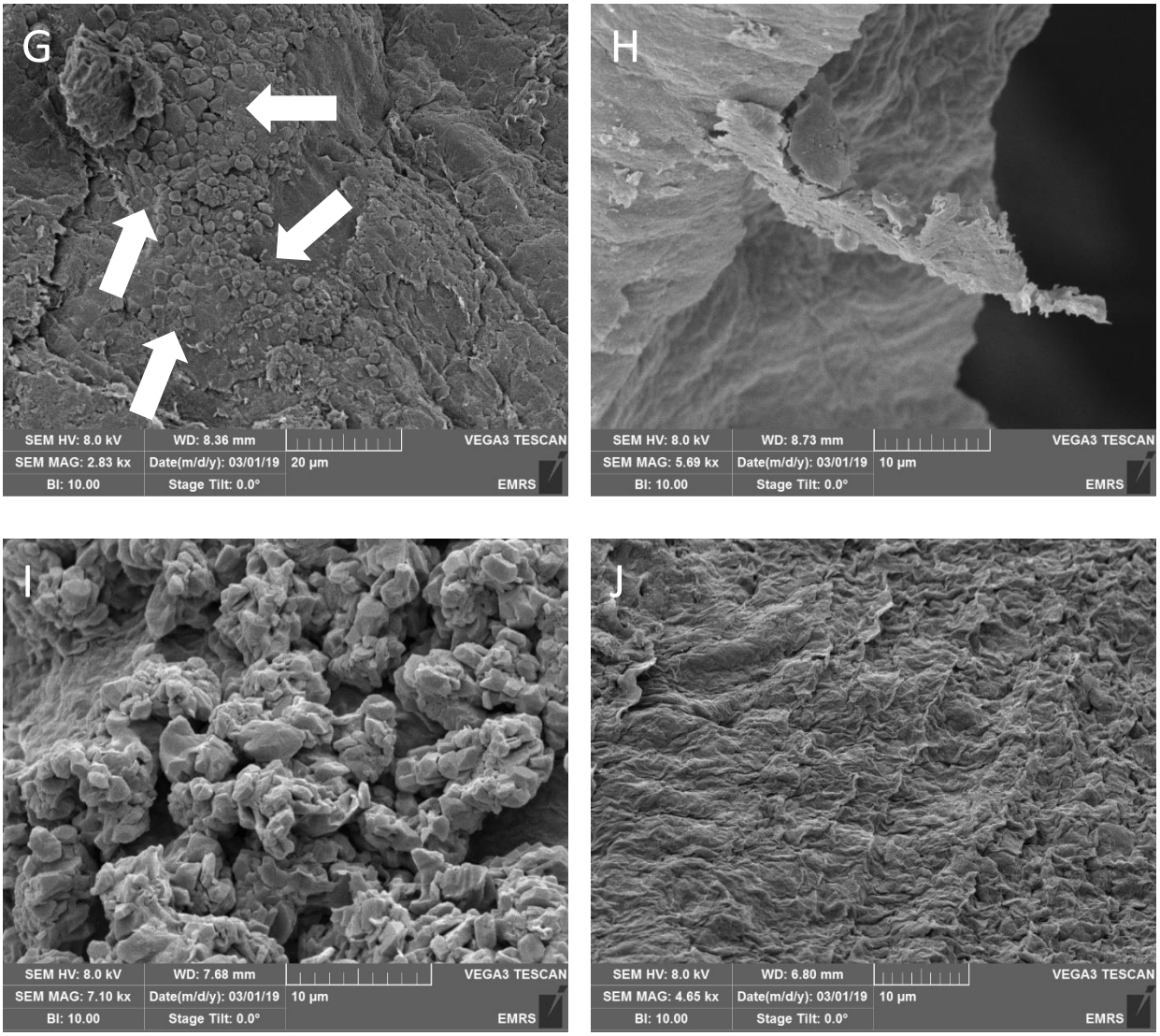

Figure 6.2: SEM images of clay recovered from the clay/bentonite interface of batch experiments. The 40°C experiment had a lot of growths on the surface (A), and the abiotic control was completely smooth (B). The 70°C experiments had significant crystal growth (C, D), and large debris / overgrown crystals (E, F). Limited minerals were observed on the corresponding control (G). Clay from the dual temperature experiment had heavily mineralised hyphae (H) in multiple locations, and similar growths as seen in the other experiments (I). The control was smooth and no crystal structures were observed (J).

6.2.2 Plasticity measurements of the MX80 bentonite from desiccation and temperature tolerance experiments

The plastic limits (PL) and liquid limits (LL) of the MX80 bentonite changed after the experiment when microbes were present at all temperatures. The PL was between 30-39% moisture content across all samples and the LL was lower when microbes were present across all temperatures. There were significant changes to the plasticity index (PI) (figure 6.3) of MX80 bentonite following experiments at 40°C with microbes; the PI was 283 compared to 376 for the abiotic control at 40°C (p= 0.017) and 379 ±3 for the PI before the experiment. The PI of the MX80 bentonite from 70°C with microbes was also significantly lower when compared to the abiotic control (p=0.0276). There was no significant difference in PI in the dual temperature experiment when microbes were present. There is a small difference between the abiotic controls at different temperatures, and a significant difference between microbial experiments at different temperatures (p=0.0348).

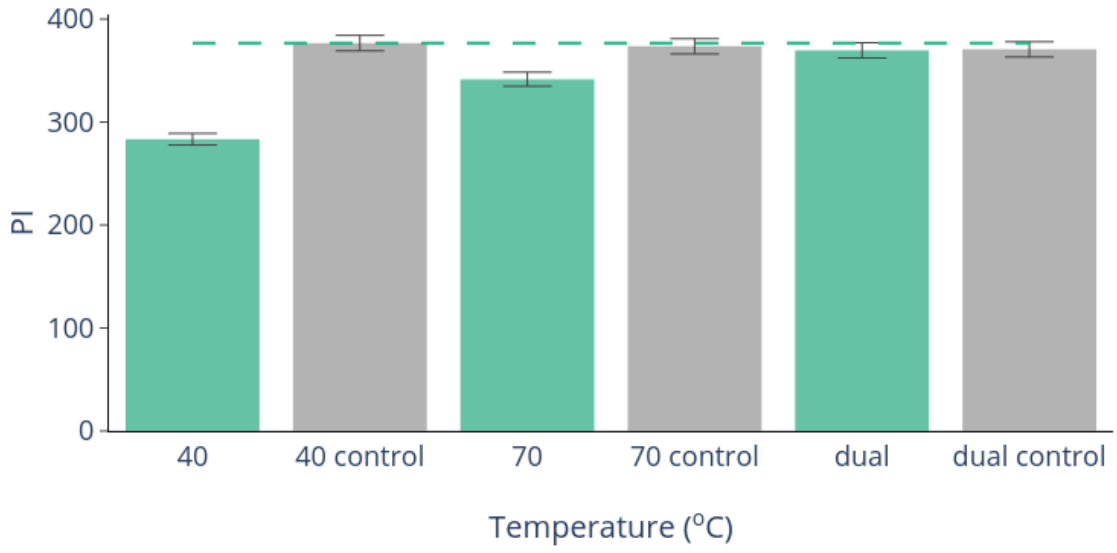

Figure 6.3: PI of MX80 bentonite recovered from desiccation tolerance experiments at different temperatures. Dotted line indicates PI of MX80 bentonite before the experiment. Error bars represent standard error.

Additionally, the %moisture content of the clay was calculated (figure 6.4). It was found that the experiments at higher temperatures had a lower moisture content than those at 40°C. Furthermore, the %moisture content of the abiotic controls was higher than the biotic experiments in all temperature treatments apart from those at 70°C which was found to be significantly higher when microbes were present ($p<0.001$). For all other temperatures, these results were found to be significantly lower when microbes were present at 40°C ($p<0.001$), and dual temperature ($p<0.001$). Similarly, a two-way ANOVA found that both microbial presence and temperature were significant factors in %moisture content ($P<0.001$).

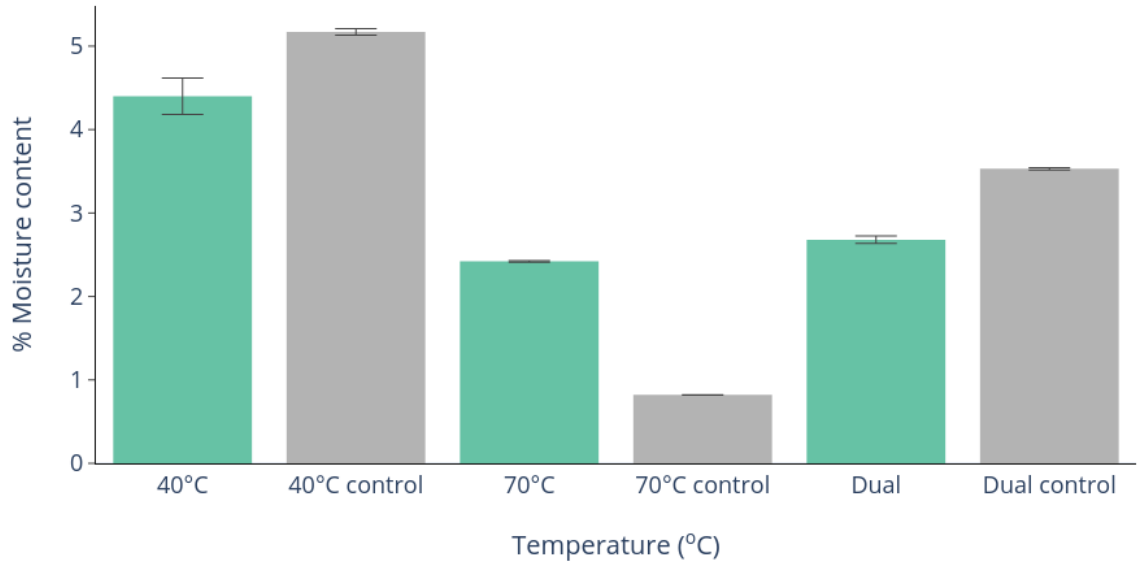

Figure 6.4: % moisture content of MX80 bentonite after desiccation tolerance experiments at elevated temperatures. Error bars show standard error.

6.2.3 Visualisation of corrosion of steel coupon recovered from desiccation tolerance experiments

The steel coupons used in these experiments did not corrode extensively. This result has been largely attributed to the dry conditions of the experiment. However, some corrosion was observed, particularly around the edges. There was visually more surface corrosion observed on steel from abiotic experiments than from experiments with microbes. This difference was

particularly clear on samples from 40°C (figure 6.5). ImageJ measurements of the area of the steel surface visually corroded suggested that this result was significant (P=0.0374) with a mean of 14% of the surface area corroded in biotic samples, compared to 35% in abiotic samples.

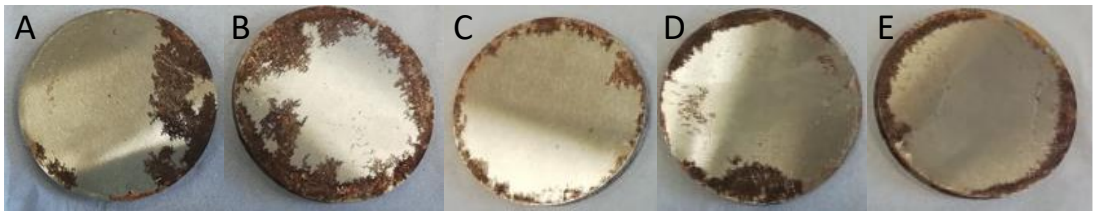

Figure 6.5: Photograph of steel coupons recovered from 40°C where from abiotic control experiments (A, B) and biotic experiments (C-E). Photographs show the steel surface that was in contact with the clay.

6.2.4 Community analysis of the desiccation tolerance experiments at various temperatures

Nine 16S rRNA libraries were derived from sequencing outputs of desiccation tolerance experiments at various temperature regimens. These library sequences have been deposited in the NCBI's Sequence Read Archive (SRA) available under BioProject PRJNA594313. The sequencing yielded average reads of 78,872 ±3693 for 40°C, 50,577 ±7706 for dual temperature and 31,116 ±9425 for 70°C with an average read length of 227 bp across all libraries. The number of reads was significantly lower from 70°C compared to 40°C (p=0.0435). From this, an average of 25 (40°C), 47 (dual temperature), and 51 (70°C) ASVs were identified from the QIIME2 pipeline. Low sequence reads from control experiments and negative sequencing controls indicate no contamination took place during the experiment or subsequently during DNA extraction and sequencing. The resulting microbial communities of MX80 bentonite was largely composed of taxa assigned to the phylum firmicutes, most abundantly, taxa related to the genus *Bacillus* (figure 6.6).

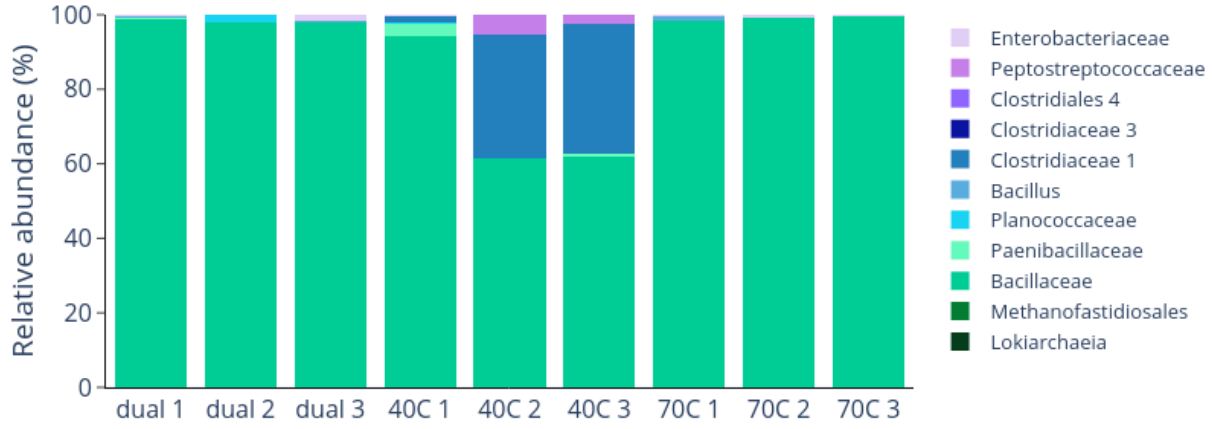

Figure 6.6: Level 5 microbial community constructed using 16S rRNA QIIME2 output and presented as %relative abundance.

However, there was also a significant population of *Clostridaceae* species in the 40°C experiment (P=0.027) which was found to be most closely related to *Clostridum beijerinickii* and *Clostridium subterminale* (figure 6.7). Whereas ASVs identified from the dual temperature experiments were most closely related to solely *Bacillus sp.* and *Paenibacillus sp.* (figure 6.8). It should also be noted that most of the nearest neighbours were isolated from high salinity environments such as salt lakes and marine sediments. This isolation source is similar to those identified as nearest neighbours to ASVs from the 70°C experiments (figure 6.9). Similarly, this community was of lower diversity relative to the 40°C incubation and was composed of mainly firmicutes, particularly *Bacillus*, albeit there was also a small population of gammaproteobacteria (comprising 0.1% relative abundance). As expected, due to the survival of spore-formers reported in previous experiments (Masurat, 2010; Stroes-Gascoyne et al., 2002) many species identified in these communities are putative spore-formers. However, there are differences between the different temperature treatments. By considering all sequences which were able to be assigned to species level, 100% of species identified in the dual temperature experiments are putatively capable of forming spores and 98.2% of the community at 70°C are spore-forming. Only 83.72% of species are putatively able to form spores at 40°C.

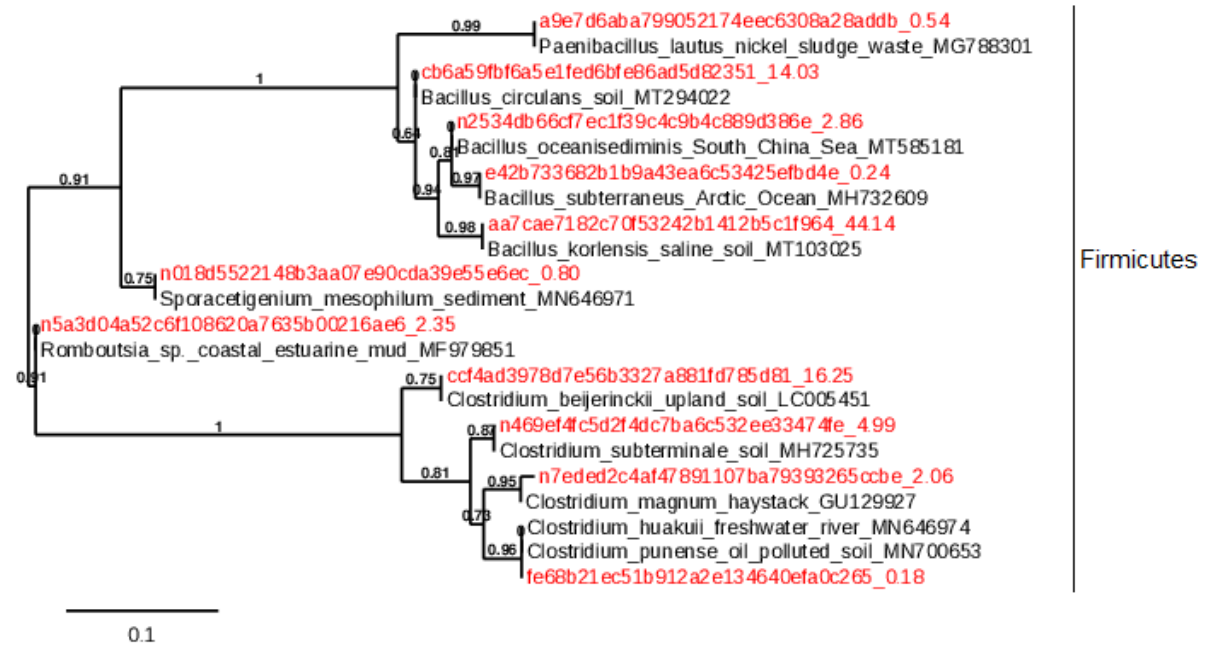

Figure 6.7: Phylogenic distance trees based on comparative analysis of partial 16S rRNA sequences recovered from desiccation tolerance experiments at 40°C. Sequences were analysed by the nearest neighbour using BLASTN (GenBank database), and then aligned and trees constructed using MEGA7. Scale bar denotes 10% sequence divergence

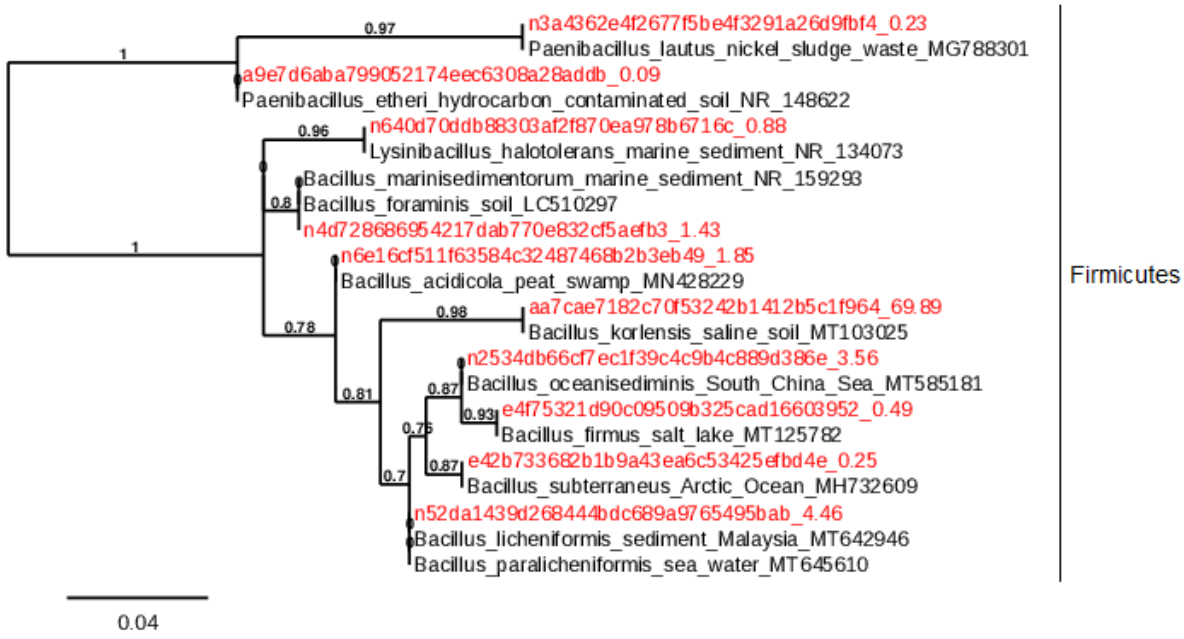

Figure 6.8: Phylogenic distance trees based on comparative analysis of partial 16S rRNA sequences recovered from desiccation tolerance experiments conducted at dual temperatures. Sequences were analysed by the nearest neighbour using BLASTN (GenBank database), and then aligned and trees constructed using MEGA7. Scale bar denotes 4% sequence divergence

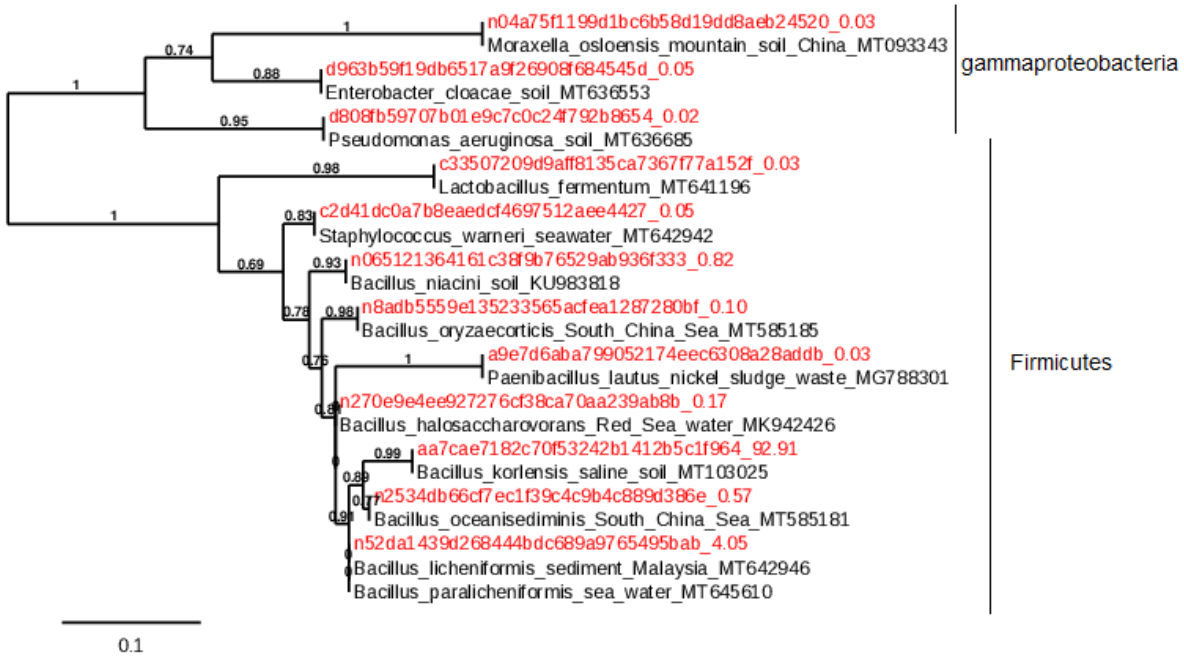

Figure 6.9: Phylogenic distance trees based on comparative analysis of partial 16S rRNA sequences recovered from desiccation tolerance experiments at 70°C. Sequences were analysed by the nearest neighbour using BLASTN (GenBank database), and then aligned and trees constructed using MEGA7. Scale bar denotes 10% sequence divergence

A PCA plot of the sequencing results for these experiments was created (figure 6.10). It demonstrates that the 70°C microbial communities have very low diversity and are also very similar in structure to the dual temperature microbial communities, although these are somewhat more widely spread. Samples from the 40°C treatment were the most widely spread, therefore indicating that they are the most diverse between samples. This diversity is likely because a wider variety of microbes were able to survive in these conditions. The diversity between these samples is still relatively low compared to other environmental samples.

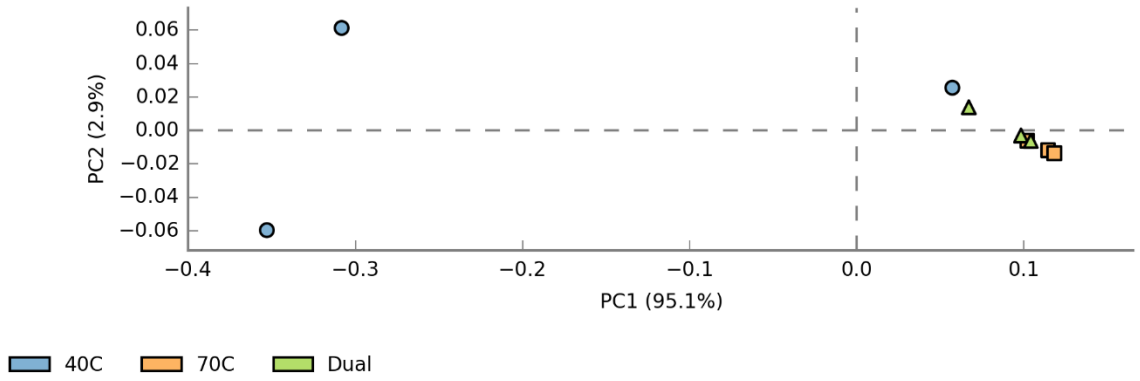

Figure 6.10: PCA plot of microbial communities at different temperatures. Constructed from outputs from QIIME2 and 16S rRNA Illumina sequencing using Stamp.

In addition to the above PCA plot, Stamp was also used to determine whether the relative abundance of different genera was significant depending on the temperature of the incubation. The only genera that proved significant were *Bacillus*, with a p-value of 0.033, and *Clostridia* (P=0.004)

6.3 Discussion

There are several conclusions to be drawn from these desiccation tolerance studies related to the survival of IRBs and fermentative bacteria indigenous to MX80 bentonite in unfavourable conditions related to those likely to occur in nuclear waste repositories. These conclusions are principally supported by the geotechnical and mineralogical data of the MX80 bentonite and further supported by the putative functions of such organisms identified in the community.

It should be noted that bacteria added to these experiments were of a higher concentration than would naturally occur in MX80 bentonite and that the clay was not compressed in these experiments. Therefore, increased activity may have occurred relative to the repository where higher compaction, resulting in a lower pore size may contribute to decreased microbial activity. However, toward the end of the repository lifespan when the edges of MX80 bentonite have been corroded there may be potential for increased activity at the clay / host rock interface. Equally, some gaps may be present at this interface much earlier where the clay has

not fully swelled allowing for some microbial growth (Wilson et al., 2010; Jalique et al., 2016; Stroes-Gascoyne et al., 2011).

During the repository closure, there may also be microbes introduced from other sources such as the local groundwater. The UK has not yet selected a repository site, so microbes from such a source have not been considered. However, Chi and Athar (2008) suggest that groundwater microbes would not be suited to survival within the clay barrier.

6.3.1 Survivability of indigenous bacteria of MX80 bentonite

To ensure DNA extracted from MX80 bentonite was indicative of active bacteria, a location geographically distant from the inoculation site was chosen for sampling. Therefore, the bacterial communities presented are representative of those able to survive in high temperature, low water conditions.

As expected, many of the bacteria identified in the sequence libraries from the incubation experiments are putatively spore-formers, particularly in the higher temperature experiments. Spore-forming bacteria can withstand harsher conditions by entering a period of dormancy (Rättö M. & Itävaara M, 2012). In this way, bacteria in the repository will be able to withstand the unfavourable habitat for decades and become active when conditions improve (e.g., as the temperature decreases, or groundwater becomes available). The lack of diversity between samples from experiments at dual temperature and 70°C indicates that the community was uniform throughout the clay and that only a limited number of species were able to survive.

Many of the bacteria present in the 40°C community are closely related to those able to grow optimally at this temperature, and many more species indigenous to MX80 bentonite are also able to tolerate this heat (see section 4.1). Therefore, there was some diversity between samples indicating that different species were more dominant in particular samples. Interestingly, *Clostridia* are lost from communities at the higher temperatures and do not survive to become active as the temperature cools (as illustrated in the dual temperature experiments), despite the ability for identified species to form spores (*C. beijernickii* (Patakova et al., 2019)). This may be due to heat or oxygen stress because many *Clostridia* are obligate anaerobes rather than *Bacillus* which is a genus that is facultatively anaerobic. The higher temperatures may have

accelerated drying conditions causing the clay to shrink from the edges and introducing a higher concentration of oxygen.

The difference in community observed between the dual temperature experiments and 70°C experiments is also interesting. It suggests that species such as *Lysinibacillus halotolerans*, and certain *Bacillus sp.* were outcompeted at 70°C or only able to survive as spores and later became active as the temperature cooled. As highlighted previously, species identified as nearest neighbours were isolated from high saline environments. Due to the low water availability, it is likely that adaptations to high saline environments would also be advantageous in the study presented here and, in the repository, even though the groundwater is low salinity.

6.3.2 Putative activities of the indigenous bacterial community

Within the bacterial communities presented there are some known IRBs; *Bacillus subterraneus* is capable of dissimilatory iron reduction (Kanos et al., 2002), as is *C. beijerinckii* (Dobbin et al., 1999). Reduction of iron in iron-containing silicate minerals in the MX80 bentonite will result in a loss of silica and transformation to non-swelling minerals, making the clay more prone to weathering (Pusch & Kasbohm, 2002). This would decrease the ability of the clay to act as an effective barrier to nuclear waste. Although abiotically this transformation is slow and requires high temperatures to proceed abiotically, biogenic dissolution of smectite does not have the same requirements (Kim, 2012). Smectite to illite transformations occur biogenically as dissolution of smectite and reprecipitation as K / Al illite – this has been shown to be catalysed by IRBs reducing Fe(III) present in silicate minerals (Kim, 2012; Fang et al., 2017; Bradbury et al., 2014). There is also evidence that the role of organic secretions in iron reduction will lead to smectite - illite transformations (Kim, 2012).

Also present in the community when incubated at 40°C is *C. subterminale* which although connected to iron reduction has not been shown to reduce iron conclusively (Kato et al., 2015). Some species of *Romboutsia* are also known to reduce iron (Gerritsen et al., 2017) however, it is not possible to know if those particular species are present here.

Even in the community from the 70°C experiments there are species with a putative iron-reducing ability. *Lactobacillus fermentim* is able to reduce iron (González et al., 2017) and *Bacillus licheniformis* is implicated in iron-reduction, but only in the presence of oxygen (Mclean et al.,

1992). Additionally, *L. halotolerans* has been shown to adhere to iron surfaces and therefore it is likely that there is some interaction and possibly iron reduction (Douterelo et al., 2014). Likewise, *Paenibacillus etheri* has been implicated in iron reduction (Loyaux-Lawniczak et al., 2019).

Additionally, some of these species are known to interact with silica. Both *P. aeruginosa* and *B. licheniformis* activity has been shown to lead to loss of silica from clays (Mohanty et al., 1990; Radhapriya et al., 2015). Such a change in mineralogy could be linked in changes in geomechanical properties which could alter the ability of MX80 bentonite to act as an effective barrier in the repository system.

It is well known that fermenting bacteria, such as firmicutes identified in these microbial communities can produce volatile fatty acids (VFAs) which can further interact with metals such as iron (Parrello et al., 2016) and support the growth of other members of the community (Bengtsson et al., 2017; Svensson et al., 2011; Gilmour et al., 2021). This process may have aided in the survival of non-fermenting species in the community in these experiments. The VFA production, in addition to the acetate added, may also lead to increases in iron-reduction (Parrello et al., 2016; Bengtsson et al., 2017; Svensson et al., 2011), which in turn could cause a release of silica from iron-containing silicate minerals (Bennett et al., 2001). Indeed, Hiebert & Bennett (1992) found that organic acid production by fermentative bacteria such as those identified here, increased the rate of silicate weathering from feldspar and quartz minerals. Furthermore, CO_2 is produced by acetogenic bacteria (*C. beijerinckii, C. magnum; C. huakuii*). In this environment, the CO_2 could also contribute to an increase in pH and further silicate weathering (equation 1) resulting in loss of silica through production of silicic acid and aqueous bicarbonate. This was not measured during this experiment as the jars were not airtight to allow water evaporation to escape and desiccation to occur. In the repository this process would cause alterations to the clay minerals but would also limit gas pressure through utilisation of the produced CO_2. MX80 is composed of 81.4% wt. montmorillonite (31% wt. silicon) and 4% wt. iron (Karnland, 2010). Changes to these minerals could therefore result in widespread mineralogical changes to the structure and properties of the clay.

$$4H_2O + 2CO_2 + SiO_2 = 2HCO_3^- (aq) + 2H^+ + H_4SiO_4 \quad [1]$$

6.3.3 Potential corrosion protection afforded by microbial activity

As indicated in the results, there was significantly less corrosion of the surface of the steel coupon when microbes were present. Although this does not account for the depth of corrosion or the overall weight loss from the steel coupon, it does suggest that microbial presence directly or indirectly limited contact of oxidants with the steel surface. This is likely due to bacteria utilising all available oxygen in the system through aerobic respiration. As Leupin et al., (2017) suggests, microbes within the repository will utilise gases produced which could aid in accelerating the transition to anaerobic conditions therefore decreasing early corrosion of the waste canister. Although, *in situ* studies by Stroes-Gascoyne et al., (2000) suggest that microbial presence has no significant effect on gas composition. However, it may be that microbial hydrogen and CO_2 products are being utilised elsewhere in the repository – such as in iron-reduction or weathering of silicate minerals (equation 1), rather than not being produced.

There is evidence of mineral precipitation (cristobalite, and iron oxides such as magnetite) at the clay / steel interface, as seen in SEM images. This is contradicted by the photographs of the steel surface which indicate more extensive corrosion (and thereby iron oxides) in the sterile experiments. An explanation for this is that microbial presence increases the ability of rust products to diffuse into the clay, or that the iron oxides observed in microbial experiments are from reduction of minerals within the clay, rather than from the steel. This explanation would be supported by the decrease in PI observed in microbial experiments.

Magnetite, lepidocrocite and goethite are all common corrosion products (Antunes et al., 2013). Whilst magnetite is not known to inhibit corrosion (Dong et al., 2000; Boin et al., 2000), other iron oxides may contribute to corrosion protection (Necib et al., 2017). Nitrate-reducing bacteria such as those present here (*P. etheri, L. halotolerans, B. korlensis* and *B. licheniformis* (Zhang et al., 2009; Loyaux-Lawniczak et al., 2019; Kong et al., 2014; Albert et al., 2005; Lee et al., 2017)) have been implicated in rust formation to inhibit corrosion (Etique et al., 2014). The low porosity of these rust layers inhibits electrons from reaching the steel surface and therefore prevents further corrosion. In these studies, this method of protection may have been limited due to the reduced activity of the microbes under the unfavourable conditions. Limited corrosion took

place across all experiments due to the low water / oxygen conditions, but there is potential for these layers to develop in the repository over time.

6.3.4 Potential mineralogical alterations to MX80 bentonite

The most notable differences between the biotic and abiotic clay samples are the presence of iron oxides at 40°C and 70°C. Although samples for XRD analysis were taken from throughout the clay, it is not clear if these iron oxides are corrosion products which have moved into the clay, or from structural iron within the MX80 bentonite. Sodium iron oxide was also observed in XRD analysis and is likely the product of microbially-influenced iron-reduction (Usman et al., 2012). The lack of moisture may have induced the formation of sodium iron-oxide through an increase in salinity. The presence of IRBs may contribute to magnetite and goethite formation as they are produced as secondary minerals during dissimilatory iron-reduction coupled to oxidation of organic matter (Lovley, 1991; Shimizu et al., 2013). Iron-reduction can also be catalysed by the presence of Fe(II) which accounts for 0.8 % wt. of the total iron in MX80 bentonite (Karnland, 2010). Therefore, there is another route in which abiotic iron-reduction may have progressed.

Magnetite was observed in the abiotic experiments at 70°C, one possible explanation for this is that drying can inadvertently cause magnetite formation (Schwertmann & Murad, 1983; Lovley et al., 1987). As these experiments have dried out the most during the experiment, it is possible that this caused increased abiotic magnetite formation. As can be seen in the PI results, the higher temperatures did correlate with minor decreases to clay plasticity.

There were no iron oxides observed in the dual temperature experiments, either with or without microbes. A possible explanation for this is that the microbes present were not active for long enough to promote any widespread alterations. These samples had the lowest number of ASVs identified and the community does not contain any known iron-reducers. Whilst there are plenty of fermentative bacteria present, they are all spore-formers. Therefore, it may be the case that these microbes were only active during the first two months at 70°C and remaining as dormant spores for most of the incubation. Those bacteria which would have been active at 40°C have likely been lost at 70°C. This lack of iron-oxides could be an indication that no mineralogical changes have occurred on iron-containing silicate minerals. This conclusion is reflected in the PI of MX80 bentonite.

There were significant decreases in PI of MX80 bentonite from biotic experiments at 40°C and 70°C. This reflects the experiments which had IRBs in their microbial community. Furthermore, the SEM images of these experiments showed the presence of iron-oxides which were also identified in XRD. Similar decreases in PI following exposure to heat were seen in Davies et al. (2017). The decrease in PI is likely due to formation of non-swelling Fe(II) minerals and a loss of silica from the clay matrix because of iron-reduction (Flórez-Góngora et al., 2020).

40°C is the temperature which supports most microbial growth and activity within this experiment as evidenced in the sequencing results and PI. It was therefore expected that the biggest change in PI occurred in experiments at this temperature. However, the lack of any significant change in PI at the dual temperatures suggest that the population of microbes which causes changes to iron minerals at 40°C is distinct from the community at 70°C and it cannot recover from exposure to higher temperatures. This conclusion is supported by microbial community data which shows differences in communities between all three temperature treatments.

In terms of the repository, a higher PI is advantageous. This property indicates the MX80 bentonite will respond to changes in moisture content whilst remaining an effective barrier (Wilson et al., 2010). The decrease in PI reported here was largely due to a lower liquid limit which could result in the canister sinking into the clay during periods of high moisture content. Further geomechanical tests were not possible due to the volume of clay used in these experiments. However, previous experiments by Svensson et al. (2011) detected a significant difference in swelling pressure before and after bentonite was exposed to high temperatures. However, that experiment did not consider microbial activity or specifically the resulting iron redox states which may have contributed to these changes. Likewise, experiments by Davies et al. (2018) found that incubating highly compacted MX80 bentonite at elevated temperatures with steel decreased both the plasticity and swell index. Indeed, the results show that PI continued to decrease as time increased. However, these experiments also did not consider the possibility of microbially-influenced mineralogical changes.

6.3.5 Conclusions

Species present in the viable indigenous iron-reducing community of MX80 bentonite are able to survive the highest temperatures expected at the host rock / clay interface in low water conditions. These microbes are largely spore-forming species. However, if limited activity can occur in areas where clay swelling has not fully occurred, biologically-influenced iron-reduction may take place due to the presence of IRBs. This biogenic process may lead to a decrease in plasticity through associated loss of silica from the clay matrix. There is also evidence to support the conclusion that microbes can enter dormancy at 70°C in order to survive to a more favourable habitat. Finally, there is likely utilisation of oxygen by aerobic microbial respiration which acts to indirectly protect steel from corrosion. Further biogenic protection may occur and, considering the species identified in the community, this protection could be through formation of a low porosity rust layer or by biofilm formation.

Chapter 7. Biotic MX80 / steel interface test cells to simulate repository pressure

7.1 Introduction

The experiments reported in this chapter aimed to mimic, to some extent, the environment within the repository in terms of pressure, heat and space. MX80 bentonite and steel were inoculated with the microbial community presented in section 4.1 and incubated in test cells under high pressure for 12 weeks. Water pumps were used to create a water pressure gradient across the clay (figure 3.7, see section 3.7.1). The steel used in these experiments represented the waste canister and so potential interactions at the canister / MX80 interface could be investigated. 40°C was chosen as the incubation temperature because the repository will be 40-50°C for the vast majority of its lifespan. The set-up of this experiment was replicated from previous work by Davies (2017), although the temperature and groundwater were altered to be in keeping with this project. Previously, test cell experiments investigating the clay / steel interface had observed green and orange corrosion products, however, the role of microbes in the formation of these products had not been evaluated. Therefore, these experiments (run in triplicates) were repeated with and without microbes (biotic and abiotic). The experiment was also repeated with microbes but without steel to attribute changes in the clay to the microbes and not to microbially-influenced (or abiotic) corrosion processes. Due to the set-up of the water pumps, each of these experimental designs was run consecutively.

As set out in section 1.6, it was hypothesised that microbial activity would increase corrosion and potentially alter the mineralogy of MX80 bentonite leading to potentially disadvantageous changes to its geomechanical properties. The results of this experiment explained below suggest that microbial activity did result in changes to the mineralogy and geomechanical properties of the MX80 bentonite in support of the hypothesis. However, the effect of microbial activity on corrosion in these experiments appears to contradict the original hypothesis, similar to the results of chapter 5 and chapter 6.

7.2 Results

Upon dismantling the test cells, the most obvious difference between the biotic and abiotic experiments was the visible change in corrosion products that diffused from the steel into the

clay, against the water gradient (figure 7.1). The microbial experiment with the steel coupon showed two bands of corrosion products, one green (adjacent to the steel surface) and one orange (further from the steel surface), this was consistent across three replicates and mirrored previous results (Davies, 2017). Whereas, in the sterile experiment, only orange corrosion products were observed. There was no corrosion layer observed in the experiment without steel, as expected. Additionally, there were differences in the pH of the clay and effluent between the different experimental set-ups. The iron-reducing ability of the resulting microbial community differed between the experiment with steel and without steel and varied depending on proximity to the steel.

Figure 7.1: Steel and clay recovered from test cells. Layers of green and orange corrosion were observed in inocculated experiment with steel (left), whereas no green layer was observed in the sterile experiment (right).

7.2.1 Effluent measurements including pH, Fe(II), and groundwater parameters

Due to the nature of the set-up, effluent could only be collected at the termination of the experiment and effluent from all triplicate test cells was collected from the same tap, therefore only one measurement could be taken per triplicate. It should be noted that all effluent measurements were taken immediately at the termination of the experiment. Differences in the

appearance of the effluent collected from each of the experiments were initially observed and photographed. Most notably, the effluent from the microbial experiment with steel present was green in colour, while the effluent from the other experiments remained colourless (or only slightly green) (figure 7.2). There was also more particulate material in the effluent when microbes were present compared to the sterile control.

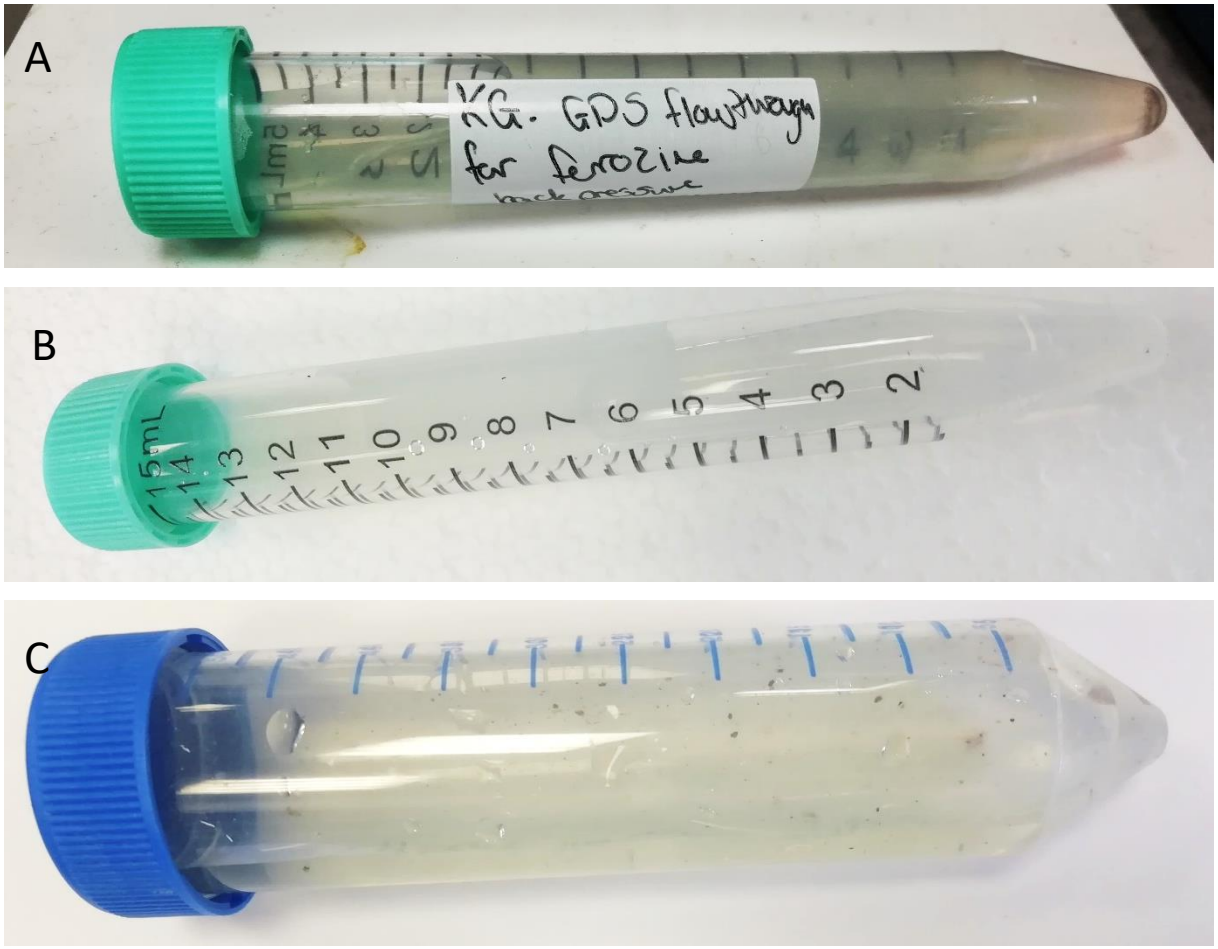

Figure 7.2: Effluent collected from Microbe_Steel experiment (A) was green in colour, the effluent from Sterile_Steel was colourless (B), and the effluent from Microbe_NoSteel (C) was less green than the Microbe_Steel experiment.

7.2.1.1 pH of the effluent collected from MX80 / steel interface test cell experiments

The groundwater used in each set-up was around pH 7. This was consistent across the experiments (figure 7.3). However, the pH of the resulting effluent was higher across all experiments including steel. This result is expected as the corrosion will result in an increase in

alkalinity (Prawoto et al., 2009) as H^+ ions are used up in corrosion processes. As the microbes were predicted to increase the corrosion, a greater increase in the pH is expected compared to the sterile experiment. The microbial experiment containing no steel remained circumneutral.

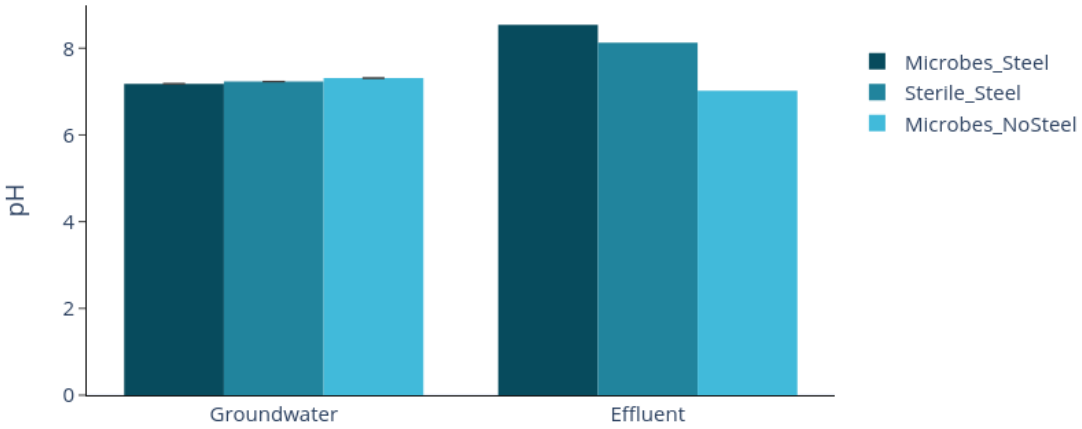

Figure 7.3: pH of initial groundwater and resulting effluent collected from test cell experiments. Error bars show standard error (groundwater only).

7.2.1.2 Fe measurements of effluent collected from test cell experiments

Fe(II) aqueous, Fe(II) total and Fe(total) measurements were measured in each sample of effluent (figure 7.4). The microbial experiments with steel were predicted to have the most corrosive activity, and therefore, the most iron present in the effluent, this is reflected in the results. The only samples containing Fe(II) were the microbial experiments with steel, which also had the highest concentration of Fe(total). The experiment with no steel did have a concentration of 0.048 mM (Karnland, 2010) of iron from structural iron within the clay. The sterile experiment with steel had a slightly higher iron concentration in the effluent (0.096 mM) but this was still far lower than the Microbial_Steel experiment (0.384 mM).

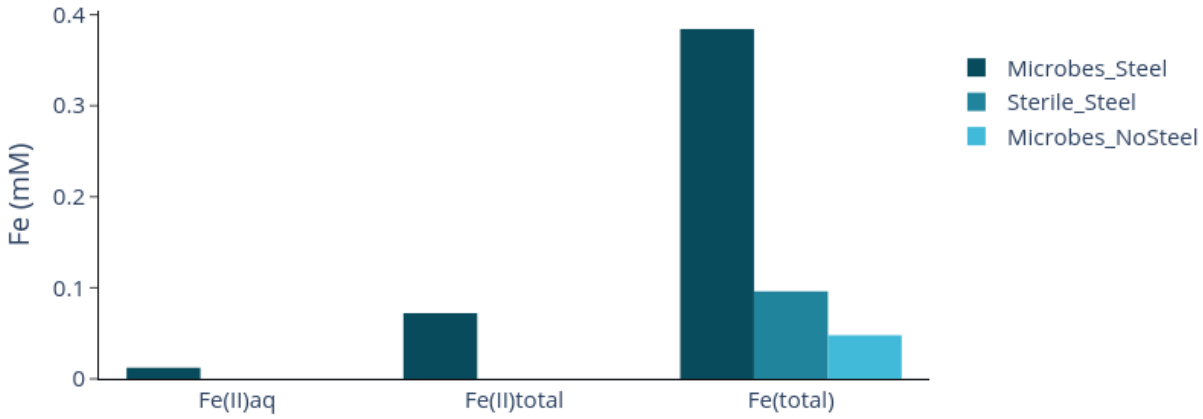

Figure 7.4: Iron concentration in the effluent recovered from test cell experiments.

7.2.1.3 Further effluent measurements from test cells using an Ultrameter

An ultrameter was used to measure the total dissolved solids (TDS) and oxidation-reduction potential (ORP) of the effluent samples (figure 7.5). The microbial experiment with the steel coupon had the highest TDS at 2362 PPM, whereas, the other experiments were both significantly lower at 550-650 PPM. The sterile experiment did have the highest ORP at 256 mV, and the microbial experiment with steel had the lowest at 180 mV. The ORP of the microbial experiment without steel was 202 mV. When considering the relation of pH and Eh (Rose, 2010) to iron redox couples, the effluent from the microbial experiments is likely to favour dissolved Fe(II) and ferric hydroxide ($Fe(OH)_3$) as the conditions sit on the boundary of these two iron species. The higher Eh of the sterile experiments shifts this to be more favourable for ferric hydroxide formation.

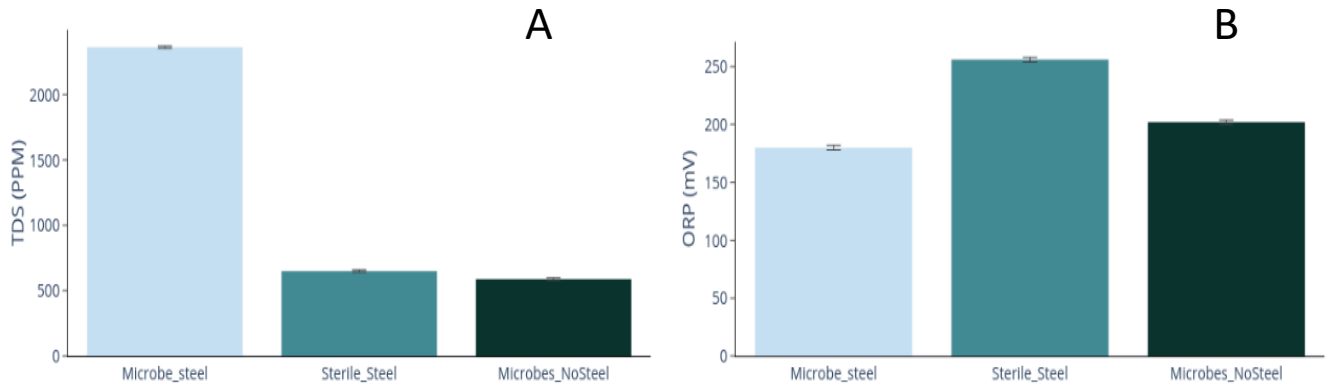

Figure 7.5: Ultrameter measurements of the effluent from test cells included TDS (A), and ORP (B). Error bars show ultrameter accuracy.

VFA analysis of the effluent revealed that the microbial experiment without steel had the highest concentration of all 3 VFAs measured (figure 7.6). The sterile experiment had the lowest concentration, with no butyric acid or formic acid present. It should be noted that the groundwater included in these experiments did have 12 mg/L acetate, which accounts for the presence of acetate in the sterile sample. All 3 VFAs – acetic, butyric and formic acids– were present in the microbial experiment with steel, though at significantly lower concentrations than the experiment without steel.

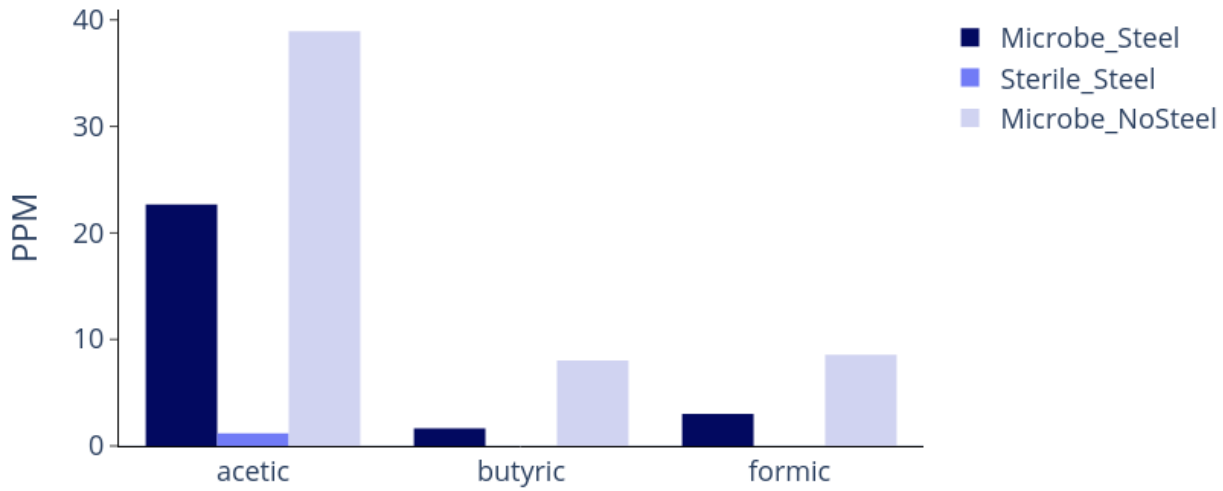

Figure 7.6: VFA analysis of effluent collected at the termination of test cell experiments.

7.2.2 Analysis of corrosion of the steel coupon recovered from test cell experiments

The steel coupon was recovered from each test cell and cleaned. Visible changes were observed (figure 7.7), both between the sterile and microbial experiments and steel that had not been used in the experiment. It was clear that the microbial activity had increased reactions at the steel surface and resulted in a black colouration, whereas the steel recovered from the sterile experiment appeared dull orange in colour.

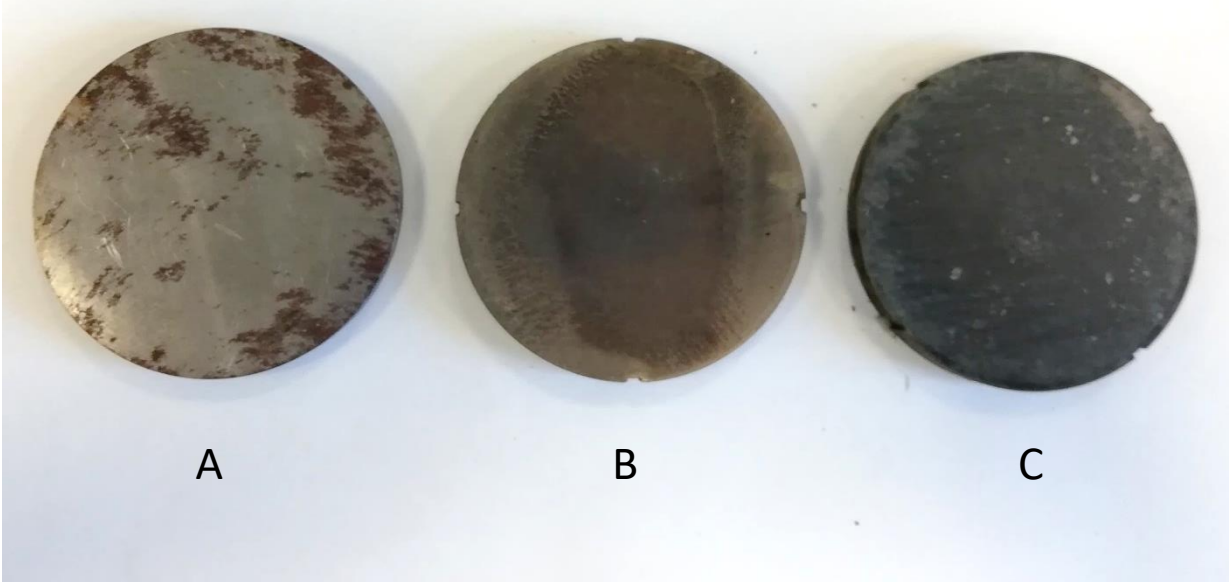

Figure 7.7: Steel coupons recovered from test cells appeared visually different. The steel before the experiment (A) was largely shiny, the steel in the sterile experiment (B) was dull and orange in colour, and the steel recovered from the microbial experiment (C), was black in colour with some green spots.

Further to this, corrosion layers formed (see section 7.1) that also differed depending on microbial presence. The depth of these layers was measured (figure 7.8) and the results suggest that corrosion products diffused further into the clay when microbes were present, and therefore, there may have been more corrosion. There was a greater diffusion of orange corrosion product into the clay in the sterile experiment than in the microbial experiment which may indicate that the orange forms before the green corrosion product.

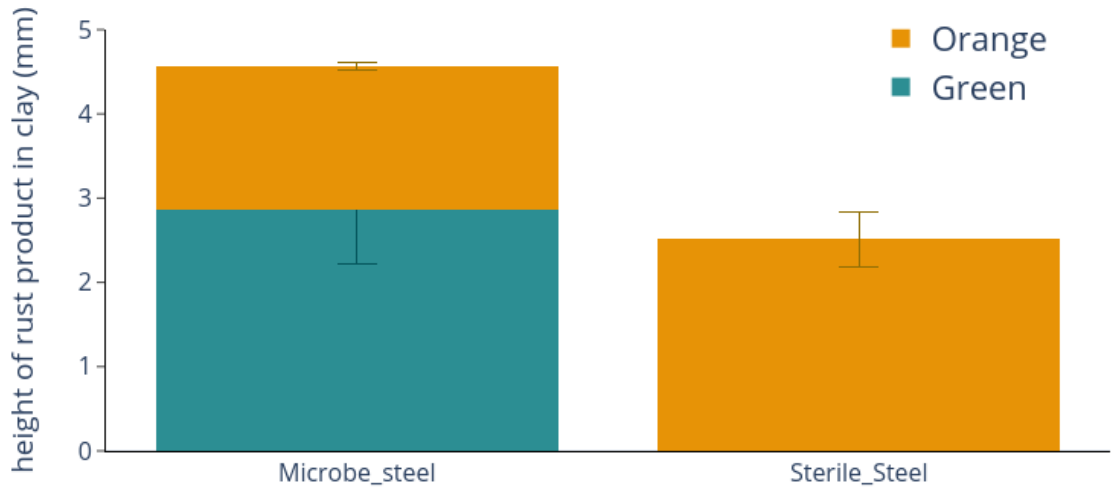

Figure 7.8: Height of rust products diffusion into the MX80 from the steel surface after test cell experiment (from photographs). Orange refers to the orange rust layer, and green refers to the green metastable Fe(II/III) oxide layer. Error bars show standard error.

7.2.2.1 SEM images of the steel coupon and corrosion layers

SEM images were taken of the steel discs from both the microbial (figure 7.9) and sterile experiments. Figure 7.10 shows evidence of corrosion and micropitting on steel from the sterile experiments. The micropitting in the microbial experiment is much less extensive than that of the sterile experiment, perhaps due to protective films of corrosion products or the microbial activity itself. The orange and green layers did not show any distinct mineralogy and so XRD was the main tool used to identify the iron (hydr)oxides present (figure 7.11).

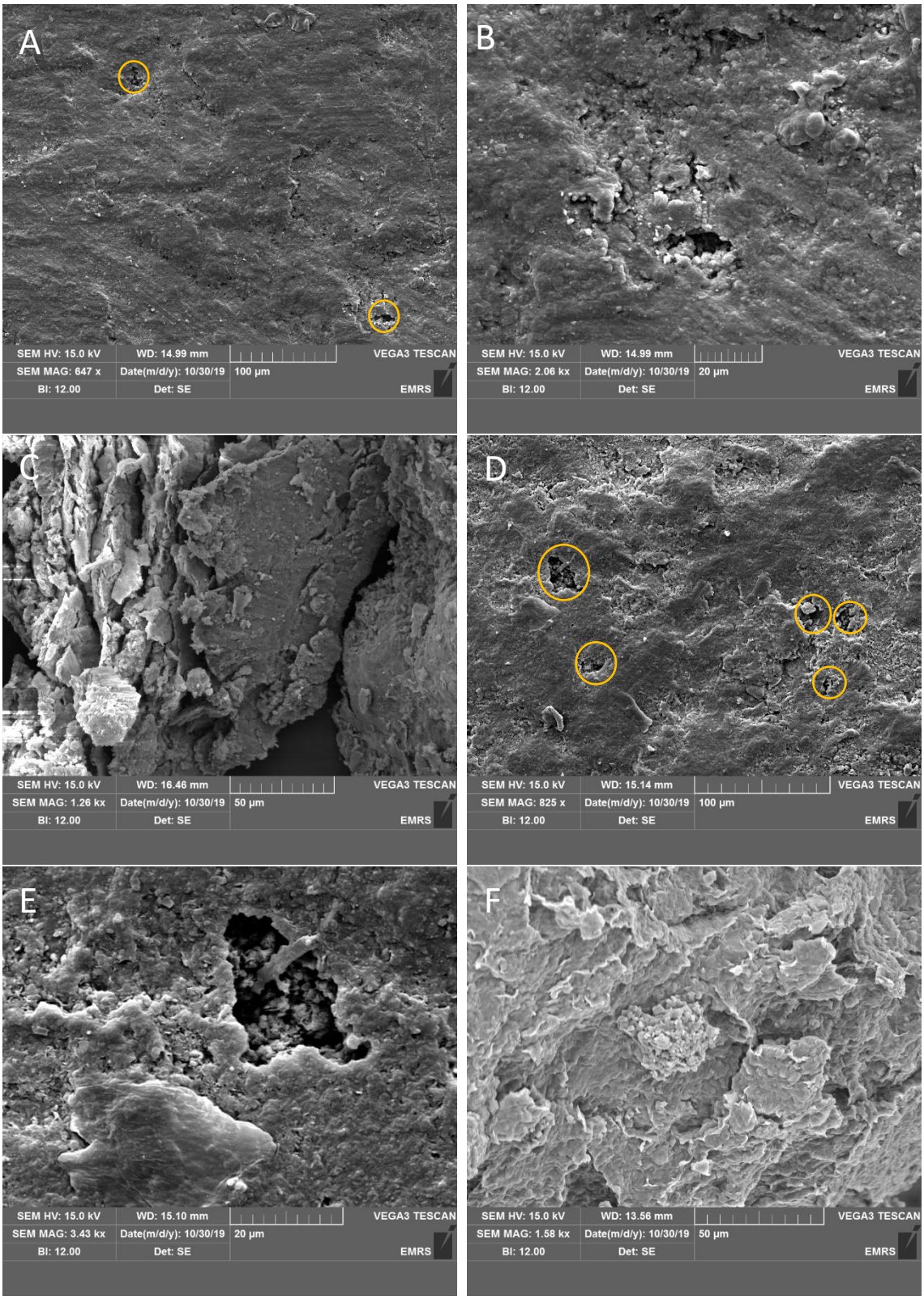

Figure 7.9: SEM images of steel disc recovered from test cells with microbes. Steel from the outer edge of the steel disc (surface is the clay/steel interface) (A, B) shows limited pitting.

Images of green rust (C) did not show any obvious mineral formations, but layers and some debris were observed. Pitting was observed in steel from the centre of the steel disc (surface is the clay/steel interface) (D, E). No notable structures were observed on the orange rust (F). Yellow circles highlight micropits.

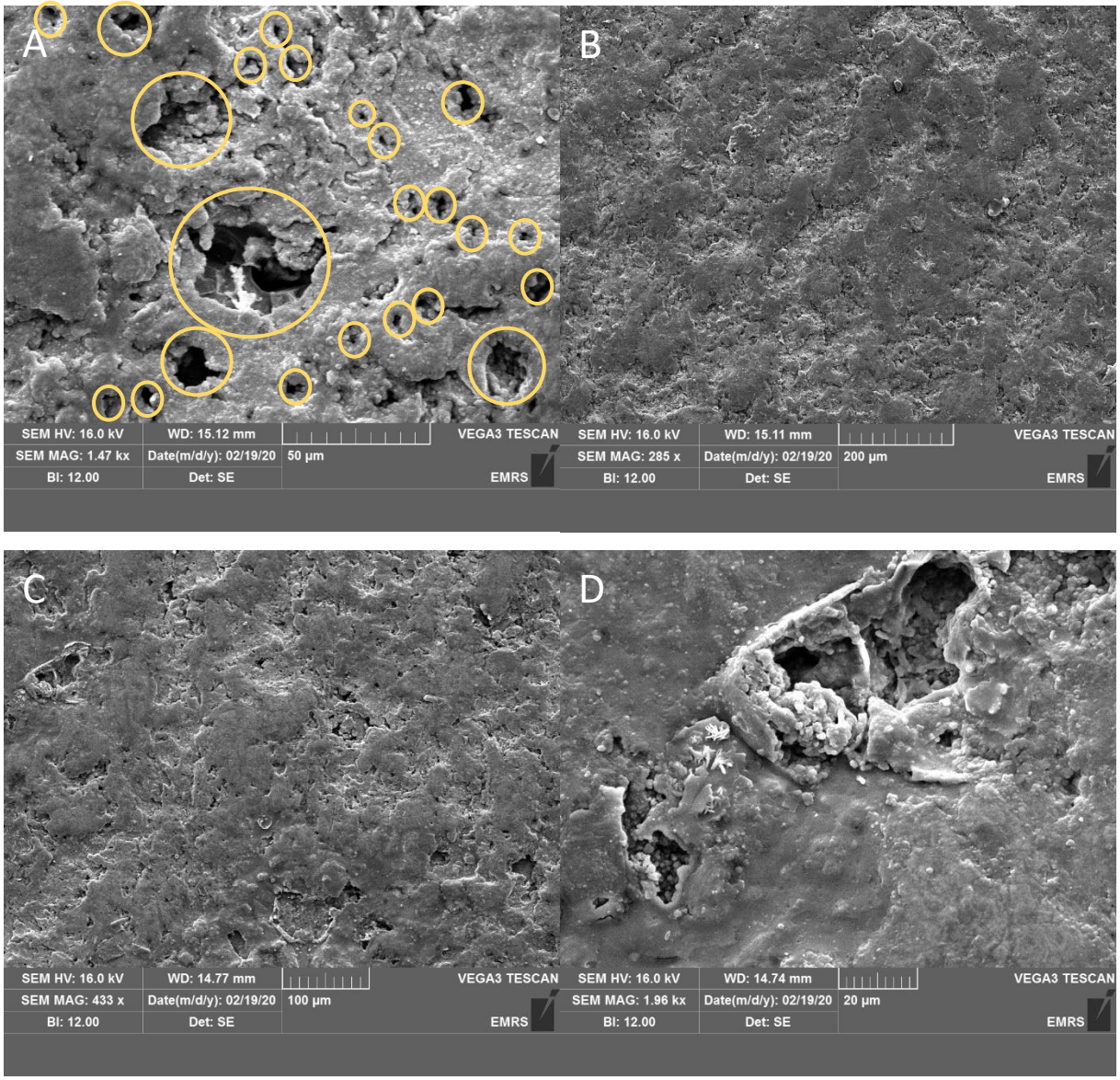

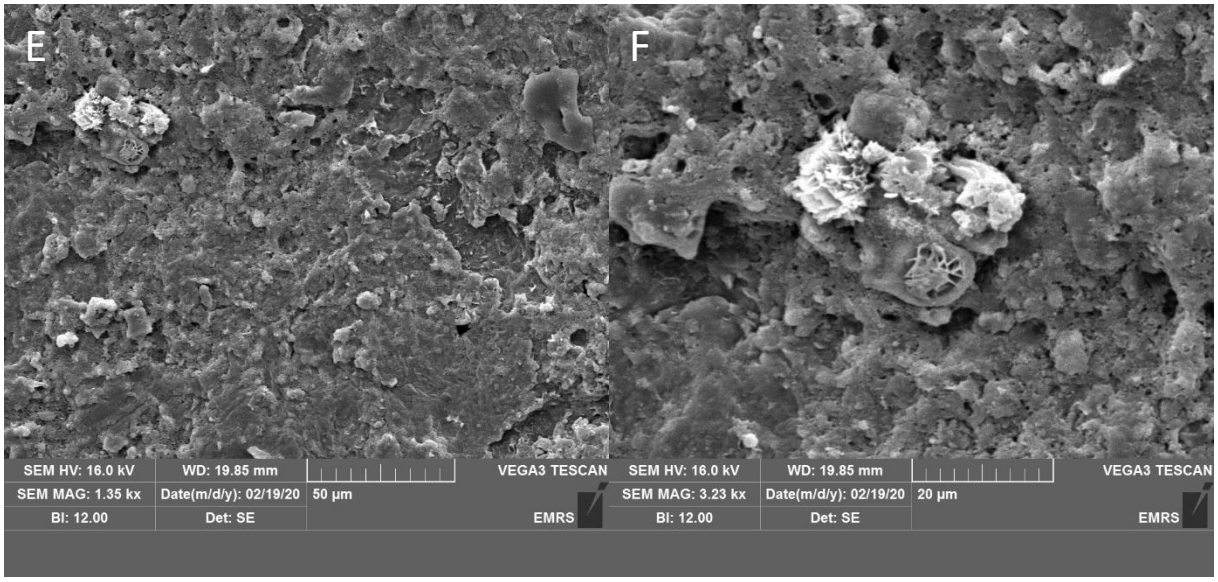

Figure 7.10: SEM images of steel recovered from sterile test cell experiments. The outer edge of the steel had some evidence of micropitting (A. B) – yellow circles indicate pitting. The inner area of the steel had more extensive pitting (C, D), and the orange rust did not indicate any mineralogical structures (E, F).

7.2.2.2 XRD analysis of the corrosion layers

XRD analysis of the green layer observed in the Microbe_Steel experiments contained iron (II) sulfate, which does appear green in colour, and iron (III) sulfate (figure 7.11A). Calcite was also present in the green corrosion layer, but was absent in the orange layer. The orange layer which was observed in both the Microbe_Steel and Sterile_Steel experiment was found to contain iron (III) sulfate which is orange in colour as well as a small percentage of magnetite (< 1%). This result was consistent across replicates and between the sterile and microbial experiments (data not shown). Both the orange and green layers contained clay minerals in addition to corrosion products.

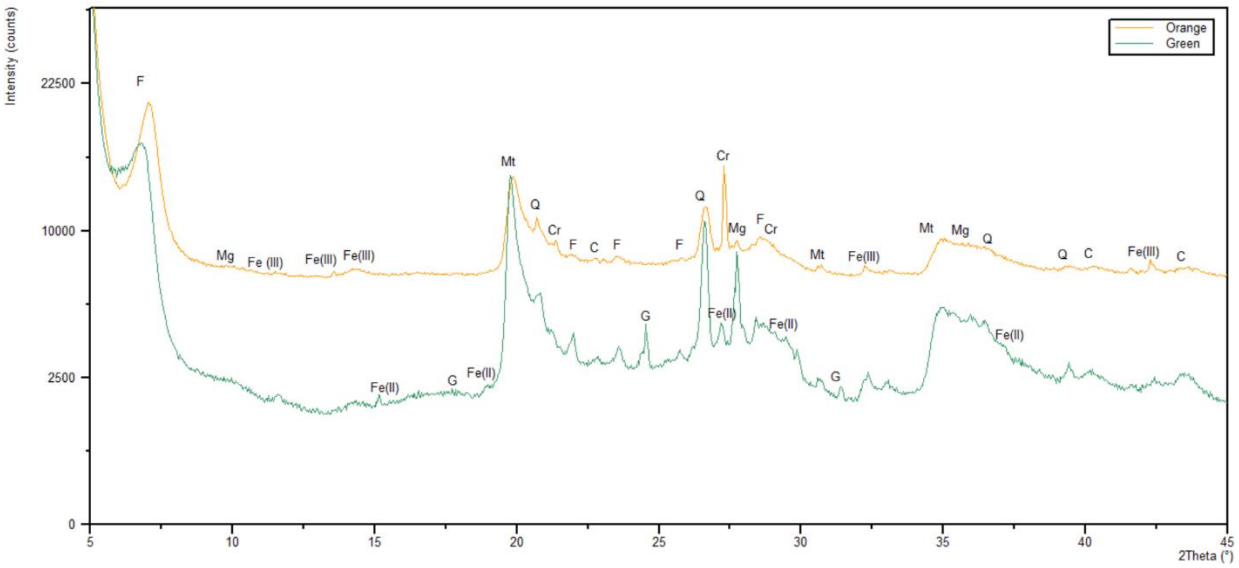

C	**Cr**	**F**	**Fe(II)**	**Fe(III)**
Calcite	Cristobalite	Feldspar	Iron (II) sulfate	Iron (III) sulfate
G	**Mg**	**Mt**	**Q**	
Goethite	Magnetite	Montmorillonite	Quartz	

Figure 7.11: XRD analysis of corrosion products from test cell experiments

7.2.3 Analysis of changes to clay mineralogy and geomechanics

7.2.3.1 pH of the clay surface

The pH of the clay surface (figure 7.12) at the top of the test cell, furthest from the steel and the point at which groundwater enters, was neutral in the sterile experiment. In the microbial experiment, this area was more acidic. This area is also the point of inoculation and so there may have been a higher concentration of microbes here compared to throughout the MX80 bentonite. The acidic pH could therefore be explained by microbial VFA production. The experiment without steel had a more variable pH between replicates. [Due to the UK National Lockdown in March 2020 and Covid-19 restrictions and the resulting restricted lab access, the pH of the clay surface was not measured immediately at the termination of the experiment, but after 3 months in storage at 4°C. During this time, microbes may have consumed VFAs, or died, contributing to pH changes].

The pH at the clay/steel interface, or the bottom of the test cell, was alkaline when steel was present. The microbial experiment with steel had the highest pH at 9.41, however, the sterile experiment had a similar pH at 9.14. The microbial experiment which excluded steel had a significantly lower pH (6.93), with a p-value of 0.0183 when compared to the microbial experiment with steel. There were no other significant changes in pH. Therefore, these results suggest that the pH on this surface is controlled by corrosion processes which use up H^+ (see section 5.3.3), rather than microbial activity.

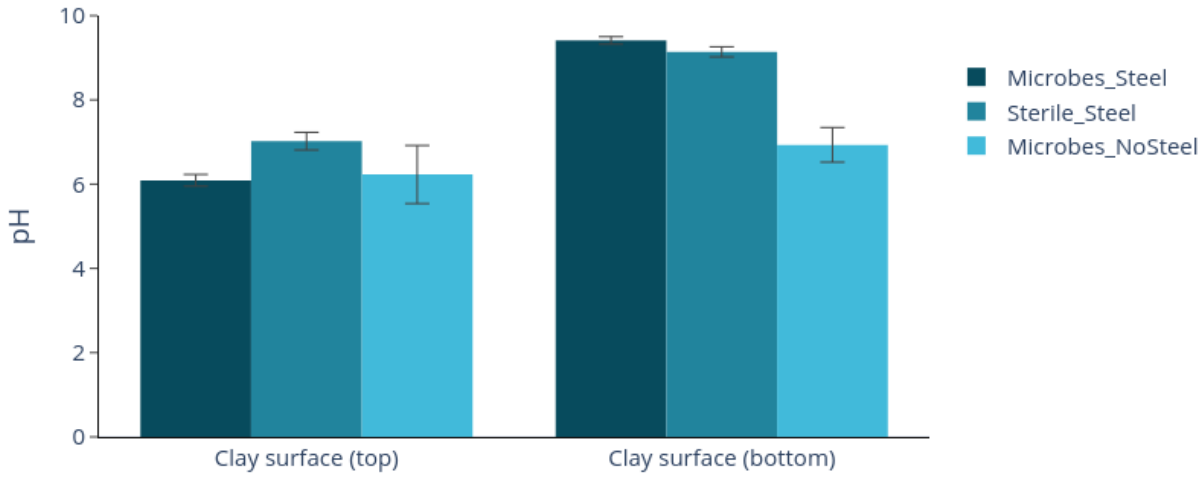

Figure 7.12: pH of the MX80 recovered from test cells at each surface. Error bars show standard error.

7.2.3.2 Plasticity index of MX80 bentonite recovered from test cell experiments

The PI of the MX80 bentonite changed significantly between treatments. In an effort to ensure the effects of the rust entering the clay did not affect the PI test, only bentonite from the top half of the test cell was used. When microbes and steel were present, the LL was lower and PL was higher, resulting a in a significantly lower PI (figure 7.13), compared to the sterile experiment ($P < 0.001$). When steel was excluded, there was also a decrease in PI compared to the sterile control, but the PI remained greater than the microbial steel experiment. The difference between

the microbial experiments with and without steel was also significant ($P < 0.001$), this difference was caused by both an increase in LL and decrease in PL. The PI results from microbial experiments, although lower, still indicate a highly plastic clay. There was a slight decrease in PI in the Sterile_Steel compared to the "as received" clay (see chapter 6), although this difference was not significant.

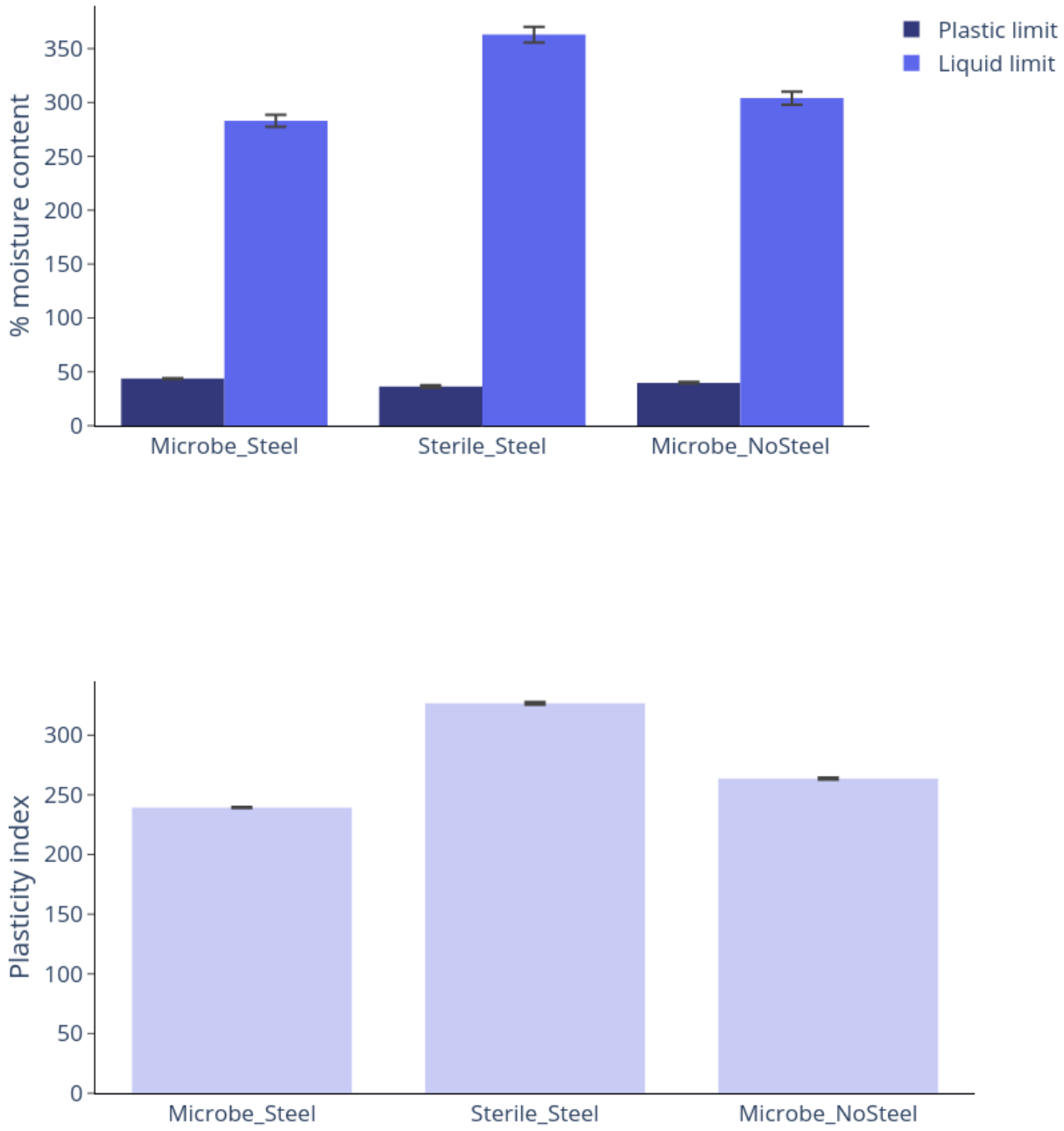

Figure 7.13: The liquid limit and plastic limit of MX80 bentonite recovered from test cells (top) revealed that both microbes and steel increase PL and decrease LL. The resulting PI (bottom) reflect this. Error bars show standard error.

7.2.3.3 SEM images of MX80 bentonite recovered from test cell experiments

SEM images of the clay do not show any notable distinctions between the sterile and microbial, steel and no steel experiments (figure 7.14 – 16). The Microbe_NoSteel experiments did, however, have some structures at the cracks in the clay (figure 7.15D), which may be the remains of biofilms – the corresponding EDX data defined this structure as 25% carbon, 28% silicon, 47% other including oxygen, calcium and sodium. Unlike the samples without steel, there are no indications of microbial biofilm formation in the MX80 bentonite recovered from test cells with steel. It is possible that these biofilms formed during the UK National Lockdown when the Microbe_NoSteel test cells were in storage (at 5°C for 3 months) rather than during the test cell experiment.

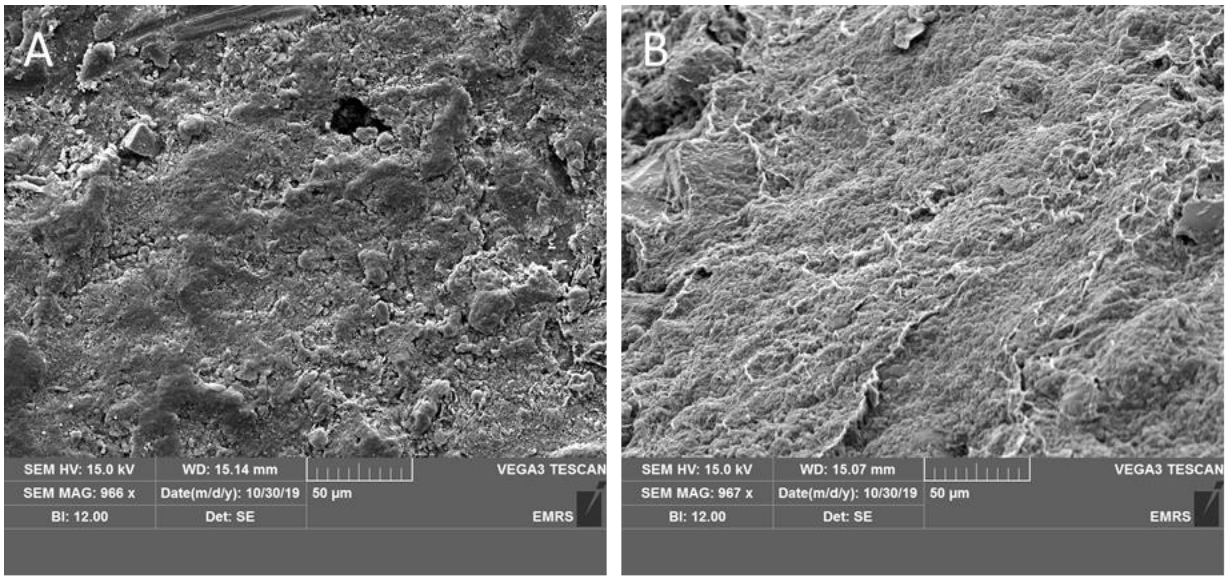

Figure 7.14: SEM images of MX80 bentonite recovered from Microbe_Steel test cells, both MX80 from the top of the test cell (A), and the bottom (B) are shown.

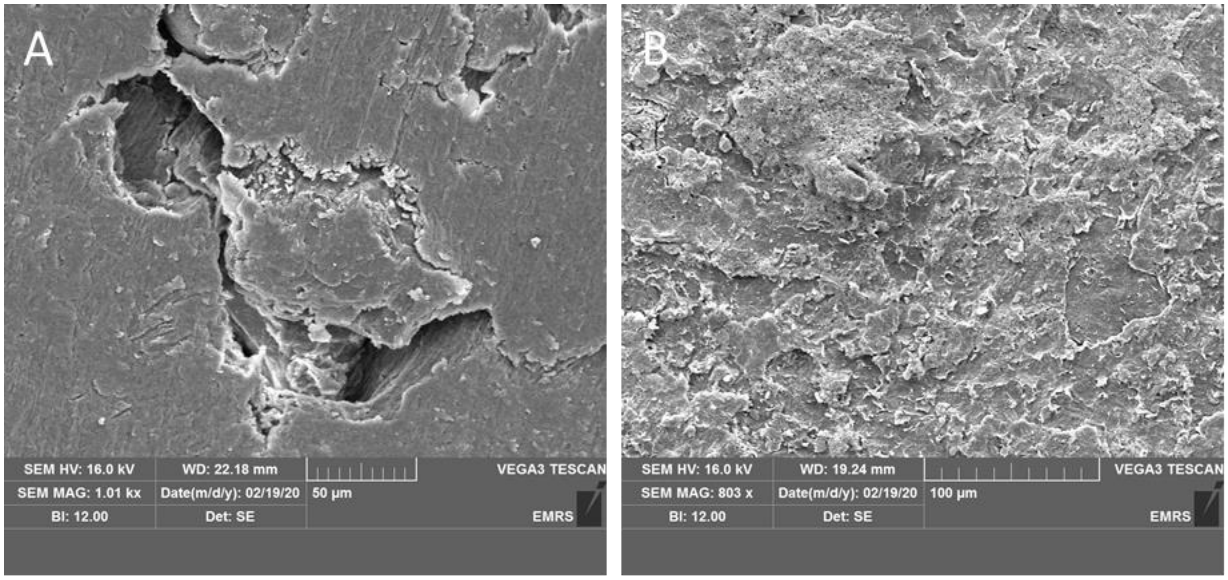

Figure 7.15: SEM images of MX80 bentonite recovered from Sterile_Steel test cells, both MX80 from the top of the test cell (A), and the bottom (B) are shown.

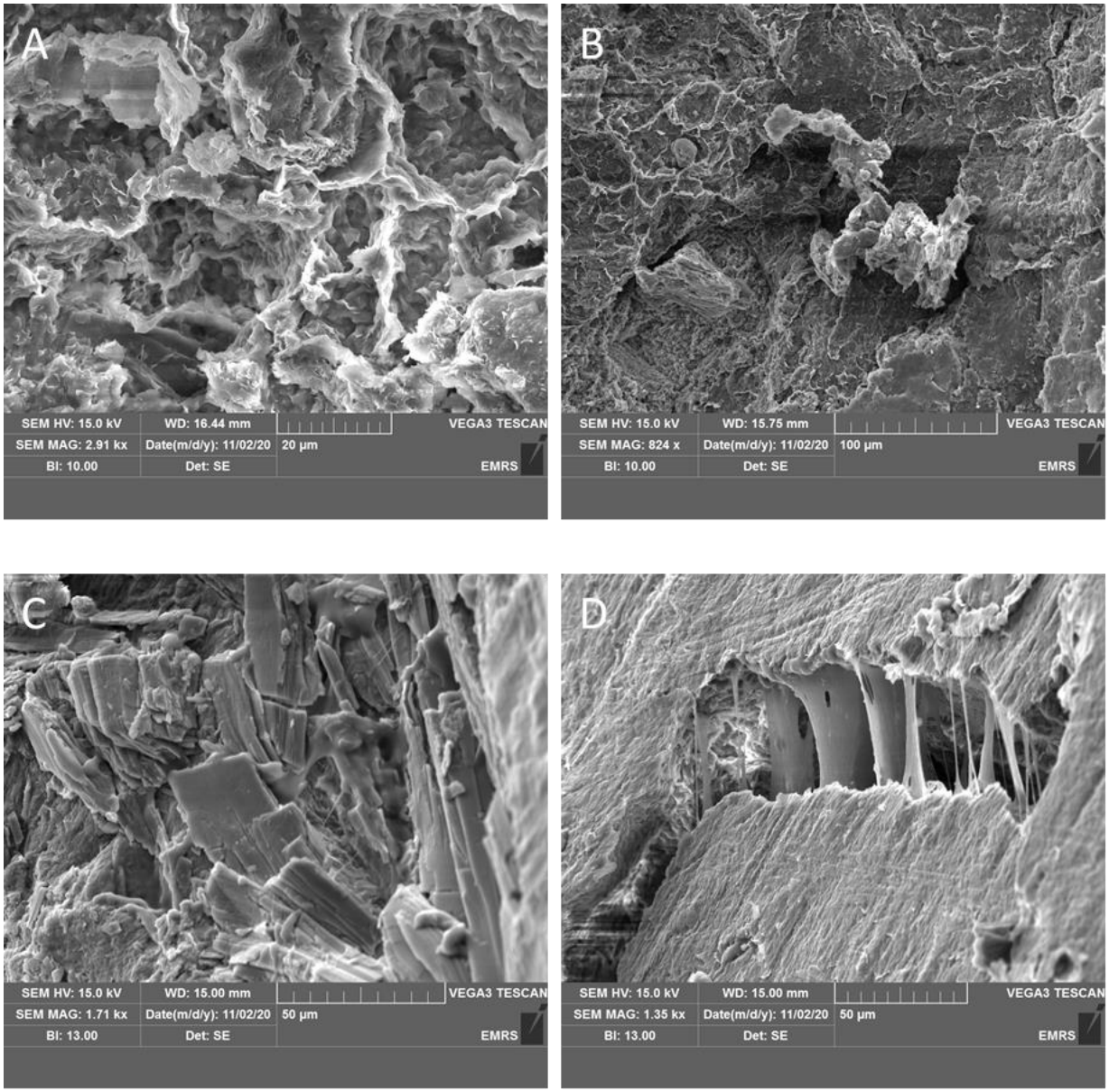

Figure 7.16: SEM images of clay recovered from Microbe_NoSteel test cells. No distinct or significantly abundant minerals were observed in samples taken from the bottom of the test cell (A, B). Samples taken from top of the test cell (C, D) show some mineralization or biofilm formation.

7.2.3.4 XRD analysis of MX80 bentonite recovered from test cell experiments

XRD analysis of MX80 bentonite recovered from the top of the test cells from the Microbe_Steel and Sterile_Steel experiments is shown in figure 7.17. Samples from the bottom are presented in

section 7.2.2.2. The XRD analysis of MX80 bentonite recovered from the top of the test cells with microbes and steel contained several iron products – magnetite, goethite and ferrihydrite – as well as the clay minerals quartz, montmorillonite and muscovite. Whilst quartz and montmorillonite were expected it is possible that this pattern is in fact illite, not muscovite, as the patterns are similar and commonly confused (Verdel et al., 2011). There is one unassigned peak around 10 2θ, which would indicate illite rather than muscovite.

The XRD analysis of the top of the clay from the sterile experiment did have some similarities to the microbial experiment: goethite and ferrihydrite were present in both. Another similarity was the presence of montmorillonite and quartz in both samples. However, muscovite, illite and magnetite did not appear in the sterile experiment (figure 7.17). As previously discussed in chapter 5 and chapter 6, illitisation is a concern as it would negatively change the ability of the MX80 bentonite to act as a barrier. These results suggest that illitisation is occurring when microbes are present.

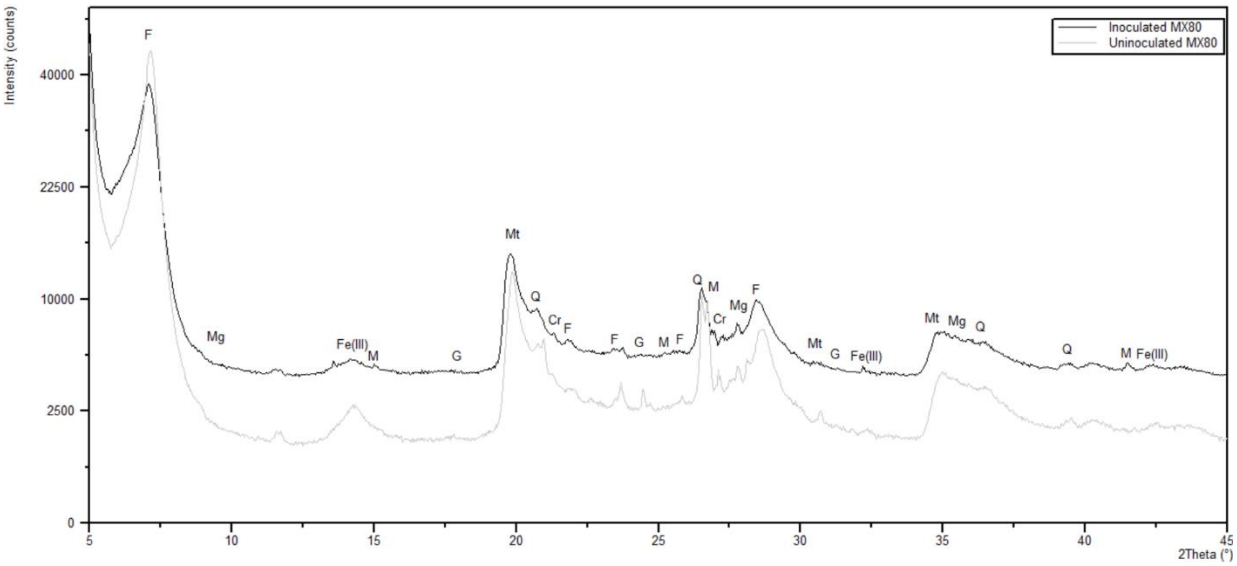

Cr	**F**	**Fe(III)**	**G**
Cristobalite	Feldspar	Iron (III) sulfate	Goethite
M	**Mg**	**Mt**	**Q**
Muscovite	Magnetite	Montmorillonite	Quartz

Figure 7.17: XRD analysis of the top of MX80 recovered from test cells including steel.

XRD analysis of MX80 bentonite recovered from test cells (figure 7.18) showed calcite precipitation in Microbe_NoSteel experiments. For consistency and to observe whether the water gradient caused any changes to the homogeny of the clay, samples were taken from the top and bottom of the test cell. Calcite was only present at the top of the cell. The bottom of these experimental samples did not contain calcite, but they did match muscovite. As mentioned previously, it is likely that muscovite is in fact illite (Verdel et al., 2011).

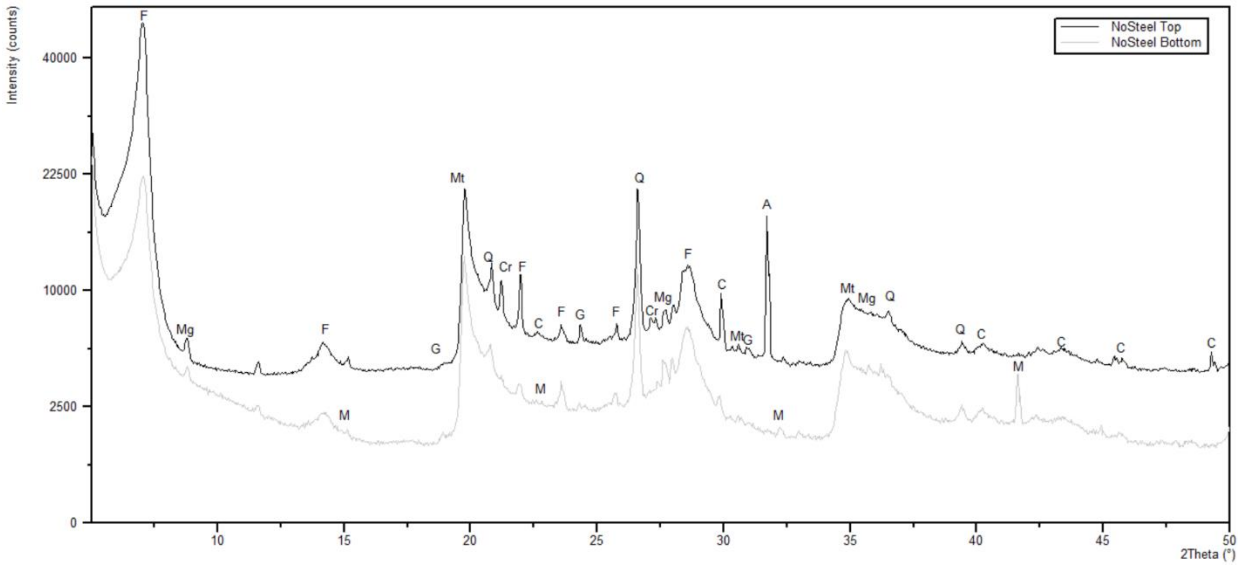

A	**C**	**Cr**	**F**
Albite	Calcite	Cristobalite	Feldspar
G	**M**	**Mt**	**Q**
Goethite	Muscovite	Montmorillonite	Quartz

Figure 7.18: XRD analysis of MX80 betonite recovered from Microbe_NoSteel test cells.

7.2.4 Iron-reducing enrichment experiments with MX80 bentonite recovered from test cells

These experiments aimed to determine if the ability of the indigenous microbial community to reduce iron, and if the structure of the community had been impacted by: the addition of steel; the diffusion of the corrosion products into the clay; and the high pressure. At the beginning of these experiments, groundwater was allowed to flow into the test cells at low pressure for 48 hours after inoculation to ensure the clay had fully swelled. This may have washed bacteria

around the test cell. Enrichments were set up after the test cell experiments were dismantled (see section 3.7 and figure 3.2). Due to COVID-19, it should be noted that the iron-reducing enrichments with MX80 bentonite recovered from the microbial experiments without steel were set up after a further 3 months in storage at 4°C.

7.2.4.1 pH of the iron-reducing enrichments

The pH of these experiments differed between experimental set ups (figure 7.19). The sterile experiments had an alkaline pH on day 0, 8.3-8.4, which decreased throughout the experiment to neutral. All inoculated experiments were circumneutral on day 0, and became acidic during the first three weeks of the experiment. This difference in alkalinity on day 0 may indicate that more corrosion took place in the sterile experiments (as reflected in the corrosion results). After this point, the Microbe_Steel experiments recovered to pH ~6.5. The *S. oneidensis* control and the experiments with clay from the Microbe_NoSteel test cells remained below pH 6 for the duration of the experiment. The Microbe_NoSteel had the greatest pH drop, 4.08-4.11 on day 7. The “No MX80” control remained between pH 6.1-7 throughout the experiment.

Both the sterile experiments were significantly different compared to the corresponding pH of the Microbe_Steel experiment, giving p-values of <0.001 for “top” (MX80 recovered from the top of the test cell, furthest from the steel) and “bottom” (MX80 recovered from the bottom of the test cell at the clay / steel interface). Similarly, the Microbe_NoSteel experiments were significantly different from the microbial experiments with steel in both the “top” and “botttom” with p-values <0.001. However, there was no significant difference found between the “top” and “bottom” experiments from the same test cells.

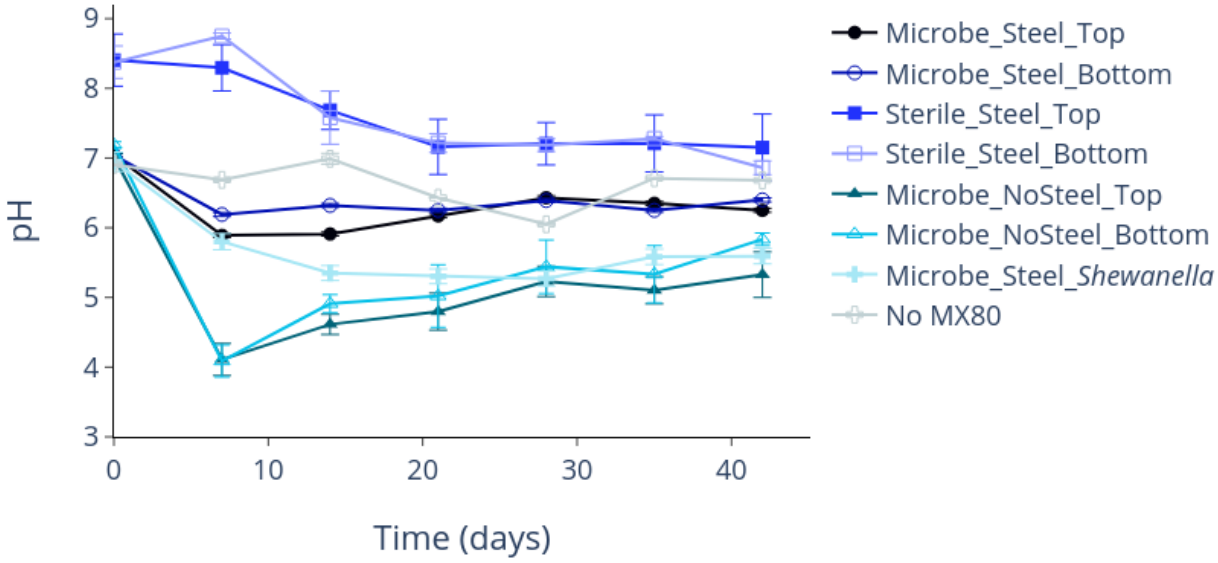

Figure 7.19: pH of the iron-reducing enrichments conducted with clay recovered from test cells. Standard error is shown as error bars.

7.2.4.2 Concentration of iron in slurry subsamples from iron-reducing enrichments

As with previous enrichments, the soluble Fe(II) remained below 0.1 mM throughout the experiment, and so the values are not reported here. The concentration of total Fe(II) was significantly different between experiments (figure 7.20). The first interesting observation is that in all experiments, including Microbes_NoSteel, using clay from the bottom of the test cell – "bottom" (at the clay steel interface) - had higher concentrations of Fe(II) than the experiments with clay taken from the top of the test cell. The p-value for comparison of Microbe_Steel_Top compared to Microbe_Steel_Bottom was significant ($p < 0.001$).

The sterile controls had the lowest concentration of Fe(II) by day 42 (3.1 - 3.5 mM), apart from the "No MX80" control which remained below 0.1 mM throughout the experiment. When the sterile experiments were compared to the corresponding Microbe_Steel experiment, the results were significant in both the "top" ($p < 0.001$) and "bottom" ($p < 0.001$) experiments. The microbial experiments all had high concentrations of Fe(II), up to 12.4 mM, however, only the "top" experiment was significantly different compared to the corresponding NoMicrobe_Steel

experiment ($p < 0.001$). The experiment containing *S. oneidensis*, had the lowest concentration of the unsterilised experiments at 7.46 mM on day 42.

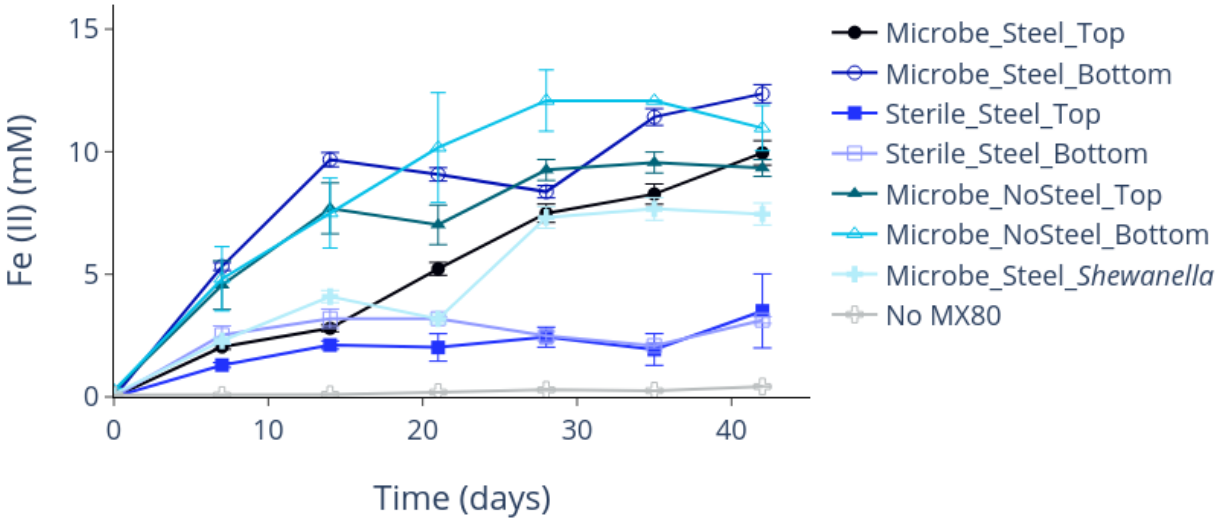

Figure 7.20: Fe(II) concentration of iron-reducing enrichments. Error bars show standard error

7.2.4.3 VFA concentrations in the iron-reducing enrichments

The concentration of acetic, butyric and formic acids changed throughout the duration of the enrichments (figure 7.21). The most significant changes were observed in concentration of acetic acid (acetate) which increased in all unsterilised samples from the organic matter provided (see section 3.7.2). The microbial experiments without steel and the *S. oneidensis* control increased the most (>410 PPM). This concentration was significantly higher than the microbial experiment with steel, with p-values of 0.000112 for "bottom" and 0.000476 for "top". The Microbe_Steel experiment reached acetic acid concentrations of 214 PPM (Top) and 167 PPM (bottom), which, whilst not the highest concentrations, were significantly higher than the sterile experiment, with P-values of <0.0001. The sterile samples remained low, averaging ~ 40 PPM. The concentration of acetic acid was also low in the "No MX80" enrichment, equivalent to the concentration of acetate added to the groundwater.

The concentration of butyric acid was somewhat like that of acetic acid, with the *S. oneidensis* and microbial experiment without steel having the highest concentrations. The *S. oneidensis*

control has the highest concentration (246 PPM), while the enrichments using MX80 bentonite from Microbe_NoSteel reached concentrations of 120-140 PPM by day 42 having previously spiked to 115-170 on day 14. This concentration was significantly higher than the microbial experiment with steel, in both the "bottom" ($P < 0.001$) and "top" ($P < 0.001$) experiments. Both the sterile experiments and the microbial experiment with steel remained low throughout this experiment, with no significant comparison.

The concentration of formic acid was also low throughout the duration of the experiment. Noting the initial spike in concentration in some samples of day 7, by day 14 all experimental samples and the *S. oneidensis* control had concentrations below <10 PPM. There were no significant differences. The "No MX80" control had a constant concentration of formic acid of ~45 PPM.

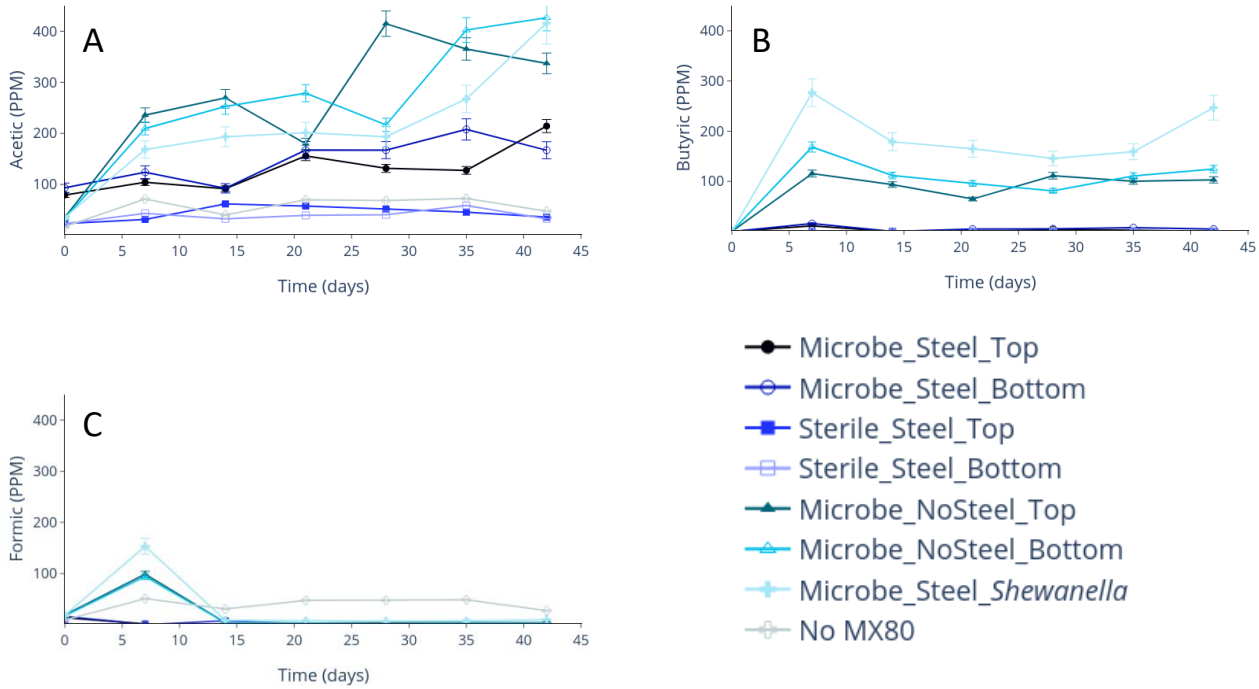

Figure 7.21: VFA concentrations of iron reducing enrichments with MX80 bentonite recovered from test cells. Acetic acid increased in all unsterilised experiments (A); whereas formic acid only increased in the positive control with S. oneidensis *and the microbial experiment without steel (B). Formic acid concentrations remained low throughout the experiment and were highest in the "No MX80" control (C). Error bars show standard error.*

7.2.5 Microbial communities of MX80 bentonite after incubation in test cell and enrichment

Microbial communities were sampled from the clay in three ways: prior to enrichment (after opening test cells) without nested PCR; prior to enrichment with nested PCR; and, enriched. As can be seen in figure 7.22 the unenriched samples without nested PCR vary greatly between samples. There was also very low yield in these samples (250-300 sequences) and therefore, only nested and enriched samples will be presented and discussed further below.

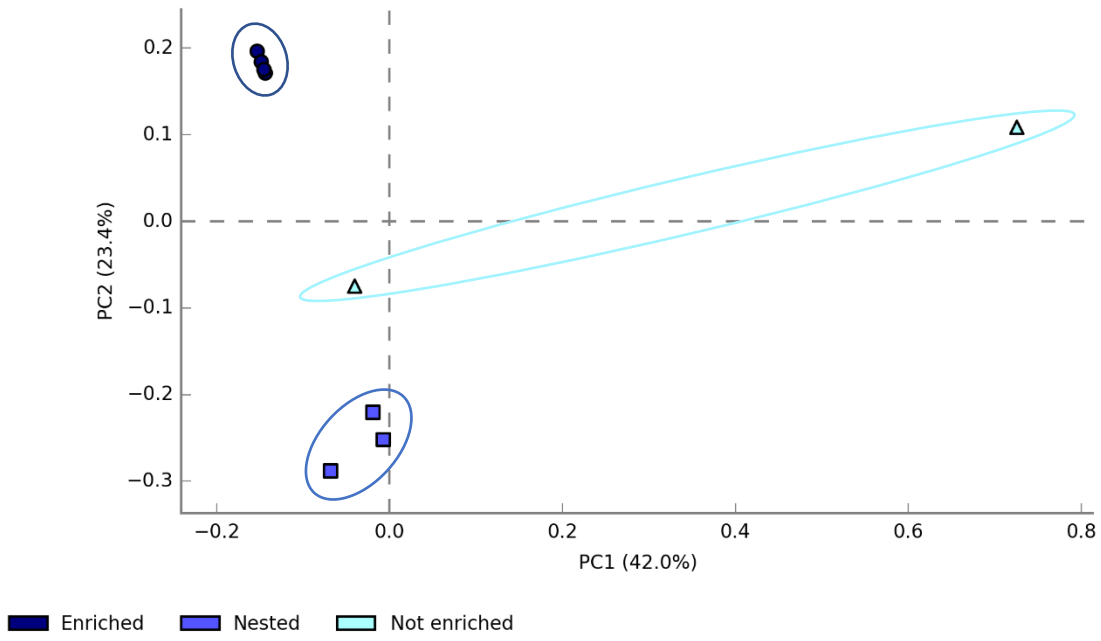

Figure 7.22: PCA plots of microbial communities from Microbes_Steel_Top. Distinct groups for enriched and nested samples when all samples are included

Twelve 16S rRNA libraries were derived from sequencing outputs from the Microbe_Steel experiments (3 for each top and bottom, nested and enriched). The sequencing yielded average reads of 20,175 ±1,847 for nested PCR samples taken from the top, 14,008 ±4,352 for nested PCR samples taken from the bottom, 31,594 ±3,267 from enrichments using clay from the top of the test cell, and 61,668 ±9,987 for enrichments using clay from the bottom of the test cell; with an average read length of 227 bp across all libraries. From this, an average of 26 (nested, top), 30

(nested, bottom), 141 (enriched, top) and 197 (enriched, bottom) ASVs were identified from the QIIME2 pipeline.

7.2.5.1 Microbial community of MX80 bentonite from the top and bottom of test cells before enrichment

The microbial community was characterised using nested PCR. *Actinobacteria, Gammaproteobacteria,* and *Alphaproteobacteria* are most abundant in the nested samples from Microbe_Steel_Top and Bottom (figure 7.23).

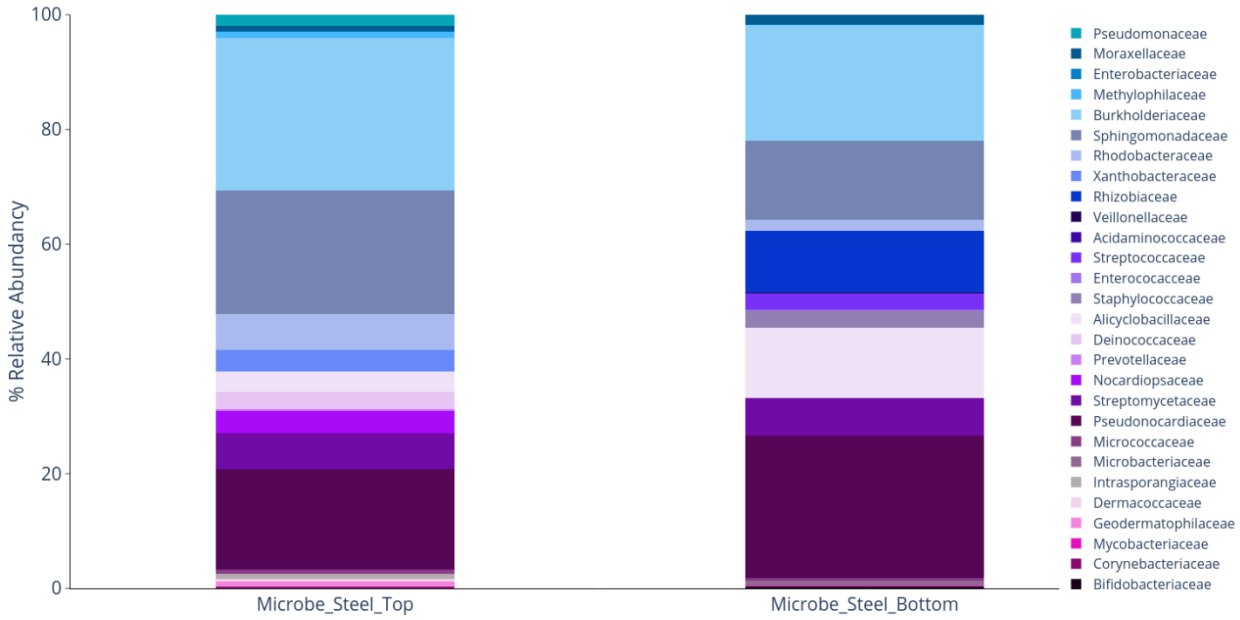

Figure 7.23: Barplots displaying the microbial communities of MX80 recovered from test cells using nested PCR. Families are shown as mean relative abundance across 3 replicates.

Blast did not return species level until <95% similarity for vast majority of ASVs, so entries with higher % similarity were chosen where possible (possibly only to genus level). The nested product of MX80 bentonite furthest from the clay/steel interface (figure 7.24) prior to enrichment produced sequences which matched to aerobic and facultatively anaerobic bacteria. No obviously iron-interacting bacteria were identified. However, sequences of the nested product of Microbe_Steel_Bottom prior to enrichment (figure 7.25) matched to known iron-oxidisers including *Acidovorax* and *Curvibacter* (Byrne-Bailey et al., 2010; Gülay et al., 2018) as well as some

possible IRBs or SRBs such as *Aquimicrobium* (Bambauer et al., 1998). Some species which are known to possess iron siderophores are also present in these nested samples. There is a limited number which produce spores or hyphae.

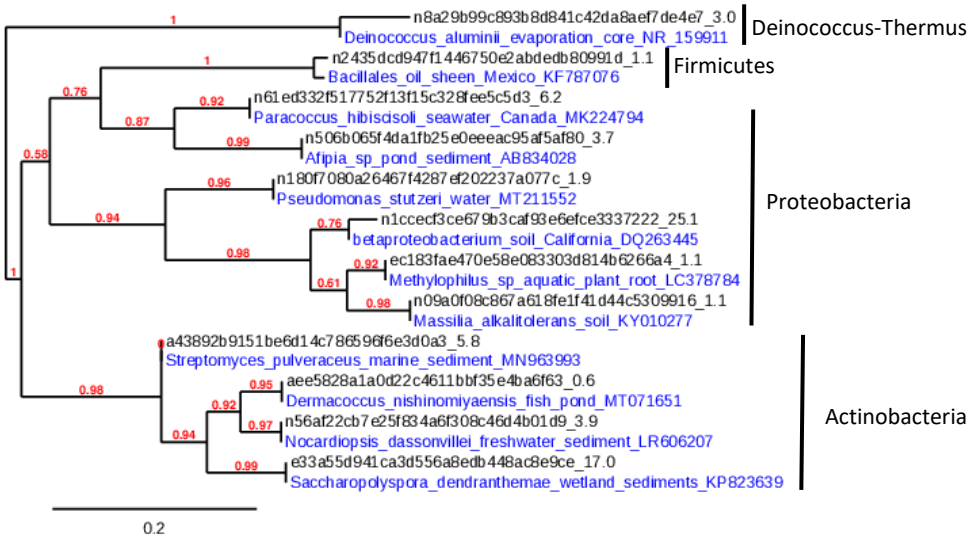

Figure 7.24: Phylogenic tree of sequences generated from 16S rRNA sequencing of the nested product of DNA extraction from Microbe_Steel_Top. Bootstrap value are included on branches and % relative abundance of ASVs is presented at the end of each leaf.

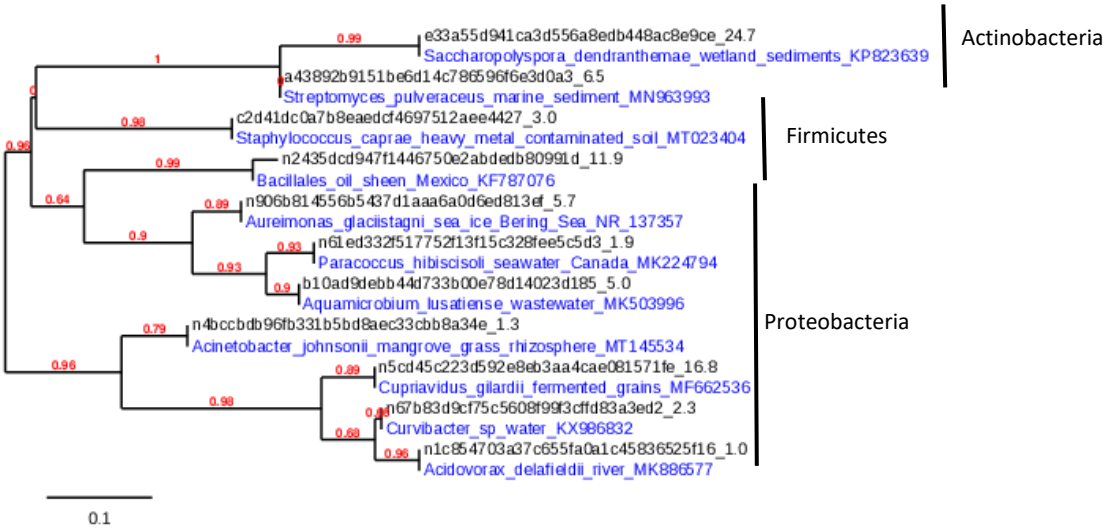

Figure 7.25: Phylogenic tree of sequences generated from 16S rRNA sequencing of the nested product of DNA extraction from Microbe_Steel_Bottom. Bootstrap value are included on branches and % relative abundance of ASVs is presented at the end of each leaf.

7.2.5.2 Microbial community of iron-reducing enrichments using MX80 bentonite from the top and bottom of test cells

Barplots from iron-reducing enrichments (figure 7.26) show that both Microbe_Steel_Top and Bottom are mostly comprised of *Clostridium* species, whereas in previous enrichments presented in this thesis, this has been mainly *Bacillus sp*..

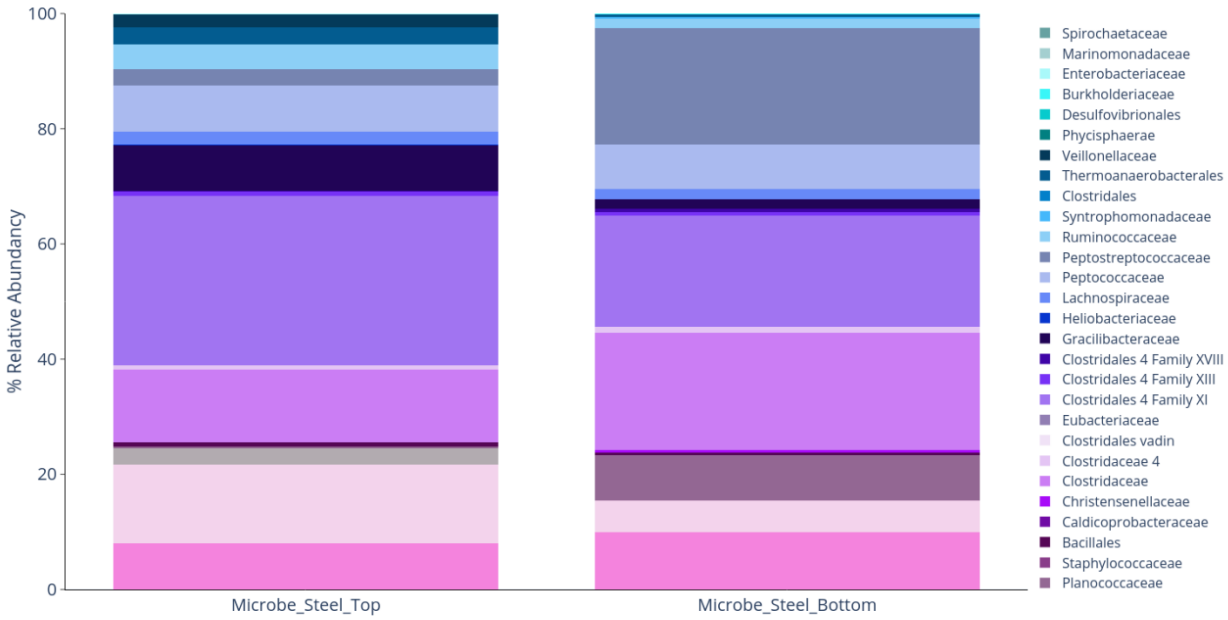

Figure 7.26: Barplots displaying the microbial communities of MX80 recovered from test cells following iron-reducing enrichments. Families are shown as mean relative abundance from 3 replicates.

Trees were constructed using only the most dominant ASVs. Blast did not return species level until <95% similarity for the vast majority of ASVs, so entries with higher % similarity were chosen where possible (although these may have only been identified to genus level). Sequences identified as being dominant in the Microbe_Steel_Top iron-reducing enrichments (figure 7.27) matched several putative iron-reducing bacteria such as two species of *Desulfosporosinus* (Pester et al., 2012), and *Gracilibacter* (Lee et al., 2006). Sequences from iron-reducing enrichments with Microbe_Steel_Bottom (figure 7.28) also matched iron-reducing bacteria such as

Desulfosporosinus (Pester et al., 2012), and *Gracilibacter* (Lee et al., 2006). There were also more species of *Clostridium sp*. in these samples than in samples from the top of the test cell.

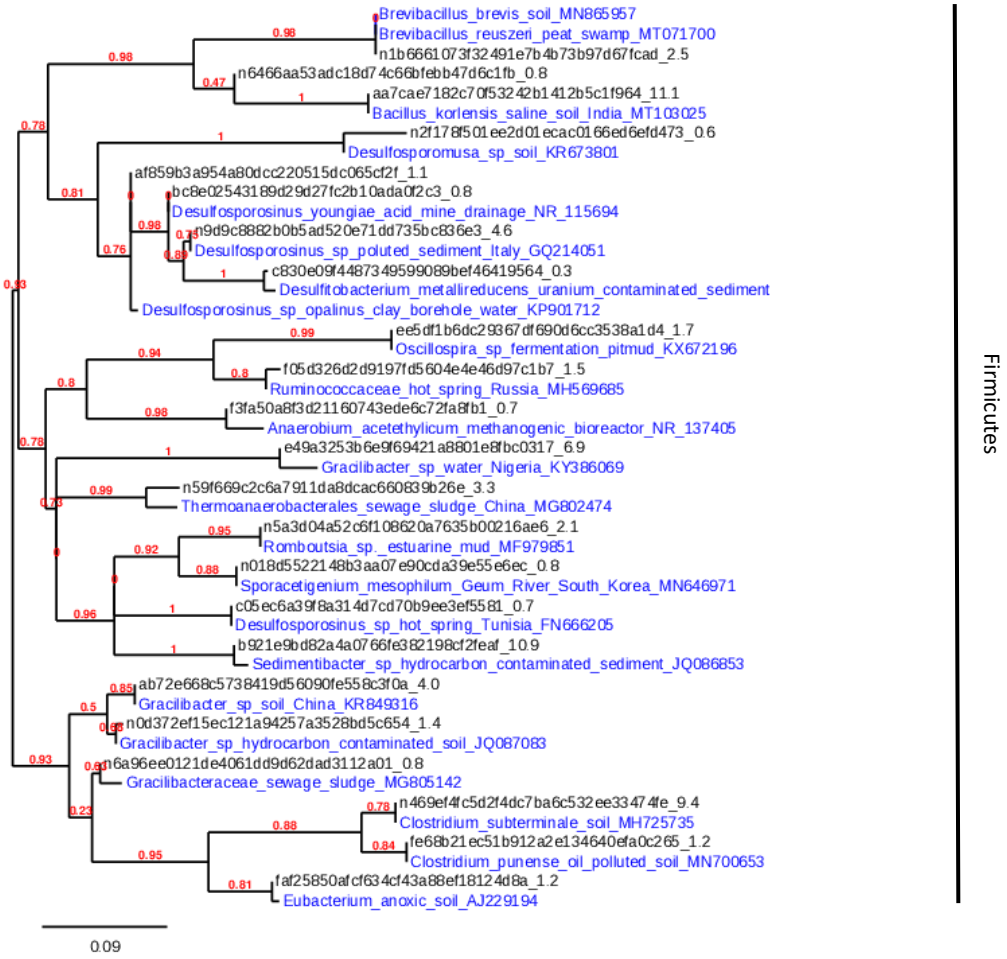

Figure 7.27: Phylogenic tree of sequences generated from 16S rRNA sequencing of iron-reducing enrichments using MX80 recovered from Microbe_Steel_Top. Bootstrap value are included on branches and % relative abundance of ASVs is presented at the end of each leaf.

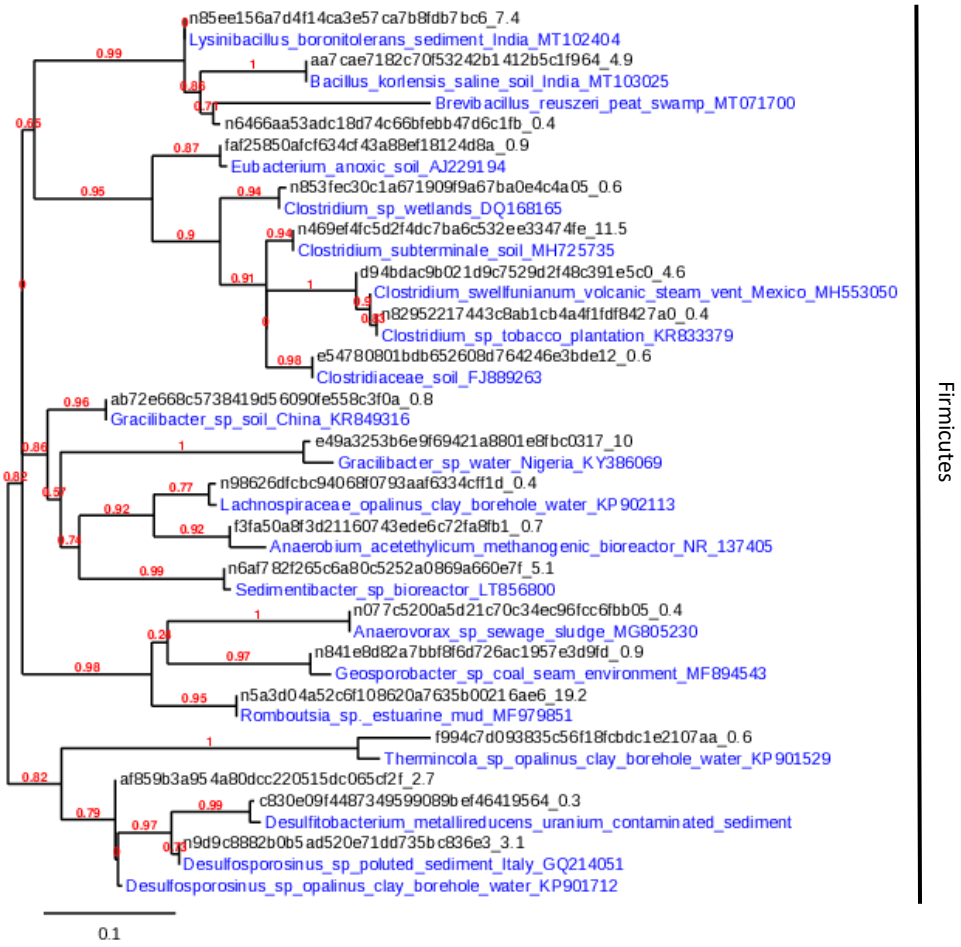

Figure 7.28: Phylogenic tree of sequences generated from 16S rRNA sequencing of Microbes_Steel_Bottom after iron-reducing enrichment. Bootstrap values are included on branches and % relative abundance of ASVs is presented at the end of each leaf.

7.2.5.3 Comparison of enriched and nested microbial communities from test cell experiments

The microbial community from enriched samples from the Microbe_Steel test cells was like previous communities (see section 4.1), whereas the microbial community from non-enriched samples was mainly composed of aerobic bacteria with some facultative anaerobes which may indicate that oxidisation processes are occurring in the test cells (such as aerobic corrosion). There was some species of *Actinobacteria* which produce hyphae and both communities included several thermo- and halotolerant bacteria. There may be some underestimates because BLASTN did not return specific matches for all ASVs. Barplots of individual families or geneses from Microbes_Steel (figure 7.29), show that sequences that were labelled as *Christesenellaceae* (through QIIME2 taxonomic assignment) are present in both nested and enriched samples.

However, the ASV sequence does not match any entries on BLASTN other than “iron-reducing bacterium”.

Desulfosporosinus is an IRB, but it only appears in enriched samples and was significantly more abundant in these samples with a P-value <0.05. This significant abundance in enriched samples was also observed with other IRBs such as *Desulfitobacterium. Anaerosolibacter* is an anaerobic bacterium – as the name suggests. It was found to be significantly more abundant in enriched samples than in unenriched. Similarly, other obligate anaerobes such as *Anaerocolumna, Anaerosporobacter* and *Anaerobacterium* were also significantly more abundant in enriched samples. *Pseudomonas stutzeri* has appeared in all samples previously and although it was present in much higher abundance in non-enriched samples, there was no significant difference. Aerobic bacteria such as *Saccharopolyspora* were also only present in non-enriched samples. They have iron-siderophore action, form spores and produce hyphae (Zhang et al., 2008) so could be good candidates for surviving in the repository.

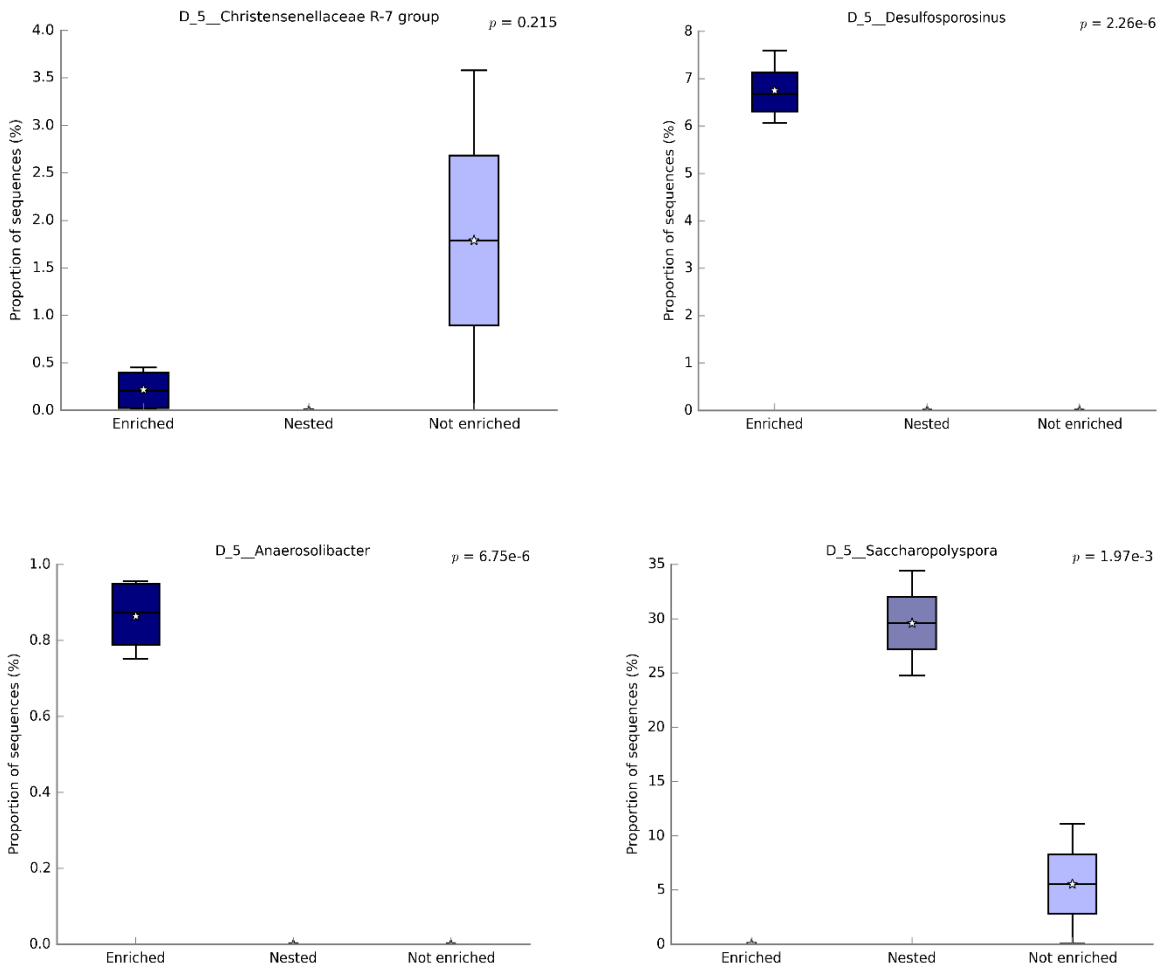

Figure 7.29: Boxplots of % relative abundance of individual species or genera from the Microbe_Steel test cells combining the top and bottom communities. Blast cannot identify Christensenellaceae *to species level, matches to "iron-reducing bacterium".*

7.3 Discussion and conclusions

7.3.1 Microbially influenced corrosion products may produce a protective layer on the steel surface

Interestingly, the SEM images of the steel recovered from these experiments show that micropitting on steel is more evident when microbes are absent. It is unlikely that MIC is causing a more even corrosion without the addition of pitting (Videla & Herrera, 2005; Miller et al., 2018), therefore, this result indicates that less corrosion has occurred when microbes were present.

The explanation for this is likely due to green rust (GR) formation as seen in figure 7.1 and the XRD data presented in figure 7.11. GRs are Fe(II/III) layered double hydroxysalts hydroxides, the presence of both Fe(II) sulfate and Fe(III) sulfate in the XRD spectrum does suggest that the green layer is a mixed oxide layer. However, due to the nature of GRs, and the limitation of XRD discussed previously, an exact mineral match was not possible. The crystallographic structure of GRs consists of positively charged trioctahedral metal sheets alternating with negatively charged hydrated interlayers of anions (Zegeye et al., 2007). GR contains 2x more Fe(II) than magnetite and is much less dense, allowing it to form much quicker in aqueous solution (Usman et al., 2012), although magnetite is more thermodynamically stable. Additionally, the presence of phosphates, silicic acid, or quartz particles promote formation of GR over magnetite (Zegeye et al., 2010; Zegeye et al., 2012; Jorand et al., 2011) –quartz and silica were likely present in the test cells and so favoured formation of GR. Although this corrosion material did diffuse further into the clay than the corrosion products from the sterile experiment, this is not a measure of the quantity of corrosion as the density of the corrosion product cannot be measured.

The protection afforded by GR formation is well documented (Zegeye et al., 2014; Boin et al., 2000; Abdikheibari et al., 2015), particularly biogenic GRs which are less reactive due to a lower surface:volume ratio owing to biofilm formation and EPS production (Zegeye et al., 2014; Volkman et al., 2000; Zegeye et al., 2010). According to the XRD analysis there was iron (II) sulfate (which is green/blue) present in the green layer and iron (III) sulfate in the green and orange layer which is yellow. In these experiments, sulfate is present in the groundwater and as gypsum in MX80 bentonite. Further analysis would be useful to identify exactly which minerals are formed such as a combination of the analytical data already collected with Mössbauer, electron probe microanalysis and Raman spectroscopy. Previous work (Davies, 2017) which utilized the same test cell set-up, also observed green and orange minerals, however, the process by which they were formed was not explained, nor were they fully identified. It can be seen from results presented here, that the same corrosion products were formed despite a different temperature / groundwater being used, and critically, formation of the green corrosion product can be linked to microbial activity.

Iron (II) sulfate has been known to provide corrosion protection by blocking reactants from the surface (Guilbaud et al., 2013). As presented above, the Eh/pH of the effluent from microbial experiments does suggest that formation Fe(II) would be favoured under these conditions. However, there may also be some carbonate green rust formation as indicated by the presence of calcite. There is some evidence that calcite would form in association with green rust and ferrihydrite immediately at the steel surface (Furukawa et al., 2002). However, there is also evidence that carbonate GR offers less protection than sulfate GR (Boin et al., 2000) due to a decrease in porosity. Magnetite, goethite and ferrihydrite were all identified in the MX80 bentonite or orange corrosion layer. All are common corrosion products (Burger et al., 2011) and have been discussed previously in section 6.3 and 4.7.

There is ample evidence to implicate microbes in GR formation (Usman et al., 2012; Zegeye et al., 2007; Volkland et al., 2000; Zegeye et al., 2014; Jorand et al., 2007; Jorand et al., 2011). Importantly, experiments by Volkland et al. (2000) showed GR formation (identified as vivianite ($Fe^{2+}_3(PO_4)_2 \bullet 8(H_2O)$)) only occurred when live bacteria were present. Magnetite was produced in the absence of bacteria, or if bacteria were initially present and then died. Therefore, dead mass sorption does not provide the correct environment for GR formation. One explanation for this is EPS allows larger aggregates to form and this is a favourable environment for GR formation over magnetite. In addition to EPS, it was observed that GR would only form above a certain cell density (Zegeye et al., 2014; Zegeye et al., 2010). The cell density of the experiments presented here was far below this threshold but this experimental set-up was very different from those described in Zegeye et al., 2014 and Zegeye et al., 2010 (liquid media experiments) so biogenic GR formation may still have occurred in this way.

Another factor in GR formation in these experiments is lack of oxygen. Although these experiments were thought to be anaerobic, it is probable that there was some residual oxygen in the system which would have driven aerobic corrosion processes resulting in the orange rust observed in both the sterile and biotic experiments. However, microbial consumption of O_2 will have accelerated the drive to anaerobic conditions in the biotic experiment, therefore resulting in different corrosion mechanisms. In the repository, there is evidence to support the theory that

microbes will be beneficial to the system by consuming oxygen that would otherwise contribute to canister corrosion (RWM, 2017).

Furthermore, if oxygen were to become available after GR formation, ferric green rusts would likely form. This mechanism involves electron transfer and a progressive deprotonation of the hydroxyl groups of the Fe−(O−H) octahedral sheets (Zegeye et al., 2014). It has been shown that this ferric GR can be a source of Fe(III) for IRBs and GR can reform at a high reduction rate due to the similarities between GR and ferric GR (Jorand et al., 2007).

Magnetite was observed in the orange layer and, along with ferrihydrite, was also seen in the clay furthest from the steel. Magnetite was only identified in samples from the Microbe_Steel experiments and is likely to be the oxidisied product of GR as it has degraded (Boin et al., 2000) and diffused through the clay.

There is evidence to suggest that diffusion of oxidised corrosion products into the clay may destabilise the MX80 bentonite; indeed, it has been estimated that up to 30% of MX80 bentonite would be converted to non-swelling Fe(II) rich clay if enough iron were corroded from the canister (Wersin et al., 2008), which in conjunction with silica dissolution would explain the decrease in PI. As previously discussed, (see section 4.1), Fe(II) can act as a catalyst for reduction of Fe(III), therefore, the formation of GR instead a more oxidized orange rust may help protect against this conversion to Fe(II) rich clay.

The presence of steel and its associated corrosion products caused an expected increase in pH (due to H^+ consumption to form hydrogen) (Prawoto et al., 2009), however, the presence of microbes neutralized this effect to some extent, probably due to VFA production. From analysis of the groundwater, it is possible to conclude that iron is more likely to leach out of the system through groundwater when microbes are present, and redox changes are also more likely. This difference may be because there is more iron corroded, although from the SEM images this seems unlikely, or because diffusion products travel further and are in a different redox state (Fe(II), not just Fe(III)). Increased iron mobilisation was evidenced by both the Fe measurements, which show higher concentrations of Fe(III), Fe(II) and $Fe(II)_{aq}$ in the microbial effluent than the sterile, as well as the measurement of diffusion of corrosion products into the clay. However, this iron may have been from the clay rather than the steel. Ultrameter readings also support this

conclusion as there was higher TDS in the Microbe_Steel than the Sterile_Steel experiments. Therefore, it is not possible to unequivocally conclude that the steel from sterile experiments were more corroded than those from microbial experiments.

7.3.2 Putative microbial activity could alter the plasticity and mineralogy of MX80 bentonite

Whilst microbial presence appears to be positive for the protection of steel from corrosion due to GR formation, microbial activity significantly lowers the PI of MX80 bentonite; although corrosion products from steel also lower the PI, as seen in the sterile experiment. This change in PI has the potential to be detrimental to the ability of the MX80 bentonite to act as a barrier (see section 6.5.4).

The presence of calcite at the top of the test cell was surprising, especially as the pH differed greatly between these two areas – calcite is more readily precipitated at alkaline pH (Thorley et al., 2015). However, microbially induced calcite precipitation (MICP) has been observed in montmorillonite clay (Chen et al., 2017) and by bacteria species presented here such as *Bacillus* (Sharma & Ramkirshnan, 2016). The process is complex and can proceed due to several different microbial activities including urea hydrolysis and denitrification (Van Paasen et al., 2010). The processes converge to produce Ca^{2+} at the cell membrane, and the microbe acts as a nucleation site to form calcium carbonate crystals through interactions with local CO_3^{2-}. In these experiments there are two calcium sources; there is calcium present in the clay (0.66% wt. CaO), and in the groundwater (0.05 g/L). Therefore, calcite observed in the GR is not from the steel. However, *S. oneidensis* inhibits calcite dissolution (Luttge & Conrad, 2004), by blocking the mineral surface – this species was identified in the original iron-reducing microbial community but did not seem to be active or survive in the test cell conditions.

Muscovite was identified in XRD analysis of the MX80 bentonite recovered from experiments with microbes, but as discussed in the results, this is more likely to be illite. Muscovite ($KAl_2(Si_3AlO_{10})(OH)_2$) is found in several rock types, most notably granitic rock. Whilst smectites can transform to muscovite through illitisation and silica loss (Kamp, 2008), it is unlikely that this progressed further than illite formation during the 3-month duration of this experiment, at relatively low temperatures. If it is in fact illite, this could explain the decrease in PI observed and

could also result in decreased swelling and sorption of the clay and possible increase in hydraulic conductivity (Bradbury et al., 2014; Pusch & Kasbohm, 2002). The transformation of montmorillonite to illite is commonly observed in nature and, for the reasons stated above, is a concern in nuclear waste repository design (Sellin & Leupin 2013). Illitisation is more widely described in chapter 2. In terms of silica solubilization, this may cause an increase in Ca^{2+} (Vasanthi et al., 2016), which could drive the calcite precipitation observed elsewhere in the clay.

Although in nature the illitisation process is slow and requires high temperatures to proceed abiotically, biogenic illitisation does not have the same requirements (Kim, 2012). Smectite to illite transformations occur biogenically as dissolution of smectite and reprecipitation as K / Al illite - this can be catalysed by IRBs and SRBs via reduction of structural Fe(III) (Kim, 2012; Fang et al., 2017; Bradbury et al., 2014). Access to Fe(III) and its surface area is the rate limiting step. This access is increased if smectite can expand, but this was not possible in these constricted test cells. Reduction of Fe(III) and the associated change in charge attracts K^+ into the interlayer space. As microbes and smectites are slightly negatively charged (illite is more negatively charged) the process is slow (Dong, 2005). However, there is a possibility of positive charges at the clay edge sites (due to proton associations and disassociations) that may allow microbes to attach themselves here (Bishop et al., 2011). There is also evidence that the role of organic secretions in iron reduction will lead to smectite - illite transformations (Kim, 2012).

7.3.3 Iron-reducing enrichments show evidence of iron-reducing ability of indigenous microbial community after test cell incubation

The results from the microbial iron-reducing enrichments showed an increase in the concentration of Fe(II) in samples taken from the bottom of the test cells, which is likely due to diffusion of rust into the clay from the steel. There is, therefore, more iron present in the 4g sample taken from the bottom of the test cell, than the top, (and more than previous enrichments presented in chapter 4) which may have contributed to the higher concentration of Fe(II) observed in these samples. Nonetheless, it is clear in all biotic samples that iron reduction is increased when microbes are present. However, unlike the original iron-reducing enrichments (see section 4.1), addition of *S. oneidensis* resulted in a lower concentration of Fe(II). It is possible that *S. oneidensis* is outcompeted in iron-reducing enrichments due to a different community, or

there was some oxygen present so it was not acting as an iron reducer. The latter seems unlikely as these experiments were carried out in an anaerobic cabinet and so there is less likely to be residual oxygen present unlike during the test cell experiments. These enrichments do further evidence the ability of the indigenous community to reduce iron, with clear differences between the Fe(II) concentration when microbes are present compared to when they are absent.

Also in contrast to the original enrichments is the concentration of acetate. The production of acetate, or the microbes that produce acetate, seem to be inhibited when steel is present in the test cells. Or alternatively, the actetate is all being utilized in iron-reduction (see section 4.1) or as energy by other members of the community and so it is not in excess. Addition of *S. oneidensis* appeared to reverse this and caused an increase in acetate. This acetate was likely produced from the consumption of other carbon sources as *S. oneidensis* is a known acetate producer (Liu et al., 2005).

7.3.4 Microbial communities from test cell experiments are altered during enrichment

The nested sequencing results revealed distinct microbial communities at the top and bottom of the test cell. These nested communities did vary somewhat between samples, likely because the microbes are not evenly distributed throughout the clay, and with no enrichment there has been no chance to grow into a more homogenous community. Although there are not many differences between microbial communities following enrichment*, Clostridia* are more abundant in samples taken from the bottom of the test cell, as is *Desulfosporosinus.* IRBs including *Desulfosporosinus* (Pester et al., 2012) and *Brevibacillus* (El-Rab et al., 2018) were identified. They are not fermenting bacteria but can use fermentation products such as acetate and amino acids. These species may have therefore contributed to the low concentration of acetate observed in these enrichments.

Present in the nested, unenriched microbial community from Microbe_Steel experiments, there are mainly aerobic bacteria that can withstand some oxygen stress or facultatively anaerobic bacteria. It is therefore likely that, as previously assumed, there was some residual oxygen in the test cells. *Methylotenera* is only present at the top of the test cell from the experiment with steel. It is a denitrifying bacterium and is capable of mixed acid fermentation (Mustakhimov et al.,

2013). Also, notably, *Deinococcus,* which was similarly only present at the top of the test cell with steel, is a thick cell walled, piezophilic bacterium, some species of which have been shown to be radiation resistant (Makarova et al., 2001).

All species identified in the Microbe_Steel iron-reducing enriched communities are anaerobic or facultatively anaerobic and the vast majority are capable of sporulation and fermentation. The results from enriched communities also suggest that the iron-reducing community can recover even after high pressure and confinement. Almost all bacteria present are known to produce acetate among other fermentation products such as butyrate and carbon dioxide. All *Clostrdium sensu stricto* species and several other species present produce hydrogen (Lin et al., 2007), whereas there are not many species present in this community that are known to utilise H_2. *Brevibacillus* is also present. This is interesting as studies have indicated that the presence of iron increases the hydrogenase activity of this bacterium (El-Rab et al., 2018). In the repository, increased H_2 may lead to an increase in gas pressure, and eventually lead to increased corrosion via hydrogen embrittlement (see section 5.6.3).

Sporomusa was also identified in the microbial community at the bottom of the test cells. It is an acetogenic bacteria that increases corrosion by using Fe(0) as an electron donor in place of H_2 (Philips et al., 2019). In addition, *Thermincola* is a chemolithoautotroph which produces hydrogen and is both thermophilic and halotolerant (Zavarzina et al., 2007). *Gracilibacter* (Lee et al., 2006)*, Thermoanaerobacterales* (Balk et al., 2009)*, Desulfosporosinus* (Pester et al., 2012)*, Fonticella* (Fraj et al., 2013)*, Brevibacillus* (El-Rab et al., 2018)*, Sporacetigenium* (Chen et al., 2006)*,* and *Desulfitobacterium* (Villemur et al., 2006; Finnerman et al., 2002) are also present and are also halotolerant or thermotolerant. Interestingly, *Desulfosporosinus* and *Gracillibacter sp.* were identified in these samples and in clay from *in situ* experiments carried out at Mount Terri 15 years after closure (Leupin et al., 2017). They are therefore likely candidates for longer-term survival in the repository.

Pantke et al. (2012) showed the production of GR by iron-oxidizing nitrate-reducing bacteria *Acidovorax* sp. (present in the nested microbial community from Microbe_Steel_Bottom). This occurred by hexagonal mineral formation on the cell surface. These crystals then grew rounder

over time, eventually leading to cell death due to constriction of the plasma membrane and blockage of cell receptors. It is therefore possible that the microbial community changes as GR is formed. Other denitrifying bacteria have also been implicated in GR formation by reacting with Fe(II) to form ammonia, goethite (identified as a corrosion product in these experiments) and GR (Etique et al., 2014).

Further evidence implicates SRBs such as *Desulfosporosinus*, in the formation of GR. Although the links to sulfate GR are obvious, SRB activity can also lead to carbonate GR (Zegeye et al., 2007). Furthermore, the relationship between SRBs and GRs is not only during formation, sulfate GRs can provide sulfate for further SRB activity (Zegeye et al., 2007), and so the structure of the GR may change or be maintained due to continued microbial presence.

Chapter 8. Conclusions

A series of experiments were designed and carried out to achieve the main aim of this project as set out in section 1.5. Firstly, these experiments were used to identify an indigenous iron-reducing microbial community of MX80 bentonite; secondly experiments tested the limits and activity of that community; and thirdly experiments assessed changes to the MX80 bentonite due to the activity of that community. All experiments were set up with a focus specifically on iron chemistry due to both the iron present in MX80 bentonite, and the UK concept for nuclear waste disposal using a carbon steel canister which could contribute iron-rich rust products to the environment.

Through these experiments, the objectives set out in section 1.2 were achieved. Enrichment experiments characterised the indigenous iron-reducing bacterial community of the MX80 bentonite (chapter 4) and found that there was sufficient iron-interacting ability to potentially alter clay minerals or influence corrosion of the canister. Indirect interaction experiments supported the second objective of this project by determining whether secreted products from the indigenous community could interact with iron-minerals. These experiments (chapter 5) were important in terms of the repository design as they suggest that isolated microbial growth (likely limited to the host rock / clay interface) could still contribute to changes in iron silicate minerals throughout the clay and or contribute to corrosion of the canister despite being spatially distant.

Further experiments presented in chapters 5-7 supported the final objectives by assessing further activities of these microbes, such as silica solubilisation and H_2 production, and the survivability of the microbial community in unfavourable conditions related to those predicted for the repository. Additionally, results from these experiments were able to suggest what, if any, microbially influenced geomechanical changes had occurred within the clay, with a focus on clay plasticity which could have implications for the ability of the clay to perform as a barrier. These results were then be analysed and the potential implications for the repository could be identified.

8.1 Summary of findings

The hypotheses as set out in section 1.6 were supported by the results presented in this thesis, except for hypothesis C which stated that corrosion would be limited in the absence of microbes. The conclusions presented below indicate that the results in fact suggest that corrosion was only limited when microbes were present.

From this project, it can be concluded that a robust and viable microbial community exists regardless of source, prior treatment and storage in compacted MX80 bentonite which is metabolically and functionally diverse. More specifically, this community can reduce iron; interact indirectly with minerals; and is not eliminated by high pressure (see chapter 7), salinity (see chapter 4), temperature (see chapter 6), or low carbon availability (see chapter 6 &7). Additionally, as evidenced in these experiments, it is likely that this microbial community could alter the gas composition of the repository by consuming O_2 and producing H_2 and, possibly, CO_2 (provided fermentable material is available).

The indirect interactions with minerals, notably iron-containing minerals, can lead to silica dissolution, calcite precipitation, and may contribute to biotically mediated illitisation of smectite (Kim, 2012). This transformation to non-swelling clay minerals would be a disadvantage in the repository system and would decrease the ability of the MX80 to perform as a barrier. However, these changes may only occur at the clay/ host rock interface or backfill, in areas where swelling has not fully occurred, rather than being widespread throughout the clay buffer (Jalique et al., 2016; Wilson et al., 2010). These changes and the loss of silica led to a decrease in the plasticity index (PI) of the clay in the presence of microbes, even at elevated temperatures. This change was likely caused by microbe-mineral interactions and could indicate a decrease in the swelling capacity of the MX80 bentonite; however, it is not clear if this would be a local effect (e.g., at the clay edge sites), or to what extent the swelling capacity may be altered.

Whilst these observations do not appear positive for the ability of the clay to perform as an effective barrier, the microbial concentration used in these experiments is higher than what is naturally present in MX80 bentonite. The swelling ability of the MX80 bentonite should also limit the microbial activity more than was observed in many of these experiments. Conversely, positive

effects of microbial presence of protection of steel from corrosion were also observed. It would appear that protection was afforded in a passive manner in most instances, by consumption of oxygen that would otherwise have contributed to aerobic corrosion. However, formation of a green corrosion product was also observed and XRD analysis suggests this product is primarily a sulfate GR, which also provides passive protection. The results of these experiments (chapter 7) suggest that microbes may be involved in maintaining the metastability of this mixed oxide layer, but further experiments and analysis (such as low angle XRD, Mossbauer analysis, or further microscopy) would be necessary to fully characterize the GR and define the microbial role fully.

8.1.1 MX80 bentonite carries a robust bacteria community capable of iron-reduction

To characterize the iron-reducing microbial community indigenous to the MX80 bentonite, anaerobic enrichments were set up at different salinities to represent the range of possible groundwaters in the repository environment. Whilst this allowed the measurement of the iron-reducing capability of the bacteria present, which was significant, enrichment was also necessary to generate enough DNA for its extraction and sequencing. This process was advantageous as it allowed for the characterisation of the activated microbial community rather than the extracellular DNA bound in the clay, or that of unviable organisms.

The enrichments in this project, however, did not replicate the repository conditions in terms of pressure, temperature, or water or carbon availability and therefore, the true active microbial community in the repository will likely be more limited. Nevertheless, these experiments did show that there are indigenous bacteria to the clay that would be good candidates for repository survival across all salinities, and a microbial community capable of significant iron-reduction in salinities up to sea-water concentrations. These iron-reducing bacteria included *Desulfosporosinus* (Kunapuli et al., 2010; Pester et al., 2012), *Desulfitobacterium* (Villemur et al., 2006), and *Shewanella* (Ruebush et al., 2006). It is noteworthy that despite the obvious iron-reduction, *Geobacter* (a common model organism for iron-reduction, and perhaps most studied) was not identified in any enrichments of MX80 bentonite presented here.

The microbial community from all enrichments was overwhelming composed of firmicutes, both spore-forming *Bacillus* and putatively fermentative *Clostidium* species were abundant. Based on

the known functions of these species it was possible to conclude that the oxidation of organic matter and H_2, and degradation of amino acids by fermenting bacteria was coupled to iron-reduction in this system. The fermentation products could be utilized by other members of the community as an energy source given the scarcity of bioavailable carbon in the repository.

These enrichment experiments also indicated that compaction, and subsequent storage of the clay as a compacted block, had little effect on the microbial community when compared to the community enriched from experiments with MX80 bentonite powder. Therefore, two conclusions can be drawn; firstly, that microbes native to the MX80 bentonite are robust and can survive in compacted clay blocks. Secondly, that microbes introduced during the commercial compaction process do not have a significant effect on the overall microbial community composition. However, salinity had a significant selective effect on the composition and diversity of the indigenous iron-reducing microbial community, as well as decreasing the ability of the indigenous community to reduce iron. Indeed, most of the high salinity enriched microbial community were spore-forming bacteria. Unsurprisingly, a BLASTN search identified that most of the members of this community were most closely related to halophilic bacteria isolated from or at least identified in salt lakes and other high salinity environments. No iron-reduction was observed in high salinity enrichments. Therefore, the conclusion that repository sites with highly saline groundwater will hugely limit microbial growth, particularly IRBs, was made.

Further enrichments were carried out under aerobic conditions and again found a viable but distinctively different microbial community; however, while many of the species identified previously were facultatively anaerobic, some of the species found in these enrichments were putatively aerobic. Therefore, the microbial community will have to change somewhat as conditions become anaerobic following repository closure, allowing the facultative anaerobes to become dominant over the strict aerobes in the community.

Furthermore, these findings also suggest that some of the bacteria that could be active during the anaerobic period of enclosure will have been active from the start of the repository as aerobic bacteria, thus giving them more time to become established before full swelling of MX80 bentonite occurs – a process which will limit microbial growth. My findings therefore justify the

need to ensure that highly compact MX80 bentonite is used in repositories and steps taken to ensure swelling takes place to seal gaps because there is a robust, viable, and functionally and metabolically diverse indigenous microbial community in MX80 bentonite which will therefore be present in the repository.

8.1.2 The indigenous iron-reducing community of MX80 bentonite is capable of further activities

A range of follow-on experiments was carried out to assess the microbial activities of the previously characterized iron-reducing microbial community. These experiments were designed in line with the obstacles microbes might face in the repository environment including pore size exclusion and clay recolonisation. These experiments also assessed the hydrogen producing and silica solubilising abilities of the community.

To first investigate the possibility of recolonization of MX80 bentonite, etching experiments were carried out. After one month of growth on agar plates, a previously sterilsied block of MX80 bentonite was cut open. SEM images showed clear microbial growth and colonisation within the block of compacted MX80 bentonite. SEM images of a sterile control showed no microbial presence – in relation to that observed in the inoculated experiment - and therefore confirmed that both the initial sterilization had been successful, and that the microbial growth observed in the experimental MX80 bentonite was new growth. Although these experiments did allow for limited expansion of the clay, and so the true pore size may have been larger than 0.02 μm (which is 10x smaller than the average microbe and, therefore, thought to inhibit microbial growth), the observable recolonization despite the decrease in carbon and water (as experienced in the clay) compared to the surrounding agar is important.

In keeping with pore spaces and their connectivity, a series of indirect interaction experiments were set up to determine whether microbial secretions, or electron transport, could interact with minerals through the clay if the microbes were unable to travel around the clay barrier due to the pore size. Mineralogical changes were observed across all iron substrates in these experiments when microbes were present. These changes included some iron oxidization when iron powder was used as the substrate and changes to MX80 bentonite powder and PCFeO. XRD

analysis showed that iron powder had been transformed to magnesioferrite. It can therefore be concluded that the iron-reducing indigenous microbial community is capable of both iron-reduction and iron oxidization by organic acid production at spatially distant locations from the minerals. This experiment is directly linked to objective 2 (see section 1.5).

Furthermore, silica solubilization was also observed by direct interaction between clay and the indigenous iron-reducing microbial community of MX80 bentonite. The outcome of interactions such as these is likely to be a loss of plasticity and, by extension, swelling capacity of the clay. Illitisation by interactions coupled to the reduction of iron (III) results in a release of silica from clay minerals. This result further evidences the previously measured iron-reducing activity of the indigenous microbial community of the MX80 bentonite and supports the conclusion that this activity could lead to geomechanical changes to the MX80 bentonite in the repository which could affect its ability to perform as a barrier.

Finally, bacterial hydrogen production was considered. Both CO_2 and H_2 are likely gas products of bacterial metabolism – particularly as end products of fermentation. H_2 was focused on as there will be abiotic production of H_2 in the repository from water splitting in the corrosion of the carbon steel canister (Hultquist et al., 2011; RWM, 2017) which could lead to an unfavourable increase in pressure within the repository. There are predictions that the bacteria would be able to utilise the H_2 (Rawlings, 2005), thus avoiding a dangerous build-up of gas pressure and indeed, the indigenous iron-reducing community characterized here are closely related to organisms known to be capable of H_2 consumption. However, results suggest that after 10 months growth there was significantly more H_2 in the microbial experiments than in the sterile. This result confirmed the presence of hydrogen production by the indigenous microbes and suggested than any utilization of H_2 was minimal. However, there was more evidence of hydrogen embrittlement on the steel when microbes were absent. In the presence of microbes, there was a build-up of lepidocrocite which may have protected the steel surface to some extent. Therefore, conclusions were drawn which stated the microbial community will contribute to an overall build-up of H_2 within the repository. Furthermore, it was concluded that, in relation to objective 1 (see section 1.5), the microbes present do affect the corrosion of steel discs (as representatives of the repository canister) indirectly through formation of a protective iron-oxide mineral layer. This

conclusion did not support our initial hypothesis because corrosion was more limited with microbes than without.

8.1.3 The indigenous iron-reducing community of MX80 bentonite can survive high temperature in desiccated environments

In line with the repository obstacles to life - low water and high temperature - longer-term desiccation tolerance experiments were set up to test the limits of the indigenous iron-reducing community. The findings of these experiments showed identifiable and distinct (and therefore viable as evidenced by enrichment) microbial communities at 40°C and 70°C, the most obvious difference being that non spore-forming *Clostridum* were absent from the microbial community at 70°C, and did not appear in the dual temperature community either. It can therefore be concluded that in order to survive the higher temperature, and later become active, spore-formation and flexible metabolic and respiratory functions are important factors which allows for microbial activity over a broad range of conditions.

Further to this, the presence of a microbial community at 70°C, and the changes observed in the PI of the MX80 bentonite, indicates that these species are active under these conditions, despite the obvious challenges. This community was found to be most closely related to species which are halotolerant which suggests that they may be suited to low water conditions.

Further conclusions from these experiments are supported by changes to clay plasticity. At 40°C, when most bacteria were likely to be active, there was a significant decrease in PI due to an increase in plastic limit and decrease in liquid limit. This temperature is within the activity range of both thermophiles and mesophiles and is also the predicted temperature for most of the repository lifespan at the clay / host rock interface. The same change, although less extensive was seen at 70°C. It was concluded that microbial activity, likely iron-reduction leading to a loss of silica from iron silicate minerals, resulted in the decrease in PI which would be unfavourable in a repository setting. However, there was no change between the sterile and nonsterile dual temperature experiments. This result suggests that while non-spore formers are not able to survive higher temperatures, those bacteria active and causing changes to clay mineralogy must have an optimum temperature above 40°C, below which they are not active.

Also of interest in these results was the condition of the steel coupons when retrieved at the end of the experiment. Like the H_2 production experiment, it seemed that there was less corrosion on the biotic samples than the abiotic. This lack of corrosion was attributed to microbial consumption of oxygen. Therefore, it can again be concluded that microbial presence indirectly inhibits corrosion of steel.

8.1.4 Summary of findings from microbial clay /steel interface experiments under high pressure

Finally, test cell experiments were set up to mimic to a greater extent, the repository conditions. In these experiments obstacles to microbial growth included high pressure, small pore size and temperature as well as low carbon availability. Carbon steel discs were included to represent the canister.

Results from these test cells had to be taken at the end of the experiment as subsampling was not possible during the interim. Significant and obvious colour changes were observed between the sterile and unsterile experiments. In the sterile experiment orange rust products were observed to have diffused into the clay from the steel coupon, against the water gradient. The steel coupon was a dull orange colour but SEM images revealed extensive pitting corrosion. Whereas in the unsterile experiment, orange and green corrosion products were observed to have diffused into the clay, with green nearest to the steel surface. The steel coupon in this experiment had turned black; however, SEM imaging suggested the surface was much smoother than the sterile coupon. These differences suggested that the microbes were implicated in some form of protection of the steel surface from corrosion. Further analysis of the green layer suggested it was a sulfate GR – a mixed metastable iron oxide product of anaerobic corrosion (Zegeye et al., 2010; Zegeye et al., 2012; Jorand et al., 2011), which has been shown to cause passive protection of steel surfaces by blocking access of oxidants (Guilbaud et al., 2013). As previously, it was concluded that microbes indirectly protected the steel surface from corrosion through consumption of oxygen and formation of a protective iron-oxide layer. Further analysis such as low-angle XRD and Mössbauer analysis would aid in an effort to confirm which mineral was formed.

It was also concluded that the indigenous microbial community reduced iron in the MX80 bentonite which caused a decrease in the PI. This conclusion was supported by measurements from groundwater which revealed that there was more iron in the effluent from microbial experiments, present as both Fe(III) and Fe(II), as well as a higher concentration of total dissolved solids. Additionally, observations of corrosion (green and orange) further suggest that the microbes are directly involved in changes to iron redox state. However, it is not clear if this iron is from the steel, or if it is structural iron from the clay. It is clear that changes to iron mobilization are likely to change the MX80 bentonite mineralogy. Furthermore, XRD analysis of these samples revealed the possibility of illitisation. This transformation would certainly explain the changes in PI, and would also indicate a decrease in swelling capacity, as smectite is much more able to swell than Fe(II) rich phyllosilicates (Wersin et al., 2008).

In these test cell experiments nested PCR allowed for sequencing of the microbial communities direct from the clay without enrichment. As previously found, this community was comprised largely of spore-forming bacteria, however, two distinct microbial communities were observed in these experiments, one present at the top of the test cell, furthest from the steel, and one at the clay / steel interface. It was therefore concluded that the concentration and redox state of iron puts a selective pressure on the microbial community. As these test cells were inoculated at the top of the test cell, and the pore space prevents movement of microbes around the test cell, some explanation is needed for the presence of community at the bottom of the cell. As part of the setup of the experiment, groundwater was allowed to flow into the test cells for 48 hours at a low pressure. This allowed full swelling to occur, but also will have carried the microbial community around the outer edges of the clay before the swelling had occurred.

Although many of the same species were found in both samples, there were some key differences. For example, the rust community had a higher abundance of *Actinobacteria* and *Acidobacter* than the community more distant from the steel. Both *Acidobacter* and *Actinobacteria* have been implicated, either directly or indirectly, in GR formation and silica mobilization (Sauro et al., 2018). Whereas the community at the other end of the test cell had more species of IRB present, compared to the rust community which was comprised of some iron-reducing species but also iron-oxidisers and denitrifying bacteria.

The presence of both iron-reducers and oxidisers at the bottom of the test cell suggests that some redox cycling may have occurred. Although there is some nitrate in the groundwater, the abundance of denitrifying bacteria was unexpected. These bacteria were found alongside a limited number of nitrogen-fixing bacteria. This finding suggests that there may be a small nitrogen cycle occurring which is coupled to iron-oxidation (Liu et al., 2009). It is also suggestive that the composition of groundwater, including the concentration of nitrate, may be an important factor in microbial community composition.

Interestingly, unlike previous enrichments, when steel was present there was only a low concentration of acetate produced over the 6-week post-test cell enrichment. As the addition of *S. oneidensis* led to an increase in acetate, it seems likely that there are simply not many species present that are actively producing acetate. The acetate concentration of the microbial experiment without steel did not show the same decrease so perhaps the high concentration of iron is causing a selective pressure which negatively affects fermenting bacteria. Significant iron-reduction was observed in all unsterile enrichments, in fact more so than the positive *S. oneidensis* control. It can therefore be concluded that the high pressure and challenges caused by small pore size do not eliminate IRBs.

8.2 Suggestions for further study

While this project shed light on the iron-reducing ability of the bacteria present in the MX80 bentonite, and its potential activity and survivability in the repository, there are still unanswered questions which have been raised from the results which give rise to new objectives. It would be important for RWM to conduct long-term experiments similar to those carried out internationally at sites such as Mont Terri (Leupin et al.; Necib et al., 2017; Stroes-Gascoyne et al., 2002; Hadi et al., 2019), to fully understand the possibility of iron-reduction or silica loss to the bentonite barrier and the potential corrosion protection afforded to the waste canister in a UK repository site.

8.2.1 Green rust analysis

Principally, a full characterisation of the GR formed during test cell experiments and the associated protection it could afford to the canister against corrosion should be carried out.

Current literature in connection to nuclear waste, does not consider potential carbon steel canister protection by GR. Indeed, there is very limited research which has aimed to generate and investigate GR in relation to nuclear waste containment and its associated environment, rather it has appeared as a by-product of an experiment which aimed to investigate something else (as it did in the experiments presented here). Some research groups investigating the alteration of bentonite due to corrosion products have observed GR formation in some samples, but this has not been reproducible across replicates (Hadi et al., 2019; Kumpulainen et al., 2011) (reproducible green mineral formation has been achieved in this project); the following reasons can be offered as explanation for these discrepancies: the research did not explicitly consider the role of microbes, the controls have not been sterilised correctly, or the corrosion products have oxidised before analysis was possible.

There is some research which has been conducted on host rocks and groundwater which has identified the presence of GR and suggests this product could be beneficial to the repository system as its low porosity could limit radionuclide transport to the external environment (Skovbjerg et al., 2010). Therefore, formation of this product closer to the source of radioactive waste (i.e., the steel canister) could act as a previously unanticipated barrier to both shield the canister surface from oxidants and thus in turn leading to a decrease in corrosion, and as a barrier limiting the movement of radionuclides from the canister.

Further work should aim to characterise this putative GR and assess its longevity to determine if it will survive the different phases of the repository, be able to reform, or will be lost after a certain point. Due to the metastable nature of GRs, an array of microscopy techniques should be used to fully understand the protective (or non-protective) properties of the GR including SEM, Raman spectroscopy, micro probe analysis, Mössbauer, and XRD.

8.2.2 Microbially influenced changes to swelling capacity

Moreover, this project aimed to investigate what effect microbial activity may have on the geomechanical properties of MX80. Whilst changes to PI were measured and found to significantly decrease when microbes were present, further investigation of microbially-induced changes to the geomechanical properties of the clay is needed, with a specific focus on swelling

capacity. Time and experimental design did not allow for any direct changes of swelling capacity to be measured, but a decrease in PI suggests there was some change to swelling capacity occurring.

8.2.3 External microbial species and the role of fungi

Furthermore, no attempt was made to identify any fungal species present or assess what alterations may occur due to fungal activity. Additionally, there is the possibility that microbial species from local groundwater may alter the microbial community through competition; or local geochemistry (such as nitrate) may put different selective pressures on the community. Therefore, special attention should be paid to local groundwaters during site selection.

8.2.4 Microbial gas production

More information and further study are also needed on gas production of microbes; experiments presented here observed significant increases in H_2 which was not used in hydrogen embrittlement of the steel and so could cause an undesirable increase in pressure in the repository. Despite predictions, and the presence of several fermenting bacterial species, no change in CO_2 was observed, this also should be further investigated. It is inevitable that CO_2 is produced during oxidation of organic acids, it is not clear where it is then utilised – perhaps in weathering of minerals within MX80 bentonite.

Bibliography

Albert R. A., Archambault J., Rosello-Mora R., Tindall B. J., Matheny M., (2005). *Bacillus acidicola* sp. nov., a novel mesophilic, acidophilic species isolated from acidic Sphagnum peat bogs in Wisconsin. *International Journal of Systemic and Evolutionary Microbiology,* 55(5)

Alcántara J., Chico B., Simancas J., Díaz I., de la Fuente D., Morcillo M., (2016) An attempt to classify the morphologies presented by different rust phases formed during the exposure of carbon steel to marine atmospheres. *Mater. Charact.,* 118; 65–78

Allard & Calas (2009). Radiation effects on clay mineral properties. *Applied Clay Science,* 43(2); 143-149

Altschul S. F., Gish W., Miller W., Myers E. W., Lipman D. J., (1990). Basic local alignment search tool. *J. Mol. Biol.,* 215; 403-410

Amcoff O., Holenyi K., (1996). Mineral formation on metallic copper in a `future repository site environment'. *SKI Technical Report,* SKI-R-96-38

Amoozegar M. A., Sánchez-Porro C., Rohban R., Hajighasemi M., Ventosa A., (2009). *Piscibacillus halophilus* sp. nov., a moderately halophilic bacterium from a hypersaline Iranian lake. *Int J Syst Evol Microbiol*., 59(12); 3095-3099

Amoozegar M. A., Shahinpei A., Makzum S., Rafieyan S., Nikou M. M., Sproer C., Ventossa A., (2018). *Salipaludibacillus halalkaliphilus sp. nov*., a moderately haloalkaliphilic bacterium from a coastal-marine wetland. *Int J Syst Evol Microbiol*., 68(7); 2214-2219

An S.Y., Asahara M., Goto K., Kasai H., Yokota A., (2007) *Terribacillus saccharophilus* gen. nov., sp. nov. and *Terribacillus halophilus* sp. nov., spore-forming bacteria isolated from field soil in Japan. *Int J Syst Evol Microbiol*., 57(1); 51-55

Antunes A., Costa I., Faria D. L. A., (2003). Characterization of corrosion products formed on steels in the first months of atmospheric exposure. Mat. Res. 6: 3

Aragno M., Schlegel H. G., (1981). The Hydrogen-Oxidizing Bacteria. In: Starr M. P., Stolp H., Trüper H. G., Balows A., Schlegel H. G., *The Prokaryotes*. Springer, Berlin, Heidelberg

Arlinger J., Bengtsson A., Edlund J., Eriksson L., Johansson J., Lydmark S., Rabe L., Pedersen K., (2013). Prototype repository – Microbes in the retrieved outer section. *Report P-13-16 Swedish Nuclear Fuel and Waste Management Co.*

Ashassi-Sorkhab H., Moradi-Haghighi M., Zarrini G., Javaherdashti R., (2012). Corrosion behavior of carbon steel in the presence of two novel iron-oxidizing bacteria isolated from sewage treatment plants. *Biodegradation*, 23; 69-79

Aubineau J., El Albani A., Bekker A., Somogyi A., Bankole O. M., Macchiarelli R., Meunier A., Riboulleau A., Reynaud J. Y., Konhauser K. O., (2019). Microbially induced potassium enrichment in Paleoproterozoic shales and implications for reverse weathering on early Earth. *Nature Communications,* 10; 2670

Aunqué L. F., Gimeno M. J., Gómez J. B., Puigdomenech I., Smellie J., Tullborg E-L., (2006). Groundwater chemistry around a repository for spent nuclear fuel over a glacial cycle. *SKB;* TR-06-31

Bakar M. A., McKimm J., Haque S. Z., Majumder M. A. A., Haque M., (2018). Chronic tonsillitis and biofilms: a brief overview of treatment modalities. *Journal of Inflammation Research*, 11:329-337

Balk M., Heilig H. G., van Eekert M. H., Stams A. J., Rijpstra I. C., Sinninghe-Damsté J. S., de Vos W. M., Kengen S. W. (2009). Isolation and characterization of a new CO-utilizing strain, *Thermoanaerobacter thermohydrosulfuricus* subsp. carboxydovorans, isolated from a geothermal spring in Turkey. *Extremophiles : life under extreme conditions*; 13(6): 885–894

Bambauer A., Rainey F. A., Stackebrandt E., Winter J., (1998). Characterization of *Aquamicrobium defluvii* gen. nov. sp. nov., a thiophene-2-carboxylate-metabolizing bacterium from activated sludge. *Archives of microbiology*; 169(4): 293–302

Banerjee D., Cairns A. J., Liu J., Motkuri R. K., Nune S. K., Fernandez C. A., Krishna R., Strachan D. M., Thallapally P. K., (2015). Potential of metal-organic frameworks for separation of xenon and krypton. *Accounts of Chemical Research*, 48(2); 211–219

Bagnoud A., Chourey K., Hettich R., Brujin I., Andersson A. F., Leupin O. X., Schwyn B., Bernier-Latmani R., (2016). Reconstructing a hydrogen-driven microbial metabolic network in Opalinus Clay rock. *Nat Commun*; 7

Bardelli F., Mondelli C., Didier M., Vitillo J. G., Cavicchia D. R., Robinet J. C., Leone L., Charlet L., (2014). Hydrogen uptake and diffusion in Callovo-Oxfordian clay rock for nuclear waste disposal technology. Applied Geochemistry; 49: 168-177

Barlow P. M., Reichard E. G., (2010). Saltwater intrusion in coastal regions of North America. *Hydrogeology Journal,* 18; 247-260

Barns S. M., Cain E. C., Sommerville L., Kuske C. R., (2007). *Acidobacteria* phylum sequences in uranium-contaminated subsurface sediments greatly expand the known diversity within the phylum. *Appl Environ Microbiol*, 73(9); 3113-3116

Barschall H., (1976). The Production and Use of Neutrons for Cancer Treatment: After earlier unfavorable results, recent clinical experience has renewed the hope that fast neutrons may be useful in curing cancer. *American Scientist*, 64(6); 668-673

Bath A., Richards H., Metcalfe R., McCartney R., Degnan P., (2006). Littleboy A., Geochemical indicators of deep groundwater movements at Sellafield. *Journal of Geochemical Exploration*, 90(1–2); 24-44

Bazylinski D. A., Frankel R. B., Konhauser K., (2006). Modes of Biomineralization of Magnetite by Microbes. *Geomicrobiology Journal,* 24(6); 465-475

Begg C. B. M., Kirk G. J. D., Mackenzie A. F., Neue H. U., (1994). Root-induced iron oxidation and pH changes in the lowland rice rhizosphere. *New Phytol*., 128; 469-477

Bejarano A., Sauer U., Mitter B., Preininger C., (2017). Parameters influencing adsorption of Paraburkholderia phytofirmans PsJN onto bentonite, silica and talc for microbial inoculants. *Applied Clay Science*, 141; 138-145

Bengtsson A., Edlund J., Hallbeck B., Heed C., Pedersen K., (2015). Microbial sulphide-producing activity in MX-80 bentonite at 1750 and 2000 kg m–3 wet density. *Report R-15-05*

Bennett P. C., Rogers J. R., Choi W. J., Hiebert F. K., (2001). Silicates, Silicate Weathering, and Microbial Ecology. *Geomicrobiology Journal;* 18: 3-19

Berger G., Beaufort D., Lacharpagne J., (2002). Experimental dissolution of sanidine under hydrothermal conditions: Mechanism and rate. *American Journal of Science,* 302(8); 663-685

Bertel D., Peck J., Quick T. J., Senko J. M., (2011). Iron transformations induced by an acid-tolerant *Desulfosporosinus* species. *Applied and Environmental Microbiology,* 78(1);81-88

Beveridge T. J., Murray R. G., (1976). Uptake and retention of metals by cell walls of Bacillus subtilis. *Journal of Bacteriology,* 127; 1502–1518

Bidle K. B., Brzezinski M. A., Long R. A., Jones J. L., Azam F., (2003). Diminished efficiency in the oceanic silica pump caused by bacteria-mediated silica dissolution. *Limnology and Oceanography*, 48(5); 1855-1868

Biezma M. V., (2001). The role of Hydrogen in Microbiologically Influenced Corrosion and Stress Corrosion Cracking. *International Journal of Hydrogen Energy*, 26(5); 515-520

Birkle P., Bundschuh J., Sracek O., (2010). Mechanisms of arsenic enrichment in geothermal and petroleum reservoirs fluids in Mexico. *Water Res.,* 44(19); 5605-17

Boin P. M. L., Odziemkowski M. S., Reardon E. J., Gillham R. W., (2000). *In Situ* Identification of Carbonate-Containing Green Rust on Iron Electrodes in Solutions Simulating Groundwater. *Journal of Solution Chemistry*; 29: 10

Bomberg M., Nyyssönen M., Pitkänen P., Lehtinen A., Itävaara M., (2015). Active microbial communities inhabit sulphate-methane interphase in deep bedrock fracture fluids in Olkiluoto, Finland. *Biomed Research International*, 979530

Borisova D., Möhwald H., Shchukin D. G., (2011). Mesoporous silica nanoparticles for active corrosion protection. *ACS Nano;* 5(3): 1939-1946

Börjesson, (2010). Design, production and initial state of the buffer. SKB technical report, *Report TR-10-15*

Bosak T., Newman D. K., (2005). Microbial kinetic controls on calcite morphology in supersaturated solutions. J*ournal of Sedimentary Research,* 75(2); 190-199

BP (2019). BP Energy Outlook. *2019 edition*

Bradbury M. H., Berner U., Curti E., Hummel W., Kosakowski G., Thoenen T., (2014) The Long Term Geochemical Evolution of the Nearfield of the HLW Repository. *Nagra Technical Report TR-12-01*

Braissant O., Cailleau G., Aragno M., Verrecchia E. P., (2004). Biologically induced mineralization in the tree Milicia excelsa (Moraceae): its causes and consequences to the environment. *Geobiology,* 2; 59–66

Brietenstein A., Wiegel J., Haertig C., Weiss N., Andreesen J. R., Lechner U., (2002). Reclassification of *Clostridium hydroxybenzoicum* as *Sedimentibacter hydroxybenzoicus* gen. nov., comb. nov., and description of *Sedimentibacter saalensis* sp. nov. *International Journal of Systematic and Evolutionary Microbiology;* 52(3): 801-807

Brown A. R., Boothman C., Pimblott S. M., Lloyd J. R., (2015). The impact of gamma radiation on sediment microbial processes. *Applied and Environmental Microbiology*; 81(12); 4014-4025

Brown S. D., Podar M., Klingeman D. M., Johnson C. M., Yang Z. K., Utturkar S. M., Land M. L., Mosher J. L., Hurt R. A., Phelps T. J., Palumbo A. V., Arkin A. P., Hazen T. C., Elias D. A., (2012). Draft Genome Sequences for Two Metal-Reducing *Pelosinus fermentans* Strains Isolated from a Cr(VI)-Contaminated Site and for Type Strain R7. *Journal of Bacteriology;* 194(18): 5147-5148

Burdige, D. J., (1993). The biogeochemistry of manganese and iron reduction in marine sediments. *Earth Science Reviews*; 35: 249–284

Bryce C., Blackwell N., Schmidt C., Otte J., Huang Y. M., Kleindienst S., Tomaszewski E., Schad M., Warter V., Peng C., Byrne J. M., KAppler A., (2018). Microbial anaerobic Fe(II) oxidation – Ecology, mechanisms and environmental implications. *Environmental Microbiology,* 20(10); 3462-3483

Burger E., Monnier J., Berger P., Neff D., L'Hostist V., Perrin S., Dillman P., (2011). The long-term corrosion of mild steel in depassivated concrete: Localizing the oxygen reduction sites in corrosion products by isotopic tracer method. *Journal of Materials Research*; 26: 3107–3115

Burkhardt E. M., Bischoff S., Akob D. M., Büchel G., Küsel K., (2011). Heavy metal tolerance of Fe(III)-reducing microbial communities in contaminated creek bank soils. *Applied and environmental microbiology*, *77*(9); 3132-6

Byrne-Bailey K. G., Weber K. A., Chair A. H., Bose S., Knox T., Spanbauer T. L., Chertkov O., Coates J. D., (2010). Completed Genome Sequence of the Anaerobic Iron-Oxidizing Bacterium *Acidovorax ebreus* Strain TPSY. *Journal of Bacteriology*; 192(5): 1475-1476

Callahan B. J., McMurdie P. J., Rosen M. J., Han A. W., Johnson A. J. A., Holmes S. P., (2016). DADA2: High resolution sample inference from Illumina amplicon data. Nature methods; 13(7): 581-583

Campbell S. E., Cole K., (1984). Developmental studies on cultured endolithic conchocelis (Rhodophyta). *Hydrobiologia*, 116/117; 201-208

Canfona L., Bacci G., Pinzari F., Lo Papa G., Dazzi C., Bennedetti A. (2014). Salinity and Bacterial Diversity: To What Extent Does the Concentration of Salt Affect the Bacterial Community in a Saline Soil? *PLoS One*, 9(9)

Caporaso J. G., Kuczynski J., Stombaugh J., Bittinger K., Bushman F. D., Costello E. K., Fierer N., Gonzalez Pena A., Goodrich J. K., Gordon J. I., Huttley G. A., Kelley S. T., Knights D., Koenig J. E., Ley R. E., Lozupone C. A., McDonald D., Muegge B. D., Pirrung M., Reeder J., Sevinsky J. R., Turnbaugh P. J., Walters W. A., Widmann J., Yatsunenko T., Zaneveld J., Knight R., (2010). QIIME allows analysis of high-throughput community sequencing data. Nature Methods; 7(5): 335-336

Carlson L., (2004). Bentonite Mineralogy. *POSIVA 2004-02*

Chekroun K., Rodriguez-Navarro C., Gonzalez-Munoz M. T., Arias J. M., Cultrone G., Rodriguez-Gallego M., (2004). Precipitation and Growth Morphology of Calcium Carbonate Induced by *Myxococcus Xanthus*: Implications for Recognition of Bacterial Carbonates. *Journal of Sedimentary Research*, 74(6); 868-876

Chen S., Song L., Dong X., (2006). *Sporacetigenium mesophilum* gen. nov., sp. nov., isolated from an anerobic digester treating municipal solid waste and sewage. *International Journal of Systematic and Evolutionary Microbiology*, 56(4)

Chen T., Li J., Shi P., Li Y., Lei J., Zhou J., Hu Z., Duan T., Tang Y., Zhu W., (2017). Effects of Montmorillonite on the Mineralization and Cementing Properties of Microbiologically Induced Calcium Carbonate. *Advances in Materials Science and Engineering*; ID 7874251

Chi Fru E., Athar R., (2008). In situ bacterial colonization of compacted bentonite under deep geological high-level radioactive waste repository conditions. *Applied Microbiology and Biotechnology*, 79(3); 499-510

Chiancone E., Ceci P., (2010). The multifaceted capacity of Dps proteins to combat bacterial stress conditions: Detoxification of iron and hydrogen peroxide and DNA binding. *Biochimica et Biophysica Acta (BBA) - General Subjects,* 1800(8); 798-805

Cleary H. J. & Greene N. D., (1967). Corrosion properties of iron and steel. *Corrosion Science*; 7(12); 821-831

CNSC (2006). Summary of CNSC Pre-Licensing Reviews, Conceptual Design and Post-Closure Safety Assessment for a Deep Geological Repository for Used Nuclear Fuel Crystalline and Sedimentary Host Rock Formations

Cornell R. M., Schwertmann U., (2003). The iron oxides: structure, properties, reactions, occurrences and uses. *John Wiley & Sons;* 365–407

Cui Y. J. (2017). On the hydro-mechanical behaviour of MX80 bentonite-based materials. *Journal of Rock Mechanics and Geotechnical Engineering*, 9(3); 565-574

Das S., Hendry J. M., Essilfie-Dughan J., (2011). Transformation of Two-Line Ferrihydrite to Goethite and Hematite as a Function of pH and Temperature. *Environ. Sci. Technol.*; 45(1): 268–275

Davies C., (2017). Investigation of the Thermo-Hygro-Chemico-Mechanical performance of the Bentonite Barrier at the High-Level Radioactive Waste Canister Interface. *Newcastle University (Thesis)*

Davies C.W., Davie C.T., Edward C.A., White M.L., (2018). Physicochemical and Geotechnical Alterations to MX-80 Bentonite at the Waste Canister Interface in an Engineered Barrier System. *Geosciences*, 7(3); 69

Department of Energy (2002). Yucca Mountain Science and Engineering Report (Revision 1). *DOE/RW-0539-1*

Department of Environment and Climate Change (2013)

Dhanasekaran D., Jiang Y., (2016). Actinobacteria: Basics and Biotechnological Applications. *InTech*, Ch.2

Dinh H. T., Kuever J., Mußmann M., Hassel A. W., Stratmann M., Widdel F., (2004). Iron corrosion by novel anaerobic microorganisms. *Nature,* 427; 829–832

Dobbin P. S., Carter J. P., San Juan C., von Hobe M., Powell A. K., Richardson D. J., (1999). Dissimilatory Fe(III) reduction by *Clostridium beijerinckii* isolated from freshwater sediment using Fe(III) maltol enrichment. *FEMS Microbiology Letters*, 176(1); 131–138

Dong H., Fredrickson J. K., Kennedy D. W., Zachara J. M., Kukkadapu R. K., Onstott T. C., (2000). Mineral transformation associated with the microbial reduction of magnetite. *US Department of Energy;* 143

Douterelo I., Husband S., Boxall J. B., (2014). The bacteriological composition of biomass recovered by flushing an operational drinking water distribution system. *Water Research,* 54; 100-114

Dupont C. L., Grass G., Rensing C., (2011). Copper toxicity and the origin of bacterial resistance—new insights and applications. *Metallomics*, 3; 1109-1118

Eduok U., Khaled M., Khalil A., Suleiman R., Ali B., (2016). Probing the corrosion inhibiting role of a thermophilic Bacillus licheniformis biofilm on steel in a saline axenic culture. *RSC Advances,* 6; 18246-18256

Edwards U., Rogall T., Blocker H., Emde M., Bottger E. C., (1989). Isolation and direct complete nucleotide determination of entire genes. Characterization of a gene coding for 16S ribosomal RNA. *Nucl Acids Res,* 17; 7843–7853

Ehrlich H. L., Newman D. K., (2009). *Geomicrobiology*, fifth edition. Ch16 and 19

El-Rab S. M. F. G., Hifney A. F., Abdel-Basset R., (2018). Costless and huge hydrogen yield by manipulation of iron concentrations in the new bacterial strain *Brevibacillus invocatu*s SAR grown on algal biomass. *International Journal of Hydrogen Energy*; 43(41): 18896-18907

Engel K., Ford S. E., Coyotzi S., McKelvie J., Diomidis N., Slater G., Neufeld J. D., (2019). Stability of Microbial Community Profiles Associated with Compacted Bentonite from the Grimsel Underground Research Laboratory. *mSphere;* 4(6): 601-619

Enning D., Garrelfs J., (2014). Corrosion of iron by sulfate-reducing bacteria: New views of an old problem. *Applied and Environmental Microbiology,* 80(4); 1226–1236

Erbs M., Spain J., (2002). Microbial iron metabolism in natural environments. *Microbial Diversity*

Etique M., Jorand F. P. A., Zegeye A., Grégoire B., Despas C., Ruby C., (2014). Abiotic Process for Fe(II) Oxidation and Green Rust Mineralization Driven by a Heterotrophic Nitrate Reducing Bacteria (Klebsiella mobilis). *Environmental Science & Technology*, 48 (7); 3742-3751

Eydal H. S. C., Jägevall S., Hermansson M., Pedersen K., (2009). Bacteriophage lytic to *Desulfovibrio aespoeensis* isolated from deep groundwater. *The ISME Journal,* 3; 1139-1147

Fang Q., Churchman G. J., Hong H., Chen Z. Q., Liu J., Yu J., Han W., Wang C., Zhao L., Furnes H., (2017). New insights into microbial smectite illitization in the Permo-Triassic boundary K-bentonites, South China. *Applied Clay Science*; 140: 96-111

Fei Y., Hua J., Liu C., Li F., Zhu Z., Xiao T., Chen M., Gao T., Wei Z., Hao L., (2018). Aqueous Fe(II)-induced phase transformation of ferrihydrite coupled absorption/immobilisation of rare earth elements. *Minerals,* 8; 357.

Felsenstein J., (1987). Phylogenies and the comparative method. The American Naturalist; 125(1): 1-15

Feofilova E. P., Ivashechkin A. A., Alekhin A. I., and Sergeeva Y. E., (2012). Fungal Spores: Dormancy, Germination, Chemical Composition, and Role in Biotechnology (A Review). *Applied Biochemistry and Microbiology,* 48(1); 5-17

Ferrier J., Yang Y., Csetenyi L., Gadd G. M., (2019). Colonization, penetration and transformation of manganese oxide nodules by *Aspergillus niger*. *Environ Microbiol*, 21; 1821-1832

Finneran K. T., Forbush H. M., Gaw Vanpraagh C. V., Lovley D. R., (2002*). Desulfitobacterium metallireducens* sp. nov., an anaerobic bacterium that couples growth to the reduction of metals and humic acids as well as chlorinated compounds. *International Journal of Systematic and Evolutionary Microbiology,* 52; 1929-1935

Flórez-Góngora C. H., Garzón-Peña A. T., Molina-Giraldo R. D., (2020). Testing stabilization of high-plasticity clays used in sloping terrain by adding sodium silicate. *J. Phys.: Conf. Ser.;* 1587: 012036

Fraj B., Ben Hania W., Postec A., Hamdi M., Ollivier B., Fardeau M. L. (2013). *Fonticella tunisiensis* gen. nov., sp. nov., isolated from a hot spring. *International journal of systematic and evolutionary microbiology*; 63(6): 1947–1950

Freeze G. A., Stein E., Brady P. V., (2019). Post-Closure Performance Assessment for Deep Borehole Disposal of Cs/Sr Capsules. *Energies,* 12; 1980

Gadd G. M., (2010). Metals, minerals and microbes: geomicrobiology and bioremediation. *Microbiology*, 156(3)

Gallagher K. L., Kading T. J., Braissant O., Dupraz C., Visscher P. T., (2012). Inside the alkalinity engine: the role of electron donors in the organomineralization potential of sulfate-reducing bacteria. *Geobiology,* 10; 518–530

Gaudin A., Gaboreau S., Tinseau E., Bartier D., Petit S., Grauby O., Foct F., Beaufort D., (2009). Mineralogical reactions in the Tournemire argillite after in situ interaction with steels. *Applied Clay Science*, 43

Gerritsen J., Hornung B., Renckens B., van Hijum S., Martins Dos Santos V., Rijkers G. T., Schaap P. J., de Vos W. M., Smidt H., (2017). Genomic and functional analysis of Romboutsia ilealis CRIBT reveals adaptation to the small intestine. *PeerJ*, 5; e3698.

Gilmour K. A., Davie C. T., Neil G., (2021). An indigenous iron-reducing microbial community from MX80 bentonite - A study in the framework of nuclear waste disposal. A*pplied Clay Science*, 205: 106039

Gilmour R., Krulwich T. A., (1997). Construction and Characterization of a Mutant of Alkaliphilic *Bacillus firmus* OF4 with a Disrupted cta Operon and Purification of a Novel Cytochrome bd. *Journal of Bacteriology,* 863-870

Glatstein D. A., Francisca F. M., (2014). Hydraulic conductivity of compacted soils controlled by microbial activity. *Environ Technol.;* 35(13-16): 1886-92

González A., Gálvez N., Martín J., Reyes F., Pérez-Victoria I., Dominguez-Vera J. M., (2017). Identification of the key excreted molecule by Lactobacillus fermentum related to host iron absorption. Food *chemistry*, 228; 374–380

Guan F., Xhai Z., Duan J., Zhang M., HouB., (2016). Influence of Sulfate-Reducing Bacteria on the Corrosion Behavior of High Strength Steel EQ70 under Cathodic Polarization. *Plos one,* 11(9)

Guisado I. M., Purswani J., Gonzales-Lopez J., Pozo C., (2016). Paenibacillus etheri sp. nov., able to grow on media supplemented with methyl tert-butyl ether (MTBE) and isolated from hydrocarbon-contaminated soil. *International Journal of Systemic and Evolutionary Microbiology,* 66(2)

Gülay A., Çekiç Y., Musovic S., Albrechtsen H. J., Smets B. F., (2018). Diversity of Iron Oxidizers in Groundwater-Fed Rapid Sand Filters: Evidence of Fe(II)-Dependent Growth by *Curvibacter* and *Undibacterium spp*. *Front. Microbiol*; 9: 2808

Hadi J., Wersin P., Serneels V., Greneche J., (2019). Eighteen years of steel–bentonite interaction in the FEBEX in situ test at the Grimsel Test Site in Switzerland. *Clays and Clay Minerals;* 67(2): 111-131

Hagdu T., Karra s., Kalinina E., Makedonska N., Hyman J. D., Klise K., Viswanathan H. S., Wang Y., (2017). A comparative study of discrete fracture network and equivalent continuum models for simulating flow and transport in the far field of a hypothetical nuclear waste repository in crystalline host rock. *Journal of Hydrology,* 553; 59-70

Haigh S., Vardanega P., Bolton M., (2013). The plastic limit of clays. Géotechnique, 63; 435-440

Hammes F., Boon N., Villiers J., Verstraete W., Siciliano S. D., (2003). Strain-Specific Ureolytic Microbial Calcium Carbonate Precipitation. *Applied and Environmental Microbiology*, 69(8); 4901-4909

Han R., Liu T., Li F., Li X., Chen D., Wu Y., (2018). Dependence of Secondary Mineral Formation on Fe(II) Production from Ferrihydrite Reduction by Shewanella oneidensis MR-1. *ACS Earth and Space Chemistry*, 2(4); 399-409

Haveman S. A., Pedersen K., (2002). Microbially mediated redox processes in natural analogues for radioactive waste. *Journal of Contaminant Hydrology,* 55(1-2); 161-174

Hedin P., Almqvist B. S. G., Berthet T., Juhlin C., Buske S., Simon H., Giese R., Krauß F., Rosberg J.-E., Alm P.-G., (2016). 3-D reflection seismic imaging at the 2.5 km deep COSC-1 scientific borehole, central Scandinavian Caledonides. *Tectonophysics*

Hedrich S., Schlomann M., Johnson D. B., (2011). The iron-oxidizing proteobacteria. *Microbiology*, 157; 1551-1554

Hellä P., Pitkänen P., Löfman J., Partamies S., Vuorinen U., Wersin P., (2014). Safety Case for the Disposal of Spent Nuclear Fuel at Olkiluoto - Definition of Reference and Bounding Groundwaters, Buffer and Backfill Porewaters. *Posiva*. 171

Hendry J. H., Simon S. L., Wojcik A., Sohrabi M., Burkart W., Cardis E., Laurier D., Tirmarche M., Hayata I., (2009). Human exposure to high natural background radiation: what can it teach us about radiation risks?. *Journal of radiological protection : official journal of the Society for Radiological Protection*, 29(2A); A29–A42

Henry D., Eby N., Goodge J., Mogk D., (2018). X-ray reflection in accordance with Bragg's Law. Accessed online [01/06/2021]: https://serc.carleton.edu/msu_nanotech/methods/BraggsLaw.html

Herrera L. K., Videla H. A., (2009). Role of iron-reducing bacteria in corrosion and protection of carbon steel. *International Biodeterioration & Biodegradation*, 63(7); 891-895

Hiebert F. K., Bennett P. C., (1992). Microbial Control of Silicate Weathering in Organic-Rich Ground Water. *Science;* 258(5080): 278-281

Hofstetter T. B., Schwarzenbach R. P., Haderlein S. B., (2003). Reactivity of Fe(II) Species Associated with Clay Minerals. *Environmental Science and Technology,* 37; 519-528

Hölting B., Coldewey W. G., (2019). Hydrogeology. *Springer* Ch.13

Horwell C. J., Williamson B. J., Llewellin E. W., Damby D. E., Le Blond J. S., (2013). The nature and formation of cristobalite at the Soufrière Hills volcano, Montserrat: implications for the petrology and stability of silicic lava domes. *Bull Volcanol*; 75: 696

Hua B., Xu H., Terry J. & Deng B. (2006). Kinetics of Uranium(VI) Reduction by Hydrogen Sulfide in Anoxic Aqueous Systems. *Environ. Sci. Technol.,* 40(15); 4666-4671

Huang M. & Hull C. M., (2017). Sporulation: How to survive on planet Earth (and beyond). *Current Genetics,* 63(5); 831-838

Hultquist G., Graham M. J., Szakalos P., Sproule G. I., Rosengren A., Gråsjö L., (2011). Hydrogen gas production during corrosion of copper by water. *Corrosion Science,* 53; 310-319

IAEA, (2018a). Status and Trends in Spent Fuel and Radioactive Waste Management, *IAEA Nuclear Energy Series,* No. NW-T-1.14

IAEA (2018). Contents and Sample Arguments of a Safety Case for Near Surface Disposal of Radioactive Waste. *IAEA-TECDOC-1814*

ICRP, (1995). Age-dependent doses to members of the public from intake of radionuclides. *ICRP,* 69-71

Idiart A., Maia F., Arcos D., (2013). Geochemical evaluation of the near-field for future HLW repository at Olkiluoto. *POSIVA--13-5*

IEA (2019), Nuclear Power in a Clean Energy System, IEA, Paris https://www.iea.org/reports/nuclear-power-in-a-clean-energy-system

Iino T., Ito K., Wakai S., Tsurumaru H., Ohkuma M., Harayama S., (2015). Iron corrosion induced by nonhydrogenotrophic nitrate-reducing *Prolixibacter* sp. strain MIC1-1. *Applied and Environmental Microbiology,* 81(5); 1839-1846

Ilgen A. G., Kukkadapu R. K., Leung K., Washington R. E., (2019). “Switching on” iron in clay minerals. *Environmental Science: Nano,* 6

Ishikawa T., Mizunoe Y., Kawabata S., Takade A., Harada M., Wai S. N., Yoshida S. (2003). The iron-binding protein Dps confers hydrogen peroxide stress resistance to Campylobacter jejuni. *Journal of bacteriology*, *185*(3); 1010-7

Itävaara M., Nyyssönen M., Kapanen A., Nousiainen A., Ahonen L., Kukkonen I., (2011). Characterisation of bacterial diversity to a depth of 1500m in the Outokumpu deep borehole, Fennoscandian Shield. *FEMS Microbiology Ecology,* 77(2); 295-309

Jalique D. R., Stroes-Gascoyne S., Hamon C. J., Priyanto D. G., Kohle C., Evenden W. G., Wolfaardt G. M., Grigoryan A. A., McKelvie J., Korber D. R., (2016). Culturability and diversity of microorganisms recovered from an eight-year old highly-compacted, saturated MX-80 Wyoming bentonite plug. *Applied Clay Science;* 126: 245-250

Jayaraman A., Earthman J. C., Wood T. K., (1997). Corrosion inhibition by aerobic biofilms on SAE 1018 steel. *Applied Microbiology and Biotechnology;* 47: 62-68

Jiang Z., Tosca N., (2019). Fe(II)-carbonate precipitation kinetics and the chemistry of anoxic ferruginous seawater. *Earth and Planetary Sciences Letters*, 506; 231-242

Jonsson (2012). Radiation effects on materials used in geological repositories for spent nuclear fuel. *Internation Scholarly Research Notices*

Jönsson B., Åkesson T., Jönsson B., Meehdi S., Janiak J., Wallenberg R., (2009). Structure and forces in bentonite MX-80. *SKB, TR-09-06*

Jorand F., Zegeye A., Ghanbaja J., Abdelmoula M., (2011). The formation of green rust induced by tropical river biofilm components. *Science of the Total Environment*, 409; 2586-2596

Jorand F., Zegeye A., Landry F., Ruby C., (2007). Reduction of ferric green rust by *Shewanella putrefaciens. Letters in Applied Microbiology*, 45; 515-521

Kamp P. C., (2008). Smectite-illite-muscovite transformations, quartz dissolution, and silica release in shales. Clays and Clay Minerals; 56 (1): 66–81

Kang M., Jackson R. B. (2016). Salinity of deep groundwater in California: Water quantity, quality, and protection. *Proceedings of the National Academy of Sciences*

Kanos S., Greene A. C., Patel B. K. C., (2002). Bacillus subterraneus sp. nov., an iron- and manganese-reducing bacterium from a deep subsurface Australian thermal aquifer. *International Journal of Systemic and Evolutionary Microbiology,* 52(3).

Karnland O., (1998). Bentonite swelling pressure in strong NaCI solutions. *POSIVA 98-01*

Karnland O., (2010). Chemical and mineralogical characterization of the bentonite buffer for the acceptance control procedure in a KBS-3 repository. *SKB, TR*-10-60

Kasana R. C., Padney C. B., (2017). *Exiguobacterium*: an overview of a versatile genus with potential in industry and agriculture. *Critical Reviews in Biotechnology*; 38(1): 141-156

Kashefi K., Shelobolina E. S., Elliott W. C., Lovley D. R., (2008). Growth of Thermophilic and Hyperthermophilic Fe(III)-Reducing Microorganisms on a Ferruginous Smectite as the Sole Electron Acceptor. *Applied and Environmental Microbiology,* 74(1); 251-258

Kashefi K., Lovley D. R., (2003). Extending the Upper Temperature Limit for Life. *Science,* 301

Kato S., Yumoto I., Kamagata Y., (2015). Isolation of Acetogenic Bacteria That Induce Biocorrosion by Utilizing Metallic Iron as the Sole Electron Donor. *Appl Environ Microbiol*.; 81(1): 67–73

Keith-Roach M. J., Livens F.R., (2002). "Interactions of microorganisms with radionuclides". Pg 304

Keller L. M., Seiphoori A., Gasser P., Lucas F., Holzer L., Ferrari A., (2014). The Pore Structure of Compacted and Partly Saturated MX-80 Bentonite at Different Dry Densities. *Clays Clay Miner,* 62; 174–187

Kieft T., (2000). Size matters: Dwarf cells in soils and subsurface terrestrial environments. In: Colwell, R. & Grimes, J. (Eds.) Nonculturable Microbes in the environment. *ASM Press*

Kim B. H., Gadd G. M., (2008). Bacterial Physiology and Metabolism. *Cambridge University Press*, pg41-43, 139, 306, 310-320

Kim J., (2012). Overviews of biogenic smectite-to-illite reaction. *Clay Science,* 16(1); 9-13

Kim J., Dong H., Seabaugh J., Newell S. W., Eberl D. D., (2004). R ole of Microbes in the Smectite-to-Illite Reaction. *Science;* 303(5659): 830-832

Kip N., Veen J., (2015) The dual role of microbes in corrosion. ISME Journal, 9; 542–551

Kiviranta L., Kumpulainen S., (2011). Quality Control and Characterization of Bentonite Materials. *POSIVA 2011-84*

Knoll A. H., Canfield D. E., Konhauser K. O., (2012). Fundamentals of Geobiology. *Wiley-Blackwell* ch 6, 8, 9, 12

Kong D., Wang Y., Zhao B., Li Y., Song J., Zhai Y., Zhang C., Wang H., Chen X., Zhao B., Ruan Z., (2014). *Lysinibacillus halotolerans* sp. nov., isolated from saline-alkaline soil. *International Journal of Systemic and Evolutionary Microbiology,* 64(8)

Konhauser K., (2007). Introduction to Geomicrobiology. *Blackwell,* ch4 and 5

Konhauser K. O., (1997). Bacterial iron biomineralisation in nature. *FEMS Microbiology Reviews,* 20(3-4); 315-326

KORAD, (2018). Management Policy, https://www.korad.or.kr/korad-eng/html.do?menu_idx=32 [accessed 04/01/2022]

Kostka J. E., Dalton D. D., Skelton H., Dollhopf S., Stucki J. W., (2002). Growth of Iron(III)-Reducing Bacteria on Clay Minerals as the Sole Electron Acceptor and Comparison of Growth Yields on a Variety of Oxidized Iron Forms. *Applied and Environmental Microbiology*

Kostka J. E., Haefele E., Viehweger R., Stucki J. W., (1999). Respiration and Dissolution of Iron(III)-Containing Clay Minerals by Bacteria. *Environ. Sci. Technol*.; 33: 3127-3133

Kotelnikova S., Pedersen K., (1998). Distribution and activity of methanogens and homoacetogens in deep granitic aquifers at Äspö Hard Rock Laboratory, Sweden. FEMS Microbiology Ecology, 26(2); 121–134

Kumpulainen S., Kiviranta L., Carlsson T., Muurinen A., Svensson D., Sasamoto H., Yui M., Wersin P., Rosch D., (2011). Long-term alteration of bentonite in the presence of metallic iron *Posiva Working Report 2010-71*

Kunapuli U., Jahn K., Lueders T., Geyer R., Heipieper H. J., Meckenstock R. U., (2010). *Desulfitobacterium aromaticivorans* sp. nov. and *Geobacter toluenoxydans* sp. nov., iron-reducing bacteria capable of anaerobic degradation of monoaromatic hydrocarbons. *International Journal of Systematic and Evolutionary Microbiology;* 60(3)

Lalucat J., Bennasar A., Bosch R., García-Valdés E., Palleroni N. J., (2006). Biology of *Pseudomonas stutzeri*. *Microbiology and molecular biology reviews: MMBR*; 70(2): 510–547

Landlot D., Davenport A., Payer J., Shoesmith D., (2009). A Review of Materials and Corrosion Issues Regarding Canisters for Disposal of Spent Fuel and High-level Waste in Opalinus Clay. *Nagra technical report TR-09-02*

Lanjekar V. B., Marathe N. P., Shouche Y. S., Ranade D. R., (2015). *Clostridium punense* sp. nov., an obligate anaerobe isolated from healthy human faeces. *International journal of systematic and evolutionary microbiology*, 65(12); 4749–4756

Lantenois S., Lanson B., Muller F., Bauer A., Jullien M., Plançon A., (2005). Experimental study of smectite interaction with metal Fe at low temperature: 1. Smectite destabilization. *Clays Clay Miner.*; 53: 597–612

Last W. M., Ginn F. M., (2005). Saline systems of the Great Plains of western Canada: an overview of the limnogeology and paleolimnology. *Saline Systems,* 1; 10

Laverov N. P., Yudintsev S. V., Kochkin B. T., Malkovsky V. I., (2016) The Russian Strategy of using Crystalline Rock as a Repository for Nuclear Waste. *Elements,* 12; 253-256

Leafe M., (2017). End in sight for reprocessing nuclear fuel at Sellafield. *Waste Management, NDA.*

Leban M. B., Kosec T., (2017). Characterization of corrosion products formed on mild steel in deoxygenated water by Raman spectroscopy and energy dispersive X-ray spectrometry. *Engineering Failure Analysi*s; 79: 940-950

Lee C., Kim J. Y., Song H. S., Kim Y. B., Choi Y. E., Yoon C., Nam Y., Roh S. W., (2017). Genomic Analysis of *Bacillus licheniformis* CBA7126 Isolated from a Human Fecal Sample. *Frontiers in Pharmacology,* 8; 724

Lee J. O., Lim J. G., Kang I. M., Kwon S., (2012). Swelling pressures of compacted Ca-bentonite. *Engineering Geology*; 129-130: 20-26

Lee Y. J., Romanek C. S., Mills G. L., Davis R. C., Whitman W. B., Wiegel J., (2006). *Gracilibacter thermotolerans* gen. nov., sp. nov., an anaerobic, thermotolerant bacterium from a constructed wetland receiving acid sulfate water. *International Journal of Systematic And Evolutionary Microbiology*; 56(9)

Lentini C. J., Wankel S. D., Hansel C. M., (2012). Enriched iron(III)-reducing bacterial communities are shaped by carbon substrate and iron oxide mineralogy. *Front. Microbiol.*

Leupin O. X., Bernier-Latmani R., Bagnoud A., Moors H., Leys N., Wouters K., Stroes-Gascoyne S., (2017). Fifteen years of microbial investigation in Opalinus Clay at the Mont Terri rock laboratory (Switzerland). *Swiss Journal of Geosciences,* 110(1); 343-354

Lin E. C., (2010). Radiation risk from medical imaging. *Mayo Clinic proceedings*, 85(12); 1142–1146

Lin P. Y., Whang L. M., Wu Y. R., Ren W. J., Hsiao C. J., Li S. L., Chang J. S., (2007). Biological hydrogen production of the genus *Clostridium*: Metabolic study and mathematical model simulation. *International Journal of Hydrogen Energy*; 32(12): 1728-1735

Lindsay D., Brözel V. S., Von Holy A. (2006). Biofilm-spore response in *Bacillus cereus* and *Bacillus subtilis* during nutrient limitation. *Journal of food protection,* 69(5); 1168-1172

Little B., Wagner P., Mansfield F., (1992). An overview of microbiologically influenced corrosion. *Electrochemica Acta*, 37(12); 2185-2194

Liu D., Dong H., Bishop M. E., Zhang J., Wang H., Huang L., Eberl D. D., (2012). Microbial reduction of structural iron in interstratified illite-smectite minerals by a sulfate-reducing bacterium. *Geobiology*; 10(2): 150-162

Liu J., (2006) Transport/Reaction Modelling of Copper Canister Corrosion Aided by Coupled Microbial Processes. *SKI Report 2006:07*

Liu T., Chen D., Li X., Li F., (2019). Microbially mediated coupling of nitrate reduction and Fe(II) oxidation under anoxic conditions, FEMS Microbiology Ecology; 95(4)

Liu W., Xu X., Wu X., Yang Q., Luo Y., Christie P., (2006). Decomposition of silicate minerals by *Bacillus mucilaginosus* in liquid culture. *Environmental Geochemistry and Health,* 28; 133-140

Liu X., Huang Y., Li J., Yang D., Xu Y., Kunte H. J., (2020). Effect of microbial hydrogen consumption on the hydrogen permeation behaviour of AISI 4135 steel under cathodic protection. *International Journal of Hydrogen Energy*, 45(7); 4054-4064

Liu Y., Gao W., Wang Y., Wu L., Liu X., Yan T., Alm E., Arkin A., Thompson D. K., Fields M. W., Zhou J., (2005). Transcriptome Analysis of *Shewanella oneidensis MR-1* in Response to Elevated Salt Conditions. *Journal of Bacteriology*, 187(7); 2501-2507

Liu Y., (2010). Influence of heating and water-exposure on the liquid limits of GMZ01 and MX80 bentonites. *Journal of Rock Mechanics and Geotechnical Engineering,* 2(2); 188-192

Lloyd J. R., Leang C., Hodges Myerson A. L., Coppi M. V., Cuifo S., Methe B., Sandler S. J., Lovley D. R., (2003). Biochemical and genetic characterization of PpcA, a periplasmic c-type cytochrome in *Geobacter sulfurreducens. Biochemical Journal,* 369; 153-161

López-Fernández M., Fernández-Sanfrancisco O., Moreno-García A., Martín-Sánchez I., Sánchez-Castro I., Merroun M. L., (2014). Microbial communities in bentonite formations and their interactions with uranium. *Applied Geochemistry*, 49; 77-86

Lovley D. R., Walker D. J. F., (2019). *Geobacter* Protein Nanowires. *Front. Microbiol.;* 10:2078

Lovley D. (2013) 'Dissimilatory Fe(III)- and Mn(IV)-Reducing Prokaryotes', in Rosenberg E., DeLong E. F., Lory S., Stackebrandt E., Thompson F., The Prokaryotes: Prokaryotic Physiology and Biochemistry. Berlin, *Heidelberg: Springer Berlin Heidelberg*, pp. 287-308

Lovley D. R., Stolz J. F., Nord Jr. G. L., Phillips E. J. P., (1987). Anaerobic production of magnetite by a dissimilatory iron-reducing microorganism. *Nature*, 330; 252-254

Lovley D. R., (1991). Magnetite Formation During Microbial Dissimilatory Iron Reduction. *Iron Minerals;* 151-166

Loyaux-Lawniczak S., Vuilleumier S., Geoffroy V. A., (2019). Efficient Reduction of Iron Oxides by *Paenibacillus* spp. Strains Isolated from Tropical Soils. *Geomicrobiology Journal,* 36(5); 423-432

Luef B., Fakra S. C., Csencsits R., Wrighton K. C., Williams K. H., Wilins M. J., Downing K. H., Long P. E., Comolli L. R., Banfield J. F., (2012). Iron-reducing bacteria accumulate ferric oxyhydroxide nanoparticle aggregates that may support planktonic growth. *The ISME Journal,* 7; 338-350

Luidold S., Antrekowitsch H., (2007). Hydrogen as a reducing agent: State-of-the-art science and technology. *JOM*, 59; 20–26

Lüttge A., Conrad P. G., (2004). Direct Observation of Microbial Inhibition of Calcite Dissolution. *Applied and Environmental Microbiology*, 70(3); 1627-1632

Lyles C. N., Le H. M., Beasley W. H., McInerney M. J., Suflita J. L., (2014). Anaerobic hydrocarbon and fatty acid metabolism by syntrophic bacteria and their impact on carbon steel corrosion. *Frontiers in Microbiology*, 5(114)

Mahony S., Benos P. V., (2007). STAMP: a web tool for exploring DNA-binding motif similarities. *Nucleic acids research*, 35

Mahony S., Auron P. E., Benos P. V., (2007). DNA familial binding profiles made easy: comparison of various motif alignment and clustering strategies. *PLoS computational biology*, 3(3); e61

Malik S., Hewitt I., Powell A., (2016). Electron Microscopy of Anionic Surfactant-Directed Synthesis of Magnetite Nanoparticles. *Chemistry Journal of Moldova*, 11; 69-73

Makarova K. S., Aravind L., Wolf Y. I., Tatusov R. L., Minton K. W., Koonin E. V., Daly M. J., (2001). Genome of the extremely radiation-resistant bacterium *Deinococcus radiodurans* viewed from the perspective of comparative genomics. *Microbiology and molecular biology reviews : MMBR*; 65(1): 44–79

Marshall M. H. M., McKelvie J. R., Simpson A. J., Simpson M. J., (2015). Characterization of natural organic matter in bentonite clays for potential use in deep geological repositories for used nuclear fuel. *Applied Geochemistry;* 54: 43-53

Marsili E., Baron D. B., Indraneel S. D., Coursolle D., Gralnick J. A., Bond D. R., (2008). *Shewanella* secretes flavins that mediate extracellular electron transfer. *Proceedings of the National Academy of Sciences*, 105:(10); 3968-3973

Masurat, P., Eriksson, S., Pedersen, K. (2010). Evidence of indigenous sulphate-reducing bacteria in commercial Wyoming bentonite MX80. *Applied Clay Science*, 47; 51–57

Matthies C., Evers S., Ludwig W., Scgink B., (2000). *Anaerovorax odorimutans* gen. nov., sp. nov., a putrescine-fermenting, strictly anaerobic bacterium. *International Journal of Systematic and Evolutionary Microbiology;* 50(4): 1591-1594

Mauri A., Brambilla M., Chiarinotti D., Matheoud R., Carriero A., Leo M., (2011). Estimated Radiation Exposure from Medical Imaging in Hemodialysis Patients. *Journal of the American Society of Nephrology,* 22; 571-578

McLean R. J., Beauchemin D., Beveridge T. J., (1992). Influence of oxidation state on iron binding by *Bacillus licheniformis* capsule. *Applied and Environmental Microbiology, 5*8(1); 405-408

Mehrshad M., Amoozegar M. A., Didari M., Bagheri M., Fazeli S., Schumann P., Spröer C., Sánchez-Porro C., Ventosa A., (2013). *Bacillus halosaccharovorans* sp. nov., a moderately halophilic bacterium from a hypersaline lake. *International journal of systematic and evolutionary microbiology*, 63(8); 2776–2781

Merkel B J., Planer-Freidrich B., (2008). *Groundwater Geochemistry, 2nd Edition*

Miller R. B., 2nd, Lawson K., Sadek A., Monty C. N., Senko J. M., (2018). Uniform and Pitting Corrosion of Carbon Steel by Shewanella oneidensis MR-1 under Nitrate-Reducing Conditions. *Applied and environmental microbiology;* 84(12): e00790-18

Milodowski A. E., Constantinou C. A., Alexander W. R., Rigas M., Tweed C. J., Sellin P., Korkeakoski P., Kemp S. J., Rushton J. C., (2009). Reaction of bentonite in low alkali cement leachates : preliminary results from the Cyprus Natural Analogue Project (CNAP). *American Society of Mechanical Engineers.*

Mohanty B., Ghosh S., Mishra A., (1990), The role of silica in *Bacillus licheniformis*. *Journal of Applied Bacteriology*, 68; 55-60

Moore D. M., Reynolds R. C. (1997). X-ray identification of clay minerals. *Oxford university press.*

Morgado L., Fernandes A. P., Dantas J. M., Silva M. A., Salgueiro C. A., (2012). On the road to improve the bioremediation and electricity-harvesting skills of *Geobacter sulfurreducens*: functional and structural characterization of multihaem cytochromes. *B iochem Soc Trans,* 40(6); 1295–1301

Motamedi M., Karland O., Pedersen K., (1996). Survival of sulfate reducing bacteria at different water activities in compacted bentonite. *FEMS Microbiology Letters*, 141(1); 83-87

Müller-Vonmoos M., Kahr G., (1983). Mineralogische Untersuchungen von Wyoming Bentonit MX-80 und Montigel. *Nagra Tech*., 83; 12

Murad E., (1998). Clays and Clay Minerals: What Can Mossbauer Spectroscopy Do to Help Understand Them? *Hyperfine Interact*., 117; 39–79.

Mustakhimov I., Kalyuzhnaya M. G., Lidstrom M. E., Chistoserdova L., (2013). Insights into Denitrification in *Methylotenera mobilis* from Denitrification Pathway and Methanol Metabolism Mutants. *Journal of Bacteriology*; 195(10): 2207–2211

Muurinen A., Carlsson T., Root A., (2013). Bentonite pore distribution based on SAXS, chloride exclusion and NMR studies. *Clay Minerals,* 48(2); 251-266

Nagel M, Andreesen J. R., (1991). *Bacillus niacini* sp. nov., a Nicotinate-Metabolizing Mesophile Isolated from Soil. *International Journal of Systemic and Evolutionary Microbiology,* 41(1)

NDA, (2010). Summary of generic designs. *Geological Disposal*

NDA (2016). Geological Disposal Waste Package Evolution Status Report December 2016. *NDA report no: DSSC/451/01*

NDA, (2016a). Total Wastes. *The 2016 Inventory*

Necib S., Diomidis M., Keech P., Nakayama M., (2017). Corrosion of carbon steel in clay environments relevant to radioactive waste geological disposals, Mont Terri rock laboratory (Switzerland). *Swiss Journal of Geosciences,* 110(1): 329-342

Neumann A., Olson T., Scherer M., (2013). Spectroscopic evidence for Fe(ii)-Fe(iii) electron transfer at clay mineral edge and basal sites. *Environmental Science and Technology*, 47; 6969-6977

Newman A. C. D., Brown G., 1987. The chemical constitution of clays. Newman. Chemistry of clays and clay minerals. Harlow: Longman. *Mineralogical Society monograph 6*

Newsome L., Morris K., Trivedi D., Atherton N., Lloyd J. R., (2014). Microbial reduction of uranium(VI) in sediments of different lithologies collected from Sellafield. *Applied Geochemistry*, 51; 55-64

Nie Z., Korre A., Durucan S., (2011). Life cycle modelling and comparative assessment of the environmental impacts of oxy-fuel and post- combustion CO2 capture, transport and injection processes. *Energy Procedia;* 4: 2510-2517

Nixon S. L., Telling J. P., Wadham J. L., Cockell J. S., (2017). Viable cold-tolerant iron-reducing microorganisms in geographically diverse subglacial environments. *Biogensciences,* 14; 1445-1455

NRC (2017). Radiation Basics. *NRC,* last viewed: 06/07/2020 < https://www.nrc.gov/about-nrc/radiation/health-effects/radiation-basics.html>

NRC (2017a). Measuring Radiation. *NRC,* last viewed: 06/07/2020 < https://www.nrc.gov/about-nrc/radiation/health-effects/measuring-radiation.html>

NRC (2018). What we regulate. *NRC,* last viewed: 07/04/2020 <https://www.nrc.gov/waste/hlw-disposal/what-we-regulate.html >

Nugent D., Sovacool B. K., (2014). Assessing the lifecycle greenhouse gas emissions from solar PV and wind energy: A critical meta-survey. *Energy Policy,* 65; 229-244

NWMO (2016). Deep Geological Repository Conceptual Design Report Crystalline / Sedimentary Rock Environment. *APM-REP-00440-0015 R001*

Okonkwo P. C., Shakoor R. A., Benamor A., Mohamed A. M. A., Al-Marri M. J. F. A., (2017). Corrosion Behavior of API X100 Steel Material in a Hydrogen Sulfide Environment. *Metals*, 7; 109

Orcutt, B. N., LaRowe, D. E., Biddle, J. F., Colwell, F. S., Glazer, B. T., Reese, B. K., et al. (2013). Microbial activity in the marine deep biosphere: progress and prospects. *Frontiers Microbiology*; 4: 189

O'Sullivan L. A., Roussel E. G., Weightman A. J., Webster G., Hubert C. R., Bell E., Head I., Sass H., Parkes, R. J., (2015). Survival of *Desulfotomaculum* spores from estuarine sediments after serial autoclaving and high-temperature exposure. *The ISME Journal*, *9*(4); 922–933

Oulkadi D., Balland-Bolou-Bi C., Michot L. J., Grybos M., Billard P., Mustin C., Banon S., (2013). Bioweathering of nontronite colloids in hybrid silica gel: implications for iron mobilisation. *Jounral of Applied Microbiology*, 116(2); 325-334

Park J. Y., Patel D., Choi E. S., Baek M. J., Chang Y., Kim T. J., Lee G. H., (2010). Salt effects on the physical properties of magnetite nanoparticles synthesized at different NaCl concentrations. *Colloids and Surfaces A: Physicochemical and Engineering Aspects*, 367(1-3); 41-46

Parkinson S. M., Wainwright M., Killham K., (1989). Observations on oligotrophic growth of fungi on silica gel. *Mycological Research*, 93:4; 529-534

Parrello D., Zegeye A., Mustin C., Billard P., (2016). Siderophore-mediated iron dissolution from nontronites is controlled by mineral cristallochemistry. *Frontiers Microbiology*, 7; 423

Parsley L. C., Linneman J., Goode A. M., Becklund K., George I., Goodman R. M., Lopanik N. B., Liles M. R., (2011). Polyketide synthase pathways identified from a metagenomic library are derived from soil *Acidobacteria. FEMS Microbiology Ecology,* 78(1); 176-187

Pashang R., Laursen A. E., (2020). Searching for bacteria in sticky situations: Methods for investigating bacterial survival at solid-air interfaces involving Wyoming MX-80 bentonite. *Applied Clay Science;* 188

Patakova P., Branska B., Sedlar K., Vasylkivska M., Jureckova K., Kolek J., Koscova P., Provaznik I., (2019). Acidogenesis, solventogenesis, metabolic stress response and life cycle changes in *Clostridium beijerinckii* NRRL B-598 at the transcriptomic level. *Sci Rep;* 9: 1371

Patel R., Punshon C., Nicholas J., Bastid P., Zhou R., Schneider C., Bagshaw N., Howse D., Hutchinson E., Asano R., King F., (2012). *Nagra Technical Report*, NTB 12-06.

Pedersen A., Hermansson M., (1991). Inhibition of metal corrosion by bacteria. *Biofouling*, 3(1); 1-11

Pedersen K., (2012). Subterranean microbial populations metabolise hydrogen and acetate under *in situ* conditions in granitic groundwater at 450m depth in the Äspö Hard Rock Laboratory, Sweden. *FEMS Microbiology Ecology,* 81(1); 217-229

Pedersen K., Bengtsson A., Blom A., Johansson L., Taborowski T., (2017). Mobility and reactivity of sulphide in bentonite clays – Implications for engineered bentonite barriers in geological repositories for radioactive wastes. *Elsevier,* 146; 495-502

Pederson K., Motamedi M., Karnland O., Sanden T., (2000). Mixing and sulphate-reducing activity of bacteria in swelling, compacted bentonite clay under high-level radioactive waste repository conditions. *Journal of Applied Microbiology,* 86(6); 1038-1047

Pedersen K., Karlsson F., (1995). Investigation of subterranean microorganisms: Their importance for performance assessment of radioactive waste disposal. *SKB Technical Report 95-10*.

Pedersen K., (2000a). Microbial processes in radioactive waste disposal. *SKB Technical Report: TR-00-04*

Perdrial J. N., Warr L. N., Perdrial N., Lett M., Elsass F., (2009). Interaction between smectite and bacteria: Implications for bentonite as backfill material in the disposal of nuclear waste. *Chemical Geology*, 264(1–4); 281-294

Penas D., Periera A. S., Tavares P., (2018). Direct Evidence for Ferrous Ion Oxidation and Incorporation in the Absence of Oxidants by Dps from Marinobacter hydrocarbonoclasticus. *A ngew.Chem.Int.Ed,* 58; 1013-1018

Pentrakova L., Su K., Pentrak M., Stucki J. W., (2013). A review of microbial redox interactions with structural Fe in clay minerals. *GeoScience World: Clay Minerals,* 48(3); 543-560

Pesek J., Buchler R., Albrecht R., Boland W., Zeth K., (2011). Structure and Mechanism of Iron Translocation by a Dps Protein from Microbacterium arborescens. *Journal of Biological Chemistry,* 286; 34872-34882

Pester M., Brambilla E., Alazard D., Rattei D., Weinmaier T., Han J., Lucas S., Lapidus A., Cheng J. F., Goodwin L., Pitluck S., Peters L., Ovchinnikova G., Teshima H., Detter J. C., Han C. S., Tapia R., Land M. L., Hauser L., Kyrpides N. C., Ivanova N. N., Pagani I., Huntmann M., Wei C. L., Davenport K. W., Daligault H., Chain P. S. G., Chen A., Mavromatis K., Markowitz V., Szeto E., Mikhailova N., Pati A., Wagner M., Woyke T., Ollivier B., Klenk H. P., Spring S., Loy A., (2012). Complete Genome Sequences of *Desulfosporosinus orientis* DSM765^{T}, *Desulfosporosinus youngiae* DSM17734^{T}, *Desulfo sporosinus meridiei* DSM13257^{T}, and *Desulfosporosinus acidiphilus* DSM22704^{T}. *Journal of Bacteriology,* 194(22); 6300-6301

Philp J. C., Taylor K. J., Christofi N., (1991). Consequences of sulphate-reducing bacterial growth in a lab-simulated waste disposal regime. *Experientia,* 47(6); 553-559

Philips J., Monballyu E., Georg S., Paepe K., Prévoteau A., Rabaey K., Arends J. B. A., (2019). An Acetobacterium strain isolated with metallic iron as electron donor enhances iron corrosion by a similar mechanism as *Sporomusa sphaeroides. FEMS Microbiology Ecology*; 95(2)

Peirce J. J., Weiner R. F., Vesilind P. A., (1998). Chapter 16 - Radioactive Waste, *Environmental Pollution and Control (Fourth Edition),* Butterworth-Heinemann

Posiva (2000). Groundwater salinity at Olkiluoto and its effects on a spent fuel repository. *POSIVA2000-11*

Poulain S., Sergeant C., Simonoff M., Le Marrec C., Altmann S., (2008). Microbial investigations in opalinus clay, an agrillaceous formation under evaluation as a potential host rock for a radioactive waste repository. *Geomicrobiology Journal,* 25(5); 240-249

Prawoto Y., Ibrahim K. M., Nik S., (2009). Effect of ph and chloride concentration on the corrosion of duplex stainless steel. *Arabian Journal for Science and Engineering*, 34(2)

Purvis G., Gray N., Sano N., Barlow A., Cockell C., Abbott G. D., Land C., Cumpson P., (2017). Decontamination of geological samples by gas cluster ion beam etching or ultra violet/ozone. *Chemical Geology*

Pusch R., Kasbohm J., (2002). Alteration of MX-80 by hydtrothermal treatment under high salt content conditions. *SKB Technical Report TR-02-06*

Pusch R., Karnland O., Lajudie A., Decarreau A., (1992). MX 80 clay exposed to high temperatures and gamma radiation. *SKB Report TR-93-03*

Qi Y., Luo H., Zheng S., Chen C., Lv Z., Xiong M., (2014). Effect of temperature on the corrosion behavior of carbon steel in hydrogen sulphide environments. *Int. J. Electrochem. Sci.,* 9; 2101-2112

Quiquet A., Colleoni F., Masina S., (2016). Long-term safety of a planned geological repository for spent nuclear fuel in Forsmark, Sweden and Olkiluoto, Finland Phase 2: impact of ice sheet dynamics, climate forcing and multi-variate sensitivity analysis on maximum ice sheet thickness. *Posiva*

Radhapriya P., Ramachandran A., Anandham R., Mahalingam S., (2015). *Pseudomonas aeruginosa* RRALC3 Enhances the Biomass, Nutrient and Carbon Contents of *Pongamia pinnata* Seedlings in Degraded Forest Soil. *PloS one,* 10;(10)

Raiko H., Sandström R., Rydén H., Johansson M., Kärnbränslehantering S., (2010). Design analysis report for the canister. *TR-10-28 Technical Report, Swedish Nuclear Fuel and Waste Management Co*.

Raman R. K. S., Javaherdashti R., Panter C., Pereloma E. V., (2005). Hydrogen embrittlement of a low carbon steel during slow strain testing in chloride solutions containing sulphate reducing bacteria. *Materials Science and Technology*, 21(9); 1094-1098

Rancourt D. G., (1998). Mössbauer spectroscopy in clay science. *Hyperfine Interactions,* 117; 3–38

Rättö M., Itävaara M. (2012). Microbial Activity in Bentonite Buffers. *VTT Technology* 20. 30

Rawlings D. E. (2005). Characteristics and adaptability of iron- and sulfur-oxidising microorganisms used for the recovery of metals from minerals and their concentrates. *Microbial Cell Factories,* 4; 13

Reisz J. A., Bansal N., Qian J., Zhao W., Furdui C. M., (2014). Effects of ionizing radiation on biological molecules--mechanisms of damage and emerging methods of detection. *Antioxidants & redox signaling*, 21(2); 260–292

Reitner J., Thiel V., (2011). *Encyclopaedia of Geobiology*. Pg 36-53, 81-89, 182-189, 322, 362-373, 486-502

Ronholm J., Schumann D., Sapers H. M., Izawa M., Applin D., Berg B., Mann P., Vali H., Flemming R. L., Cloutis E. A., Whyte L. G., (2014). A mineralogical characterization of biogenic calcium carbonates precipitated by heterotrophic bacteria isolated from cryophilic polar regions. *Geobiology*, 12; 542-556

Rose A. W., (2010). Advances in Passive Treatment of Coal Mine Drainage 1998-2009. *Penn State University*

Rosnes, J. T., Torsvik, T., & Lien, T. (1991). Spore-Forming Thermophilic Sulfate-Reducing Bacteria Isolated from North Sea Oil Field Waters. *Applied and Environmental Microbiology*, 57(8); 2302–2307

Roxburgh (1987). Geology of high-level nuclear waste disposal - An introduction. *Chapman and Hall*. New York

RS®Minerals, (2017). MX-80 Delivery Specification Sheet. Available online: http://www.rsminerals.co.uk/bentonite (Accessed 23rd October 2020)

RStudio Team (2020). RStudio: Integrated Development for R. RStudio, PBC, Boston, MA URL http://www.rstudio.com/.

Ruan Z., Wang Y., Zhang C., Song J., Zhai Y., Zhuang Y., Wang H., Chen X., Li Y., Zhao B., Zhao B., (2014). *Clostridium huakuii* sp. nov., an anaerobic, acetogenic bacterium isolated from methanogenic consortia. *International journal of systematic and evolutionary microbiology*, 64(12); 4027–4032

Ruebush S. S., Brantley S. L., Tien M., (2006). Reduction of Soluble and Insoluble Iron Forms by Membrane Fractions of *Shewanella oneidensis* Grown under Aerobic and Anaerobic Conditions. *Applied and Environmental Microbiology,* 72(4); 2925-2935

RWM (2020). Site Evaluation - How we will evaluate sites in England.

RWM (2017) Contractor Report to RWM The impact of ionizing radiation on microbial cells pertinent to the geological disposal of radioactive waste. *Contractor Report no. RWM/UManchester/01*

RWM (2017a) Contractor Report to RWM FEBEX-DP: THM modelling. *Contractor Report no. QRS-1713A-R2, V1.8*

RWM (2016) Geological Disposal: Generic Specification for waste packages containing high heat generating waste. *WPSGD no. WPS/240/01*

Sahin U., Eroğlu S., Sahin F., (2011). Microbial application with gypsum increases the saturated hydraulic conductivity of saline–sodic soils. *Applied Soil Ecology;* 48(2): 247-250

Saitou N. and Nei M., (1987). The neighbour-joining method: a new method for reconstructing phylogenetic trees. Molecular Biology Evolution; 4(4): 406-425

Saleh M., Sarhan M., Mourad E., Hamza M., Abbas M., Othman A., Youssef H., Morsi A., Youssef G., El-Tahan M., Amer W., Fayez M., Ruppel S., Hegazi N., (2017). A novel plant-based-sea water culture media for in vitro cultivation and in situ recovery of the halophyte microbiome. *Journal of Advanced Research,* 8; 577–590

Sanchez-Porro C., Amoozegar M. A., Rohban R., Hajighasemi M., Ventosa A., (2009). *Thalassobacillus cyri s*p. nov., a moderately halophilic Gram-positive bacterium from a hypersaline lake. *Int J Syst Evol Microbiol*., 59(10); 2565-2570

Sauro, F., Cappelletti, M., Ghezzi, D*.,* Columbu A., Hong P. Y., Zowawi H. M., Carbone C., Piccini L., Vergara F., Zannoni D., Waele J., (2018). Microbial diversity and biosignatures of amorphous silica deposits in orthoquartzite caves. *Sci Rep* 8

Sauzeat E., Villiéras T. F., François M., Pelletier M., Barrés O., Yvon J., Guillaume D., Dubbessy J., Pfeiffert C., Ruck R., Cathelineau M., (2001). Caractérisation minéralogique, cristallochimique et texturale de l'argile MX-80, *ANDRA Technical Report*

Savage D., (2005). The Effects of High Salinity Groundwater on the Performance of Clay Barriers. *SKI Report 2005:54*

Savage D., (2012). Geochemical Constraints on Buffer Pore Water Evolution and Implications for Erosion. *SSM report 2012:61*.

Sawayama S., (2006). Possibility of anoxic ferric ammonium oxidation. *Journal of Bioscience and Engineering;* 101(1): 70-72

Schaefer M. V., Gorski C. A., Scherer M. M., (2010). Spectroscopic Evidence for Interfacial Fe(II)−Fe(III) Electron Transfer in a Clay Mineral. *Environmental Science and Technology,* 45(2); 540-545

Scheldeman P., Goossens K., Rodriguez-Diaz M., Pil A., Goris J., Herman L., Vos P., Logan N. A., Heyndrickx M., (2004). Paenibacillus lactis sp. nov., isolated from raw and heat-treated milk. *International Journal for Systemic and Evolutionary Microbiology,* 54(3)

Schink B., (1984). *Clostridium magnum* sp. nov., a non-autotrophic homoacetogenic bacterium. *Archives of Microbiology,* 137; 250-255

Schlekat C. E., Decho A. W., Chandler G. T., (1999). Dietary assimilation of cadmium associated with bacterial exopolymer sediment coatings by the estuarine amphipod *Leptocheirus plumulosus*: effects of Cd concentration and salinity. *Marine Ecology Progress Series,* 183; 205-216

Schneider M., Froggatt A., Hazemann J., Katsuta T., Ramana M. V., Rodriguez J. C., Rüdinger A., Stienne A., (2017). The World Nuclear Industry Status Report

Schütz M. K., Schlegel M. L., Libert M., Bildstein O., (2015). Impact of Iron-Reducing Bacteria on the Corrosion Rate of Carbon Steel under Simulated Geological Disposal Conditions. *Environmental Science & Technology*, 49(12); 7483-7490

Schwertmann U., Murad E., (1983). Effect of pH on the formation of goethite and hematite from ferrihydrite. *Clays and Clay Minerals,* 31(4); 277-284

Sellin P., Leupin O. X., (2013). The use of clay as an engineered barrier in radioactive-waste management – a review. *GeoScience World,* 61(6); 477-498

Semenkova A., Evsiunina M., Verma P., Mohapatra P., Petrov V., Seregina I., Bolshov M., Krupskaya V., Romanchuk A., Kalmykov S., (2018). Cs^+ sorption onto Kutch clays: Influence of competing ions. *Applied Clay Science,* 166; 88-93

Shariatmadari N., Saeidijam S., (2012). The effect of thermal history on thermo-mechanical behavior of bentonite-sand mixture. *International Journal of Civil Engineering,* 10(2)

Sharma A., Ramkrishnan R., (2016). Study on effect of Microbial Induced Calcite Precipitates on strength of fine grained soils. *Perspectives in Science*; 8: 198-202

Shelobolina E. S., Nevin K.P., Blakeney-Hayward J.D., Johnsen C.V., Plaia T.W., Krader P., Woodard T., Holmes D.E., Vanpraagh C.G., Lovley D.R. (2007). *Geobacter pickeringii* sp. nov., *Geobacter argillaceus* sp. nov. and *Pelosinus fermentans* gen. nov., sp. nov., isolated from subsurface kaolin lenses*. Journal of Systematic and Evolutionary Microbiology*; 57: 126-135

Shimizu M., Zhou J., Schröder C., Obst M., Kappler A., Borch T., (2013). Dissimilatory Reduction and Transformation of Ferrihydrite-Humic Acid Coprecipitates. *Environ. Sci. Technol*.; 47: 13375−13384

Shiratori H., Ohiwa H., Ikeno H., Ayame S., Kataoka N., Miya A., Beppu T., Ueda K., (2008*). Lutispora thermophila* gen. nov., sp. nov., a thermophilic, spore-forming bacterium isolated from a thermophilic methanogenic bioreactor digesting municipal solid wastes. *International Journal of Systematic and Evolutionary Microbiology;* 58(4): 964-969

Shukla A., Parmar P., Saraf M., (2007). Radiation, radionuclides and bacteria: An in-perspective review. *Journal of Environmental RadioactivityI*, 180; 27-35

Simoncic P., Armbruster T., (2004). Peculiarity and defect structure of the natural and synthetic zeolite mordenite: A single-crystal X-ray study. *American Mineralogist,* 89; 421-431

Singh S., Bhatta U. M., Satyam P, V., Dhawan A., Sastry M., Prasad B. L. V., (2008). Bacterial synthesis of silicon/silica nanocomposites. *Journal of Materials Chemistry*; 22

SKB (2015). Microbial sulphide-producing activity in MX-80 bentonite at 1750 and 2000 kg m–3 wet density. *Report R-15-05*

SKB, (2010). Design, production and initial state of the buffer. *Svensk Kärnbränslehantering AB*. *Technical Report TR-10-15*

SKB (2010a). Chemical and mineralogical characterization of the bentonite buffer for the acceptance control procedure in a KBS-3 repository. *TR-10-60*

SKB (2006). Groundwater chemistry around a repository for spent nuclear fuel over a glacial cycle. *TR-06-31*

Skopp J., Jawson M. D., Doran J. W., (1990). "Steady-State Aerobic Microbial Activity as a Function of Soil Water Content" *Soil Scientific Society American Journal,* 54; 1619-1625

Skovbjerg L. L., Christiansen B. C., Nedel S., Dideriksen K., Stipp S. L. S. (2010). The role of green rust in the migration of radionuclides: An overview of processes that can control mobility of radioactive elements in the environment using as examples Np, Se and Cr. *Radiochim. Acta*; 98: 607–612

Slobodkin A. I., Tourova T. P., Kuznetsov B. B., Kostrikina N. A., Chernyh N. A., Bonch-Osmolovskaya E. A., (1999). *Thermoanaerobacter siderophilus* sp. nov., a novel dissimilatory Fe(III)-reducing, anaerobic, thermophilic bacterium. *International Journal of Systematic Bacteriology*, 49; 1471 - 1478

Smart N. R., Reddy B., Rance A. P., Nixon D. J., Frutschi M., Bernier-Latmani R., Diomidis N., (2017). The anaerobic corrosion of carbon steel in compacted bentonite exposed to natural Opalinus Clay porewater containing native microbial populations. *Corrosion Engineering, Science and Technology,* 52(1); 101-112

Song Y., Jiang G., Chen Y., Zhao P., Tian Y., (2017a). Effects of chloride ions on corrosion of ductile iron and carbon steel in soil environments. Sci Rep, 7; 6865

Song D., Li X., Cheng Y., Xiao X., Lu Z., Wang Y., Wang F., (2017). Aerobic biogenesis of selenium nanoparticles by *Enterobacter cloacae* Z0206 as a consequence of fumarate reductase mediated selenite reduction. *Sci Rep,* 7; 3239

Spring S., Rosenzweig F., (2006). The Genera *Desulfitobacterium* and *Desulfosporosinus*: Taxonomy in *The Prokaryotes* (Ch1.2.24), *Springer*Stone W., Kroukamp O., Moes A., McKelvie J., Korber D. R., Wolfaardt G. M., (2016). Measuring microbial metabolism in atypical environments: Bentonite in used nuclear fuel storage. *Journal of Microbiological Methods*; 120: 79-90

Steiglmeier M., Wirth R., Kminek G., Moissl-Eichinger C., (2009). Cultivation of Anaerobic and Facultatively Anaerobic Bacteria from Spacecraft-Associated Clean Rooms. *Applied and Environmental Microbiology,* 75(11); 3484-3491

Stevenson M. A., Faust J. C., Andrade L. L., Freitas F. S., Gray N. D., Tait K., Hendry K. R., Hilton R. G., Henley S. F., Tessin A., Leary P., Papadaki S., Ford A., Marz C., Abbott G. D., (2020). Transformation of organic matter in a Barents Sea sediment profile: coupled geochemical and microbiological processes. *Phil. Trans. R. Soc*. A 378: 20200223

Stewart D. I., Studds P., Cousens T. W., (1998). The effects of salt solutions on the properties of bentonite-sand mixtures. *Clay Minerals;* 33: 651-660

Stone W., Kroukamp O., Moes A., McKelvie J., Korber D. R., Wolfaardt G. M., (2016). Measuring microbial metabolism in atypical environments: Bentonite in used nuclear fuel storage. *Journal of Microbiological Methods*, 120; 79-90

Strobel H.J., (2009). Basic Laboratory Culture Methods for Anaerobic Bacteria. *Mielenz J. (eds) Biofuels. Methods in Molecular Biology (Methods and Protocols),* 581. Humana Press, Totowa, NJ

Stroes-Gascoyne S., West J. M., (1997). Microbial studies in the Canadian nuclear fuel waste management program. *FEMS: Microbiology Reviews,* 20; 573-590

Stroes-Gascoyne S., Hamon C.J., Vilks P., Gierszewski P., (2002). Microbial, redox and organic characteristics of compacted clay-based buffer after 6.5 years of burial at AECL's Underground Research Laboratory. *Appl. Geochem.;* 17: 1287–1303

Stroes-Gascoyne S., Hamon C. J., Maak P., (2011). Limits to the use of highly compacted bentonite as a deterrent for microbially influenced corrosion in a nuclear fuel waste repository. *Physics and Chemistry of the Earth;* 36: 1630-1638

Stroes-Gascoyne S., Hamon C. J., Vilks P. (2000). Microbial analysis of the isothermal test at AECL's Underground Research Laboratory.Prepared by Atomic Energy of Canada Limited for Ontario Power Generation. *Ontario Power Generation Nuclear Waste Management Division,* Report 06819-REP-01200-10023-R00.

Stucki J. W., (2006). Properties and behaviour of iron in clay minerals. *Handbook of Clay Science* (F. Bergaya, B.K.G. Theng and G. Lagaly, editors). Elsevier, Amsterdam. 423–475

Stucki J. W., Lee K., Zhang L., Larson R. A., (2009). Effects of iron oxidation states on the surface and structural properties of smectites. *Pure Appl. Chem*., 74: 2145–2158

Svemar C., Johanneson L. E., Grahm P., Svensson D., Kristensson O., Lönnqvist M., Nilsson U., (2016). Opening and retrieval of outer section of Prototype Repository at Äspö Hard Rock Laboratory. *SKB, TR-13-22*

Svensson D., Dueck A., Nilsson U., Olsson S., Sanden T., Lydmark S., Jagerwall S., Pedersen K., Hansen S., (2011). Status of the ongoing laboratory investigation of reference materials and test package 1. *SKB, TR-11-06*

Taylor P., (1995). Interactions of silica with iron oxides: Effects on oxide transformations and sorption properties. *AECL*, 11257

Thorley R. M. S., Taylor L. L., Banwart S. A., Leake J. R., Beerling D. J., (2015). The role of forest trees and their mycorrhizal fungi in carbonate rock weathering and its significance for global carbon cycling. *Plant, Cell and Environment*; 38: 1947–1961

Tiago I., Pires C., Mendes V., Morais P. V., Costa M. S., Verissimo A., (2006). *Bacillus foraminis* sp. nov., isolated from a non-saline alkaline groundwater. *International Journal of Systemic and Evolutionary Microbiology,* 56(11)

Tomaszewski E. J., Cronk S. S., Gorski C. A., Ginder-Vogel M., (2016). The role of dissolved Fe(II) concentration in the mineralogical evaluation of Fe(hydr)oxides during redox cycling. *Chemical Geology,* 438; 163-170

Tor J. M., Kashefi K., Lovley D. R., (2001). Acetate Oxidation Coupled to Fe(III) Reduction in Hyperthermophilic Microorganisms. Applied and Environmental Microbiology; 67(3): 1363-1365

Turnbull P. C. B., (1996). Bacillus. In: Baron S., editor. *Medical Microbiology. 4th edition*. University of Texas Medical Branch at Galveston, Ch 15

Ulrich N., Nagler K., Laue M., Cockell C. S., Setlow P., Moeller R., (2018). Experimental studies addressing the longevity of *Bacillus subtilis* spores - The first data from a 500-year experiment. *PLoS One*, 13(12)

Urios L., Marsal F., Pelligrini D., Magot M. (2012). Microbial Diversity of the 180 million-year-old Toarcian argillite from Tounemire, France. *Applied Geochemistry*, 27(7); 1442-1450

Uroz S., Calvaruso C., Turpault M.-P., Frey-Klett P. (2009). Mineral weathering by bacteria: ecology, actors and mechanisms. *Trends Microbiol;* 17: 378–387

Usman M., Hanna K., Abdelmoula M., Zegeye A., Faure P., Ruby C., (2012). Formation of green rust via mineralogical transformation of ferric oxides(ferrihydrite, goethite and hematite). *Applied Clay Science*, 64; 38-43

Valencia-Cantero E., Peña-Cabriales J. J., (2014). Effects of iron-reducing bacteria on carbon steel corrosion induced by thermophilic sulfate-reducing consortia. *Journal of Microbiology and Biotechnology*, 24(2); 280-286

Van Paassen L. A., Ghose R., Van der Linden T. J. M., Van der Star W. R. L., Van Loosdrecht M. C. M., (2010). Quantifying biomediated ground improvement by ureolysis: large-scale biogrout experiment. *J. Geotech. Geoenviron. Eng*.; 136(12): 1721-1728

Vasanthi N., Saleena L. M., Anthoni Raj S. (2016). Silica Solubilization Potential of Certain Bacterial Species in the Presence of Different Silicate Minerals. *Silicon*, 10(2); 267-275

Verdel C., Niemi N., Van der Pluijm B., (2011). Variations in the Illite to Muscovite Transition Related to Metamorphic Conditions and Detrital Muscovite Content: Insight from the Paleozoic Passive Margin of the Southwestern United States. *The Journal of Geology*; 119(4): 419-437

Videla H. A., Herrera L. K., (2009). Understanding microbial inhibition of corrosion. A comprehensive overview. International Biodeterioration & Biodegradation, 63(7); 896-900

Videla H. A., Herrera L. K., (2005). Microbiologically influenced corrosion: looking to the future. *International Microbiology;* 8: 169-180

Villar M. V., (2005). MX-80 Bentonite Thermo-Hydro-Mechanical Characterisation Performed at CIEMAT in the Context of the Prototype Project. *IAEA*

Villemur R., Lanthier M., Beaudet R., Lépine F., (2006). The Desulfitobacterium genus. *FEMS Microbiol Rev*., 30(5); 706-733

Vorhies J. S. & Gaines R. R., (2009). Microbial dissolution of clay minerals as a source of iron and silica in marine sediments. *Nature Geoscience*, 2; 221-225

Wang S., Xu D., Wang B., Sheng L.Y., Han E., Dong C., (2016). Effect of solution treatment on stress corrosion cracking behavior of an as-forged Mg-Zn-Y-Zr alloy. *Scientific reports,* 6; 29471

Warner E. S., Heath G. A., (2012). Life Cycle Greenhouse Gas Emissions of Nuclear Electricity Generation, *Journal of Industrial Ecology*, 16(1); 73-92

Wersin P., Birgersson M., Olsson S., Karnland O., Snellman M., Oy S., Oy R., (2008). Impact of corrosion-derived iron on the bentonite buffer within the KBS-3H disposal concept. *SKB* SKB Rapport R-08-34

West J., McKinley I. G., Stroes-Gascoyne S., (2002). Microbial effects on waste repository materials. *Interactions of Microorganisms with Radionuclides,* ch9

Wilins M. J., Livens F. R., Vaughan D. J., Lloyd J. R., Beadle I., Small J. S., (2010). Fe(III) Reduction in the Subsurface at a Low-level Radioactive Waste Disposal Site. *Geomicrobiology Journal,* 3(27); 231-239

Wilke S., Holtz F., Neave D. A., Almeev R., (2017). The Effect of Anorthite Content and Water on Quartz–Feldspar Cotectic Compositions in the Rhyolitic System and Implications for Geobarometry. *Journal of Petrology*, 58(4); 789–818

Williamson A. J., Morris K., Shaw S., Byrne J. M., Boothman C., Lloyd J. R., (2013). Microbial Reduction of Fe(III) under Alkaline Conditions Relevant to Geological Disposal. *Applied and Environmental Microbiology,* 79(11); 3320-3326

Wilkins M.J., Livens F.R., Vaughan D.J., Beadle I., Lloyd J.R., (2007). The influence of microbial redox cycling on radionuclide mobility in the subsurface at a low-level radioactive waste storage site. *Geobiology*; 5: 293–301.

Wilson (2017). FEBEX-DP: Geochemical Modelling of Iron-Bentonite Interactions. *Quintessa QRS-1713A-R3 v1.3*

Wilson J., Savage D., Bond A., Watson S., Pusch R, Bennett D., (2010). Bentonite. *NDA*

Wong D. , Suflita J. M., McKinley J. P., Krumholz L. R., (2003). Impact of Clay Minerals on Sulfate-Reducing Activity in Aquifers. *Microbial Ecology,* 47(1); 80-86

Yang Q., Toijer E., Olsson P., (2019). Analysis of radiation damage in the KBS-3 canister materials. *SKB TR-19-14*

Yeates, C., Gillings, M., Davison, A., Altavilla, N., Veal, D., (1998). Methods for microbial DNA extraction from soil for PCR amplification. *Biological Procedures Online*, 1; 40–47

Yee N., Shaw S., Benning L. G., Nguyen T. H., (2006). The rate of ferrihydrite transformation to goethite via the Fe(II) pathway. *American Mineralogist*, 91; 92-96

Yoon S., Cho W. H., Lee C. S., Kim G. Y., (2018). Thermal Conductivity of Korean Compacted Bentonite Buffer Materials for a Nuclear Waste Repository. *Energies,* 11

Yumoto I., Hirota K., Nodasaka Y., Nakajima K., (2005). *Oceanobacillus oncorhynchi* sp. nov., a halotolerant obligate alkaliphile isolated from the skin of a rainbow trout (Oncorhynchus mykiss), and emended description of the genus *Oceanobacillus*. *Int J Syst Evol Microbiol*, 55; 1521-1524

Zavarzina D. G., Sokolova T. G., Tourova T. P., Chernyh N. A., Kostrikina N. A., Bonch-Osmolovskaya E. A., (2007). *Thermincola ferriacetica* sp. nov., a new anaerobic, thermophilic, facultatively chemolithoautotrophic bacterium capable of dissimilatory Fe(III) reduction. *Extremophiles: life under extreme conditions*; 11(1): 1–7

Zegeye A., Huguet L., Abdelmoula M., Cateret C., Mullet M., Jorand F., (2007a). Biogenic hydroxysulfate green rust, a potentialelectron acceptor for SRB activity. *Geochimica et Cosmochimica Acta*, 71; 5450-5462

Zegeye A., Ruby C., Jorand F., 2007. Kinetic and Thermodynamic Analysis During Dissimilatory γ-FeOOH Reduction: Formation of Green Rust 1and Magnetite. *Geomicrobiology Journal*; 24; 51-64

Zegeye A., Etique M., Carteret C., Ruby C., Schaaf P., Francius G., (2014). Origin of the Differential Nanoscale Reactivity of Biologically and Chemically Formed Green Rust Crystals Investigated by Chemical Force Spectroscopy. *The Journal of Physical Chemistry*

Zegeye A., Bonneville S., Benning L. G., Sturm A., Fowle D. A., Jones C. A., Canfield D. E., Ruby C., MacLean L. C., Nomosatryo S., Crowe S. A., Poulton S. W., (2012). Green rust formation controls nutrient availability in a ferruginous water column. *Geology*, 40(7); 599-602

Zegeye A., Mustin C., Jorand F., (2010). Bacterial and iron oxide aggregates mediate secondary iron mineral formation: green rust versus magnetite. *Geobiology*, 8; 209-222

Zhang J., Wu D., Zhang J., Liu Z., Song F., (2008). *Saccharopolyspora shandongensis* sp. nov., isolated from wheat-field soil. *International Journal of Systematic and Evolutionary Microbiology*; 58(5)

Zhang J., Wang Y., Dai J., Tang Y., Yang Q., Luo X., Fang C., (2009). *Bacillus korlensis* sp. nov., a moderately halotolerant bacterium isolated from a sand soil sample in China. *International Journal of Systemic and Evolutionary Microbiology,* 59(7).

Zhang J., Wang J., Fang C., Song F., Xin Y., Qu L., Ding K., (2010). *Bacillus oceanisediminis sp.* nov., isolated from marine sediment. *International Journal of Systemic and Evolutionary Microbiology,* 60(12).

Zhang Q., Huang Y., Blackwood D. J., Zhang B., Lu D., Yang D., Xu Y., (2020). On the long term estimation of hydrogen embrittlement risks of titanium for the fabrication of nuclear waste container in bentonite buffer of nuclear waste repository. *Journal of Nuclear Materials*; 533: 152092

Zhang T., Wang S., (2019). Explanation of the influence of sodium chloride solution on volume deformation and permeability of normally consolidated clays. *Materials*, 12; 1671

Zhang X., Mandelco L., Wiegel J., (1994) *Clostridium hydroxybenzoicum* sp. nov., an amino acid-utilizing, hydroxybenzoate-decarboxylating bacterium isolated from methanogenic freshwater pond sediment. *International Journal of Systematic and Evolutionary Microbiology*; 44: 214-222

Zhang Z., Schwartz S., Wagner L., Miller W., (2000). A greedy algorithm for aligning DNA sequences. *J Comput Biol*; 7(1-2): 203-14

Zhu W., Winterstein J. P., Yang W. C. D., Yuan L., Sharma R., Zhou G., (2017). In Situ Atomic-Scale Probing of the Reduction Dynamics of Two-Dimensional Fe2O3 Nanostructures. *ACS Nano,* 11; 656−664

Zhu W., Mu T., Zhang Y., Duan T., Luo X., (2014). Coating of microbially produced calcium carbonate onto stone materials. *Science China Technological Sciences*; 58(2): 266–272

Zhu Y., Li Y., Lu A., Wang H., Yang X., Wang C., Cao W., Wang Q., Zhang X., Pan D., Pan X., (2011). Study of the interaction between bentonite and a strain of *Bacillus mucilaginosis. Clays and Clay Minerals,* 59(5); 538-585